The Formation of Microstructure in Shape-Memory Alloys

Konstantinos Koumatos
The Queen's College
University of Oxford

A thesis submitted for the degree of
Doctor of Philosophy in Mathematics

Hilary Term 2012

This thesis is dedicated to my Parents,
for their unending and unconditional support, and to
Katrina who has been my anchor over these years.

Acknowledgements

My research - presented in this thesis - would not have been possible without the support, encouragement, guidance and contribution of a number of people, who I dearly thank and would like to acknowledge.

First and foremost, I am forever grateful to Professor John M. Ball, my supervisor, for all his assistance and guidance. He has been an inspirational figure for me in Oxford, I have learned a great deal from him and I feel truly indebted. I am also obliged to Hanuš Seiner whose remarkable work has been invaluable for my research and has given me the opportunity to take part in research that crosses disciplinary boundaries.

I would also like to particularly thank, Professor Endre Süli who, as a Principal Investigator at OxMOS, has often given me advice, guided me through my research and has helped me immensely with issues outside my research. Likewise, my whole-hearted gratitude goes to Professor Jon Chapman, Principal Investigator at OxMOS, and Professors Bernd Kirchheim and Jan Kristensen for their truly valuable suggestions and help. I am also grateful to Professors Kaushik Bhattacharya and Yury Grabovsky for the extremely helpful discussions during their respective visits at Oxford as well as Dr. Christoph Ortner for his part in the process leading to this thesis.

My research has been supported by the EPSRC critical mass programme 'OxMOS: New Frontiers in the Mathematics of Solids' and I am grateful for their financial support, as well as for the support I have received from 'The Queen's College' and, during my first year in Oxford, the MULTIMAT research and training network. I am also thankful to the Mathematical Institute of the University of Oxford and the Oxford Centre for Nonlinear PDE for offering me an ideal environment to conduct my doctoral research. Special gratitude goes to the project administrators and support stuff at the Gibson Building.

I could never forget my fellow students at OxMOS and OxPDE for the insightful conversations we have had - mathematical or otherwise - and above all, all my friends for making my stay in Oxford an unforgetable experience. Lastly, I wish to thank my family whose support - financial and emotional - as well as guidance have been more than decisive over the years and a true driving force, for which I am grateful.

Abstract

The application of techniques from nonlinear analysis to materials science has seen great developments in the recent years and it has really been a driving force for substantial mathematical research in the area of partial differential equations and the multi-dimensional calculus of variations.

This thesis has been motivated by two recent and remarkable experimental observations of H. Seiner[1] in shape-memory alloys which we attempt to interpret mathematically. Much of the work is original and has given rise to deep problems in the calculus of variations.

Firstly, we study the formation of non-classical austenite-martensite interfaces. Ball & Carstensen (1997, 1999) theoretically investigated the possibility of the occurrence of such interfaces and studied the cubic-to-tetragonal case extensively. In this thesis, we present an analysis of non-classical austenite-martensite interfaces recently observed by Seiner et al. in a single crystal of a CuAlNi shape-memory alloy, undergoing a cubic-to-orthorhombic transition. We show that these can be described by the general nonlinear elasticity model and we make some predictions regarding the admissible volume fractions of the martensitic variants involved, as well as the habit plane normals.

Interestingly, in the above experimental observations, the interface between the austenite and the martensitic configuration is never exactly planar, but rather slightly curved, resulting from the pattern of martensite not being exactly homogeneous. However, it is not clear how one can reconstruct the inhomogeneous configuration as a stress-free microstructure and, instead, a theoretical approach is followed. In this approach, a general method is provided for the construction of a compatible curved austenite-martensite interface and, by exploiting the structure of quasiconvex hulls, the existence of curved interfaces is shown in two and three dimensions. As far as the author is aware of, this is the first construction of such a curved austenite-martensite interface.

Secondly, we study the nucleation of austenite in a single crystal of a CuAlNi shape-memory alloy consisting of a single variant of stabilized 2H martensite. The

[1]Institute of Thermomechanics ASCR, Dolejškova 5, 182 00 Prague 8, Czech Republic

nucleation process is induced by localized heating and it is observed that, regardless of where the localized heating is applied, the nucleation points are always located at one of the corners of the sample - a rectangular parallelepiped in the austenite.

Using a simplified nonlinear elasticity model, we propose an explanation for the location of the nucleation points by showing that the martensite is a local minimizer of the energy with respect to localized variations in the interior, on faces and edges of the sample, but not at some corners, where a localized microstructure can lower the energy. The result for the interior, faces and edges is established by showing that the free-energy function satisfies a set of quasiconvexity conditions at the stabilized variant throughout the specimen, provided this is suitably cut. The proofs of quasiconvexity are based on a rigidity argument and are specific to the change of symmetry in the phase transformation. To the best of the author's knowledge, quasiconvexity conditions at edges and corners have not been considered before.

Contents

List of Figures

Chapter 1

Introduction

As the title reveals, this thesis is primarily concerned with the problem of pattern formation in shape-memory alloys. These are crystalline solids undergoing a broad class of solid-to-solid phase transformations referred to as *martensitic* - named after the German materials scientist Adolf Martens ($1850 - 1914$). A primary goal set out for this thesis is to be as self-contained as possible and as such, in this introduction, we give a brief account of martensitic transformations from a materials science point of view; we describe precisely what they are and give an appropriate definition for the context of this work. In doing so, we lay out and explain some fundamental concepts regarding crystalline solids and their phase transitions.

Having provided the necessary background, we proceed to discuss shape-memory alloys and highlight their importance with respect to applications. A description of the shape-memory phenomenon is given and we show how this is manifested in martensitic transformations.

Moreover, a complete overview of the proceeding chapters is included and the introduction ends with a very brief discussion of issues related to martensitic transformations which go beyond the scope of this thesis and have thus been omitted.

1.1 Martensitic Phase Transformations

A *crystalline solid* is a material in which the atoms or groups of atoms are arranged in an orderly repeating pattern extending in all three spatial dimensions within the body; this pattern is referred to as the *crystal lattice* or simply *lattice*. A *unit cell* for a crystal lattice is a group of neighbouring atoms which, if repeated, can generate the entire lattice structure. The dimensions of this unit cell, i.e. the interatomic distances, are given by the *lattice parameters* which can be determined experimentally.

Crystalline solids can be *single crystals* or *polycrystals*. A single crystal is a crystalline solid in which the crystal lattice of the entire undeformed body is uniform throughout the specimen. On the other hand, a polycrystal is a solid that comprises a large number of regions, each having the same lattice structure but different orientations. These regions of different orientation are referred to as *grains* and are separated by *grain boundaries*. Hence, we could define single crystals as crystalline solids that have no grain boundaries. Polycrystals are more common in nature and in industrial usage; however, in this thesis we shall only be concerned with single crystals.

Many of the commonly used materials are *alloys*; that is, they are a mixture of different elements. Variations in the composition of such an alloy can result in regions with different lattice structure or, even when the composition of regions remains the same, these may have different crystal lattices. The regions described by the latter are called *phases* and like grains are separated by interfaces referred to as *phase boundaries*. Martensitic phase transformations are a manifestation of such a coexistence of phases and they have a profound effect on the macroscopic properties of the body.

A *phase transformation* in a material system is the transition from one phase to another. During a phase transformation, the arrangement of the crystal lattice changes from the *reference configuration* to a different one. When this structural change in the crystal lattice occurs by the coordinated movement of atoms (or groups of atoms) relative to their neighbours the transformation is called *displacive* and, in particular, there is no diffusion.

We now define the class of martensitic phase transformations: these are displacive, solid-to-solid phase transformations during which the structure of the lattice changes abruptly at some critical temperature (i.e. first-order transformations[1]). The high-temperature phase is called the *austenite*, whereas the low-temperature phase is referred to as the *martensite*. Assuming that the body is in the austenite phase, if cooled a little, the only change will be that due to ordinary thermal contraction. However, that is only until we reach a critical temperature M_S, the *martensite start temperature*, at which the lattice structure suddenly changes as the body transforms into the martensite phase. During this process austenite and martensite coexist until

[1]We note that certain transformations, such as the R-phase in NiTi or the modulated phases in NiMnGa, share similar features to martensitic transformations and, in some literature, might be referred to as martensitic; however, these are not of first-order; this is also true for certain ceramics as well as ferroics. In this thesis, we retain the term martensitic only for transitions of first-order.

a temperature M_F, the *martensite finish temperature*, when the body has fully transformed to martensite; this coexistence of phases is common in first-order transitions. Despite the nature of this change, there is no diffusion and the relative positions of atoms remain the same. Further cooling will only result in further thermal contraction. If, upon heating and at some other critical temperature A_S, *the austenite start temperature*, the lattice structure abruptly changes back to its original configuration, the transformation is called *reversible*; as with the forward transition, the two phases coexist until the *austenite finish temperature* A_F is reached. These form a subclass of martensitic transformations, known as thermoelastic. Henceforward, we will only be concerned with reversible martensitic transformations and we drop the term thermoelastic. In the above process, the critical temperature for the forward and the reverse transformations need not be the same and in fact, it is not. This difference between the two critical temperatures is called *thermal hysteresis*. Understanding hysteresis is far from trivial and it is not accounted for in this thesis. A common way to ignore this is to consider the mean value of the two transformation temperatures to be the critical temperature θ_c both for the forward and reverse transformations, i.e. $\theta_c = (M_S + A_S)/2$.

An important feature of such transformations is that, in general, the high-temperature phase possesses greater crystallographic symmetry than the low-temperature phase. In particular, we will be interested in transitions in which there is only one *variant of austenite* whereas there are several distinct *variants of martensite*. The latter are symmetry-related and their number depends on the change of symmetry during the transformation. For example, in a cubic-to-tetragonal transformation (see Fig. 1.1), there are three distinct symmetry-related variants of martensite. As these have the same energy, the material cannot distinguish between them and prefer one over the other. In fact, not only is there no reason for one martensitic variant to be preferable to another, but there is also no reason why the austenite should transform into a particular single variant of martensite. Indeed, different regions of the crystal may transform into different variants of martensite and this occurs for a number of reasons, the most important being the need for the martensite to be geometrically compatible with itself and the austenite.

This brings us to another feature of martensitic transformations which is the ability to produce *microstructure*. The coexistence of different martensitic variants occurs in such a way that the lattice remains unbroken across interfaces between such variants. This need for coherence forces the martensitic variants to form patterns at length-scales much smaller than the size of the solid body, e.g. Fig. 1.2. As a result,

microstructure is formed which has a profound impact on the macroscopic properties of materials undergoing martensitic transformations.

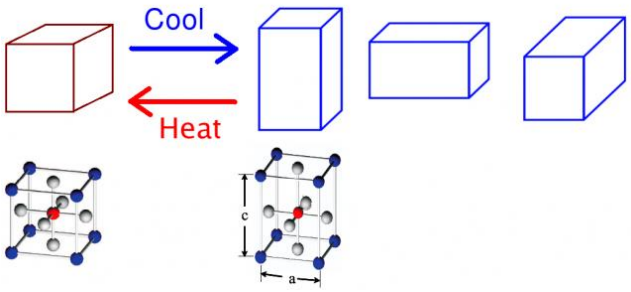

Figure 1.1: Variants of martensite in a cubic-to-tetragonal transformation; a and c represent the lattice parameters.

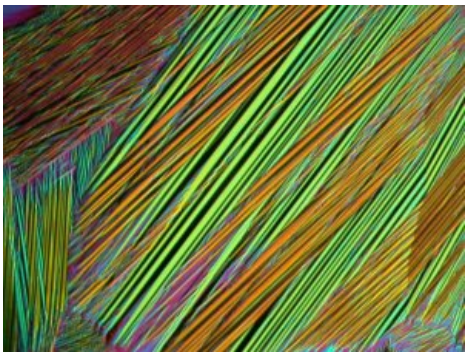

Figure 1.2: Microstructure of martensite in CuZnAl (M. Morin, INSA de Lyon).

Transformations of this type may also be induced by applying loads, a phenomenon known as a *stress-induced martensitic transformation*. This means that, above the critical temperature, the austenite can be transformed into *stress-induced martensite* by applying some mechanical load rather than cooling the specimen. In this case, applying and removing loads take the place of cooling and heating. The process is not much different: as the loads are applied, the specimen only exhibits small elastic deformation but, at some critical load, the crystal transforms to the martensitic phase. Being above the transformation temperature, the martensite is unstable without the presence of loads and hence, upon unloading, the crystal starts the reverse transformation back to the austenite phase. After complete unloading, the crystal recovers all the deformation and returns to its reference configuration. Hysteresis, in the sense of critical loads, remains present and is dependent on the relative stability

of the austenite and the martensite and, hence, on the temperature. It should be noted, however, that after suitable mechanical treatment many materials exhibit a certain stabilization effect. In particular, the mechanical treatment leads to an energy barrier which can significantly increase the temperature needed for the transition back to austenite; this effect is known as the *mechanical stabilization of martensite*. In this case, upon unloading, the reverse transformation does not occur due to this rise in the critical temperature. The mechanical stabilization effect will play an important role in Chapter 4 where a detailed description is given. We do not elaborate further on stress-induced transformations as a detailed account for these is perpetually connected to hysteresis and heat transfer. As such, they go beyond the scope of this thesis and we refer the reader to the work of Huo and Müller [79], Shaw and Kyriakides [125] and of Sittner et al. [127, 128] for an extensive study.

Martensitic phase transformations have been observed in a number of materials, including ceramics, biological systems and alloys. In particular, a category of alloys that are of special interest in applications, as well as one of the main driving forces for the development of mathematical models of martensitic transformations, is that of the so-called *shape-memory alloys*. We draw attention to these and see how martensitic transformations allow us to understand their properties.

Shape-memory phenomenon

Shape-memory alloys (SMAs) can be elastically deformed and, upon heating beyond some critical temperature, they return to their original configuration in a process known as *shape recovery*. SMAs have been used in a wide range of applications including eyeglass frames, dentistry and piping but also aircraft engineering and robotics, amongst others, existing or potential. The following quote, borrowed from Richard Lin (Stanford University), highlights the importance of such materials: *'With the innovative ideas for applications of SMAs and the number of products on the market using SMAs continually growing, advances in the field of shape memory alloys for use in many different fields of study seem very promising'*. However, existing SMAs present limitations in their usage because of factors such as large hysteresis and there is a need to discover and manufacture new SMAs. Thus, understanding their properties is very important and in recent years this has motivated substantial mathematical research.

The shape-memory phenomenon is really a manifestation of martensitic phase transformations. In particular, at temperatures higher than the transformation tem-

perature, the specimen is in the high-symmetry austenite phase and, upon cooling, the austenite transforms into the low-temperature, low-symmetry martensite phase. As we mentioned already, this transformation needs to be done coherently and, as a result, microstructure of martensite is formed. In fact the transformation from the parent, austenite phase to the product, martensite phase often happens in such a way that the shape of the specimen remains macroscopically undistorted; this is known as *self-accommodation* (see [26] for a mathematical treatment).

Upon deformation, the crystal rearranges the martensitic variants and creates a new microstructure so that the deformation can be accommodated. However, these different martensitic variants have the same energy and the crystal is able to change its shape to accommodate the deformation without any energetic costs. Once the loads are removed, the crystal remains in the deformed configuration since the self-accommodated state and its current deformed state are energetically equivalent.

When the specimen is heated to its transformation temperature, martensite transforms back to austenite. However, since austenite possesses high symmetry, it can no longer accommodate the deformed shape and the crystal is forced to return to its original high-temperature reference configuration. Fig. 1.3 below provides a schematic description of the shape-memory phenomenon. This unique high-temperature, low-energy state, the various low-temperature, low-energy states and the ability of the crystal to form microstructure at low temperatures are crucial for the properties of materials undergoing martensitic phase transformations and, ultimately, are the elements giving rise to the shape-memory phenomenon.

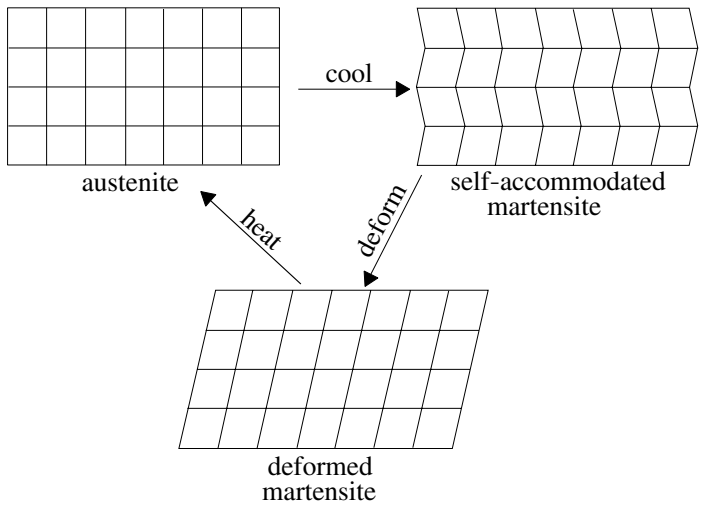

Figure 1.3: Schematic description of the shape-memory phenomenon.

1.2 Overview

The chapters of this thesis are organized as follows: In Chapter 2, we introduce the continuum model for martensitic transformations, as proposed by J.M. Ball and R.D. James, which we follow in our analysis. This is a variational model where the crystal is modelled as a nonlinear elastic material and the free-energy density is invariant with respect to both rigid-body rotations and the appropriate crystallographic symmetries; the variants of austenite and martensite are represented by energy wells for this density. This chapter is split into two main parts: firstly, so as to help keep the thesis self-contained, we include a review of the vectorial calculus of variations to the extent that is necessary for the chapters that follow. However, this review is by no means exhaustive and the reader is referred to [46, 105] and the references therein for a more complete account. In particular, we present the direct method of the calculus of variations, make the passage from constrained to generalized minimization problems via relaxation methods and discuss some fundamental aspects of the theory of Young measures. Finally, we introduce all appropriate generalized convexity conditions for functions and sets, discuss their connections and present relevant results.

We then proceed to introduce the continuum theory, beginning with an atomistic description. We present an elementary review regarding lattices, their deformations and symmetries and establish a link with the continuum theory based on the Cauchy-Born hypothesis. As we aim to concentrate on the continuum viewpoint, this presentation is condensed and the reader is referred to [19] for a more extensive treatment.

Having established our mathematical framework, we describe how this applies in the continuum model and we discuss the origin of microstructure which, in this context, is viewed as a result of energy minimization and geometric compatibility accounting for discontinuities of the deformation gradient along phase boundaries. This geometric compatibility gives rise to the so-called *compatibility equations*, a generalization of which will be central in Chapter 3. We also review some of the achievements of the continuum theory in recovering the crystallographic theory of martensite and we introduce the *parallelogram microstructure* which will concern us in Chapter 3. Lastly, we comment briefly on a geometrically linear variation to this theory and discuss why the nonlinear model is preferred.

In Chapter 3, we draw attention to non-classical austenite-martensite interfaces. The theory described in Chapter 2 naturally leads to the prediction of more complex austenite-martensite interfaces compared to the classical crystallographic theory. In

these interfaces, a pure phase of austenite meets a complicated microstructure of martensite and not necessarily a single laminate as in the classical case. Ball and Carstensen [13, 14] provided a theoretical investigation of such interfaces which was exhaustive for the cubic-to-tetragonal transformation. They fully identified the set of admissible microstructures for the two-well problem and made predictions regarding the possible interfaces and habit plane normals. A brief review of their work is included. We then proceed to the description of experimental results obtained by H. Seiner et al. [123], where a non-classical austenite-martensite interface is observed in a CuAlNi single crystal. In the observed interface, the martensite is arranged in a parallelogram microstructure and the actual interface appears to be slightly curved due to a variation in the volume fraction of the martensitic configuration. Based on the variational model of Ball and James, we provide an analysis of the homogeneous non-classical interface which neglects the curvature of the interface. We deduce that it is predictable by the theory and we present results concerning the admissible volume fractions and habit plane normals; these can also be found in [20]. CuAlNi undergoes a cubic-to-orthorhombic transformation and, due to algebraic complexity, the results we obtain are not as sharp as those of Ball and Carstensen; nevertheless, similarities are clear and comparisons can be drawn.

The remainder of Chapter 3 is devoted to the investigation of curved interfaces. Attempts to include the inhomogeneity of the martensitic configuration and directly construct the curved interface of the experiment as a stress-free microstructure proved to be unsuccessful. We briefly discuss these attempts not only to motivate the theoretical investigation of curved interfaces that follows, but also because they contain calculations (not included) that are of some interest. We then depart from the strict experimental set-up and proceed into a theoretical investigation where, via a new method exploiting the structure of quasiconvex hulls, we prove the existence of a curved austenite-martensite interface in two and three dimensions.

To ensure that the deformation remains Lipschitz continuous across a non-planar surface, a modification of Hadamard's jump condition is proved. This provides necessary and sufficient conditions for a map $z \in W^{1,\infty}\left(\Omega, \mathbb{R}^d\right)$ to have a gradient taking the values Dy^+ and Dy^- on either side of a C^1 surface, for $y^\pm$ appropriately smooth.

A general method of constructing a compatible curved interface is presented which works for any relevant quasiconvex hull K^{qc} provided that its relative interior is non-empty and contains a point F which is rank-one connected to the identity; 'relative' is meant with respect to a set of the form $\mathcal{D} = \{A \in M^{d\times d} : \det A = \Delta\}$ and 'relevant' refers to $SO(d)$-invariant sets K satisfying such a determinant constraint.

In two dimensions, the existence of such a point is established by using a known abstract characterization of quasiconvex hulls to show that double laminates correspond to relative interior points. In three dimensions, no general characterization exists and it can be shown that explicitly known hulls have empty (relative) interiors, whereas, the limited existing examples of relative interior points (cf. [41, 53]) cannot be rank-one connected to the identity. However, using an idea originated by B. Kirchheim along with results in [41], we prove - modulo assumptions - the existence of such a point for compact sets K such that K^{qc} contains a three well configuration of the form $\bigcup_{i=1}^{3} SO(3)\, U_i$ where the U_i, $i = 1, 2, 3$, are diagonal matrices permuting η_2, η_1, η_1 on the diagonal; examples of such sets K are those corresponding to the cubic-to-tetragonal transition but also the cubic-to-orthorhombic which is the transition Seiner's specimen undergoes. We end this chapter by making some concluding remarks.

In Chapter 4, we draw attention to a different problem also motivated by recent experimental observations of H. Seiner which - in a simplified setting - has much in common with the Weierstrass problem[2] in the vectorial calculus of variations. In particular, using a localized heat source, austenite is nucleated in a bar-shaped specimen of a CuAlNi single crystal which is mechanically stabilized as a pure phase of a single martensitic variant. It is observed that, regardless of where the localized heating is applied, the nucleation points are always located at a corner of the specimen, while the martensite remains stable throughout the interior, faces and edges. A brief review of the Weierstrass problem is presented, including the recent and truly remarkable developments of Y. Grabovsky and T. Mengesha in [70], and the experimental results of Seiner are described, along with a more detailed description of the mechanical stabilization effect.

We then proceed to discuss the problem in mathematical terms. The viewpoint taken is that the stability of the martensite is related to certain quasiconvexity conditions on the energy density throughout the domain, conditions which fail at some corners, thus allowing for the nucleation of austenite. The problem is phrased in terms of Young measures where an energy functional is derived rigorously, via the means of Γ- convergence, that is infinite off the set K of the martensitic and austenitic energy wells - assuming that the latter has lower energy. The quasiconvexity conditions in the interior and at the boundary of a bar-shaped domain are defined in terms of

[2]The Weierstrass problem consists of finding necessary and sufficient conditions for strong local minimizers in the calculus of variations. The resolution of this problem in the scalar case is attributed to Weierstrass, thus bearing his name (see Chapter 4 for more details).

Young measures and amount to the stabilized variant being a local minimizer with respect to a certain set of localized variations. In the interior and on faces these conditions are a mere re-phrasing of the classical conditions of quasiconvexity in the interior (Morrey [103]) and at the boundary (Ball and Marsden [22]), whereas, at edges and corners, a natural extension of these is considered.

For a class of parallelepipeds, including that of the experiment, these quasiconvexity conditions are proved for the interior, faces and edges while, at some corners, the instability is shown by an explicit construction of an inhomogeneous gradient Young measure that lowers the energy (see also [21][3]). The proof of quasiconvexity uses the minors relations and for the faces and edges, a more elaborate method is followed involving a notion of *maximal directions* which is defined. For the method to be applicable, one needs to rule out interpenetration of matter and a certain type of self-contact of the boundary, conditions which are achieved by employing the constraint of Ciarlet and Nečas [39], combined with results from the theory of mappings with bounded distortion.

1.3 Omissions

Throughout this thesis, there are issues related to the modelling of martensitic phase transformations that fail to be addressed, either by the model itself or by the author, and we briefly account for these.

First and foremost, the model is only concerned with statics and not dynamics. The issue of the evolution of microstructure is not addressed, whereas this is a problem of pattern formation and, as such, should be treated with a dynamical model. A static model could never be fully predictive as there is an excess of energy minimizers. In the low-temperature martensite phase, there are numerous configurations of the martensitic variants that minimize the total energy and are, therefore, allowed by the model. However, the static theory fails to distinguish between these and the microstructure cannot be uniquely determined. Instead, the geometry of the microstructure is assumed *a priori* and we decide on whether or not it is predictable by showing its consistency with the theory. Nevertheless, the theory can predict various interesting aspects of the microstructure, such as the orientation of the habit planes and the volume fractions in twinned martensite, without making assumptions additional to the change in symmetry and the transformation strains. Further, there

[3]In [21] it is claimed that an appropriate Young measure lowering the energy can be constructed at all corners. However, it is not clear whether or not this stronger statement is true; this is subject to further investigation.

is no consensus on the appropriate dynamical equations and for all models the resulting equations are in general too difficult to treat rigorously, with few analytic results known. Despite that, such models have been very useful in computations and have provided great insight in problems of increasing complexity. Many authors have developed dynamical models following various approaches and the reader is referred to Andrews and Ball [5], Kloucek and Luskin [88] as well as Wang and Khachaturyan [142] for relevant descriptions. We should also point out that we do not provide any justification for the variational approach to microstructure; this is itself motivated by dynamic considerations and we refer the reader to [11, 17, 67] which also provide additional references for the dynamic approach.

Another issue that we do not address is the incorporation of interfacial energy into the model. In the model used here, the infimum of the energy is not in general attained but, rather, there are energy-minimizing sequences approaching it which, in the limit, give rise to infinitely fine microstructures. However, in reality, the observed microstructures may be very fine indeed but have a characteristic length scale which is not accounted for in the model precisely due to the non-attainment of the infimum. This problem can be dealt with by adding an interfacial energy term to the energy functional. The form of this interfacial energy should be naturally derived from an atomistic model and, although there have been several models, the way of doing so is not clear. For treatments of such models the reader is referred to Ball and Crooks [16], Conti and Schweizer [42], Kohn and Müller [90], Müller [105] and references therein.

Finally, this thesis concerns the modelling of single crystals where the lattice of the austenite phase is uniform along the specimen; nonetheless, typical commercial specimens are polycrystals. As mentioned already, these are an agglomeration of a large number of grains with an identical lattice but oriented differently. In such martensitic materials, each grain undergoes a martensitic transformation and forms a microstructure that may well be different from that in other grains. Still, these different microstructures cannot be entirely independent as the grains are bonded with each other. As a result, the properties and behaviour of a polycrystal may differ notably from those of a single crystal and, indeed, experimental results confirm this. Work has been conducted in order to model polycrystals effectively in which a linearized version of the elasticity model is preferred. This is because the nonlinear setting gets too involved and sets restrictions to the extent up to which we can investigate the behaviour of polycrystals. The reader is referred to the work of Bhattacharya and Kohn [33, 34], as well as of Shu and Bhattacharya [126] and references therein for a more in-depth study of polycrystals.

Chapter 2

The Calculus of Variations and the Nonlinear Elasticity Model

At this point we take a detour and provide the mathematical background necessary for the description of the model and, ultimately, the prediction of microstructure formation in martensitic materials. The results described in this section are well established and we do not include any proofs; instead, the reader is referred to the appropriate literature where these can be found.

2.1 The Calculus of Variations

In general, the calculus of variations is concerned with the problem of minimizing an integral of the form

$$I(y) = \int_{\Omega} \varphi(x, y(x), Dy(x))\, dx$$

over some set of *admissible* maps

$$\mathcal{A} = \left\{ y : \Omega \to \mathbb{R}^N \in X : \; y_{|\partial\Omega_1} = \bar{y} \right\}$$

In the above, $\Omega \subset \mathbb{R}^d$ is a bounded domain (i.e. open and connected) where d, $N \geq 1$ and $\partial\Omega_1$ is a portion of the boundary of Ω - possibly the entire boundary; X is a function space to be specified and $\bar{y} \in X$ is a given function; in particular, $\mathcal{A}$ is non-empty. For the purposes of this thesis, we restrict attention to the case of no lower order terms, i.e. when φ depends only on the gradient Dy, and we assume that $d = N > 1$ which is relevant for the modelling of martensitic transformations. We note that the general flavour of the results presented remains the same in the case of lower order terms but the assumptions tend to be more technical. For statements and proofs in the general case, the reader is referred to Dacorogna's book [46], as well

as the references given in this chapter. The case $d = 1$ or $N = 1$, the scalar case, will not be of interest to us and it is not covered in this exposition. The scalar case is generally more straightforward and standard textbooks, including [46], cover it.

Hence, we consider the minimization problem

$$I(y) = \int_\Omega \varphi(Dy(x))\,dx \quad \text{over} \tag{2.1.1}$$

$$\mathcal{A} = \left\{y : \Omega \to \mathbb{R}^d \in X :\ y_{|\partial\Omega_1} = \bar{y}\right\}, \tag{2.1.2}$$

where $\Omega \subset \mathbb{R}^d$ and $\bar{y} \in X$ making $\mathcal{A}$ non-empty.

A powerful tool in dealing with the minimization problem (2.1.1)-(2.1.2) is the *direct method in the calculus of variations* and we focus on this. The idea is as follows: Suppose that $\inf_{\mathcal{A}} I(y) = l > -\infty$. Then, there exists a sequence $\left\{y^k\right\}$ such that $I\left(y^k\right) \to l$ as $k \to \infty$. There are two central points:

(i) assume that (up to a subsequence) y^k converges with respect to a certain topology to a limit y and that

(ii) the functional I is (sequentially) lower semicontinuous with respect to the same topology; that is $I(y) \le \liminf_{k\to\infty} I\left(y^k\right)$ whenever $y^k \to y$.

Then we may conclude that

$$l \le I(y) \le \liminf_{k\to\infty} I\left(y^k\right) = l$$

and the existence of a minimizer y is guaranteed.

Property (i) can be satisfied via an appropriate choice of the function space X and we choose the Sobolev space $W^{1,p}\left(\Omega, \mathbb{R}^d\right)$; then the boundary condition is to be understood in the sense of traces. Recall that for $1 \le p \le \infty$ a function $y : \Omega \to \mathbb{R}$ is in the space $W^{1,p}(\Omega, \mathbb{R})$ if

$$\begin{aligned} &\int_\Omega \left(|y(x)|^p + |Dy(x)|^p\right) dx < \infty, \qquad 1 \le p < \infty, \\ &\operatorname*{ess\,sup}_\Omega \left(|y(x)| + |Dy(x)|\right) < \infty, \qquad p = \infty, \end{aligned} \tag{2.1.3}$$

where $\operatorname{ess\,sup}_\Omega |y(x)| = \inf\{M > 0 :\ |y(x)| \le M \text{ for a.e. } x \in \Omega\}$, i.e. $y \in W^{1,p}(\Omega, \mathbb{R})$ if and only if both y and its generalized partial derivatives $\partial y/\partial x_i$ lie in $L^p(\Omega, \mathbb{R})$ for all $i = 1, \ldots, d$. Then, we say that $y \in W^{1,p}\left(\Omega, \mathbb{R}^d\right)$ if each component of $y = (y_1, \ldots, y_d)$ is an element of $W^{1,p}(\Omega, \mathbb{R})$. For details and an extensive treatment of Sobolev spaces see Adams [2].

When equipped with the weak topology (weak$*$ for $p=\infty$), Sobolev spaces enjoy good compactness properties. This is because for $1<p<\infty$, the space $W^{1,p}$ is reflexive and the space L^1 is separable with $(L^1)^* = L^\infty$. Consequently, from the Banach-Alaoglu theorem, every bounded sequence in $W^{1,p}$, $p>1$ has a weakly convergent subsequence (weakly$*$ for $p=\infty$). Thus, by imposing a coercivity condition on φ (i) will be satisfied. Typically, this coercivity condition is of the form

$$-c_1 + c_2|F|^p \leq \varphi(F), \ \forall F \in M^{d\times d}, \tag{2.1.4}$$

for some $c_1, c_2 > 0$ and $p>1$. The condition for $p=\infty$ becomes $\varphi(F)\to\infty$ as $|F|\to\infty$. Then, if $\{y^k\}\subset\mathcal{A}$ is an infimizing sequence such that $I(y^k)\to l = \inf_{\mathcal{A}} I$, the coercivity condition allows us to bound y^k in $W^{1,p}$ and we can extract a convergent subsequence (not relabeled) such that $y^k \rightharpoonup y$ in $W^{1,p}$. Assuming that the boundary of Ω is Lipschitz, by trace theory, $y^k_{|\partial\Omega} \to y_{|\partial\Omega}$ in L^p and the limit will also satisfy the boundary condition. Then, for

$$\mathcal{A} = \left\{ y \in W^{1,p}\left(\Omega, \mathbb{R}^d\right) : y_{|\partial\Omega_1} = \bar{y} \right\} \tag{2.1.5}$$

we deduce that $y\in\mathcal{A}$ and our choice of function space is justified.

Remark. When the boundary condition is set on the entire boundary $\partial\Omega$, we will often abbreviate this as $y \in \bar{y} + W_0^{1,p}\left(\Omega,\mathbb{R}^d\right)$ where, for $1\leq p<\infty$, $W_0^{1,p}(\Omega,\mathbb{R}^n)$ is the closure of $C_c^\infty\left(\Omega,\mathbb{R}^d\right)$ - smooth, compactly supported functions - in the $W^{1,p}$ norm; for $p=\infty$, the closure is taken with respect to the weak$*$ topology of $W^{1,\infty}\left(\Omega,\mathbb{R}^d\right)$. We note that if Ω is Lipschitz, $W_0^{1,p}\left(\Omega,\mathbb{R}^d\right) = \left\{ y\in W^{1,p}\left(\Omega,\mathbb{R}^d\right) : \ y_{|\partial\Omega}=0 \right\}$.

On the other hand, satisfaction of (ii) is not as trivial. Morrey [103] introduced the notion of quasiconvexity which is now recognized as the central convexity condition ensuring weak lower semicontinuity in the vectorial case $d>1$.

Definition 2.1.1. *Let $\varphi : M^{d\times d}\to\mathbb{R}$ be a Borel measurable and locally bounded function and $1\leq p\leq\infty$. We say that φ is $W^{1,p}$ quasiconvex at a matrix $F\in M^{d\times d}$ if for some bounded and open set $E\subset\mathbb{R}^d$ with $\mathcal{L}^d(\partial E)=0$,*

$$\varphi(F) \leq \frac{1}{\mathcal{L}^d(E)} \int \varphi(F + Dy(x))\, dx \tag{2.1.6}$$

for all $y\in W_0^{1,p}\left(E,\mathbb{R}^d\right)$. We say that φ is $W^{1,p}$ quasiconvex if it is $W^{1,p}$ quasiconvex at every $F\in M^{d\times d}$.

Above $\mathcal{L}^d(E)$ is the d-dimensional Lebesgue measure of the set E. We note that if (2.1.6) holds for one open and bounded set E with $\mathcal{L}^d(\partial E) = 0$ then it also holds for any such set E and the definition of quasiconvexity is independent of the choice of E. From now on and for simplicity, we refer to $W^{1,\infty}$ quasiconvex functions simply as quasiconvex.

Remark. Note that we required Borel measurability and local boundedness for a function to be termed $(W^{1,p})$ quasiconvex. Henceforth, whenever a function is said to be $(W^{1,p})$ quasiconvex, it is also assumed to be Borel measurable and locally bounded. This is not necessary and we refer the reader to [105] for an alternative exposition.

It is easy to see that φ is $W^{1,p}$ quasiconvex at F if the function $y = Fx$ is an absolute minimizer of the functional

$$I_E(y) = \int_E \varphi(Dy(x))\,dx$$

over the set of admissible maps

$$\mathcal{A} = \left\{y :\ y - Fx \in W_0^{1,p}\left(E, \mathbb{R}^d\right)\right\}.$$

The following central theorem in the vectorial calculus of variations is essentially due to Morrey [103] and has been refined by Acerbi and Fusco [1], Marcellini [98] and Meyers [102].

Theorem 2.1.1. *Let $I(y) = \int_\Omega \varphi(Dy)\,dx$. If $\varphi : M^{d\times d} \to \mathbb{R}$ is continuous and I is sequentially weakly$*$ lower semicontinuous in $W^{1,\infty}\left(\Omega, \mathbb{R}^d\right)$ (in particular, if I is weakly lower semicontinuous in $W^{1,p}\left(\Omega, \mathbb{R}^d\right)$) then φ is quasiconvex. Conversely, suppose that φ is quasiconvex and that:*

- *if $p = \infty$,*
$$|\varphi(F)| \le \eta(|F|), \quad \text{for all } F \in M^{d\times d}$$
and some continuous and increasing function η;

- *if $1 < p < \infty$,*
$$-c\left(1 + |F|^q\right) \le \varphi(F) \le c\left(1 + |F|^p\right), \quad \text{for all } F \in M^{d\times d}$$
and some $c > 0$, $1 \le q < p$;

- *if* $p = 1$,
$$|\varphi(F)| \leq c(1 + |F|), \quad \text{for all } F \in M^{d\times d}$$
and some $c > 0$.

Then the functional I *is sequentially weakly (weakly* if* $p = \infty$*) lower semicontinuous in* $W^{1,p}\left(\Omega, \mathbb{R}^d\right)$.

Combining Theorem 2.1.1 with our discussion so far one obtains the existence of minimizers:

Theorem 2.1.2. *Let* $\Omega \subset \mathbb{R}^d$ *have Lipschitz boundary and* $\varphi : M^{d\times d} \to \mathbb{R}$ *be a quasiconvex function such that*
$$-c_1 + c_2|F|^p \leq \varphi(F) \leq c_1(1 + |F|^p)$$
for some $c_1,\ c_2 > 0$, $1 < p < \infty$ *and all* $F \in M^{d\times d}$. *Then* I *admits a minimizer over the class of admissible maps*
$$\mathcal{A} = \{y \in W^{1,p}\left(\Omega, \mathbb{R}^d\right) :\ y_{|\partial\Omega_1} = \bar{y}\}.$$

By Theorem 2.1.2, the quasiconvexity condition, modulo technical assumptions, guarantees the existence of minimizers for the variational problem investigated here. Interestingly, we note that in some sense quasiconvexity is also necessary for the existence of minimizers. In particular, Ball and Murat [23] showed the following:

Let $\Omega \subset \mathbb{R}^d$ be a bounded, open set with $\mathcal{L}^d(\partial\Omega) = 0$, φ be a Borel measurable and bounded below function and $1 \leq p \leq \infty$. If the functional
$$J(y) = \int_\Omega [\varphi(Dy(x)) + \Psi(x, y(x))]\, dx$$
attains a minimum on $\mathcal{A} = \left\{y : y - Fx \in W_0^{1,p}(\Omega, \mathbb{R}^d)\right\}$ for all smooth, non-negative Ψ, then φ is $W^{1,p}$ quasiconvex at $F \in M^{d\times d}$.

However, in general, the absence of quasiconvexity is only indicative of non-attainment of the infimum and this will be of great importance to us since typically the integrands considered when modelling martensitic transformations are not quasiconvex. This is a consequence of the crystallographic symmetry of the material and it is an essential aspect of the model, leading to the formation of microstructure.

To overcome this difficulty, one examines a *generalized minimization problem* which does admit minimizers and views these as *generalized minimizers* of the original non-quasiconvex problem. There are two ways of generalizing the problem and we shall introduce these here.

Relaxation methods

Definition 2.1.2. *Let $\varphi : M^{d\times d} \to \mathbb{R}$ be an arbitrary function. The quasiconvexification of φ, denoted by φ^{qc}, is defined by*

$$\varphi^{qc} = \sup\left\{\psi : \psi : M^{d\times d} \to \mathbb{R} \text{ quasiconvex and } \psi \leq \varphi\right\}. \tag{2.1.7}$$

Alternatively, φ^{qc} is referred to as the quasiconvex envelope or quasiconvex hull of φ.

Note that as long as φ is bounded below by a quasiconvex function, φ^{qc} is itself quasiconvex; otherwise, $\varphi^{qc} \equiv -\infty$.

Then the relaxation method relies on replacing the non-quasiconvex integrand φ with its quasiconvexification φ^{qc}. Note that if φ satisfies a coercivity and growth condition, so does φ^{qc} and it is quasiconvex. This is trivial as $\varphi^{qc} \leq \varphi$ and the function $-c_1 + c_2|F|^p$ is quasiconvex. Then, via an application of the direct method, the minimization problem

$$I^{qc}(y) = \int_\Omega \varphi^{qc}(Dy(x))\, dx$$

admits a minimizer.

We note that there is an alternative characterization of φ^{qc} which is due to Dacorogna [45]. In particular, for φ Borel measurable and locally bounded,

$$\varphi^{qc}(F) = \inf_{y\in W_0^{1,p}\left(E,\mathbb{R}^d\right)} \left\{ \frac{1}{\mathcal{L}^d(E)} \int_E \varphi(F + Dy(x))\, dx \right\}$$

where $E \subset \mathbb{R}^d$ is bounded and open. As expected, the above infimum does not depend on the choice of the set E and it is identically equal to $-\infty$ unless φ is bounded below by a quasiconvex function.

For the purposes of the following relaxation theorem, a proof of which can be found in [46], consider the variational problems:

$$\inf\left\{ I = \int_\Omega \varphi(Dy(x))\, dx :\ y \in \mathcal{A} \right\} \qquad (P)$$
$$\inf\left\{ I^{qc} = \int_\Omega \varphi^{qc}(Dy(x))\, dx :\ y \in \mathcal{A} \right\} \qquad (P^{qc})$$

Theorem 2.1.3. *Let a Borel measurable function $\varphi : M^{d\times d} \to \mathbb{R}$ satisfy the coercivity and growth condition*

$$-c_1 + c_2|F|^p \leq \varphi(F) \leq c_1(1 + |F|^p)$$

for all $F \in M^{d\times d}$, *some* $c_1,\ c_2 > 0$ *and* $p > 1$. *Then,*

$$\min\left(P^{qc}\right) = \inf\left(P\right).$$

Furthermore, if y *is a minimizer of* (P^{qc}), *there exists a minimizing sequence* y^k *for* (P) *such that* $y^k \rightharpoonup y$ *in* $W^{1,p}$ *and* $I\left(y^k\right) \to I^{qc}\left(y\right)$ *as* $k \to \infty$. *Conversely, let* y^k *be a minimizing sequence for* (P). *Then* y^k *is also minimizing for* (P^{qc}) *and (up to a subsequence)* y^k *converges weakly to a minimizer* y *of* (P^{qc}).

Remark. In physical terms, relaxation corresponds to the passage from a micro- to a macro-energy and, respectively, solutions to the relaxed problem correspond to macroscopic minimizers.

Young measures

We now introduce an alternative way of dealing with non-quasiconvex variational problems via the use of *Young measures*. In this case, we do not alter the integrand but, rather, we enlarge the space of admissible maps to one of admissible measures in which the problem admits solutions.

Young measures, introduced by L.C. Young [144], are families of probability measures, $\nu = (\nu_x)_x$, parametrized by x, carrying the minimal information about a sequence $\left\{z^k\right\}$ that is necessary (under suitable hypotheses) to compute precisely the weak limit of $\psi\left(z^k\right)$ for all continuous functions ψ. To be more specific, we recall the Fundamental Theorem on Young measures along with necessary notation.

Definition 2.1.3. *Let* $C_0\left(\mathbb{R}^N\right)$ *be the closure under the supremum norm of compactly supported, continuous functions on* $\mathbb{R}^N$. *By* $\mathcal{M}\left(\mathbb{R}^N\right)$ *we denote the dual space of* $C_0\left(\mathbb{R}^N\right)$ *consisting of signed Radon measures with finite mass equipped with the dual norm of total variation.*

A map $\mu : \Omega \to \mathcal{M}\left(\mathbb{R}^N\right)$ *is called weak* measurable if the functions* $x \mapsto \langle \mu\left(x\right), \psi\rangle$ *are measurable for all* $\psi \in C_0\left(\mathbb{R}^N\right)$ *where* $\langle \mu\left(x\right), \psi\rangle = \int_{\mathbb{R}^N} \psi \, d\mu\left(x\right)$.

Henceforth, we denote the space of essentially bounded weak measurable functions from* Ω *to* $\mathcal{M}\left(\mathbb{R}^N\right)$ *by* $L^\infty_{w^*}\left(\Omega, \mathcal{M}\left(\mathbb{R}^N\right)\right)$; *we note that since* $C_0\left(\mathbb{R}^N\right)$ *is separable,* $L^\infty_{w^*}\left(\Omega, \mathcal{M}\left(\mathbb{R}^N\right)\right) = L^1\left(\Omega, C_0\left(\mathbb{R}^N\right)\right)^*$ *and it becomes a Banach space when equipped with the norm*

$$\|\mu\| = \operatorname*{ess\,sup}_{x\in\Omega} \|\mu_x\|_{\mathcal{M}(\mathbb{R}^N)}.$$

Remark. If $\xi \in L^1(\Omega)$ and $f \in C_0\left(\mathbb{R}^N\right)$ the tensor product $\xi \otimes f$ denotes the element of $L^1\left(\Omega, C_0\left(\mathbb{R}^N\right)\right)$ given by $x \mapsto \xi(x) f$. We note that the span of such tensor products is dense in $L^1\left(\Omega, C_0\left(\mathbb{R}^N\right)\right)$. Then, a sequence $\nu^k \in L^\infty_{w^*}\left(\Omega, \mathcal{M}\left(\mathbb{R}^N\right)\right)$ converges weakly$*$ to ν in $L^\infty_{w^*}\left(\Omega, \mathcal{M}\left(\mathbb{R}^N\right)\right)$ if

$$\int_\Omega \xi(x) \langle \nu^k, f \rangle \, dx \to \int_\Omega \xi(x) \langle \nu, f \rangle \, dx$$

for all $\xi \in L^1(\Omega)$, $f \in C_0\left(\mathbb{R}^N\right)$. We shall refer to this type of convergence as weak$*$ convergence of Young measures.

Theorem 2.1.4. *(Fundamental theorem on Young measures) Let $\Omega \subset \mathbb{R}^d$ be a measurable set of finite measure and let $z^k : \Omega \to \mathbb{R}^N$ be a sequence of measurable functions such that*

$$\sup_k \int_\Omega a\left(|z^k(x)|\right) dx < \infty \tag{2.1.8}$$

where $a : [0,\infty) \to [0,\infty)$ is some continuous, nondecreasing function such that $a(t) \to \infty$ as $t \to \infty$. Then there exists a subsequence, not relabeled, and a weak$*$ measurable map $\nu \in L^\infty_{w^*}\left(\Omega, \mathcal{M}\left(\mathbb{R}^N\right)\right)$ such that the following hold:

(i) $\nu_x \geq 0$ and $\|\nu_x\|_{\mathcal{M}(\mathbb{R}^N)} = \int_{\mathbb{R}^N} d\nu_x = 1$ for a.e. $x \in \Omega$.

(ii) if $E \subset \Omega$ is measurable, $\psi \in C\left(\mathbb{R}^N\right)$ and $\psi\left(z^k\right)$ is relatively weakly compact in $L^1(E)$ then

$$\psi\left(z^k\right) \rightharpoonup \bar{\psi} = \langle \nu_x, \psi \rangle \text{ in } L^1(E). \tag{2.1.9}$$

(iii) Let $K \subset \mathbb{R}^N$ be compact. Then

$$\operatorname{supp} \nu_x \subset K \text{ a.e.} \Leftrightarrow \operatorname{dist}\left(z^k(x), K\right) \to 0 \text{ in measure}^1. \tag{2.1.10}$$

The family of probability measures $(\nu_x)_{x\in\Omega}$ is called the Young measure associated to (a subsequence of) z^k and we say that (up to a subsequence) z^k generates $(\nu_x)_{x\in\Omega}$.

There are more general statements of the above theorem where Young measures can be generated under weaker assumptions and the reader is referred to [9] for such a version of the above theorem.

We should mention that if a sequence z^k is equi-integrable, then (2.1.8) is satisfied. Also, taking $a(t) = t^p$, one can easily see that any uniformly bounded sequence in L^p has (up to a subsequence) an associated Young measure.

[1] Convergence in measure means that $\forall\, \epsilon > 0$, $\mathcal{L}^d\left(\left\{x \in \Omega : \operatorname{dist}\left(z^k(x), K\right) \geq \epsilon\right\}\right) \to 0$ as $k \to \infty$.

An important observation which will be of great use to us is that whenever the functions z^k are uniformly bounded in $L^\infty\left(\Omega,\mathbb{R}^N\right)$, then $f\left(z^k\right)$ is uniformly bounded in $L^\infty(\Omega)$ for any continuous $f:\mathbb{R}^N\to\mathbb{R}$. In this case, there exists a subsequence and an associated Young measure ν_x such that

$$f\left(z^k\right)\overset{*}{\rightharpoonup}\langle\nu_x,f\rangle\quad\text{in } L^\infty(\Omega).$$

This is in fact the form of the theorem given by Tartar in [138].

Moreover, it is clear that whenever z^k generates a Young measure $(\nu_x)_{x\in\Omega}$ and $z^k\rightharpoonup z$ in L^p then z is the centre of mass of the corresponding Young measure; i.e. $z(x)=\langle\nu_x,\mathrm{id}\rangle$ a.e. where $\mathrm{id}:\mathbb{R}^N\to\mathbb{R}^N$ is the identity map.

Alternatively, one can give a probabilistic interpretation to Young measures [9]. In particular, let $B(x,r)\subset\Omega$ be the ball centred at x of radius r. Define a probability distribution $\nu^k_{x,r}$ by picking points $y\in B(x,r)$ uniformly at random and observe the values of $z^k(y)$ (subsequence not relabeled). For a measurable set $E\subset\mathbb{R}^N$ we obtain

$$\nu^k_{x,r}(E)=\frac{\mathcal{L}^d\left(\left\{y\in B(x,r):z^k(y)\in E\right\}\right)}{\mathcal{L}^n(B(x,r))}.$$

Then

$$\nu_x=\lim_{r\to0}\lim_{k\to\infty}\nu^k_{x,r},\tag{2.1.11}$$

the limits being weak$*$ limits of measures.

Reflecting this probabilistic interpretation, if a sequence of measurable functions $z^k:\Omega\to\mathbb{R}^N$ generates the Young measure $\nu=(\nu_x)_{x\in\Omega}$, then $z^k\to z$ in measure if and only if $\nu_x=\delta_{z(x)}$ a.e. in Ω. In particular, if $z^k\in L^p\left(\Omega,\mathbb{R}^N\right)$, $p<\infty$, $\left\{|z^k|^p\right\}$ is weakly convergent in $L^1(\Omega,\mathbb{R}^N)$ and z^k generates a Young measure $\nu=(\nu_x)_{x\in\Omega}$ such that $\nu_x=\delta_{z(x)}$ for a.e. $x\in\Omega$, then $z^k\to z$ strongly in $L^p\left(\Omega,\mathbb{R}^N\right)$.

A special class of Young measures which will be of great importance to us is that of $W^{1,p}$ *gradient Young measures* which we define next; henceforth, we identify $\mathbb{R}^N$ with the space $M^{d\times d}$ of $d\times d$ matrices with real entries.

Definition 2.1.4. *Let $\Omega\subset\mathbb{R}^d$ be a bounded domain. A weakly$*$ measurable map $\nu:\Omega\to\mathcal{M}\left(M^{d\times d}\right)$ is a $W^{1,p}$ gradient Young measure if there exists a sequence of maps $y^k:\Omega\to\mathbb{R}^d$ such that*

$$\begin{aligned}y^k\rightharpoonup y\quad &in\quad W^{1,p}\left(\Omega,\mathbb{R}^d\right)\quad\left(\overset{*}{\rightharpoonup}\ if\ p=\infty\right)\\ \delta_{Dy^k(\cdot)}\overset{*}{\rightharpoonup}\nu\quad &in\quad L^\infty_{w^*}\left(\Omega,\mathcal{M}\left(M^{d\times d}\right)\right).\end{aligned}$$

In this case, we will often say that ν is generated by the sequence y^k rather than the gradients Dy^k.

The following theorem due to Kinderlehrer and Pedregal [86, 87] provides a full characterization of $W^{1,p}$ gradient Young measures.

Theorem 2.1.5. *Let $\Omega \subset \mathbb{R}^d$ be a bounded domain. A family $(\nu_x)_{x\in\Omega}$ of probability measures on $M^{d\times d}$, depending measurably on x, is a $W^{1,p}$ gradient Young measure if and only if*

(i) $\int_\Omega \int_{M^{d\times d}} |A|^p \, d\nu_x(A)\, dx < \infty$ *for* $1 \le p < \infty$ *or* $\operatorname{supp} \nu_x \subset K$ *a.e. for some compact set* K *when* $p = \infty$.

(ii) $\bar{\nu}_x = \langle \nu_x, \mathrm{id}\rangle = Dy(x)$ *a.e. for some* $y \in W^{1,p}$ *referred to as the underlying map of* ν.

(iii) (Jensen's inequality) $\langle \nu_x, \psi\rangle = \int_{M^{d\times d}} \psi(A)\, d\nu_x(A) \ge \psi(\bar{\nu}_x)$ *a.e. for all quasiconvex* ψ *satisfying* $|\psi(A)| \le c(1 + |A|^p)$ *if* $1 \le p < \infty$*; for* $p = \infty$ *no growth condition is required.*

In particular, we note the *minors relations:*

$$\langle \nu_x, \mathrm{adj}_s\rangle = \mathrm{adj}_s(\bar{\nu_x}) \tag{2.1.12}$$

for all subdeterminants adj_s of order $s \le p$. The justification for the minors relations is provided later in our discussion on conditions of generalized convexity.

A gradient Young measure is called *homogeneous* if the map $\nu : \Omega \to \mathcal{M}\left(M^{d\times d}\right)$ is constant a.e., i.e. if there is no x-dependence. Kinderlehrer and Pedregal [86, 87] showed that if $(\nu_x)_{x\in\Omega}$ is a $W^{1,p}$ gradient Young measure, then for a.e. $\alpha \in \Omega$, the probability measure $\nu = \nu_\alpha$ is a homogeneous $W^{1,p}$ gradient Young measure. This is referred to as the *localization* principle. Moreover, they showed that whenever $\nu = (\nu_x)_{x\in\Omega}$ is a $W^{1,p}$ gradient Young measure with underlying map $y(x) = Fx$ on $\partial\Omega$, $F \in M^{d\times d}$, then the measure $\operatorname{Av}\nu$ defined for all $\psi \in C_0\left(M^{d\times d}\right)$ by

$$\langle \operatorname{Av}\nu, \psi\rangle = \frac{1}{\mathcal{L}^d(\Omega)} \int_\Omega \langle \nu_x, \psi\rangle \, dx$$

is a homogeneous $W^{1,p}$ gradient Young measure with $\overline{\operatorname{Av}\nu} = F$. In particular, if ν is a $W^{1,\infty}$ gradient Young measure, so that its support is compact, this holds for all continuous ψ. This is called the *averaging* of Young measures.

Ending our discussion on Young measures, we give a technical result due to Zhang [146] known as *Zhang's Lemma*. This says that if a sequence Dy^k is bounded in L^p, $p > 1$, and generates a Young measure $(\nu_x)_{x\in\Omega}$ with $\operatorname{supp}\nu_x \subset K$ a.e. where $K \subset M^{d\times d}$ is compact, then there exists a sequence z^k with Dz^k bounded in L^∞

which generates the same Young measure $(\nu_x)_{x\in\Omega}$. In other words, a $W^{1,p}$ gradient Young measure with compact support is a $W^{1,\infty}$ gradient Young measure. This will be particularly useful to us as, in the context of martensitic transformations, we will be concerned with gradient Young measures with compact support. Hence, using Zhang's Lemma, we may speak of $W^{1,\infty}$ gradient Young measures and restrict attention to underlying deformations in $W^{1,\infty}\left(\Omega,\mathbb{R}^d\right)$.

The remaining ingredient is to show how these Young measures can be used to tackle our minimization problem when the integrand φ fails to be quasiconvex. When discussing the relaxation method, we introduced the original and relaxed problems in the following form:

$$\inf\left\{I=\int_\Omega \varphi\left(Dy\left(x\right)\right)dx:\ y\in\mathcal{A}\right\} \qquad (P)$$
$$\inf\left\{I^{qc}=\int_\Omega \varphi^{qc}\left(Dy\left(x\right)\right)dx:\ y\in\mathcal{A}\right\} \qquad \left(P^{qc}\right).$$

Next, let

$$\inf\left\{I^{YM}=\int_\Omega \langle\nu_x,\varphi\rangle\ dx:\nu \text{ admissible}\right\} \qquad \left(P^{YM}\right)$$

where ν being admissible means that $\nu=(\nu_x)_{x\in\Omega}$ is a $W^{1,p}$ gradient Young measure subject to the compatibility condition that there exists $y\in\mathcal{A}$ such that

$$\bar{\nu}_x=\langle\nu_x,\mathrm{id}\rangle=Dy\left(x\right)\ \text{ a.e. in }\Omega.$$

Theorem 2.1.6. *Let $\varphi:M^{d\times d}\to\mathbb{R}$ satisfy*

$$-c_1+c_2|F|^p\leq\varphi\left(F\right)\leq c_1\left(1+|F|^p\right)$$

for all $F\in M^{3\times3}$, some $c_1,\ c_2>0$ and $p>1$. Then,

$$\min\left(P^{qc}\right)=\min\left(P^{YM}\right).$$

Furthermore, if $(\nu_x)_{x\in\Omega}$ is a minimizer of $\left(P^{YM}\right)$ then the map $y\in\mathcal{A}$ such that $Dy\left(x\right)=\bar{\nu}_x$ a.e. is a minimizer of $\left(P^{qc}\right)$ and

$$\varphi^{qc}\left(Dy\left(x\right)\right)=\langle\nu_x,\varphi\rangle\ \text{ a.e. in }\Omega.$$

Conversely, let y be a minimizer for $\left(P^{qc}\right)$ and $(\nu_x)_{x\in\Omega}$ be an admissible Young measure such that $\bar{\nu}_x=Dy\left(x\right)$ and $\varphi^{qc}\left(Dy\left(x\right)\right)=\langle\nu_x,\varphi\rangle$ a.e. in Ω. Then, $\nu=(\nu_x)_x$ is a minimizer of $\left(P^{YM}\right)$ and

$$\operatorname{supp}\nu_x\subset\left\{F\in M^{d\times d}:\ \varphi\left(F\right)=\varphi^{qc}\left(F\right)\right\}.$$

A proof of Theorem 2.1.6 can be found in [112]. We note that combining with Theorem 2.1.3, we deduce that if y^k is a minimizing sequence for the constrained problem (P), then (up to a subsequence) Dy^k generates a gradient Young measure minimizing $\left(P^{YM}\right)$.

Remark. The above relaxation results are utilized in this thesis to establish the existence of macroscopic minimizers in a variational model of martensitic transformations. This model is based on nonlinear elasticity and therefore one must require that $\varphi(F) \to \infty$ as $\det F \to 0^+$ in order to avoid interpenetration of matter; similarly, one also needs that $\varphi(F) \to \infty$ for matrices F such that $\det F < 0$. However, these physical conditions are clearly violated with the growth condition assumed above, i.e. $\varphi(F) \leq c_1\left(1 + |F|^p\right)$.

The reader will also notice that we did not assign the notion of quasiconvexity to infinite-valued functions (we will use such a notion in Chapter 4). There have been such definitions in the literature, e.g. Ball and Murat [23], Dacorogna and Fusco [47], which have been shown to be necessary for weak lower semicontinuity. However, proving sufficiency is a difficult problem which has not been resolved. Since quasiconvexity in the direct method is used as an equivalent to weak lower semicontinuity, the existence of minimizers under the assumptions of elasticity theory is not clear.

In his celebrated paper [7], Ball proposed a stronger convexity condition, *polyconvexity*, that allows for infinite-valued functions and he was able to obtain existence results under the constraint $\varphi(F) \to \infty$ as $\det F \to 0^+$. The reader is referred to Ball and James [19] for a treatment of these physical constraints in the context of martensitic transformations.

Generalized notions of convexity

The notion of quasiconvexity may be the correct condition to ensure the existence of minimizers but it is not at all trivial to verify the quasiconvexity condition for a given function. Indeed, in the case of smooth real-valued functions on $N \times d$ matrices $(N \geq 3, d \geq 2)$, Kristensen [91] showed that there is no local condition equivalent to quasiconvexity. Because of the intractability of quasiconvexity, other convexity conditions have been explored and already we have mentioned that of polyconvexity. Next, we aim to introduce these conditions and remark on their relation.

Definition 2.1.5. *Let $\varphi : M^{d\times d} \to \mathbb{R} \cup \{+\infty\}$. Then φ is rank-one convex if*

$$\varphi\left(\lambda A + (1-\lambda) B\right) \leq \lambda\, \varphi\left(A\right) + (1-\lambda)\, \varphi\left(B\right) \tag{2.1.13}$$

for all $A, B \in M^{d\times d}$ such that $\operatorname{rank}\left(A - B\right) = 1$ *and all $\lambda \in (0,1)$.*

Remark. We note that when $\varphi \in C^2\left(M^{d\times d}\right)$, rank-one convexity is equivalent to

$$D^2\varphi\left(F\right)\left(a \otimes m, a \otimes m\right) \geq 0$$

for all $F \in M^{d\times d}$ and $a, m \in \mathbb{R}^n$; this is the *Legendre-Hadamard condition* which appears often in variational problems as the condition ensuring the ellipticity of the Euler-Lagrange equations (if slightly strengthened).

Theorem 2.1.7. *Let $\varphi : M^{d\times d} \to \mathbb{R}$ be quasiconvex. Then φ is rank-one convex.*

A proof of the above theorem can be found in [105]. It is worth noting that even when φ is infinite-valued, rank-one convexity remains a necessary condition for the weak lower semicontinuity of the functional I. Also, note that since rank-one convex functions are continuous, Theorem 2.1.7 implies that every finite-valued quasiconvex function is continuous as well; thus the requirement that φ be continuous in Theorem 2.1.2 is redundant.

At this point, we motivate the importance of rank-one differences with a simple result known as the *Hadamard jump condition*. We note this as it will be crucial for the description of microstructure in the following section.

Lemma 2.1.8. *Let $m \in \mathbb{R}^d$ be a unit vector and A, $B \in M^{d\times d}$, $A \neq B$. Suppose that a map $y : \mathbb{R}^d \to \mathbb{R}^d$ is as in Fig. 2.1, i.e.*

$$Dy = \begin{cases} A, & x \cdot m > k \\ B, & x \cdot m < k. \end{cases}$$

Then $y \in W^{1,\infty}\left(\mathbb{R}^d, \mathbb{R}^d\right)$ if and only if

$$A - B = a \otimes m$$

for some non-zero $a \in \mathbb{R}^d$; i.e. if and only if the matrices A and B are non-trivially rank-one connected.

Through rank-one convexity we are able to get a necessary condition for a given function φ to be quasiconvex. In the scalar case, rank-one convexity and quasiconvexity are in fact equivalent. Although a series of results exist linking the two notions,

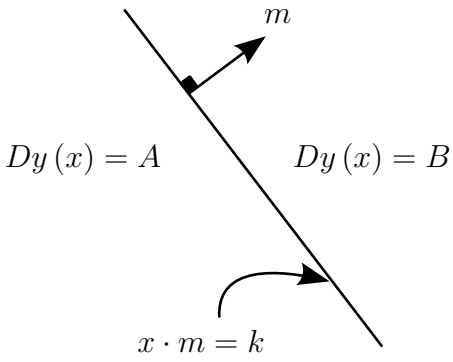

Figure 2.1: A gradient taking the values A and B on either side of the planar interface $x \cdot m = k$.

Šverák in [134], constructed an ingenious counterexample showing that for functions $\varphi : M^{N\times d} \to \mathbb{R}$ with $d \geq 2$ and $N \geq 3$ the reverse implication does not hold in general. Yet, it remains an open problem to verify whether quasiconvexity is implied by rank-one convexity in the case $d \geq N = 2$. In this thesis, we will be interested in the case $d = N = 3$ and hence rank-one convexity cannot serve as a sufficient condition for quasiconvexity.

As mentioned earlier, Ball [7] introduced a different notion that he called *polyconvexity*. For the purposes of the next definition let $\sigma(s) = \binom{d}{s}^2$ and $\tau(d) = \sum_{s=1}^{d} \sigma(s)$.

Definition 2.1.6. *A function $\varphi : M^{d\times d} \to \mathbb{R} \cup \{+\infty\}$ is called polyconvex if there exists a convex function $g : \mathbb{R}^{\tau(d)} \to \mathbb{R} \cup \{+\infty\}$ such that*

$$\varphi(F) = g(T(F)) \tag{2.1.14}$$

where $T(F) = \left(F, \operatorname{adj}_2(F), \ldots, \operatorname{adj}_{d-1}(F), \det F\right)$ and adj_s stands for the matrix of all $s \times s$ subdeterminants of F.

Hence, for $d = 3$, φ is polyconvex if

$$\varphi(F) = g(F, \operatorname{cof} F, \det F). \tag{2.1.15}$$

Polyconvexity and quasiconvexity can be linked in the following way:

Theorem 2.1.9. *Let $\varphi : M^{d\times d} \to \mathbb{R}$ be polyconvex and $p \geq d$. Then φ is $W^{1,p}$ quasiconvex; in particular, φ is ($W^{1,\infty}$) quasiconvex for any d.*

We should point out that the convex function g in the definition of polyconvexity need not be unique. Moreover, the reverse implication of Theorem 2.1.9 does not hold in general and the reader is referred to Šverák [133], among others, for examples of

quasiconvex functions that are not polyconvex. As remarked already, Ball in [7] used the notion of polyconvexity to prove that integral functionals involving polyconvex integrands are weakly lower semicontinuous and proved existence results under the constraints of nonlinear elasticity.

Another class of functions is that of quasiaffine maps which we introduce next. We note that these are very important as they enjoy remarkable weak continuity properties.

Definition 2.1.7. *A function $\varphi : M^{d\times d} \to \mathbb{R}$ is called quasiaffine if φ as well as $-\varphi$ are quasiconvex.*

This is an analogue of affine functions with respect to convex ones and it practically means that inequalities are replaced by equalities in the definition of quasiconvexity. Similarly, one can define polyaffine and rank-one affine functions in the obvious way. Nevertheless, Ball [7] asserts that they are equivalent. With the definition at hand, one can prove the following result which can be found in [7].

Theorem 2.1.10. *Let $\varphi : M^{d\times d} \to \mathbb{R}$. The following are equivalent:*

(i) φ *quasiaffine.*

(ii) φ *is a null Lagrangian, i.e. the Euler-Lagrange equations* $\mathrm{Div} D_F\varphi(Dy) = 0$ *are satisfied for all smooth functions* $y : \mathbb{R}^d \to \mathbb{R}^d$.

(iii) $\varphi(F) = c + \sum_{s=1}^{\tau(d)} c_s \mathrm{adj}_s(F)$ *where* $c =$*constant and* $c_s \in \mathbb{R}^{\sigma(s)}$.

(iv) $y \mapsto \varphi(Dy)$ *is weakly continuous (weakly* if* $p = \infty$*) as a mapping from* $W^{1,p} \to L^1$ *for* p *large enough* ($p \geq d$ *suffices).*

When discussing $W^{1,p}$ gradient Young measures, we noted the minors relations:

$$\langle \nu_x, \mathrm{adj}_s \rangle = \mathrm{adj}_s(\bar{\nu}_x) \tag{2.1.16}$$

for all subdeterminants adj_s of order $s \leq p$. This should now be clear, as Jensen's inequality holds for $\pm\mathrm{adj}_s$.

Moreover, note that for $d = 3$ the only quasiaffine functions are of the form

$$\varphi(F) = b + C \cdot F + D \cdot \mathrm{cof} F + e \det F$$

where b, $e \in \mathbb{R}$ and C, $D \in M^{3\times 3}$. To sum up, for finite-valued functions, we have the following implications:

$$\varphi \text{ convex} \Rightarrow \varphi \text{ polyconvex} \Rightarrow \varphi \text{ quasiconvex} \Rightarrow \varphi \text{ rank-one convex} \tag{2.1.17}$$

whereas, and in particular in the case $d = 3$, the reverse implications are all false.

Generalized convexity conditions for sets

We next discuss the above generalized convexity conditions for sets. These are extremely useful for the study of microstructure in shape-memory alloys as they enable us to identify the set of all recoverable strains, i.e. all the deformations that the alloy can recover upon heating.

Before discussing these conditions formally, we note that different authors follow different approaches and the definitions given here may not entirely agree with certain expositions, e.g. Dacorogna [46], Zhang [148]. However, we briefly comment on some of these differences.

Definition 2.1.8. *Let $E \subset M^{d\times d}$. We say that E is quasiconvex if there exists a non-negative, quasiconvex function $\psi : M^{d\times d} \to \mathbb{R}$ such that*

$$E = \left\{\psi^{-1}(0)\right\} = \left\{F \in M^{d\times d} : \psi(F) = 0\right\}. \tag{2.1.18}$$

Similarly, we can define polyconvexity and rank-one convexity of sets where we stress the fact that the function ψ is required to be finite-valued. In particular, since ψ is continuous, polyconvex, quasiconvex and rank-one convex sets are then closed by definition. This is a major difference between other expositions where these sets may be open; for instance, polyconvexity and rank-one convexity may be naturally defined - and indeed they are in some contexts - by requiring that the indicator function of the set is respectively polyconvex or rank-one convex. However, a different definition would then be required for quasiconvexity as the respective notion for infinite-valued functions has not been defined. For our purposes, it seems more convenient to use Definition 2.1.8 which is uniform for all notions and, without perplexing definitions or notation, provides all the desired definitions for the respective semiconvex hulls which we present next.

Definition 2.1.9. *Let $K \subset M^{d\times d}$. The quasiconvex hull of K, denoted by K^{qc}, is defined by*

$$K^{qc} = \bigcap \{E \supseteq K : E \text{ quasiconvex}\}. \tag{2.1.19}$$

Clearly, if K is quasiconvex then $K = K^{qc}$. Similarly, one can define the convex, polyconvex and rank-one convex hull of a set K denoted by K^c, K^{pc} and K^{rc} respectively.

Remark. As we shall see, in the case where $K = \bigcup_{i=1}^{N} SO(3)U_i$, the quasiconvex hull is precisely the set corresponding to the deformation gradients of all linear transformations that the alloy can recover.

Equivalently, we have the following characterization: let $K \subset M^{d\times d}$. The quasiconvex hull of K is given by

$$K^{qc} = \left\{F \in M^{d\times d} : \psi(F) \leq 0, \forall\, \psi : M^{d\times d} \to \mathbb{R} \text{ quasiconvex}, \psi|_K \leq 0\right\}, \quad (2.1.20)$$

where substituting quasiconvex for convex, polyconvex or rank-one convex we obtain a characterization for the respective hulls. To see the equivalence with Definition 2.1.9, let $\tilde{K}^{qc}$ be as in the right hand side of (2.1.20). Suppose that $F \in \tilde{K}^{qc} \setminus K^{qc}$; by definition, there exists a quasiconvex set $E \supseteq K$ such that $F \notin E$. But $E = \psi^{-1}(\{0\})$ for some finite-valued, non-negative quasiconvex ψ and hence $\psi(F) > 0$. But $K \subset E$ so that $\psi|_K \leq 0$ contradicting $F \in \tilde{K}^{qc}$. Conversely, suppose that $F \in K^{qc} \setminus \tilde{K}^{qc}$; then $\psi(F) > 0$ for some finite quasiconvex function with $\psi|_K \leq 0$; let $g = \max\{\psi, 0\}$. This is a (finite) non-negative quasiconvex function which vanishes on K, i.e. $g^{-1}(\{0\})$ defines a quasiconvex set such that $g^{-1}(\{0\}) \supseteq K$ and thus $g^{-1}(\{0\}) \supseteq K^{qc}$; but $F \notin g^{-1}(\{0\})$ contradicts $F \in K^{qc}$.

In the context of martensitic transformations, we will be interested in compact sets K and, in this case,

$$K^{qc} = \left\{F \in M^{d\times d} : \psi(F) \leq \max_K \psi, \forall\, \psi : M^{d\times d} \to \mathbb{R} \text{ quasiconvex}\right\}. \quad (2.1.21)$$

Needless to say that by replacing ψ quasiconvex by ψ convex, polyconvex, rank-one convex, one obtains the definitions of K^c, K^{pc} and K^{rc} respectively. That the set defined by (2.1.21) is contained in the set given in (2.1.20) is trivial and, as for the other direction, it suffices to consider the function $g = \max\{\psi - \max_K \psi, 0\}$. We note this characterization as it will be particularly useful.

As before, we remark that the above definitions always return a closed set. In fact, if one is interested in obtaining open hulls, one would be required to include infinite-valued functions in Definition 2.1.20, with a more elaborate definition required for quasiconvex hulls; of course, Definition 2.1.8 will no longer suffice (see [46] for details). For general sets K, including infinite-valued functions in (2.1.20) for the convex or polyconvex hull will simply return a set whose closure is K^c or K^{pc} respectively and, in particular, when K is compact including infinite-valued functions will make no difference in the case of convex or polyconvex hulls. On the other hand, rather interestingly, including infinite-valued rank-one convex functions in (2.1.20) delivers

another semiconvex hull which is called the lamination convex hull of K[2]. This will be very useful in practice and we give the definition next.

Definition 2.1.10. *A set $E \subset M^{d\times d}$ is called lamination convex if*

$$\lambda F + (1-\lambda)\, G \in E \quad \forall\, \lambda \in (0,1)$$

whenever F, $G \in E$ and rank $(F-G) = 1$. *The lamination convex hull of a compact set $K \subset M^{d\times d}$ is defined as the smallest lamination convex set containing K and is denoted by K^{lc}.*

Clearly $K^{lc} \subset K^{rc}$ and using the respective implications for functions (2.1.17) one can easily obtain the following inclusions:

$$K \subset K^{lc} \subset K^{rc} \subset K^{qc} \subset K^{pc} \subset K^{c}. \tag{2.1.22}$$

Just as in the case of the convex hull, there are alternative characterizations of the above semiconvex hulls which can prove to be much more useful in practice. We introduce these here without any proofs. These can be found in [105].

As before, let $K \subset M^{d\times d}$ be compact. The following characterizations are equivalent to (2.1.21):

- (gradient Young measures)

  $$K^{qc} = \left\{ \bar{\nu} : \nu \text{ homogeneous } W^{1,\infty} \text{ gradient Young measure with } \operatorname{supp}\nu \subset K \right\}.$$

  This is a direct consequence of the characterization of $W^{1,\infty}$ gradient Young measures given by Kinderlehrer and Pedregal in Theorem 2.1.5.

- (weak$*$ limits) There exists $y^k \in W^{1,\infty}\left(\Omega, \mathbb{R}^d\right)$ such that $\operatorname{dist}(Dy^k, K) \to 0$ in measure and $Dy^k \overset{*}{\rightharpoonup} Dy$ in L^∞ for some $y \in W^{1,\infty}\left(\Omega, \mathbb{R}^d\right)$ if and only if $Dy \in K^{qc}$ a.e.

- (linear boundary conditions)

  $$K^{qc} = \left\{ \begin{array}{c} F \in M^{d\times d} : \exists \text{ sequence } y^k \text{ bounded in } W^{1,\infty} \text{ such that} \\ y^k_{|\partial\Omega} = Fx \text{ and } \operatorname{dist}(Dy^k, K) \to 0 \text{ in measure} \end{array} \right\}.$$

As regards polyconvexity, and using the same notation as in Definition 2.1.6, we get the following equivalent characterizations:

[2]Some authors, e.g. Dacorogna [46], define this as the rank-one convex hull.

- By Carathéodory's Theorem [118] for convex sets it can be shown that (see [48])

$$K^{pc} = \left\{ F \in M^{d\times d} \,:\, T(F) = \sum_{i=1}^{\tau(d)+1} \lambda_i T(F_i)\,,\; F_i \in K,\; \lambda_i \geq 0,\; \sum_{i=1}^{\tau(d)+1} \lambda_i = 1 \right\}.$$

- K^{pc} can also be written as the projection on $d \times d$ - dimensional space of a convex set in dimension $\tau(d)$ (see [46]); that is

$$K^{pc} = \left\{ F \in M^{d\times d} \,:\, T(F) \in \tilde{K}^c \right\}$$

  where $\tilde{K} = \{T(F) \,:\, F \in K\}$.

- (probability measures) Theorem 2.1.5 showed that every homogeneous $W^{1,\infty}$ gradient Young measure satisfies Jensen's inequality for all quasiconvex functions. Let us write $\mathcal{M}^{qc}$, $\mathcal{M}^{pc}$ and $\mathcal{M}^{rc}$ for the set of homogeneous probability measures supported on K satisfying Jensen's inequality for quasiconvex, polyconvex and rank-one convex functions respectively. Rather trivially, from the implications on functions, $\mathcal{M}^{rc} \subset \mathcal{M}^{qc} \subset \mathcal{M}^{pc}$. One can show[3] that $\mathcal{M}^{pc}$ consists precisely of those measures satisfying the minors relations (2.1.16), i.e.

$$M(\bar{\nu}) = \langle \nu, M \rangle \text{ for all minors of order } s = 1, \ldots, d$$

  and then,

$$K^{pc} = \{\bar{\nu} \,:\, \nu \in \mathcal{M}^{pc}\}.$$

In a similar fashion, we can get a characterization of the rank-one convex hull in terms of probability measures; in particular,

$$K^{rc} = \{\bar{\nu} \,:\, \nu \in \mathcal{M}^{rc}\}.$$

All measures in $\mathcal{M}^{rc}$ are homogeneous gradient Young measures which are referred to as *laminates*.

Note: There are no explicit equivalent characterizations of polyconvex and rank-one convex hulls in terms of weak limits of sequences.

[3]Similarly to convex and affine functions, any (finite-valued) polyconvex function is given as the pointwise supremum of the quasiaffine maps that lie beneath it (see [7, 46]); then, taking the limit in the minors relation we obtain Jensen's inequality for polyconvex functions.

Finally, we introduce a characterization of the lamination convex hull which will prove to be very useful in the description of microstructure. Let

$$K^{(i+1)} = K^{(i)} \cup \left\{ \lambda F + (1-\lambda) G \,:\, F,\, G \in K^{(i)},\, \mathrm{rank}\,(F-G) = 1,\, \lambda \in [0,1] \right\}$$

and $K^{(1)} = K$. Then,

$$K^{lc} = \bigcup_{i=1}^{\infty} K^{(i)}. \tag{2.1.23}$$

In short, this says that we can reconstruct the lamination convex hull from the original set simply by inductively adding rank-one segments.

There is an extensive literature on such semiconvex hulls and the reader is referred to Zhang's extremely interesting work [147, 148, 149, 150], Dolzmann et al. [54] as well as Dacorogna [46] for further results. Before finishing our discussion on the calculus of variations, we note some examples of known semiconvex hulls that we will encounter later on. The known cases are relatively simple and, in general, calculating such hulls or extracting information about their structure is a rich and intricate problem which is far from trivial - this will concern us more in Chapter 3.

In the subsequent chapters, we will be interested in compact sets K that satisfy a determinant constraint and are $SO\,(d)$ invariant, i.e. K is of the form

$$K = \bigcup_{i=1}^{N} SO\,(d)\; U_i$$

where $\det U_i = \Delta$, a positive constant, and the wells $SO\,(d)\, U_i$ are (rank-one) compatible with each other; that is for all $i,\, j = 1, \ldots, N$ with $i \neq j$ there exists $R \in SO\,(d)$ such that

$$\mathrm{rank}\,(RU_i - U_j) = 1.$$

In this case some results are well established; however, the number of wells and the dimension play a crucial role. Moreover, relaxing the assumptions on rank-one compatibility or the determinant constraint can dramatically alter the results.

- *The one-well problem:* When $N = 1$ there can be no rank-one connections between a well and itself and it can be shown that the quasiconvex hull is trivial in this case, i.e. $K^{qc} = K$. Moreover, any gradient Young measure supported on one well must necessarily be homogeneous. For references see [10, 19, 85].

- *The two-well problem:* In two dimensions, it has been shown that all semiconvex hulls are trivial whenever the two wells are incompatible [135]. In fact, in

[30, 136] this is shown to hold for any number of wells. Then, as in the one-well problem, any gradient Young measure supported on two incompatible wells must be trivial (i.e. supported on only one of them) and homogeneous [100, 135].

When the two wells are compatible, i.e. rank-one connections exist between them, the situation alters entirely. If we do not set a determinant constraint but simply require that the determinants of the two wells are positive, the problem has been solved by Šverák in [136] who showed that $K^{pc} = K^{qc} = K^{rc} = K^{(3)}$. On the other hand, if we do assume that the wells have equal determinant, the quasiconvex hull is given by $K^{(2)}$; in fact, in this case, the result can be extended to an arbitrary number of wells which relies on the fact that necessarily the wells have to be compatible (see [30, 52] for proofs). We make use of this in Chapter 3.

In three dimensions, the quasiconvex hull has been computed by Ball and James [19] in the case of compatible wells with equal determinant, where they showed that $K^{qc} = K^{lc} = K^{(2)}$. If the two wells fail to have equal determinant there are no general results known to the author. On the other hand, if the two wells are incompatible there are many results which provide partial solutions, usually under strict assumptions. The reader is referred to Dolzmann, Kirchheim, Müller and Šverák in [55] for such results. In particular, they show that K^{rc} is always trivial - hence the same holds for K^{pc} and K^{qc} - if the wells satisfy certain involved conditions on their eigenvalues. However, there are examples where K^{pc} is not trivial, leaving K^{qc} open to investigation.

- *Three-wells or more:* In two dimensions we have already mentioned that a general characterization exists for the case of equal determinant and for any number of wells. In three dimensions, it is worth mentioning that in the special case of an arbitrary number of wells having an equal eigenvalue and corresponding eigenvector, the problem can be reduced to that in two dimensions to show that $K^{qc} = K^{lc} = K^{(2)}$; however, this is by no means a general result. For other cases, or more dimensions, hardly any concrete results exist. We note that Friesecke has a presented but unpublished formula for the polyconvex hull of three compatible wells [66] in three dimensions and it has been conjectured that $K^{pc} = K^{qc}$ - a conjecture which remains open. Moreover, there are interesting results of Dolzmann and Kirchheim [53] and, more recently, of Conti, Dolzmann and Kirchheim [41] showing e.g. that the problem of three compatible wells with equal determinant has a relative interior of full dimension. We do not elaborate further as we shall use their ideas in Chapter 3.

It is evident that the situation becomes dramatically complicated even for the three-well problem. In fact, for four wells or more, the problem becomes almost completely open in three dimensions. Even in the case of four incompatible wells (in fact even for four incompatible points) the quasiconvex hull can be non-trivial. The construction that exhibits this is commonly referred to as the T-4 configuration, or Tartar's square, and details can be found in [31] or [105]. We also note that throughout this discussion we have assumed that the wells have determinants of the same sign. If this is not the case, even for two incompatible wells in two dimensions the problem can be non-trivial. In [37] it is shown that indeed there can be non-trivial gradient Young measures supported on such wells. For a more detailed account of problems on semiconvex hulls, we refer the reader to [52, 105].

At this point, we put an end to our introductory discussion on the calculus of variations and embark on the description of the model for martensitic phase transformations where we see how the above ideas are implemented.

2.2 The Nonlinear Elasticity Model

Here we aim to provide a full description of the continuum theory as established by Ball and James [13, 18]. In doing so, we follow a rather standard presentation and start by introducing Bravais lattices and an atomistic description of the theory. We do that in three dimensions.

Bravais Lattices and Link to Continuum Theory

Definition 2.2.1. *A Bravais lattice* $\mathcal{L}(\mathbf{g}_i, \mathbf{o})$ *is a set of points in* $\mathbb{R}^3$ *such that there exist linearly independent vectors* $\{\mathbf{g}_1, \mathbf{g}_2, \mathbf{g}_3\} \in \mathbb{R}^3$ *with the property that*

$$\mathcal{L}(\mathbf{g}_i, \mathbf{o}) = \left\{\mathbf{x} \in \mathbb{R}^3 : \mathbf{x} = \nu^i \mathbf{g}_i + \mathbf{o},\ \textit{where}\ \nu^1, \nu^2, \nu^3 \in \mathbb{Z}\right\}, \tag{2.2.1}$$

where repeated indices denote summation.

In other words, a Bravais lattice is simply a set of points in the three-dimensional space obtained by the translation of a single point $\mathbf{o}$ through three linearly independent vectors $\{\mathbf{g}_1, \mathbf{g}_2, \mathbf{g}_3\}$. The three vectors, $\{\mathbf{g}_1, \mathbf{g}_2, \mathbf{g}_3\}$, define the unit cell for this lattice and are referred to as the *lattice vectors*. In three dimensions, there are precisely 14 Bravais lattices which are given in Fig. 2.2.

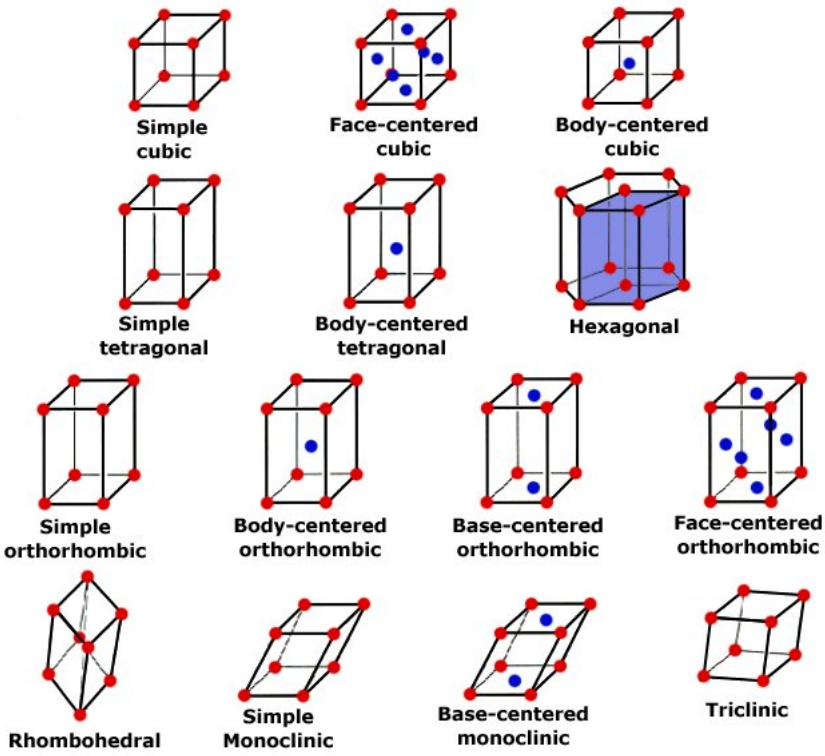

Figure 2.2: Unit cells for the 14 three-dimensional Bravais lattices.

At this point, we introduce some notation regarding lattices which will be of use for the remainder of this thesis. A *direction in a lattice*, denoted by $[uvw]$, is the direction given by the vector

$$\mathbf{d} = u\mathbf{g}_1 + v\mathbf{g}_2 + w\mathbf{g}_3.$$

Moreover, a class of crystallographically equivalent directions is denoted by $\langle uvw \rangle$ and it contains all the directions given by permutations of u, v, w including the replacement of each by its additive inverse. As an example, in a simple cubic lattice with lattice vectors parallel to the edges, the class $\langle 100 \rangle$ includes the directions $[100]$, $[\bar{1}00]$, $[010]$, $[0\bar{1}0]$, $[001]$ and $[00\bar{1}]$, where the overhead bar is used to denote the additive inverse.

It is also important to introduce *planes in a lattice*; this is done through the use of *reciprocal vectors* (see Ashcroft and Mermin [6] for details on reciprocal lattices). Assume that the unit cell of a lattice is given by the vectors $\{\mathbf{g}_1, \mathbf{g}_2, \mathbf{g}_3\}$. Then, the reciprocal vectors, $\{\mathbf{g}^1, \mathbf{g}^2, \mathbf{g}^3\}$, are such that

$$\mathbf{g}_i \cdot \mathbf{g}^j = \delta_{ij}, \quad i, j = 1, 2, 3,$$

where δ_{ij} denotes the Kronecker delta. Then, the (abc) plane is simply the plane with normal

$$\mathbf{n} = a\mathbf{g}^1 + b\mathbf{g}^2 + c\mathbf{g}^3$$

and a class of crystallographically equivalent planes is denoted by $\{abc\}$. For example, in a simple cubic lattice, $\{110\} = \{(110), (1\bar{1}0), (101), (\bar{1}01), (011), (0\bar{1}1)\}$. Notice that these exhaust all the possibilities, as multiplying a, b, c by a constant does not change the plane in any meaningful way.

Definition 2.2.2. *If the numbers u, v, w (or a, b, c) are all rational, then we say that the direction $[uvw]$ (or the plane (abc)) is a rational direction (rational plane).*

Once again we note that multiplication by a positive constant does not make a meaningful change either in a direction or a plane in the lattice, as it only changes the magnitude of the vectors $\mathbf{d}$ and $\mathbf{n}$ respectively. Therefore, in the above case, each of the rational numbers can be expressed as an integer simply by multiplying by the smallest common multiple of the denominators. This enables one to understand rational directions and rational planes, respectively, as those directions that pass through lattice points and as those planes on which a two-dimensional sub-lattice lies.

After this small elementary discussion on Bravais lattices, we proceed to discuss lattice deformations and their symmetries. This will enable us to describe the setting under which the continuum model is introduced.

A result in crystallography, [56], implies that a Bravais lattice cannot determine its lattice vectors uniquely:

Theorem 2.2.1. *Consider two Bravais lattices given by $\mathcal{L}(\mathbf{g}_i, \mathbf{o})$ and $\mathcal{L}(\bar{\mathbf{g}}_i, \mathbf{o})$. Then $\mathcal{L}(\mathbf{g}_i, \mathbf{o}) = \mathcal{L}(\bar{\mathbf{g}}_i, \mathbf{o})$ if and only if there exists a 3×3 matrix with integer entries, $\left(\mu_i^j\right)$, such that $\det\left(\mu_i^j\right) = \pm 1$ and*

$$\bar{\mathbf{g}}_i = \mu_i^j \mathbf{g}_j,$$

where again the summation convention is used.

Let

$$\mathcal{G} = \left\{\mu = \left(\mu_i^j\right) \in M^{3\times 3} : \mu_i^j \in \mathbb{Z},\ i, j = 1, 2, 3 \text{ and } \det \mu = \pm 1\right\}.$$

$\mathcal{G}$ forms a group referred to as the *invariance group* of the lattice and it consists of all those linear transformations which map a Bravais lattice into itself; in particular, $\mathcal{G}$ includes shears and rotations alike. However, large shears are associated with

plastic deformation and slip which are not elements associated with typical deformations of shape-memory alloys; additionally, the Cauchy-Born hypothesis, which will provide the link between the atomistic and the continuum model, is violated if dislocations and slips are allowed. Also, it was shown by Fonseca [60] that a variational model with $\mathcal{G}$ as a symmetry group will necessarily be extremely degenerate. Including such shears in the model would make the notion of a Bravais lattice inadequate to describe the crystal and, instead, a local theory of material symmetry is needed (e.g. Ericksen [57]). In this we only consider an appropriate neighbourhood of the lattice vectors, say $\{\mathbf{g}_i\}$, where appropriate means a neighbourhood large enough to include elastic deformations and the phase transitions relevant to martensitic transformations, whilst large shears inherent in the invariance group $\mathcal{G}$ are excluded. This neighbourhood will also serve as the domain of the free energy and, as such, it is essential that it is invariant under a group which acts as the invariance group of that free energy. Hence, before we proceed, we define the *point group* of a Bravais lattice $\mathcal{L}(\mathbf{g}_i)$ which serves as the invariance group mentioned above.

Definition 2.2.3. *The point group $\mathcal{P}(\mathbf{g}_i)$ of a Bravais lattice $\mathcal{L}(\mathbf{g}_i)$ is defined as the set*

$$\mathcal{P}(\mathbf{g}_i) := \left\{ Q \in O(3) : Q\mathbf{g}_i = \mu_i^j \mathbf{g}_j \; for \; some \; \mu \in \mathcal{G} \right\}, \tag{2.2.2}$$

where $O(3) = \left\{ R \in M^{3\times 3} : R^T R = RR^T = \mathbf{1}, \det R = \pm 1 \right\}$ is the orthogonal group.

It is easy to show that if $\mathcal{L}(\mathbf{g}_i) = \mathcal{L}(\bar{\mathbf{g}}_i)$ then also $\mathcal{P}(\mathbf{g}_i) = \mathcal{P}(\bar{\mathbf{g}}_i)$ and, hence, the point group of a lattice is associated with the lattice itself. For instance, in a cubic lattice with lattice vectors $\{\mathbf{g}_i\}$, $i = 1, 2, 3$, denote $\mathcal{P}(\mathbf{g}_i)$ by $\mathcal{P}^c$. Then, $\mathcal{P}^c$ consists precisely of the 48 orthogonal transformations that map a cube back to itself.

The existence of such a neighbourhood has been proven essentially by Ericksen [57, 58, 59] and Pitteri [114] but below, we present a version of this theorem due to Ball and James [19][4]. Prior to the statement of the theorem we introduce its notation. Given a set $\mathcal{N}$ of vector-triples, $Q\mathcal{N}$ denotes the set of all vector-triples of the form $\{Q\mathbf{f}_1, Q\mathbf{f}_2, Q\mathbf{f}_3\}$, $Q \in O(3)$, $\{\mathbf{f}_i\} \in \mathcal{N}$ and $\mu[\mathcal{N}]$ denotes the set of all vector-triples of the form $\mu_i^j \mathbf{f}_j$, $\mu \in \mathcal{G}$, $\{\mathbf{f}_j\} \in \mathcal{N}$.

Theorem 2.2.2. *Let $\mathcal{L}(\mathbf{g}_i)$ be a Bravais lattice. Then, there exists a bounded, open neighbourhood $\mathcal{N} \subset (\mathbb{R}^3)^3 = \mathbb{R}^3 \times \mathbb{R}^3 \times \mathbb{R}^3$ such that*

[4]The same idea was implicitly used by Parry [111] and another version of the theorem has also been proved by Fosdick and Hertog [65]

(i) $\{\mathbf{g}_i\} \in \mathcal{N}$;

(ii) $Q\mathcal{N} = \mathcal{N}\ \forall Q \in O(3)$, *i.e* $\mathcal{N}$ *is* $O(3)$ *invariant;*

(iii) $\forall \mu \in \mathcal{G}$, $\mu[\mathcal{N}] = \mathcal{N}$ *or* $\mu[\mathcal{N}] \cap \mathcal{N} = \emptyset$;

(iv) if $\mu \in \mathcal{G}$ *satisfies* $\mu[\mathcal{N}] = \mathcal{N}$, *then* $\mu_i^j \mathbf{g}_j = Q\mathbf{g}_i$ *for some* $Q \in \mathcal{P}(\mathbf{g}_i)$.

In addition, if $\{\mathbf{g}_i\}$ *is such that* $\mathcal{P}(\mathbf{g}_i) = \mathcal{P}^c$, *then any bounded open neighbourhood* $\mathcal{N}$ *satisfying (i), (ii) and (iii) has the property that*

$$\mu[\mathcal{N}] = \mathcal{N},\ \mu \in \mathcal{G} \quad \Longleftrightarrow \quad \mu_i^j \mathbf{g}_j = Q\mathbf{g}_i\ for some\ Q \in \mathcal{P}^c. \tag{2.2.3}$$

The neighbourhood, $\mathcal{N}$, is known as the Ericksen-Pitteri neighbourhood and the above result provides its existence. Nevertheless, it does not address whether we can find a connected neighbourhood with the desired properties. The latter has been addressed in detail by Pitteri and Zanzotto [115].

Due to the argument in Theorem 2.2.2, one is forced to restrict attention to those transformations where the symmetry of one phase is greater than that of the other. In addition, we need to choose the higher symmetry phase as the reference configuration and the point group of that phase as the set of symmetry operations. Otherwise said, the point group of the martensite, $\mathcal{P}^m$, must be a strict subset of the point group of the austenite, $\mathcal{P}^a$, i.e.

$$\mathcal{P}^m \subset \mathcal{P}^a.$$

Now assume that the austenite phase of a martensitic alloy has a Bravais lattice given by $\mathcal{L}(\mathbf{g}_i^p)$ with corresponding point group $\mathcal{P}^a$. Further, assume that there is a positive definite symmetric matrix U, depending on the lattice parameters, which represents the transformation of the lattice vectors $\{\mathbf{g}_i^p\}$, and hence of the lattice $\mathcal{L}(\mathbf{g}_i^p)$, to the martensite lattice $\mathcal{L}(U\mathbf{g}_i^p)$ with point group $\mathcal{P}^m$. Denote the Ericksen-Pitteri neighbourhood of the austenite lattice vectors $\{\mathbf{g}_i^p\}$ by $\mathcal{N}^p$ and assume that $\{U\mathbf{g}_i^p\} \in \mathcal{N}^p$. Ball and James [19], show that the point groups of the austenite and martensite phases must satisfy

$$\mathcal{P}^m = \left\{R \in \mathcal{P}^a : RUR^T = U\right\}. \tag{2.2.4}$$

The above condition characterizes the set of all positive definite, symmetric matrices that give rise to the change of symmetry from $\mathcal{P}^a$ to $\mathcal{P}^m$ in $\mathcal{N}^p$. $\mathcal{P}^m$ is clearly a subgroup of $\mathcal{P}^a$ (closed under matrix multiplication, contains multiplicative inverses and the identity matrix), containing precisely all the orthogonal transformations R

which map U into itself. Also, note that elements of $\mathcal{P}^a$ and $\mathcal{P}^m$ with determinant -1 are irrelevant for (2.2.4) as R appears twice. For this reason, we restrict attention to point groups containing rotations only; that is, only the *Laue groups* $\mathcal{P}^a \cap SO(3)$ and $\mathcal{P}^m \cap SO(3)$ are to be considered from now on. For simplicity these are not relabeled, i.e. $\mathcal{P}^{a/m} = \mathcal{P}^{a/m} \cap SO(3)$.

It is worth noting that there is a restriction set by the fact that the point group of the martensite must be a subgroup of the point group of the austenite. Namely, it discards transformations, such as the face-centered cubic to body-centered cubic, where this is not the case. However, such martensitic transformations are typically irreversible and beyond our scope.

A very important consequence of (2.2.4) is that, due to the different possible representations of the subgroup $\mathcal{P}^m$, it gives rise to multiple variants of martensite. To be more specific, consider $\bar{R} \in \mathcal{P}^a$ such that $\bar{R} \notin \mathcal{P}^m$. Then, from the definition of $\mathcal{P}^m$, it becomes clear that $\bar{R}U\bar{R}^T = V$ with $V \neq U$ a positive definite, symmetric matrix. Now, let $|\mathcal{P}^a|$ and $|\mathcal{P}^m|$ denote the order of the groups $\mathcal{P}^a$ and $\mathcal{P}^m$ respectively. Since, for any $R \in \mathcal{P}^m$, $V = \bar{R}\left(RUR^T\right)\bar{R}^T = \left(\bar{R}R\right)U\left(\bar{R}R\right)^T$, we see that there are precisely $|\mathcal{P}^m|$ elements of $\mathcal{P}^a$ that return the matrix V. Therefore, the number n of distinct symmetry related, positive definite, symmetric matrices that can be obtained as RUR^T with $R \in \mathcal{P}^a$ is exactly

$$n = \frac{|\mathcal{P}^a|}{|\mathcal{P}^m|}.$$

These distinct positive definite, symmetric matrices, $U_1, ..., U_n$ say, are called the *variants of martensite* and their number can differ significantly according to the relative symmetry of the parent and the product phase. For example, in a cubic-to-tetragonal transformation $n = 3$ whereas for a cubic-to-orthorhombic $n = 6$.

Henceforth, let us assume that the austenite lattice is cubic, i.e. $\mathcal{P}^a = \mathcal{P}^c$, and write $\mathbf{g}_i^c$ for the austenite lattice vectors and $\mathcal{N}^c$ for the Ericksen-Pitteri neighbourhood; this is the only case that will concern us in this thesis. We now make the assumption that the lattice parameters do not remain fixed but change slightly with temperature due to ordinary thermal expansion. To account for this fact, we require that the lattice parameters, and hence the lattice vectors, are dependent on the temperature $\theta \in \mathcal{I}$, where $\mathcal{I} \subset (0, \infty)$ is an interval of relevant temperatures containing the critical temperature θ_c. However, instead of defining a temperature dependent neighbourhood, we define the Ericksen-Pitteri neighbourhood $\mathcal{N}^c$ through $\mathbf{g}_i^c(\theta_c)$, the austenite lattice vectors at θ_c. Naturally, we then require that for each

$\theta \in \mathcal{I}$, $\{\mathbf{g}_i^c(\theta)\} \in \mathcal{N}^c$. Upon passage to the continuum theory, defining the Ericksen-Pitteri neighbourhood in terms of $\mathbf{g}_i^c(\theta_c)$, will lead to the interpretation of the reference configuration Ω as the undistorted austenite at θ_c. Note that the dependence of the lattice vectors on the temperature is henceforth assumed but not displayed.

The nonlinear elasticity model is based on energy minimization and, as such, on a *free-energy density* $\hat{\varphi}$ which is to be prescribed. Let $\hat{\varphi} \in C^0(\mathcal{N}^c \times \mathcal{I})$ be of the form

$$\hat{\varphi}(\mathbf{g}_1, \mathbf{g}_2, \mathbf{g}_3, \theta). \tag{2.2.5}$$

It is natural to make the two following assumptions:

(a) any two sets of lattice vectors generating the same lattice give the same value of the free energy and

(b) the free energy of a lattice is the same as the free energy of any orthogonal transformation of the lattice.

Otherwise said, we assume that for each $\theta \in \mathcal{I}$,

(a) $\hat{\varphi}\left(\mu_i^j \mathbf{g}_j, \theta\right) = \hat{\varphi}(\mathbf{g}_i, \theta)$ whenever $\{\mathbf{g}_i\} \in \mathcal{N}^c$, $\mu \in \mathcal{G}$ and $\mu_i^j \mathbf{g}_j \in \mathcal{N}^c$ and

(b) $\hat{\varphi}(R\mathbf{g}_i, \theta) = \hat{\varphi}(\mathbf{g}_i, \theta)$ for all $R \in SO(3)$.

Further, we assume that the energy is minimized by austenite for temperatures $\theta \geq \theta_c$ and by martensite for $\theta \leq \theta_c$; at the critical temperature θ_c both the austenite and the martensite are minimizers of the energy. That is,

(c) for each $\theta \in \mathcal{I}$ such that $\theta \geq \theta_c$, $\hat{\varphi}(\mathbf{g}_i^c, \theta) \leq \hat{\varphi}(\mathbf{g}_i, \theta)$ for all $\{\mathbf{g}_i\} \in \mathcal{N}^c$ and

(d) for each $\theta \in \mathcal{I}$ such that $\theta \leq \theta_c$, $\hat{\varphi}(U\mathbf{g}_i^c, \theta) \leq \hat{\varphi}(\mathbf{g}_i, \theta)$ for all $\{\mathbf{g}_i\} \in \mathcal{N}^c$.

In view of (a) and (b), the existence of minimizers from (c) and (d) implies the existence of more minimizers via invariance. In particular, for $\theta \geq \theta_c$, (b) says that $\{R\mathbf{g}_i^c\}$ also minimizes $\hat{\varphi}(\cdot, \theta)$ for all $R \in SO(3)$. Similarly, for $\theta \leq \theta_c$, $\{RU\mathbf{g}_i^c\}$ with $R \in SO(3)$ minimizes $\hat{\varphi}(\cdot, \theta)$ but, due to (a), so does $\left\{\mu_i^j RU\mathbf{g}_i^c\right\}$ for any $\mu_i^j \in \mathcal{G}$ with $\mu[\mathcal{N}^c] = \mathcal{N}^c$. Making use of Theorem 2.2.2 (iv) (see [19] for proofs), we see that the orbits $\{RU_k\mathbf{g}_i^c : R \in SO(3),\ k = 1, \ldots n\}$ are all energy-minimizing for $\theta \leq \theta_c$ where $U_1, \ldots, U_n$ are the martensitic variants obtained as RUR^T, $R \in \mathcal{P}^c$ (say, $U = U_1$). These are all the minimizers of $\hat{\varphi}(\cdot, \theta)$ and we proceed by strengthening (c) and (d):

(c´) for each $\theta \in \mathcal{I}$ such that $\theta > \theta_c$, the orbit $\{R\mathbf{g}_i^c : R \in SO(3)\}$ is a strict minimizing set for $\hat{\varphi}(\cdot, \theta)$ on $\mathcal{N}^c$ and

(d´) for each $\theta \in \mathcal{I}$ such that $\theta < \theta_c$, the orbits $\{RU_k\mathbf{g}_i^c : R \in SO(3),\ k = 1, \dots n\}$ are strict minimizing sets for $\hat{\varphi}(\cdot, \theta)$ on $\mathcal{N}^c$.

The set $\{R\mathbf{g}_i^c : R \in SO(3)\}$ represents the energy well of the austenite, whilst the sets $\{RU_1\mathbf{g}_i^c : R \in SO(3)\}, \dots, \{RU_n\mathbf{g}_i^c : R \in SO(3)\}$ represent the n energy wells of the martensite. A schematic representation of the free-energy density and its energy wells, relative to the temperature, is given in Fig. 2.3.

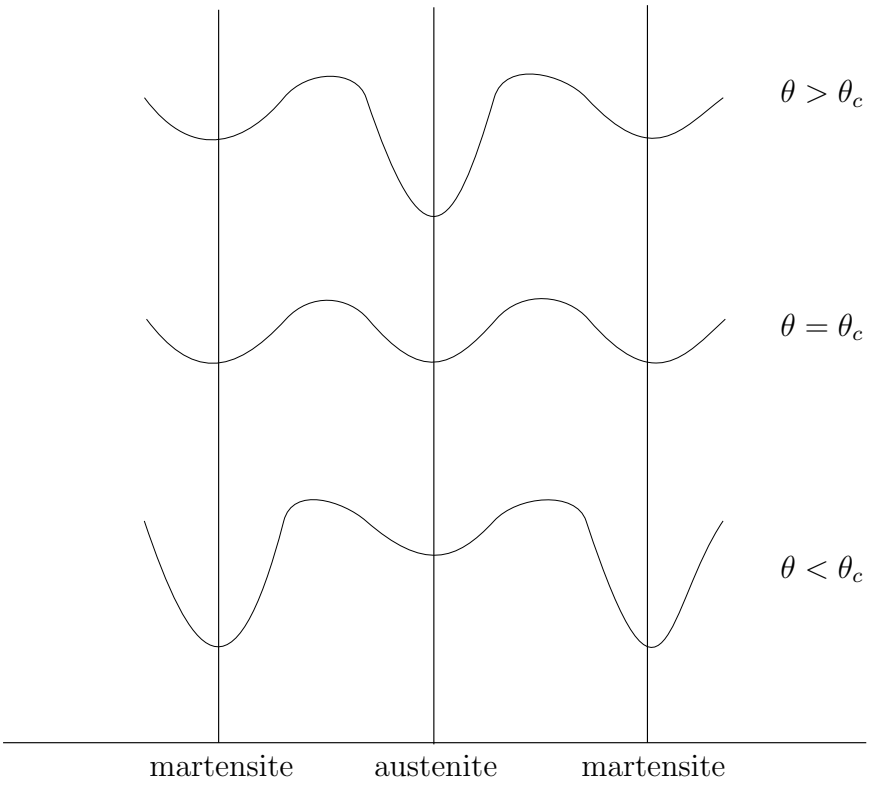

Figure 2.3: Schematic representation of the free-energy density. The relative stability of each phase is shown by the height of the corresponding energy wells.

Before we formally proceed to the description of the continuum theory, we mention that in some alloys the arrangement of atoms on the crystal lattice is such that different types of atoms appear in different periodic arrangements. These cannot be described by a Bravais lattice as it would require either to ignore the difference or to ignore one of the types of atoms. Such structures are called *ordered structures* or *superlattices* and they can be described by a collection of congruent Bravais lattices which are shifted or off-set from one another. This collection of congruent Bravais lattices is called a *multi-lattice* and Fig. 2.4 provides an example of such a 2-lattice.

An analysis similar to the above is possible where the lattice, and consequently the free energy, have a dependence on a function describing the shift or off-set. Nevertheless, according to the Cauchy-Born hypothesis, these shifts are not present in the continuum deformation and can be ignored by minimizing them out of the problem (see James [81]). The good agreement between experiments and theoretical predictions in shape-memory alloys, which are commonly multi-lattices, allows us to ignore the shift and discard it from the minimization. Yet, this agreement is satisfactory when we consider statics, as in metastable and dynamic problems, shifts can have a much greater effect [32, 81, 96].

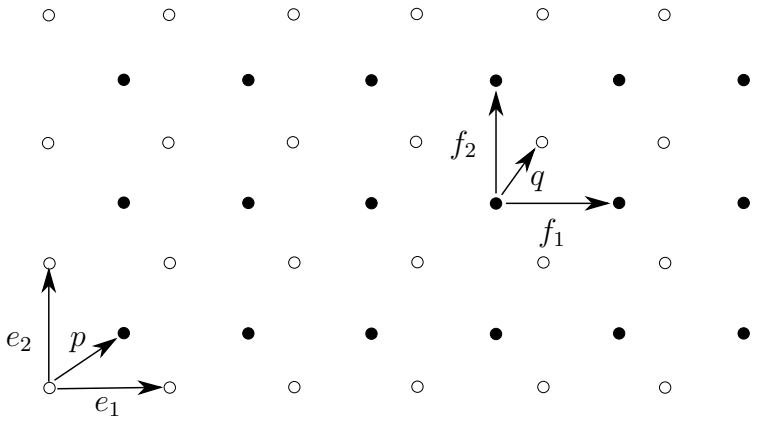

Figure 2.4: Example of a multi-lattice obtained by 2 congruent Bravais lattices.

The Continuum Model

At this point, we are in a position to make the passage from the atomistic to the continuum model by making use of the Cauchy-Born hypothesis which relates microscopic to macroscopic motion by regarding the lattice vectors as infinitesimal line segments in the continuum. To be precise, let $\Omega \subset \mathbb{R}^3$ be a bounded domain (open and connected) describing the region occupied by the crystalline solid in the reference configuration. Also, let $y : \Omega \to \mathbb{R}^3$ be a function describing the deformation of the body; that is, the material point at $\mathbf{x} \in \Omega$ in the reference configuration is displaced to the point $y(\mathbf{x})$ in the deformed configuration, and let $F = Dy$ be the deformation gradient. In the continuum theory, we restrict attention to deformations that preserve orientation and hence we impose the condition that $\det F > 0$. We note that this is related to the issue of invertibility as, for any physically realistic model, one needs to exclude interpenetration of matter, i.e. one needs to ensure invertibility of y in the

interior of Ω. We note that if $y \in C^1(\Omega, \mathbb{R}^3)$, the condition $\det F > 0$ ensures local invertibility by the inverse function theorem, i.e. invertibility in a neighbourhood of each $x \in \Omega$; this is a weaker condition and of course y will typically not be as smooth since the existence of minimizers is only established in $W^{1,p}(\Omega, \mathbb{R}^3)$. We do not remark further on the issue of invertibility as this will be a main point in Chapter 4 where references can be found. Then, the Cauchy-Born hypothesis says that a free-energy density $\varphi : \mathcal{N}_+^c \to \mathbb{R}$ is defined for each $\theta \in \mathcal{I}$ by

$$\varphi(F, \theta) = \hat{\varphi}(F\mathbf{g}_i^c, \theta) \tag{2.2.6}$$

where

$$\mathcal{N}_+^c = \left\{ A \in M^{3\times 3} : \det A > 0 \text{ and } \{A\mathbf{g}_i^c\} \in \mathcal{N}^c \right\}. \tag{2.2.7}$$

For mathematical rigour, we wish to impose standard coercivity and growth conditions on the continuum density φ and, hence, we need to assume that φ is defined on the entire space $M_+^{3\times 3}$ of matrices with positive determinant. To justify this, let us look back at the energy $\hat{\varphi}$ and consider a deformation of the lattice $\mathcal{L}(\mathbf{g}_i^c)$ associated to an element μ of the invariance group $\mathcal{G}$ which is not in the point group $\mathcal{P}^c = \mathcal{P}(\mathbf{g}_i^c)$, e.g. a lattice-restoring shear; due to Theorem 2.2.2, $\mu[\mathcal{N}^c] \cap \mathcal{N}^c = \emptyset$. On the other hand, the Ericksen-Pitteri neighbourhood contains the martensitic transformations so that, if U is the deformation associated to the martensitic transition, the vector triple $\{U\mathbf{g}_i^c\}$ belongs to $\mathcal{N}^c$. Since μ corresponds to a lattice-restoring shear, as we move from $\{U\mathbf{g}_i^c\}$ to $\{\mu_i^j \mathbf{g}_i^c\}$, one expects to find a high energy barrier as shown in Fig. 2.5. In particular, since plastic deformations are not associated to martensitic transformations in shape-memory materials, the energy barrier for the martensitic transition is expected to be lower than that of the shear deformation. Hence, in order to confine ourselves to deformations with moderate energy, it is reasonable to restrict attention to the neighbourhood $\mathcal{N}^c$; consequently, we justify redefining the continuum energy φ on $M_+^{3\times 3}$ by naturally expecting its minimizers to lie in $\mathcal{N}_+^c$. This is of course not a rigorous justification but we do not elaborate further as this is in fact a rather deep problem in the theory presented here.

In the continuum theory we consider the problem of minimizing the total free energy of the crystal

$$I_\theta(y) = \int_\Omega \varphi(Dy(\mathbf{x}), \theta) \tag{2.2.8}$$

among all deformations $y \in \mathcal{A}$ where

$$\mathcal{A} := \left\{ y \in W^{1,p}(\Omega, \mathbb{R}^3) : \det Dy > 0 \text{ a.e. and } y_{|\partial\Omega_1} = \bar{y} \right\}, \tag{2.2.9}$$

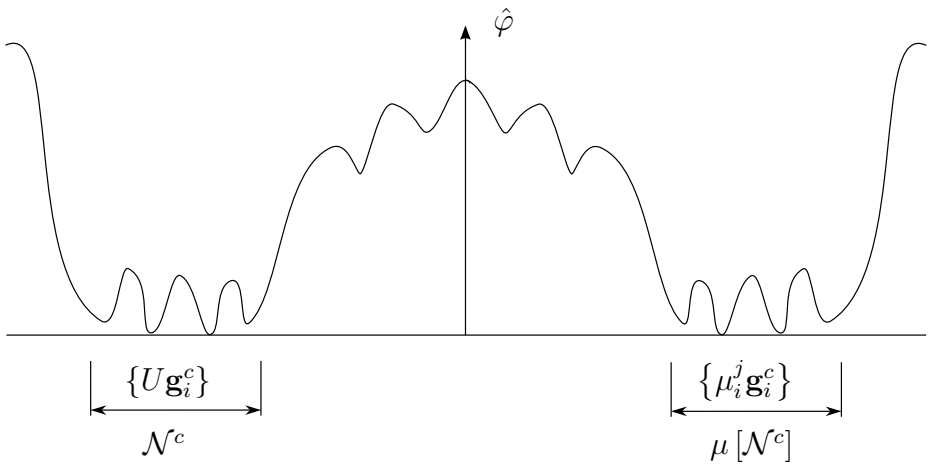

Figure 2.5: The energy density $\hat{\varphi}$ as one moves from a deformation U of the lattice $\mathcal{L}(\mathbf{g}_i^c)$ associated to the martensitic transition, to a deformation μ associated to an element in $\mathcal{G} \setminus \mathcal{P}(\mathbf{g}_i^c)$; we note the high energy barrier expected between these two points.

for some $p > 1$ as described in the previous section. The fact that there might be no condition specified for the remainder of the boundary, corresponds to a 'natural boundary condition' of surface tractions being zero there.

Following our discussion on the atomistic description, it becomes clear that the energy density φ of the continuum model immediately inherits properties (a), (b), (c´) and (d´). Thus, in the continuum setting, for each $\theta \in \mathcal{I}$ and $F \in \mathcal{N}_+^c$,

(a) $\varphi(FQ, \theta) = \varphi(F, \theta)$ for all $Q \in \mathcal{P}^c$ - material symmetry - and

(b) $\varphi(RF, \theta) = \varphi(F, \theta)$ for all $R \in SO(3)$ - frame-indifference.

Since we are considering matrices with positive determinant, from the polar decomposition theorem, we can write $F = RU$ where U is a unique positive definite, symmetric matrix and R is a rotation. Then, condition (b) now implies that only the symmetric part $U = \sqrt{F^T F}$ of any deformation gradient needs to be considered, thus justifying our assumption that the transformation matrix U was a positive definite and symmetric matrix.

We also obtain that

(c´) for each $\theta \in \mathcal{I}$ such that $\theta > \theta_c$, the orbit $\{\alpha(\theta) SO(3)\}$ is a strictly minimizing set for $\varphi(\cdot, \theta)$ and

(d´) for each $\theta \in \mathcal{I}$ such that $\theta < \theta_c$, the orbits $\{\bigcup_{i=1}^n SO(3) U_i\}$ are strictly minimizing sets for $\varphi(\cdot, \theta)$

where $\{U_i,\ i=1,\dots n\}$ is the set of martensitic variants and the function $\alpha(\theta)$ in (c´) is simply a coefficient accounting for ordinary thermal expansion such that $\alpha(\theta_c)=1$. This leads to and is consistent with the fact that we interpret the reference configuration Ω as the undistorted austenite at the critical temperature.

By adding to φ an appropriate function of the temperature θ, we may assume that $\inf_{F\in\mathcal{A}}\varphi(F,\theta)=0$. Then, in accordance with (c´) and (d´), the set K_θ of energy-minimizing deformation gradients at temperature θ, i.e.

$$K_\theta=\left\{F\in M^{3\times3}_+ : \varphi(F,\theta)=0\right\}$$

becomes

$$K_\theta=\begin{cases}\alpha(\theta)\,SO(3)\,, & \theta>\theta_c\\ SO(3)\cup\bigcup_{i=1}^n SO(3)\,U_i, & \theta=\theta_c\\ \bigcup_{i=1}^n SO(3)\,U_i, & \theta<\theta_c.\end{cases}\tag{2.2.10}$$

In what follows we shall assume that the energy density $\varphi(\cdot,\theta):M^{3\times3}_+\to[0,\infty)$ is continuous and satisfies the following growth condition:

$$-c_1+c_2|F|^p\le\varphi(F)\le c_1\left(|F|^p+1\right)\tag{2.2.11}$$

for all $F\in M^{3\times3}_+$ and for some $c_1,\,c_2>0$ and $1<p<\infty$. Above, $M^{3\times3}_+=\{A\in M^{3\times3}:\det A>0\}$. Moreover, we recall that φ satisfies conditions (a) and (b); that is, material symmetry and frame indifference.

We have already mentioned that the growth condition above is inconsistent with the natural constraint that $\varphi(F,\theta)\to\infty$ as $\det F\to0^+$. Nevertheless, for mathematical rigour, we shall assume (2.2.11) and we keep in mind that this condition can be dropped and the constraint can be effectively handled (Ball and James [19]).

As alluded to previously, energy densities for crystals which account properly for crystallographic symmetry are typically not quasiconvex. In particular, the set $K(\theta)$ usually contains rank-one connections, i.e. pairs of rank-one connected matrices, and when this is the case, φ becomes zero at two matrices whose difference is of rank-one. This implies that, were φ rank-one convex, it would become zero along the line segment connecting the two matrices and lying outside the set K_θ. This contradicts our assumption on the zero set of φ and we conclude that φ cannot be rank-one convex and, therefore, it cannot be quasiconvex either; thus, in dimension $d>1$, we cannot ensure that the infimum of I_θ, under suitable boundary conditions, is attained.

This lack of quasiconvexity is precisely what gives rise to microstructure. Any infimizing sequence will have to approach the set K_θ in measure without the limiting

configuration necessarily being a minimizer of φ. Such a sequence will involve finer and finer features (oscillations) and the hypothesis is that, in the limit, these can model the extremely fine microstructures observed. Provided our infimizing sequence is, say, bounded in $W^{1,p}$ we can deduce that - at the temperature θ - it will generate (up to a subsequence) a gradient Young measure $(\nu_x)_{x\in\Omega}$ such that

$$\operatorname{supp}\nu_x \subset K_\theta \text{ for a.e. } x \in \Omega.$$

However, from our relaxation theorems, its centre of mass $\bar{\nu}_x \in \mathcal{A}$ will be energy-minimizing for I^{qc} which was interpreted as the macroscopic energy. Therefore, $\bar{\nu}_x$ is interpreted as an energy-minimizing *macroscopic deformation gradient*.

Moreover, we made the assumption that $l = \inf_{\mathcal{A}} I_\theta = 0$. Since we will primarily be interested in linear boundary conditions, i.e. $\bar{y} = Fx$ say in (2.2.9), we restrict attention to these. In this case, it is clear that $l = 0$ if and only if, there exists a minimizing sequence y^k such that $y^k_{|\partial\Omega} = Fx$ and $\operatorname{dist}(Dy^k, K_\theta) \to 0$ in measure. Thus, in the context of the previous section, we may say that

$$\inf_{\mathcal{A}} I_\theta = 0 \Leftrightarrow F \in K_\theta^{qc} \tag{2.2.12}$$

and the set K_θ^{qc} corresponds precisely to the set of all *recoverable strains under displacement control* at temperature θ.

Simple laminates

Suppose that A, B are martensitic variants. The simplest solution to the relation $Dy \in \{A, B\}$ is a so-called *simple laminate*, as in Fig. 2.6, where Dy is constant in alternating bands bounded by the planes $x \cdot n =$ constant. We note that for the deformation to remain continuous across the interfaces $x \cdot n =$ constant, the Hadamard jump condition (Lemma 2.1.8) must hold; that is,

$$B - A = a \otimes n$$

for some non-zero $a \in \mathbb{R}^3$, i.e. A and B must be rank-one connected. This is a rather strict condition set on the two variants and the above equation needs to be solved. We elaborate on this shortly and for the purposes of this example let us assume that this is indeed the case.

As an illustration of the use of Young measures, let $F = \lambda A + (1-\lambda) B$ be a convex combination of the two variants. We wish to construct a gradient Young measure which can effectively describe a simple laminate and its underlying deformation

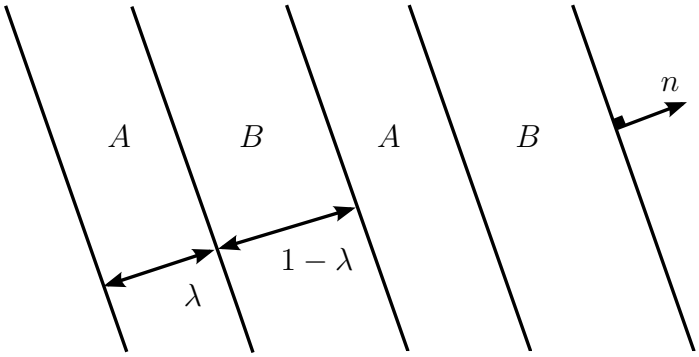

Figure 2.6: A simple laminate of martensite between the variants A and $B = A + a \otimes n$.

satisfies the linear boundary condition Fx. This is a fundamental example in the continuum model for martensitic transformations and it will be used repeatedly.

Let us consider a sequence of deformations $y^k : \Omega \to \mathbb{R}^3$ uniformly bounded in $W^{1,\infty}(\Omega, \mathbb{R}^3)$ such that

$$\begin{aligned} \operatorname{dist}\left(Dy^k, \{A, B\}\right) &\to 0 \text{ in measure,} \\ y^k(x) &= Fx \text{ on } \partial\Omega. \end{aligned}$$

Such sequences can be constructed as in Fig. 2.7 by letting Dy^k correspond to a simple laminate with bands of alternating width λk^{-1}, $(1-\lambda)\, k^{-1}$ upon which Dy^k takes the values A, B respectively, this being modified in a layer of width $1/k$ near $\partial\Omega$ so as to exactly satisfy the boundary condition (see e.g. [105] for details).

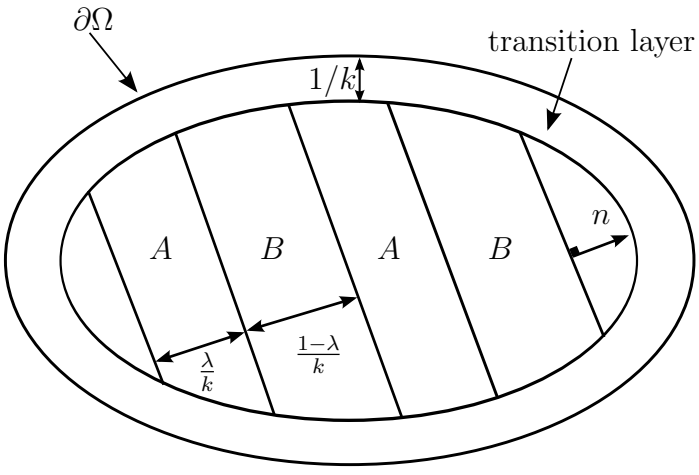

Figure 2.7: Schematic depiction of the sequence of gradients Dy^k, bounded in L^∞, approaching the set $\{A, B\}$ in measure and modified near the boundary so as to satisfy the boundary condition.

Let $\nu = (\nu_x)_{x\in\Omega}$ be the Young measure generated by (a subsequence of) Dy^k. In view of the Fundamental Theorem on Young measures (Theorem 2.1.4), we deduce that $\|\nu_x\|_{\mathcal{M}(M^{3\times 3})} = 1$ and that $\operatorname{supp}\nu_x \subset \{A, B\}$ a.e. in Ω, i.e.

$$\nu_x = \mu(x)\,\delta_A + (1-\mu(x))\,\delta_B.$$

By considering a further subsequence, we may assume that $y^k \overset{*}{\rightharpoonup} y$ in $W^{1,\infty}$. Choosing $\psi \equiv \mathrm{id}$ in Theorem 2.1.4 (ii), we infer that $Dy(x) = \langle \nu_x, \mathrm{id}\rangle$ so that

$$Dy(x) = \mu(x)\,A + (1-\mu(x)\,B) = A + (1-\mu(x))\,a\otimes n.$$

Extending y^k and y by Fx outside Ω we see that the map $y(x) - Ax$ is constant on the planes $x\cdot n =$ constant. Hence, $y(x) = Fx$ and $\mu(x) = \lambda$, i.e. the sequence Dy^k generates the unique homogeneous $W^{1,\infty}$ gradient Young measure

$$\nu = \lambda\delta_A + (1-\lambda)\,\delta_B.$$

Remark. We note that, unlike simple laminates, the microstructure corresponding to ν has no characteristic length-scale. Nevertheless, in view of the relaxed minimization problem, we refer to this microstructure as a simple laminate and interpret the centre of mass of ν, $\bar{\nu} = \lambda A + (1-\lambda)\,B$, as the macroscopic deformation gradient corresponding to a simple laminate. This will play a pivotal role in the construction of austenite-martensite interfaces.

Interfaces and Twins

Due to the Hadamard jump condition, we saw that zero-energy interfaces are in one-to-one correspondence with rank-one connections between the sets $SO(3)\,U_i$ and $SO(3)\,U_j$. Naturally, we wish to determine the conditions under which these sets are rank-one connected.

Definition 2.2.4. *Let $U, V \in M^{3\times 3}_+$. We say that the wells $SO(3)\,U$ and $SO(3)\,V$ are rank-one connected if there exist rotations $R_1, R_2 \in SO(3)$ and vectors $b, n \in \mathbb{R}^3$, $|n| = 1$, such that*

$$R_1V - R_2U = b\otimes n. \tag{2.2.13}$$

A pair (R_1V, R_2U) satisfying (2.2.13) is called a twin. Moreover, the vectors R_2^Tb and n are called the twin plane shear and twin plane normal respectively.

At this point note that, provided U, V are positive definite and symmetric, using the uniqueness of the polar decomposition, $b = 0$ implies $U = V$. Conversely, if $U = V$, multiplying (2.2.13) to the right by U^{-1} and to the left by R_2^T we deduce that

$$R = 1 + a \otimes U^{-1} n,$$

where $R = R_2^T R_1$ and $a = R_2^T b$; but then R is a rotation with two linearly independent axes of rotation (perpendicular to $U^{-1}n$) and, therefore, $R = 1$ implying that there are no rank-one connections between a well and itself.

On the other hand, for $U \neq V$, multiplying (2.2.13) to the left by R_2^T and under the notation R and a introduced above, we deduce the so-called *twinning relation* which is to be solved for R, a and n; that is,

$$RV - U = a \otimes n. \tag{2.2.14}$$

Multiply to the right by U^{-1} to get that

$$RVU^{-1} = 1 + a \otimes U^{-T} n \tag{2.2.15}$$

and let

$$C = (1 + m \otimes a)(1 + a \otimes m), \tag{2.2.16}$$

where $C = U^{-T} V^T V U^{-1}$, $m = U^{-T} n$. Clearly, $\det VU^{-1} > 0$ and thus $1 + a \cdot m > 0$. According to the polar decomposition theorem, (2.2.15) is equivalent to (2.2.16) and the problem reduces to solving the latter.

The following result due to Ball and James [18] (see also Khachaturyan [84]) provides a general method for solving the above problem.

Theorem 2.2.3. *Let $C \in M^{3\times 3}$, $C \neq \mathbf{1}$ be symmetric and let $\lambda_1 \leq \lambda_2 \leq \lambda_3$ be the ordered eigenvalues of C. Necessary and sufficient conditions for C to be expressible in the form*

$$C = (1 + m \otimes a)(1 + a \otimes m)$$

for non-zero a and m with $1 + a \cdot m > 0$ is that $\lambda_i > 0$ (i.e. $C > 0$) and $\lambda_2 = 1$. The solutions are then given by

$$a = \rho \left(\sqrt{\frac{\lambda_3 (1 - \lambda_1)}{\lambda_3 - \lambda_1}} e_1 + \kappa \sqrt{\frac{\lambda_1 (\lambda_3 - 1)}{\lambda_3 - \lambda_1}} e_3 \right), \tag{2.2.17}$$

$$m = \rho^{-1} \left(\frac{\sqrt{\lambda_3} - \sqrt{\lambda_1}}{\sqrt{\lambda_3 - \lambda_1}} \right) \left(-\sqrt{1 - \lambda_1} e_1 + \kappa \sqrt{\lambda_3 - 1} e_3 \right), \tag{2.2.18}$$

where $\rho \neq 0$ is chosen to make m of unit length, e_1, e_3 are normalized eigenvectors of C corresponding to λ_1, λ_3 respectively and $\kappa = \pm 1$. These solutions are unique up to the substitution $a \to -a$, $m \to -m$ and satisfy $1 + a \cdot m = \sqrt{\lambda_1 \lambda_3}$.

The solutions to our original problem (2.2.15) can now be specified simply by setting $n = U^T m$ and substituting back to the equation to get the rotation R.

Next, assume that U, V are positive definite, symmetric matrices and that, for some $Q \in SO(3)$, $U = QVQ^T$ - these are conditions satisfied by the martensitic variants. The following result provides a simple criterion for determining whether the sets $SO(3)U$ and $SO(3)V$ are rank-one connected.

Lemma 2.2.4. *Let $U, V \in M^{3\times 3}$ be positive definite and symmetric and assume that $U = QVQ^T$ for some $Q \in SO(3)$. Then, the sets $SO(3)U$ and $SO(3)V$ are rank-one connected if and only if*

$$\det\left(U^2 - V^2\right) = 0.$$

In fact, Forclaz [64] shows that an equivalent condition is $\det(U - V) = 0$.

Theorem 2.2.3, though useful, can in practice require many calculations. Alternatively and in specific cases, one can use a result known as *Mallard's law* (see Bhattacharya [26]), which we present next.

Theorem 2.2.5. *(Mallard's law) Let $Q = -\mathbf{1} + 2e \otimes e$ be a rotation by angle π about the axis e and suppose that*

- *$V = PUQ$ for some rotation P, or equivalently, $V^T V = QU^T UQ$ and*
- *$V^T V \neq U^T U$*

Then, there are two solutions to (2.2.14) which are given by

$$a = 2\left(\frac{U^{-T}e}{|U^{-T}e|^2} - Ue\right), \quad n = e \tag{2.2.19}$$

$$a = \rho Ue, \quad n = 2\rho^{-1}\left(e - \frac{U^T Ue}{|Ue|^2}\right) \tag{2.2.20}$$

where $\rho \neq 0$ is chosen to make n of unit length.

Recall that any two martensitic variants U, V are related by $V = QUQ^T$ for some rotation $Q \in \mathcal{P}^a$; Mallard's law says that if this rotation is by an angle π, there is always a twinning system between the wells $SO(3)U$ and $SO(3)V$; this is indeed the case at least for typical martensitic transformations (see e.g. Appendix A for the cubic-to-orthorhombic transition). In particular, when a rotation Q by angle π is in

$\mathcal{P}^a$ but not in $\mathcal{P}^m$, there exists a martensitic variant $V \neq U$, given by $V = QUQ$, and the wells $SO(3)U$ and $SO(3)V$ are rank-one connected. In turn this implies that, for any such material, an energy density φ accounting properly for its crystallographic symmetries can never be quasiconvex.

We note that when $V = QUQ$, Mallard's law also allows us to classify the twins between the wells $SO(3)U$ and $SO(3)V$. For this, we need the following definition.

Definition 2.2.5. *In the notation of (2.2.14), let*

$$s = |a||U^{-1}n|, \qquad \eta_1 = \frac{a}{|a|}, \qquad K_1 = \frac{U^{-1}n}{|U^{-1}n|} \tag{2.2.21}$$

We call s, η_1 and K_1 the twinning shear, the shearing direction and the twinning (or shearing) plane respectively.

Looking back at Mallard's law, we see that in the first solution the twinning plane K_1 is a plane of symmetry in the austenite and thus rational; such twins are called *Type-I*. Similarly, in the second solution, it is the shearing direction which is a direction of symmetry in the austenite and so rational. Then, we say that this is a *Type-II* twin. However, there are cases when there are two such rotations Q by angle π meaning that there are two solutions which can be described both by a Type-I and a Type-II twin, both having rational twinning plane and shearing direction. Such twins are called *compound*.

Next, we present a result which can be found in [145] and comes as a useful corollary to Theorem 2.2.5. For the purposes of the following corollary, we write $a \wedge b$ for the vector product of $a, b \in \mathbb{R}^3$.

Corollary 2.2.6. *Let $U, V \in M^{3\times 3}$ satisfy $U = QVQ$ for some rotation Q by angle π about some axis e. Denote by (R_1, a_1, n_1) and (R_2, a_2, n_2) the two twinning solutions corresponding to the Type-I and Type-II solutions in (2.2.19) and (2.2.20) respectively. Then*

$$R_1 = \left(-\mathbf{1} + \frac{2}{|U^{-1}e|^2} U^{-1}e \otimes U^{-1}e\right) Q. \tag{2.2.22}$$

Furthermore, the rotation R_1 has axis parallel to $e \wedge U^{-1}e$ and the angle of rotation θ_1 can be found from $\cos\theta_1 = 2\left(U^{-1}e \cdot e\right)^2 / |U^{-1}e|^2 - 1$. Also, for R_2, we have

$$R_2 = \left(-\mathbf{1} + \frac{2}{|Ue|^2} Ue \otimes Ue\right) Q. \tag{2.2.23}$$

The rotation R_2 has axis parallel to $e \wedge Ue$ and the angle of rotation θ_2 can be found from $\cos\theta_2 = 2\left(Ue \cdot e\right)^2 / |Ue|^2 - 1$.

Ending our discussion on rank-one connections, we mention another corollary to Theorem 2.2.5 which will prove useful in the following section (see [72]).

Corollary 2.2.7. *Let U, V and (R_1, a_1, n_1), (R_2, a_2, n_2) as in Corollary 2.2.6. Suppose that $\bar{U}, \bar{V} \in M^{3\times 3}$ such that $\bar{U} = \bar{Q}U\bar{Q}^T$ and $\bar{V} = \bar{Q}V\bar{Q}^T$ for some rotation $\bar{Q}$. Then, the twinning solutions $\left(\bar{R}, \bar{a}, \bar{n}\right)$ to the equation*

$$\bar{R}\bar{V} - \bar{U} = \bar{a} \otimes \bar{n}$$

are given by $\left(\bar{Q}R_1\bar{Q}^T, \bar{Q}a_1, \bar{Q}n_1\right)$ and $\left(\bar{Q}R_2\bar{Q}^T, \bar{Q}a_2, \bar{Q}n_2\right)$ for the Type-I and Type-II twins respectively.

Parallelogram microstructure

In what follows, we shall be interested in a particular configuration known as the *parallelogram microstructure* (Bhattacharya [29], Nishida et al. [106, 107]) which will concern us in Chapter 3. This microstructure involves four distinct variants of martensite and can be described by a twinning system 'zig-zagging' through a region occupied by another laminate; a small region of the parallelogram microstructure is shown schematically in Fig. 2.8 where the crucial points are the four-fold corners at which the four interfaces separating the four martensitic variants meet along the line perpendicular to the plane of the paper. The entire pattern can then be reconstructed by repeating such corners.

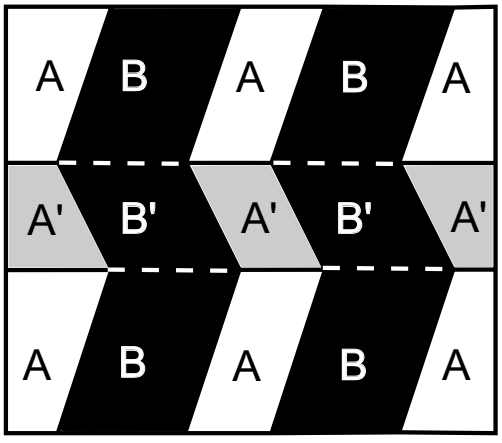

Figure 2.8: Schematic representation of a parallelogram microstructure involving the variants A, A', B and B'.

The above condition, namely that the four interfaces meet along a line, is rather interesting as it adds a constraint for kinematic compatibility; in particular, one

needs to ensure that there is no dislocation at the corner and satisfying the twinning equations on the four interfaces alone does not suffice for the reconstruction of the parallelogram microstructure.

Let $A = R_A U_A$, $A' = R_{A'} U_{A'}$, $B = R_B U_B$ and $B' = R_{B'} U_{B'}$. Then, geometric compatibility on each of the four interfaces requires the following:

$$\begin{aligned} R_B U_B - R_A U_A &= a_{AB} \otimes n_{AB} \\ R_{B'} U_{B'} - R_{A'} U_{A'} &= a_{A'B'} \otimes n_{A'B'} \\ R_{A'} U_{A'} - R_A U_A &= a_{AA'} \otimes n_{AA'} \\ R_{B'} U_{B'} - R_B U_B &= a_{BB'} \otimes n_{BB'} \end{aligned} \tag{2.2.24}$$

These are the twinning equations for each adjacent pair of variants but, as noted already, these are not sufficient. Following our discussion above and setting $R_I^T R_J = R_{IJ}$, $b_{IJ} = R_I^T a_{IJ}$ for $I,\ J \in \{A, A', B, B'\}$, we obtain the following system which needs to be satisfied:

$$\begin{aligned} R_{AB} U_B - U_A &= b_{AB} \otimes n_{AB} \\ R_{A'B'} U_{B'} - U_{A'} &= b_{A'B'} \otimes n_{A'B'} \\ R_{AA'} U_{A'} - U_A &= b_{AA'} \otimes n_{AA'} \\ R_{BB'} U_{B'} - U_B &= b_{BB'} \otimes n_{BB'} \\ R_{AB} R_{BB'} &= R_{AA'} R_{A'B'} \\ n_{AB}, n_{A'B'}, n_{AA'} &\text{ and } n_{BB'} \text{ coplanar.} \end{aligned} \tag{2.2.25}$$

Note that we added two conditions, namely that $R_{AB} R_{BB'} = R_{AA'} R_{A'B'}$ and that n_{AB}, $n_{A'B'}$, $n_{AA'}$ and $n_{BB'}$ are coplanar. Regarding the first condition note that R_{IJ} denotes the mutual rotation between U_I and U_J; then the mutual rotation between U_A and $U_{B'}$ can be written as a superposition of rotations R_{AB} and $R_{BB'}$ or, equivalently, of $R_{AA'}$ and $R_{A'B'}$, i.e. $R_{AB} R_{BB'} = R_{AA'} R_{A'B'}$. In particular, this condition is necessary to prevent a dislocation along the line of intersection. On the other hand, the condition on the coplanarity of the normals to the four interfaces ensures that all four planes meet at a line. In fact, we can say a bit more and we will in Chapter 3; for now we only present the following result due to Bhattacharya [28] giving conditions under which the parallelogram microstructure is compatible. For notational convenience, let (U_I, U_J) denote the twinning system between $R_I U_I$ and $R_J U_J$.

Lemma 2.2.8. *Suppose Q and R are rotations by angle π about axes e_1 and e_2 respectively such that $e_1 \cdot e_2 = 0$. Let e_3 be perpendicular to both e_1 and e_2 and suppose that the variants U_A, $U_{A'}$, U_B and $U_{B'}$ satisfy the conditions below:*

- *All four variants are distinct;*
- *$U_{A'} = RU_AR$, $U_{B'} = QU_{A'}Q$, $U_B = QU_AQ$;*
- *$e_3 \cdot U_A^2 e_1 \neq 0$.*

Then, there are two solutions to (2.2.25). In either solution, the twinning systems $(U_{A'}, U_A)$ and $(U_{B'}, U_B)$ are necessarily Type-I, whereas (U_B, U_A) as well as $(U_{B'}, U_{A'})$ are Type-II. Further, the Type-I interfaces are in the same plane while the Type-II interfaces are obtained by a reflection across it.[5]

In a recent experiment by H. Seiner et al. [123], this geometry was observed forming an interface with austenite and in the next chapter we explore the above observations extensively.

Austenite-martensite interfaces

Suppose that at some critical temperature θ_c a microstructure of martensite forms an interface with a uniform region of austenite. For a single variant of martensite U to form an interface with a uniform region of the austenite, we need that these are compatible, i.e. from Theorem 2.2.3, we need that U^2 be expressible in the form

$$U^2 = (1 + n \otimes a)(1 + a \otimes n)$$

for some non-zero vectors a and n. In particular, we require that $\lambda_2(U^2) = 1$.

However, in practice, this is not the case and the requirement that the middle eigenvalue be one is truly non-generic[6]. What one usually observes is a region of finely twinned martensite, in the form of a simple laminate, forming a not-so-sharp flat interface with a uniform region of austenite. These are the most commonly observed interfaces with austenite and are referred to as *classical austenite-martensite interfaces*. Before we show how these interfaces can be predicted by the nonlinear

[5]We remark that since compound twins can be interpreted both as Type-I and Type-II twins, in the necessary geometry described, the Type-I or Type-II twinning systems can be replaced by compound twins.

[6]R. D. James, J. Cui, Z. Zhang and others have done some remarkable work where the composition of alloys is 'tuned' so that $\lambda_2(U^2) = 1$. This results in very interesting phenomena and relates to thermal hysteresis [44, 83].

elasticity model, we present a result by Ball and James [18] predicting a necessarily planar geometry for a classical interface between a simple laminate and the austenite.

Theorem 2.2.9. *Let $p > 2$ and let $\Omega \subset \mathbb{R}^3$ be bounded, open and connected. Suppose that Ω can be written as $\Omega = \Omega_{A,B} \cup \Omega_C \cup \mathcal{P}$ where $\Omega_{A,B}$, Ω_C are disjoint, open and connected and where $\mathcal{P} = \Omega \cap \partial\Omega_{A,B} = \Omega \cap \partial\Omega_C$. Further assume that either $\mathcal{L}^3(\mathcal{P}) = 0$ or $p > 3$. Let $A, B, C \in M^{3\times 3}$ be distinct matrices such that neither $A - C$ nor $B - C$ is of rank one. Let $y^k \rightharpoonup y$ in $W^{1,p}(\Omega, \mathbb{R}^3)$ satisfy for every $\epsilon > 0$*

$$\lim_{k\to\infty} \mathcal{L}^d\left(\left\{x \in \Omega_{A,B} : |Dy^k - A| > \epsilon \text{ and } |Dy^k - B| > \epsilon\right\}\right) = 0 \tag{2.2.26}$$

and

$$\lim_{k\to\infty} \mathcal{L}^d\left(\left\{x \in \Omega_C : |Dy^k - C| > \epsilon\right\}\right) = 0. \tag{2.2.27}$$

Then there exists a unit vector $m \in \mathbb{R}^3$ and $c \in \mathbb{R}$ such that $\mathcal{P} \subset \{x \in \mathbb{R}^3 : x \cdot m = c\}$, i.e. the interface $\mathcal{P}$ is planar.

In the notation of the above result, let $A = U$ and $B = RV$ be martensitic variants such that $V = PUP^T$ for some rotation $P \in L^a$, the austenitic Laue group, and let $C = \mathbf{1}$ denote the undistorted austenite. Then, for the simple laminate to be compatible we require that

$$RV - U = a \otimes n.$$

On the other hand, none of U or RV are rank-one connected with the identity which implies that the deformation cannot be continuous. To overcome this, we introduce an interpolation layer of thickness $1/k$ - this time separating the uniform region of austenite and the twinned martensite - to obtain a sequence of deformations y^k as in Fig. 2.9. In the limit as $k \to \infty$, the volume of the interpolation layer tends to zero and we must make sure that the average deformations on each side are compatible so that the limiting deformation remains continuous across the interface. In the example of the simple laminate, we saw that the average deformation in the martensitic region is given by

$$F = \lambda RV + (1 - \lambda) U = U + \lambda a \otimes n. \tag{2.2.28}$$

Thus, we impose the condition

$$QF - \mathbf{1} = b \otimes m \tag{2.2.29}$$

for some rotation Q and vectors $b, m \in \mathbb{R}^3$.

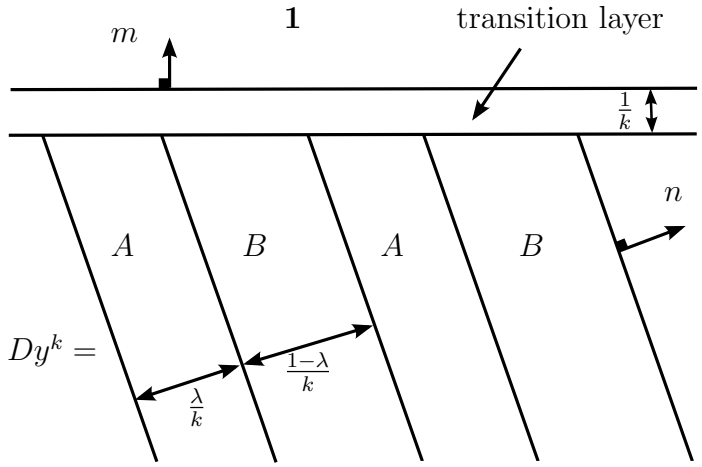

Figure 2.9: Minimizing sequence of gradients Dy^k for an austenite-twinned martensite interface.

Then, we may obtain a sequence of energy-minimizing deformations provided that

$$\begin{aligned} &(1) \qquad RV - U = a \otimes n \\ &(2) \qquad QF - \mathbf{1} = b \otimes m. \end{aligned}$$

Suppose that (1) is satisfied for some rotation R and vectors a, n and we wish to solve (2). Following Theorem 2.2.3, let $C(\lambda) := (U + \lambda n \otimes a)(U + \lambda a \otimes n)$. Then, we need $C(\lambda)$ to be expressible in the form

$$C(\lambda) = (\mathbf{1} + m \otimes b)(\mathbf{1} + b \otimes m).$$

This is possible if and only if, $\lambda_2(C(\lambda)) = 1$ and, in particular, we require that

$$\det(C(\lambda) - \mathbf{1}) = 0.$$

The following results can be found in Ball and James [18] but we present them here, along with proofs, as the methods will be useful for the calculations in Chapter 3.

Lemma 2.2.10. *Assume $C(\lambda)$ is as above and let $g(\lambda) = \det(C(\lambda) - \mathbf{1})$. Then $g(\lambda)$ is a quadratic function of λ satisfying $g(\lambda) = g(1 - \lambda)$.*

Proof. We first show that $g(\lambda)$ is quadratic. First, note that $\det V = \det U$ and $\mathrm{tr}\, V = \mathrm{tr}\, U$. This is clear since, U, V being martensitic variants, there exists a rotation P such that $V = PUP^T$. What is more, since $RV = U + a \otimes n$ we get that

$$RVU^{-1} = 1 + a \otimes U^{-1}n$$

and taking determinants, it is easy to see that

$$a \cdot U^{-1} n = 0, \tag{2.2.30}$$

i.e. $\det(U + \lambda a \otimes n) = \det U > 0$. Thus,

$$\begin{aligned} g(\lambda) &= \det\left[(U + \lambda n \otimes a)(U + \lambda a \otimes n) - \mathbf{1}\right] \\ &= \det U \det\left[(U + \lambda a \otimes n) - (U + \lambda n \otimes a)^{-1}\right] \\ &= \det U \det\left[\left(U - U^{-1}\right) + \lambda\left(a \otimes n + U^{-1} n \otimes U^{-1} a\right)\right] \end{aligned} \tag{2.2.31}$$

where the matrix multiplying λ is of rank two and, therefore, $g(\lambda)$ is at most quadratic. Also, $RV = U + a \otimes n$ and hence, $V^2 = (U + n \otimes a)(U + a \otimes n)$. In turn, this implies that

$$g(1) = \det\left[P\left(U^2 - \mathbf{1}\right) P^T\right] = \det\left(U^2 - \mathbf{1}\right) = g(0).$$

It follows that $g(\lambda) = g(1 - \lambda)$. □

From Lemma 2.2.10, we can see how to make one eigenvalue of $C(\lambda)$ equal to 1. However, in order to satisfy the conditions of Theorem 2.2.3, we must ensure that the other two eigenvalues of $C(\lambda)$ bound 1 from above and below.

Lemma 2.2.11. *Suppose that for some $\lambda^* \in [0, 1]$, $C(\lambda^*)$ has the unordered triple of eigenvalues 1, λ_1, λ_3. Then, λ_1 and λ_3 bound 1 from above and below if and only if,*

$$\operatorname{tr} U^2 - \det U^2 - 2 + \left(\lambda^{*2} - \lambda^*\right)|a|^2 \geq 0. \tag{2.2.32}$$

Proof. λ_1 and λ_3 bound 1 from above and below if and only if $(1 - \lambda_1)(\lambda_3 - 1) \geq 0$. Thus, if and only if, $(\lambda_1 + \lambda_3 + 1) - \lambda_1 \lambda_3 - 2 \geq 0$, i.e.

$$\operatorname{tr} C(\lambda^*) - \det C(\lambda^*) - 2 \geq 0.$$

Note again that $V^2 = (U + n \otimes a)(U + a \otimes n)$. Taking traces and noting that $|n| = 1$, we deduce that

$$2Ua \cdot n + |a|^2 = 0. \tag{2.2.33}$$

Then,

$$\begin{aligned} \operatorname{tr} C(\lambda^*) &= \operatorname{tr} U^2 + 2\lambda^*(Ua \cdot n) + \lambda^{*2}|a|^2 \\ &= \operatorname{tr} U^2 + \left(\lambda^{*2} - \lambda^*\right)|a|^2. \end{aligned}$$

Since also $\det C(\lambda^*) = \det U^2$, the result follows. □

We are now in a position to prove a result concerning the existence of solutions to equation (2). For the purposes of Theorem 2.2.12, we shall refer to the triple $(Q, \lambda, b \otimes m)$ as a solution of (2), if the rotation Q, the scalar $\lambda \in (0, 1)$ and the rank-one matrix $b \otimes m$ satisfy

$$U + \lambda a \otimes n = Q^T \left(\mathbf{1} + b \otimes m\right). \tag{2.2.34}$$

Theorem 2.2.12. *Let U be a positive definite, symmetric matrix such that it satisfies the twinning equation (1) for some $V = PUP^T$, $P, R \in SO(3)$ and vectors $a \neq 0$ and n with $|n| = 1$. Further, assume that U does not have an eigenvalue equal to 1. Necessary and sufficient conditions for (2.2.34) to have a solution are that*

$$\delta \leq -2 \tag{2.2.35}$$

and that

$$\operatorname{tr} U^2 - \det U^2 - 2 + \frac{1}{2\delta}|a|^2 \geq 0 \tag{2.2.36}$$

where

$$\delta = a \cdot U \left(U^2 - \mathbf{1}\right)^{-1} n. \tag{2.2.37}$$

If further,

$$\delta < -2 \tag{2.2.38}$$

then strict inequality holds in (2.2.36) and there are exactly four distinct solutions of (2.2.34) having the form

$$\begin{gathered} \left(R_1, \lambda^*, b_1^+ \otimes m_1^+\right), \\ \left(R_2, \lambda^*, b_1^- \otimes m_1^-\right), \\ \left(R_3, 1 - \lambda^*, b_2^+ \otimes m_2^+\right), \\ \left(R_4, 1 - \lambda^*, b_2^- \otimes m_2^-\right). \end{gathered} \tag{2.2.39}$$

The superscripts $\pm$ correspond to solutions of the twinning equation (2.2.34) given by Theorem 2.2.3 with $\kappa = \pm 1$ and

$$\lambda^* = \frac{1}{2}\left(1 - \sqrt{1 + \frac{2}{\delta}}\right), \tag{2.2.40}$$

so that $0 < \lambda^* < 1/2$. If equality holds in (2.2.35), then all solutions have $\lambda^* = 1/2$; if strict inequality holds in (2.2.36), then there are exactly two solutions, while if equality holds in (2.2.36) there is only one solution.

Proof. By Theorem 2.2.3 and the polar decomposition theorem, necessary and sufficient conditions that equation (2.2.34) has a solution with $\lambda = \lambda^*$ are that the eigenvalues $0 < \lambda_1 \leq \lambda_2 \leq \lambda_3$ of $C(\lambda^*)$ satisfy $\lambda_2 = 1$, $\lambda_1 > 0$ and $(\lambda_1 - 1)^2 + (\lambda_3 - 1)^2 \neq 0$.

Note that since $\det(U + \lambda a \otimes n) = \det U > 0$ for all λ the condition $\lambda_1 > 0$ is immediately satisfied. By Lemma 2.2.10, $g(\lambda) = \det(C(\lambda) - \mathbf{1})$ can be written as

$$g(\lambda) = a_0 + a_1\left(\lambda^2 - \lambda\right) \tag{2.2.41}$$

for some constants a_0, a_1 and, by direct calculation, we find that $a_0 = g(0) = \det(U^2 - \mathbf{1})$ and $a_1 = -\frac{dg}{d\lambda}(0) = -2a \cdot U\mathrm{cof}(U^2 - \mathbf{1})\, n$. Then, the condition that $C(\lambda^*)$ has an eigenvalue equal to 1 for some $\lambda^* \in (0,1)$ is that $g(\lambda^*) = 0$.

Setting $\delta = -\frac{a_1}{2a_0} = a \cdot U(U^2 - \mathbf{1})^{-1} n$, we see that $g(\lambda^*) = 0$ admits a solution $\lambda \in (0,1)$ provided that

$$\delta \leq -2$$

and, substituting back into g, we find that λ is given by

$$\lambda^{*2} - \lambda^* = \frac{1}{2\delta}. \tag{2.2.42}$$

Thus, by Lemma 2.2.11, the eigenvalues of $C(\lambda^*)$ satisfy $0 < \lambda_1 \leq \lambda_2 = 1 \leq \lambda_3$ if and only if (2.2.35) and (2.2.36) hold. The eigenvalues of $C(\lambda^*)$ cannot all be 1, as $C(\lambda^*) = \mathbf{1}$ would imply that for any vector e perpendicular to both Ua and n, $C(\lambda^*)\, e = U^2 e = e$. However, U^2 does not have an eigenvalue equal to 1.

If $\delta < -2$ then g has two distinct roots λ^* and $1 - \lambda^*$ with λ^* given by (2.2.40). By Lemma 2.2.11 equality holds in (2.2.36) if and only if, 1 is a double eigenvalue of $C(\lambda^*)$ which is impossible. This is because there would then exist a corresponding eigenvector e with $e \cdot n = 0$ such that

$$U^2 e + \lambda^*(Ua \cdot e)\, n = e.$$

Writing $(U^2 - \mathbf{1}) = \det(U^2 - \mathbf{1})\,\mathrm{cof}(U^2 - \mathbf{1})^{-1}$ and taking the dot product with Ua, we infer that

$$g(0)(Ua \cdot e) = -\frac{1}{2}\lambda^* \frac{dg}{d\lambda}(0)(Ua \cdot e).$$

Note that $Ua \cdot e \neq 0$ since, otherwise, U^2 would have an eigenvalue equal to 1. Hence,

$$a_0 = \frac{1}{2}\lambda^* a_1$$

which is only possible if $\lambda^* = \frac{1}{2}$ - a contradiction. Therefore, Theorem 2.2.3, gives four distinct solutions of (2.2.34).

If $\delta = -2$, then (2.2.42) gives $\lambda^* = \frac{1}{2}$. By Theorem 2.2.3, there are two solutions if strict inequality holds in (2.2.36) and one otherwise. □

Remark. We note that the the presentation of Ball and James [18] followed here completely recovers the predictions of the crystallographic (or phenomenological) theory of martensite developed, independently, by Bowles and MacKenzie [35] as well as Wechsler, Lieberman and Read [143] in the 1950s. Deriving the crystallographic theory as a consequence of energy minimization has several advantages, including the fact that we do not require the a priori knowledge of the twinning nodes and that it allows us to extend the theory much further than the austenite - finely twinned martensite interface; we do so with an austenite - parallelogram martensite interface in the subsequent chapter.

Having introduced the necessary terminology and main results, we end this chapter by briefly commenting on a geometrically linear version of the model presented here.

2.3 Variations of the Theory

The nonlinear elasticity model presented in this chapter is not the only one that has been suggested in order to predict the morphology of microstructure in crystalline solids. Most notably, Khatchaturyan, Roitburd and Shatalov (see e.g. [84]) have introduced another model based on linear elasticity which, although not physically linear, Ball and James [19] and Kohn [89] have shown that it can be thought of as a 'linearization' of the presented theory.

This geometrically linear version of the Ball and James model has been commonly used in the literature as it enables easier computations. Nevertheless, we do not extend further on this and for the purposes of this thesis only the nonlinear model is used. This is because, in linear elasticity not only the stress-strain relation but also rotations are linearized; this linearization of rigid body rotations results in non-physical 'phantom' stresses whereas, in nonlinear elasticity, a rigid body rotation correctly results in another stress-free state. Additionally, the nonlinear theory seems conceptually simpler and, thus, it is preferred. For a detailed comparison between the two models and their predictions, the reader is referred to Bhattacharya [27, 29]. We also note Ruddock [119] where an interesting comparison between the two models can be found regarding their predictions on the X-interface (described in [24]) and the wedge microstructure (analyzed in [25]).

Chapter 3

Non-classical and curved austenite-martensite interfaces

In Chapter 2, we saw how the nonlinear elasticity model can predict classical interfaces between austenite and martensite; these have been studied extensively in the literature [18, 19, 29]. On the other hand, the model allows for more complicated austenite-martensite interfaces in which the microstructure of martensite is not restricted to a simple laminate; such interfaces are called non-classical and will concern us in this chapter.

As a simple illustration, let us restrict attention to a planar interface, say $x \cdot m = k$. Suppose that the region below the interface, $x \cdot m < k$, is occupied by a pure phase of austenite, whilst a general microstructure of martensite, represented by a gradient Young measure ν occupies the region $x \cdot m > k$. For simplicity, suppose that the martensitic microstructure is homogeneous in the sense that $\bar{\nu} = F$ is constant in the region $x \cdot m > k$. For the microstructure of martensite to be energy-minimizing we must require that ν is supported on the set $K = \bigcup SO(3)\, U_i$ of martensitic energy wells, i.e. $\operatorname{supp} \nu \subset K$, which in turn implies that $\bar{\nu} = F \in K^{qc}$.

To make the overall deformation continuous across the planar interface we need to satisfy the Hadamard jump condition. Thus, for planar interfaces between austenite and a homogeneous microstructure of martensite, accounting for non-classical interfaces becomes equivalent to establishing rank-one connections between the austenite and the set K^{qc}, i.e. finding vectors b, m such that

$$\mathbf{1} + b \otimes m \in K^{qc}. \tag{3.0.1}$$

As we have seen, very little is known about quasiconvex hulls and predicting non-classical austenite-martensite interfaces becomes a very difficult task even in this simplified setting. If we allow the interface to be a general surface Γ and the

martensitic microstructure to depend on the position, we still need to require that $\bar{\nu}_x = Dy(x) \in K^{qc}$ almost everywhere but the jump condition no longer suffices; this will concern us in Section 3.4.

In Section 3.3, we aim to present an analysis of non-classical interfaces recently observed by Seiner et al. [123] in CuAlNi single crystals, undergoing a cubic-to-orthorhombic transition, the experimental observations being described in Section 3.2. We show that they can be described by the nonlinear elasticity model for martensitic transformations and we make some predictions regarding the volume fractions of the martensitic variants involved, as well as the habit plane normals.

In Section 3.4, we turn our attention to the issue of curved austenite-martensite interfaces where we present a method of constructing such interfaces as stress-free microstructures. To the best of the author's knowledge this is the first theoretical construction of such a curved interface. Before presenting these results we briefly recap the work of Ball and Carstensen [13, 14], who theoretically investigated non-classical austenite-martensite interfaces and studied the cubic-to-tetragonal case extensively.

3.1 Previous Work

The two-well problem for rank-one compatible wells satisfying a determinant constraint has been solved by Ball and James [19]. In this case, one may assume that the two wells, say $SO(3)U_1$, $SO(3)U_2$, are given by

$$U_1 = \operatorname{diag}(\eta_2, \eta_1, \eta_1), \quad U_2 = \operatorname{diag}(\eta_1, \eta_2, \eta_1).$$

Then, it can be shown that for $K = SO(3)U_1 \cup SO(3)U_2$,

$$K^{qc} = SO(3)\mathcal{F} \tag{3.1.1}$$

where $\mathcal{F}$ consists of all matrices $F \in M^{3\times 3}_+$, satisfying

$$F^T F = \begin{pmatrix} a & c & 0 \\ c & b & 0 \\ 0 & 0 & \eta_1^2 \end{pmatrix}$$

for some $a, b > 0$ such that

$$a + b \pm 2c \leq \eta_1^2 + \eta_2^2 \quad \text{and} \quad ab - c^2 = \eta_1^2 \eta_2^2.$$

Equivalently,

$$K^{qc} = \left\{ F \in M^{3\times 3} : \det F = \eta_1^2 \eta_2 \text{ and } |F(e_1 \pm e_2)|^2 \leq \eta_1^2 + \eta_2^2 \right\}.$$

Remark. The above sets coincide with $K^{(2)}$ - the set of second order laminates. A way of showing that K^{qc} is given by this set consists of constructing an appropriate polyconvex function which is zero precisely on the candidate set and then, the quasi-convex hull can be shown to be contained in this polyconvex set by showing that all its elements can be expressed as double laminates.

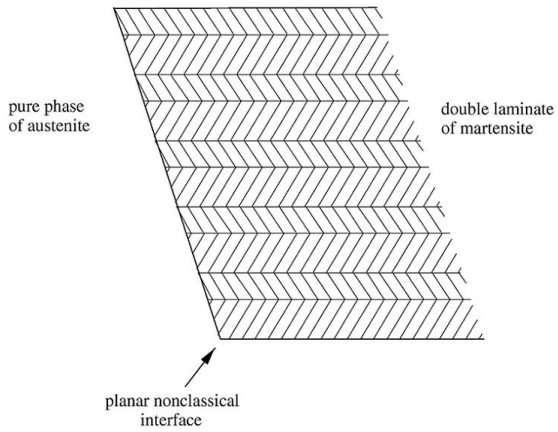

Figure 3.1: A typical double laminate in which the martensite consists of twins within twins with constant gradient on each sublayer (from [13]).

Through Theorem 2.2.3, Ball and Carstensen obtained solutions to (3.0.1) with K^{qc} as above. The set K^{qc} being much larger than K one expects to have many more possibilities for non-classical interfaces than classical ones. This is verified in Fig. 3.2, taken from [13], which shows the values of lattice parameters for which non-classical and classical interfaces are possible. It becomes clear that non-classical interfaces are indeed possible for a much larger set of lattice parameters η_1, η_2.

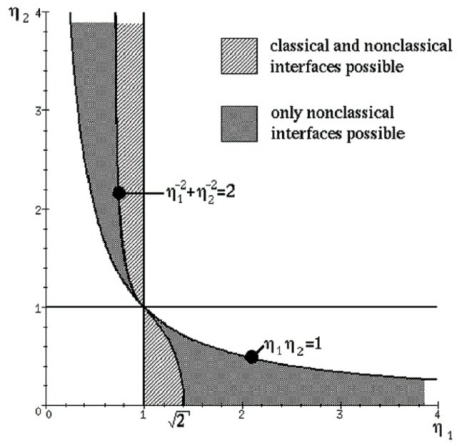

Figure 3.2: Lattice parameters (η_1, η_2) allowing non-classical interfaces.

Moreover, Ball and Carstensen showed that in the region where both classical and non-classical interfaces exist, the unit normals corresponding to the non-classical interfaces form four circular arcs on the unit sphere whose endpoints are precisely the eight habit plane normals of the classical theory as shown in Fig. 3.3.

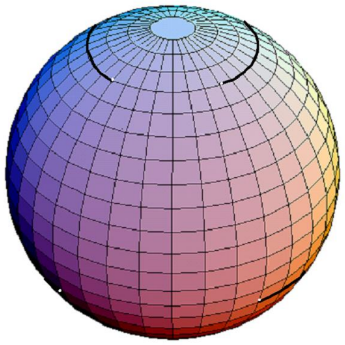

Figure 3.3: Non-classical interface normals, depicted on the unit sphere, for lattice parameters allowing for both classical and non-classical interfaces.

They also showed that the conditions on the lattice parameters allowing for non-classical interfaces remain the same even for the three-well problem [14], i.e. when

$$\begin{aligned} K &= \bigcup_{i=1}^{3} SO(3)\, U_i \quad \text{where} \\ U_1 &= \operatorname{diag}(\eta_2, \eta_1, \eta_1)\,,\ U_2 = \operatorname{diag}(\eta_1, \eta_2, \eta_1)\,,\ U_3 = \operatorname{diag}(\eta_1, \eta_1, \eta_2)\,. \end{aligned}$$

In particular, they showed that $\mathbf{1} + b \otimes m \in K^{qc} \Leftrightarrow \mathbf{1} + b \otimes m \in K^{pc} \Leftrightarrow \eta_1, \eta_2$ satisfy the same conditions as for the two wells. This is rather remarkable as neither knowledge of K^{qc} nor of K^{pc} is required.

The work of Ball and Carstensen remains theoretical as non-classical interfaces have not been observed in materials undergoing the appropriate transformations, e.g. cubic-to-tetragonal. Additionally, in Fig. 3.2, we note that for lattice parameters very close to 1 (which is typically the case) the region allowing for classical interfaces is much larger than that allowing for non-classical ones; this implies that for typical materials undergoing the cubic-to-tetragonal transition, non-classical interfaces might indeed not be preferable.

On the other hand, non-classical interfaces have been observed in materials with lower martensitic symmetry. For example, through a clever experimental procedure, Seiner and Landa [121] were able to observe a certain type of non-classical interface in a CuAlNi single crystal which is analyzed in the subsequent section. In the cubic-to-orthorhombic transformation of CuAlNi the number of martensitic variants is six

and their quasiconvex hull is far from known; as such, our analysis is not as sharp and general as that of Ball and Carstensen, though similarities can be drawn and interesting aspects are revealed.

3.2 Experimental Observations

The specimen examined was a 3.9×3.8×4.2mm rectangular parallelepiped of the austenitic phase of CuAlNi, cut from a single crystal of this alloy such that the normals to the specimen faces had approximately the principal crystallographic directions ⟨100⟩. The original single crystal was grown by a Bridgman method at the Institute of Physics ASCR in Prague. The specimen was subjected to the following sequence of mechanical and thermal loadings (see Fig. 3.4):

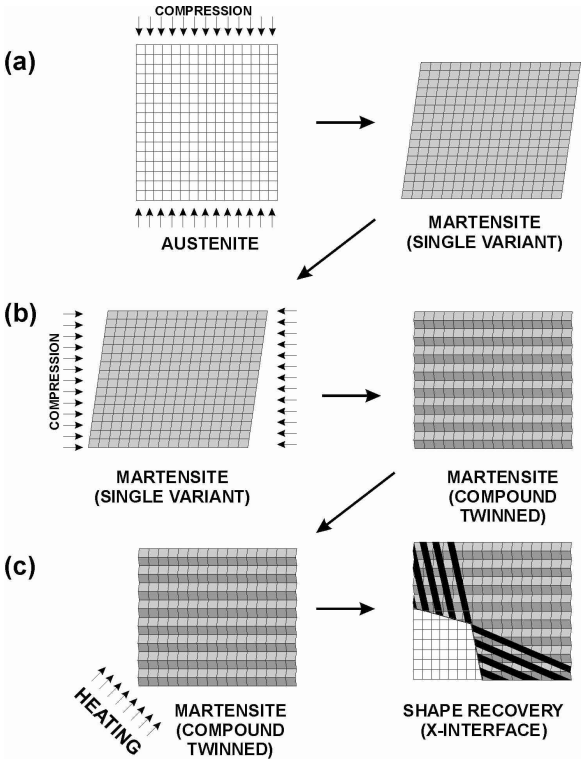

Figure 3.4: Outline of the experimental procedure.

(a) At room temperature, the specimen was transformed into a single variant of 2H martensite[1] by applying uniaxial compression (in a bench vice). Due to

[1]In Ramsdel's crystallographic notation, 2H martensite is the basic form of orthorhombic CuAlNi martensite with crystal symmetry represented by the point group P_{nmm} (for point group notation see e.g. Thurston [139]). This is the only martensitic phase which can be both stress-induced and temperature-induced.

an effect called *mechanical stabilization of martensite* (this will be explained in depth in Chapter 4), the specimen did not return to austenite after unloading, but remained as a single variant of martensite.

(b) The specimen was rotated by 90° and uniaxial compression was applied again. In this case, the loading induced the reorientation of martensite into another variant via compound twinning (for an analysis of the relation between the direction of applied compression and the activated twinning systems in CuAlNi, see [109]). The reorientation was not fully completed. Instead, the loading was interrupted at the moment when the specimen contained comparable volume fractions of both variants. By such a procedure, we obtain a finely compound twinned specimen.

(c) The finely compound twinned specimen was heated from one side using a gas lighter, which induced the shape-recovery process, i.e. the thermally driven return of the specimen into austenite. As the compound twins cannot form any compatible interface with austenite, the transition was achieved by formation of an *interfacial* microstructure, interpolating between the mechanically stabilized martensite (the compound twins) and austenite, ensuring their compatible connection. This interfacial microstructure was formed by Type-II twins crossing the original compound microstructure and getting arranged into a so called X-interface (for more details of formation of X-interfaces in CuAlNi see [123], for the theoretical analysis of this microstructure, see [119]). By removing the heating in the middle of the course of the transition, the interfacial microstructure was stopped, and the non-classical interfaces between austenite and the two mutually crossing systems of twins (compound and Type- II) were observable by optical microscopy. An example is given in Fig. 3.5.

This procedure was repeated several times, which enabled the capturing of several optical micrographs of the non-classical interfaces. An interesting observation was that, as shown in Fig. 3.6, the interface between the austenite and the system of crossing twins was never exactly planar, but rather slightly curved. This results from the fact that the pattern of compound twins induced in the specimen by the uniaxial compression in stage (b) of the experimental procedure is never exactly homogeneous. With varying volume fraction of the compound twins, the admissible orientation of the habit plane varies as well, as will be shown in the theoretical analysis given in the following section.

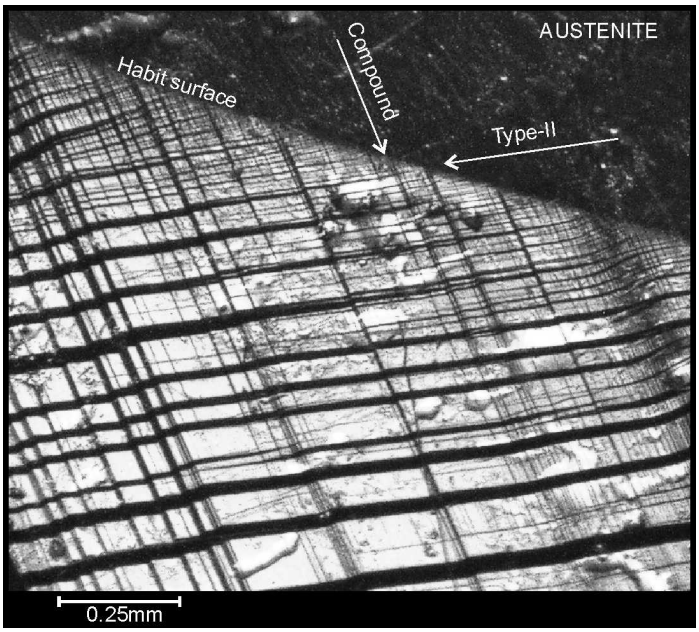

Figure 3.5: Optical micrograph of a non-classical interface between austenite and a martensitic microstructure. The arrows indicate the orientations of twinning planes of Type-II and compound twinning systems.

3.3 An Analysis of Non-Classical Austenite-Martensite Interfaces

We now present an analysis for the above non-classical austenite-martensite interface via the nonlinear elasticity model presented in Chapter 2. We note that, with lattice parameters α, β and γ, the martensitic variants for the cubic-to-orthorhombic transition are given by

$$U_1 = \begin{pmatrix} \beta & 0 & 0 \\ 0 & \frac{\alpha+\gamma}{2} & \frac{\alpha-\gamma}{2} \\ 0 & \frac{\alpha-\gamma}{2} & \frac{\alpha+\gamma}{2} \end{pmatrix} \qquad U_2 = \begin{pmatrix} \beta & 0 & 0 \\ 0 & \frac{\alpha+\gamma}{2} & \frac{\gamma-\alpha}{2} \\ 0 & \frac{\gamma-\alpha}{2} & \frac{\alpha+\gamma}{2} \end{pmatrix}$$

$$U_3 = \begin{pmatrix} \frac{\alpha+\gamma}{2} & 0 & \frac{\alpha-\gamma}{2} \\ 0 & \beta & 0 \\ \frac{\alpha-\gamma}{2} & 0 & \frac{\alpha+\gamma}{2} \end{pmatrix} \qquad U_4 = \begin{pmatrix} \frac{\alpha+\gamma}{2} & 0 & \frac{\gamma-\alpha}{2} \\ 0 & \beta & 0 \\ \frac{\gamma-\alpha}{2} & 0 & \frac{\alpha+\gamma}{2} \end{pmatrix} \tag{3.3.1}$$

$$U_5 = \begin{pmatrix} \frac{\alpha+\gamma}{2} & \frac{\alpha-\gamma}{2} & 0 \\ \frac{\alpha-\gamma}{2} & \frac{\alpha+\gamma}{2} & 0 \\ 0 & 0 & \beta \end{pmatrix} \qquad U_6 = \begin{pmatrix} \frac{\alpha+\gamma}{2} & \frac{\gamma-\alpha}{2} & 0 \\ \frac{\gamma-\alpha}{2} & \frac{\alpha+\gamma}{2} & 0 \\ 0 & 0 & \beta \end{pmatrix}.$$

Remark. As before, let (U_I, U_J) denote a twin between variants U_I and U_J. Then the twins (U_1, U_2), (U_3, U_4) and (U_5, U_6) are compound, whereas, twinning systems between any other two variants can be either of Type-I or Type-II.

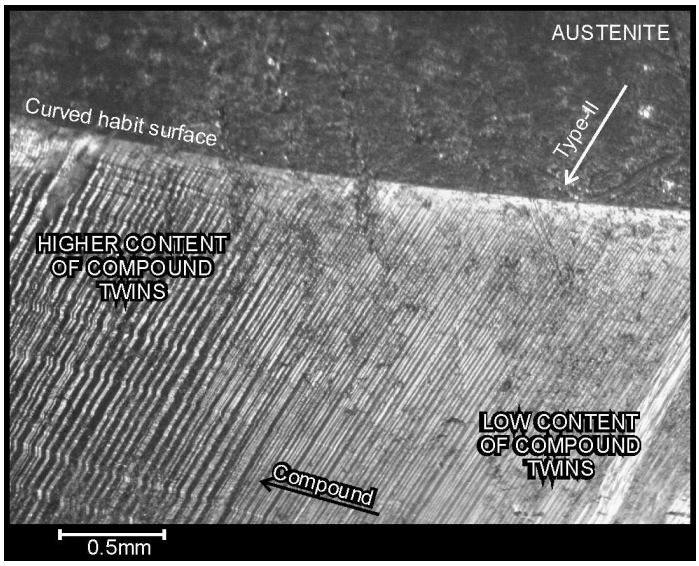

Figure 3.6: Curved interface between crossing twins and austenite resulting from the inhomogeneity of compound twinning. (Optical microscopy.)

We start by presenting a lemma in [119] which will prove to be pivotal for the analysis that follows.

Lemma 3.3.1. *Suppose that x_i and y_i are non-zero vectors with $i = 1, 2, 3$ and that $\sum_{i=1}^{3} x_i \otimes y_i = 0$. Then, both $\{x_1, x_2, x_3\}$ and $\{y_1, y_2, y_3\}$ are sets of coplanar vectors and at least one is a set of parallel vectors.*

We now concentrate on the martensite phase and we construct the microstructure consisting of compound and Type-II twin crossings, as shown in Fig. 3.7.

For the parallelogram microstructure we assume that (U_B, U_A) is a Type-II twin and the variants $U_{A'}$ and $U_{B'}$ are their respective compound counterparts, i.e. both $(U_{A'}, U_A)$ and $(U_{B'}, U_B)$ are compound twinning systems. From the remark following (3.3.1) it is trivial to see that $(U_{B'}, U_{A'})$ can also form a Type-II twin.

When discussing the parallelogram microstructure in Chapter 2 we saw that the compatibility equations deriving from Hadamard's jump condition are given by

$$R_{AB}U_B - U_A = b_{AB} \otimes n_{AB} \tag{3.3.2}$$

$$R_{A'B'}U_{B'} - U_{A'} = b_{A'B'} \otimes n_{A'B'} \tag{3.3.3}$$

$$R_{AA'}U_{A'} - U_A = b_{AA'} \otimes n_{AA'} \tag{3.3.4}$$

$$R_{BB'}U_{B'} - U_B = b_{BB'} \otimes n_{BB'} \tag{3.3.5}$$

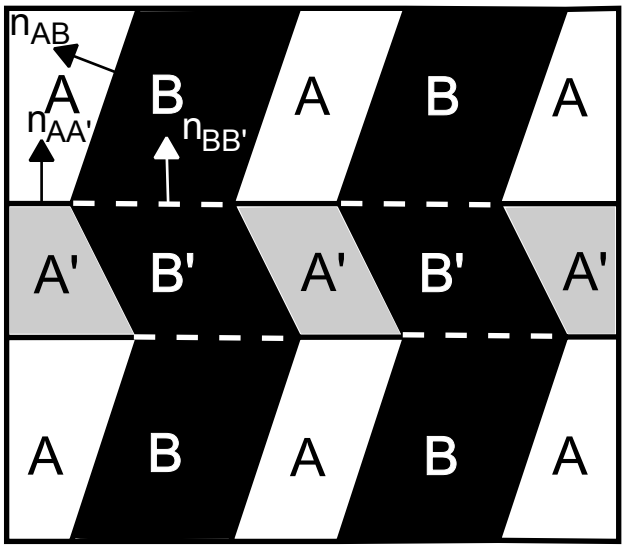

Figure 3.7: Parallelogram microstructure

where b_{IJ} and n_{IJ} are, respectively, the shearing vector and normal to the twinning plane for the system of variants U_I and U_J and R_{IJ} denotes the mutual rotation between variants U_I and U_J.

In Fig. 3.7 we note an important fact; namely, that the normals $n_{AA'}$ and $n_{BB'}$ to the two compound systems satisfy

$$n_{AA'} = n_{BB'}.$$

This relation follows from the experimental observations and it is not only in accordance with the theory but, more importantly, the theory necessitates it. This is a consequence of Lemma 2.2.8 and we shall comment on this further, once we establish the compatibility of the above parallelogram microstructure.

In addition to the compatibility equations (3.3.2)-(3.3.5), we also saw that there are two other conditions for the parallelogram microstructure to be compatible; namely that $R_{AB}R_{BB'} = R_{AA'}R_{A'B'}$ and that n_{AB}, $n_{A'B'}$, $n_{AA'}$ and $n_{BB'}$ are coplanar vectors. In fact, the former relation implies the latter and a necessary and sufficient condition for the entire parallelogram microstructure to be compatible is simply that

$$R_{AB}R_{BB'} = R_{AA'}R_{A'B'}. \tag{3.3.6}$$

The necessity of (3.3.6) is clear, since both sides describe the mutual rotation between U_A and $U_{B'}$. On the other hand, sufficiency follows from the fact that (3.3.2)-(3.3.5) imply that the normals n_{AB}, $n_{A'B'}$, $n_{AA'}$ and $n_{BB'}$ are coplanar. To see this, simply

pre-multiply (3.3.3) by $R_{AA'}$ and use the equality (3.3.6) to get that

$$R_{AB}R_{BB'}U_{B'} - R_{AA'}U_{A'} = R_{AA'}b_{A'B'} \otimes n_{A'B'}.$$

Substitute for $R_{AA'}U_{A'}$ and $R_{BB'}U_{B'}$ from (3.3.4) and (3.3.5) respectively to get that $R_{AB}U_B - U_A + R_{AB}b_{BB'} \otimes n_{BB'} - b_{AA'} \otimes n_{AA'} - R_{AA'}b_{A'B'} \otimes n_{A'B'} = 0$. Then, using (3.3.2), we deduce that

$$b_{AB} \otimes n_{AB} + R_{AB}b_{BB'} \otimes n_{BB'} - b_{AA'} \otimes n_{AA'} - R_{AA'}b_{A'B'} \otimes n_{A'B'} = 0. \tag{3.3.7}$$

Given that $n_{AA'} = n_{BB'}$, Lemma 3.3.1 simply says that $\{n_{AA'}, n_{BB'}, n_{AB}, n_{A'B'}\}$ must be coplanar. We note this equation, as we will use it again shortly.

Before forming the interface, we show the compatibility of the parallelogram microstructure between the Type-II and compound twinning systems. At the same time, we also turn our attention to the conditions of Lemma 2.2.8 on the parallelogram microstructure. The first condition requires that the four martensitic variants are distinct which is trivially true from our assumptions on the variants. From now on we write $Q = Q[\phi, e]$ for the anticlockwise rotation Q by angle ϕ about the axis e. In the subsequent parts, we shall denote vectors by e_k; these should not be confused with the standard basis vectors denoted in this thesis by i_k. Firstly, from Table A in Appendix A, note that there always exists a rotation $Q = Q[\pi, e_1] \in L^a$, the austenitic Laue group, such that $QU_AQ = U_B$ and $QU_{A'}Q = U_{B'}$ and this rotation is unique. As (U_B, U_A) as well as $(U_{B'}, U_{A'})$ form Type-II twins, from Mallard's law,

$$b_{AB} = \rho U_A e_1 \quad \text{and} \quad n_{AB} = 2\rho^{-1}\left(e_1 - \frac{U_A^2 e_1}{|U_A e_1|^2}\right) \tag{3.3.8}$$

where ρ is a factor chosen to make n_{AB} of unit length; clearly, for the twinning solutions to the system between variants $U_{A'}$ and $U_{B'}$, we simply replace U_A by $U_{A'}$ in (3.3.8). What is more, from Table A, there is precisely one rotation $R = R[\pi, e_2] \in L^a$ such that $RU_AR = U_{A'}$ and $RU_BR = U_{B'}$. In general, as $(U_{A'}, U_A)$ and $(U_{B'}, U_B)$ form compound twinning systems, there are two rotations in L^a for each of the pairs $(U_{A'}, U_A)$ and $(U_{B'}, U_B)$ taking U_A to $U_{A'}$ and similarly U_B to $U_{B'}$. However, in view of Lemma 2.2.8 and the experimental observations, we require that $n_{AA'} = n_{BB'}$; this forces us to consider the unique common rotation $R = R[\pi, e_2]$, so that

$$n_{AA'} = n_{BB'} = e_2 \tag{3.3.9}$$

and then

$$b_{AA'} = 2\left(\frac{U_A^{-1}e_2}{|U_A^{-1}e_2|^2} - U_A e_2\right) \quad \text{and} \quad b_{BB'} = 2\left(\frac{U_B^{-1}e_2}{|U_B^{-1}e_2|^2} - U_B e_2\right). \tag{3.3.10}$$

We note that the existence of these rotations is also a condition of Lemma 2.2.8.

Through a careful examination of the appropriate rotations in Appendix A, it can also be checked that whenever (U_B, U_A) is a Type-II twin and $U_{A'}$, $U_{B'}$ are their compound counterparts, the vectors e_1 and e_2 above always satisfy

$$e_1 \cdot e_2 = 0 \tag{3.3.11}$$

and $e_3 \cdot U_A^2 e_1 \neq 0$ for a vector e_3 perpendicular to both e_1 and e_2 provided that $\beta^2 \neq (\alpha^2 + \gamma^2)/2$; this is true for Seiner's specimen and the remaining conditions of Lemma 2.2.8 are satisfied[2].

It can then be checked that for the above solutions of the twinning equations, $R_{AB}R_{BB'} = R_{AA'}R_{A'B'}$. The simplest way to see this is the following: by Corollary 2.2.7, we deduce that the triple $(QR_{AA'}Q, Qb_{AA'}, Qn_{AA'})$ is the solution to the equation $R_{BB'}U_{B'} - U_B = b_{BB'} \otimes n_{BB'}$ so that, staying consistent with our choice of solutions, $QR_{AA'}Q = R_{BB'}$. Similarly, for the Type-II solutions, we deduce that $RR_{AB}R = R_{A'B'}$. Therefore,

$$R_{AA'}R_{A'B'} = R_{AB}R_{BB'} \Leftrightarrow R_{AA'}RR_{AB}R = R_{AB}QR_{AA'}Q.$$

Moreover, writing

$$Q = -\mathbf{1} + 2e_1 \otimes e_1, \quad R = -\mathbf{1} + 2e_2 \otimes e_2,$$

and using the fact that $e_1 \cdot e_2 = 0$, a simple calculation reveals that $RQ = QR$. We may now utilize Corollary 2.2.6 to get that, with our choice of solutions,

$$\begin{aligned} R_{AA'} &= (-\mathbf{1} + \frac{2}{|U_A^{-1}e_2|^2} U_A^{-1}e_2 \otimes U_A^{-1}e_2)R \\ R_{AB} &= (-\mathbf{1} + \frac{2}{|U_A e_1|^2} U_A e_1 \otimes U_A e_1)Q. \end{aligned}$$

Combining with the fact that $RQ = QR$, we infer that $R_{AA'}R_{A'B'} = R_{AB}R_{BB'}$ if and only if the matrices

$$-\mathbf{1} + \frac{2}{|U_A^{-1}e_2|^2} U_A^{-1}e_2 \otimes U_A^{-1}e_2 \quad \text{and} \quad -\mathbf{1} + \frac{2}{|U_A e_1|^2} U_A e_1 \otimes U_A e_1$$

[2]Simply note that e_2 is always one of the standard basis vectors of $\mathbb{R}^3$ whereas e_1 is of the form $i_k \pm i_l$ where i_k, i_l are the other two basis vectors, e.g. for $A = 1$, $B = 4$ say, $A' = 2$ and $B' = 3$ and $e_1 = (i_1 + i_2)/\sqrt{2}$ whereas $e_2 = i_3$ so that $e_1 \cdot e_2 = 0$. It is also easy to check that, for any choice of variants, the expression $e_3 \cdot U_A^2 e_1$ reduces to $\beta^2 - (\alpha^2 + \gamma^2)/2$. For instance, in the previous example, $e_3 = (i_1 - i_2)/\sqrt{2}$ and $U_1^2 e_1 = (2\beta^2 i_1 + (\alpha^2 + \gamma^2)i_2 + (\alpha^2 - \gamma^2)i_3)/2\sqrt{2}$, i.e. $e_3 \cdot U_1^2 e_1 = (2\beta^2 - \alpha^2 - \gamma^2)/4$.

commute. However, this is trivially the case due to (3.3.11); then all the compatibility equations for the parallelogram microstructure are satisfied and the constructed microstructure is indeed compatible.

We also remarked that, under our assumed variants and twinning solutions, all the conditions of Lemma 2.2.8 are satisfied. Hence, the lemma says that there are indeed solutions to the compatibility equations for the parallelogram microstructure between the assumed variants. By Lemma 2.2.8 we also deduce that these solutions necessarily alternate between a Type-I and a Type-II twin interface and the Type-I interfaces (here compound) are in the same plane; hence the requirement $n_{AA'} = n_{BB'}$ is justified. Note that having fixed the unique rotation $R = R[\pi, e_2]$ such that $RU_AR = U_{A'}$ and $RU_BR = U_{B'}$, it is the interpretation of the twinning systems as 'Type-I' twins in Mallard's law[3] that returned the correct normals. Indeed, were they not compound, Lemma 2.2.8 would have forced us to consider the twinning solutions corresponding to the Type-I system and, hence, the solutions with $n_{AA'} = n_{BB'}$ so that the Type-I systems are in the same plane. This is a rather remarkable agreement between theory and experiments.

Forming the Interface

We now wish to construct the non-classical interface between the homogeneous parallelogram microstructure and the pure phase of austenite. We stress that, for the time being, we are only concerned with the homogeneous microstructure and we therefore exclude the possibility of a curved interface. Let

$$M_{AB}(\lambda) = (1-\lambda)U_A + \lambda R_{AB}U_B \tag{3.3.12}$$

$$M_{A'B'}(\lambda) = (1-\lambda)U_{A'} + \lambda R_{A'B'}U_{B'} \tag{3.3.13}$$

represent the macroscopic deformation gradients corresponding to the Type-II structures. We note that the geometry of the parallelogram structure requires that the Type-II volume fraction λ be the same in (3.3.12) and (3.3.13).

Assume that the compound volume fraction of variant $U_{A'}$ in U_A, as well as that of $U_{B'}$ in U_B, is Λ. Then, the macroscopic deformation gradient of the entire microstructure is given by

$$M(\lambda, \Lambda) = (1-\Lambda)M_{AB}(\lambda) + \Lambda R_{AA'}M_{A'B'}(\lambda). \tag{3.3.14}$$

[3]Since these are compound twins both solutions can be interpreted as either a Type-I or a Type-II twin. Here, by a 'Type-I' twin we mean the first solution (2.2.19) in Theorem 2.2.5.

Whether the interface between the parallelogram microstructure and the austenite can be formed is a question of finding λ and Λ such that the middle eigenvalue of $M^T(\lambda,\Lambda)M(\lambda,\Lambda)$ is equal to 1, which is equivalent to finding rank-one connections between the austenite and $SO(3)M(\lambda,\Lambda)$. In particular, we require that

$$\det(M^T(\lambda,\Lambda)M(\lambda,\Lambda)-\mathbf{1})=0. \tag{3.3.15}$$

We note that the above determinant is a priori a sixth order polynomial in both λ and Λ and in order to solve it we need to simplify it. Thus, we start by proving some key results that, though simple, will be essential in the subsequent calculations.

We first show that $\det M_{A'B'}(\lambda)=\det M_{AB}(\lambda)$. This is trivially true since the compatibility equations (3.3.2)-(3.3.5) imply that $M_{AB}(\lambda)$, $M_{A'B'}(\lambda)\in K^{(1)}$, the set of first order laminates, and the function $\det : M^{3\times 3}\to\mathbb{R}$ is quasiaffine. However, we follow a more basic approach which provides us with more and much needed information. Consider equation (3.3.2); then

$$R_{AB}U_B=U_A(1+U_A^{-1}b_{AB}\otimes n_{AB})$$

and by taking determinants, we obtain

$$\det U_B=\det U_A(1+U_A^{-1}b_{AB}\cdot n_{AB}).$$

Clearly $\det U_B=\det U_A$ and thus,

$$U_A^{-1}b_{AB}\cdot n_{AB}=0. \tag{3.3.16}$$

That is, $\det M_{AB}(\lambda)=\det U_A\det\left(1+\lambda U_A^{-1}b_{AB}\otimes n_{AB}\right)=\det U_A$ and similarly, $\det M_{A'B'}(\lambda)=\det U_{A'}=\det U_A$ for all $\lambda\in[0,1]$, i.e. $\det M_{A'B'}(\lambda)=\det M_{AB}(\lambda)$. This result has a simple physical interpretation. Since the determinants have the meaning of volume change and the microstructures M_{AB} and $M_{A'B'}$ are just mixtures of variously rotated single variants, the volume must remain the same.

Also, by (3.3.7) and the fact that $n_{AA'}=n_{BB'}$,

$$(b_{AA'}-R_{AB}b_{BB'})\otimes n_{AA'}-b_{AB}\otimes n_{AB}+R_{AA'}b_{A'B'}\otimes n_{A'B'}=0.$$

The normals cannot all be parallel and hence, by Lemma 3.3.1, we deduce that

$$b_{AA'}-R_{AB}b_{BB'}\parallel b_{AB}\parallel R_{AA'}b_{A'B'}. \tag{3.3.17}$$

Hence, there exists some η such that

$$\eta b_{AB}=b_{AA'}-R_{AB}b_{BB'}, \tag{3.3.18}$$

which needs to be determined. Using Corollary 2.2.6, we can identify the rotation R_{AB} as

$$R_{AB} = \left(-\mathbf{1} + \frac{2}{|U_A e_1|^2} U_A e_1 \otimes U_A e_1\right) Q, \tag{3.3.19}$$

where $Q = Q[\pi, e_1] \in L^a$ is the unique rotation such that both $QU_AQ = U_B$ and $QU_{A'}Q = U_{B'}$. As for the solutions to the twinning equations (3.3.4), Corollary 2.2.7 says that the triple $(QR_{AA'}Q, Qb_{AA'}, Qn_{AA'})$ is a solution to (3.3.5). In particular,

$$Qb_{BB'} \otimes Qn_{BB'} = b_{AA'} \otimes n_{AA'}. \tag{3.3.20}$$

We wish to calculate the expression $R_{AB}b_{BB'}$. Writing $Q = -\mathbf{1} + 2e_1 \otimes e_1$, it is easy to see that $Qn_{BB'} = -e_2 = -n_{AA'}$ simply by substituting $n_{BB'} = e_2$ and using (3.3.11). Then, (3.3.20) immediately gives $Qb_{BB'} = -b_{AA'}$; substituting back in the expression for R_{AB} and using the fact that $b_{AB} = \rho U_A e_1$,

$$R_{AB}b_{BB'} = b_{AA'} - \frac{2}{|b_{AB}|^2}(b_{AA'} \cdot b_{AB})\, b_{AB}.$$

Then,

$$\eta = \frac{2}{|b_{AB}|^2} b_{AA'} \cdot b_{AB}. \tag{3.3.21}$$

Our goal is to deduce an expression for $\det(M^T(\lambda, \Lambda) M(\lambda, \Lambda) - 1)$ which will enable us to find solutions of (3.3.15) for $(\lambda, \Lambda) \in [0,1] \times [0,1]$. To this end we seek a rank-one connection between $M_{AB}(\lambda)$ and $M_{A'B'}(\lambda)$. Indeed, using (3.3.6) and equations (3.3.2)-(3.3.5),

$$R_{AA'}M_{A'B'}(\lambda) - M_{AB}(\lambda) = (1-\lambda) b_{AA'} \otimes n_{AA'} + \lambda R_{AB} b_{BB'} \otimes n_{BB'}.$$

Since $n_{AA'} = n_{BB'}$, and using (3.3.18), we infer that

$$R_{AA'}M_{A'B'}(\lambda) - M_{AB}(\lambda) = b_*(\lambda) \otimes n_{AA'}, \tag{3.3.22}$$

where $b_*(\lambda) = b_{AA'} - \lambda\eta b_{AB}$. Next, combining (3.3.22) and (3.3.14),

$$M(\lambda, \Lambda) = M_{AB}(\lambda) + \Lambda b_*(\lambda) \otimes n_{AA'}$$

and using the expression for $M_{AB}(\lambda)$ we deduce that

$$M(\lambda, \Lambda) = U_A + \lambda b_{AB} \otimes n_{AB} + \Lambda b_*(\lambda) \otimes n_{AA'}. \tag{3.3.23}$$

Finally, we note that $\det M(\lambda, \Lambda) = \det U_A$. This is again immediate since for each $\lambda \in [0,1]$, $\operatorname{rank}(R_{AA'}M_{A'B'}(\lambda) - M_{AB}(\lambda)) = 1$, i.e. $M(\lambda, \Lambda) \in K^{(2)}$ and, in

particular, satisfies the determinant constraint. On the other hand, to extract more information, we also have that

$$\det\, M(\lambda,\Lambda) = \det\, M_{AB}(\lambda) \det\left(1 + \Lambda\, M_{AB}^{-1}(\lambda)\, b_*(\lambda) \otimes n_{AA'}\right).$$

However, from (3.3.22), we see that

$$R_{AA'} M_{A'B'}(\lambda) = M_{AB}(\lambda)\left(1 + M_{AB}^{-1}(\lambda)\, b_*(\lambda) \otimes n_{AA'}\right)$$

and taking determinants,

$$\det\, M_{A'B'}(\lambda) = \det\, M_{AB}(\lambda)\left(1 + M_{AB}^{-1}(\lambda)\, b_*(\lambda) \cdot n_{AA'}\right).$$

Since $\det\, M_{A'B'}(\lambda) = \det\, M_{AB}(\lambda)$, it follows that for all $\lambda \in [0,1]$,

$$M_{AB}^{-1}(\lambda)\, b_*(\lambda) \cdot n_{AA'} = 0. \tag{3.3.24}$$

We now concentrate on the non-classical interface where we follow an approach very similar to that of Ball and James [18]. Firstly, we present a result which enables us to solve (3.3.15), i.e. $\det\left(M^T M - \mathbf{1}\right) = 0$.

Lemma 3.3.2. *Let* $g(\lambda,\Lambda) = \det\left(M^T(\lambda,\Lambda)\, M(\lambda,\Lambda) - \mathbf{1}\right)$. *Then,* $g(\lambda,\Lambda)$ *is at most a quadratic function of* λ *and* Λ *such that*

$$g(1-\lambda,\Lambda) = g(\lambda,\Lambda) \quad \textit{and} \quad g(\lambda,1-\Lambda) = g(\lambda,\Lambda).$$

Proof. Since $\det\, M(\lambda,\Lambda) = \det\, U_A$, by factoring M^T out of the determinant,

$$g(\lambda,\Lambda) = \det U_A \det(M(\lambda,\Lambda) - M^{-T}(\lambda,\Lambda))$$

and we calculate $M(\lambda,\Lambda) - M^{-T}(\lambda,\Lambda)$. Making use of the expression for $M(\lambda,\Lambda)$ and (3.3.24) - after a short calculation - we obtain

$$M^{-T}(\lambda,\Lambda) = M_{AB}^{-T}(\lambda) - \Lambda M_{AB}^{-T}(\lambda)\, n_{AA'} \otimes M_{AB}^{-1}(\lambda)\, b_*(\lambda).$$

Similarly, using the expression for $M_{AB}(\lambda)$ in (3.3.12) and (3.3.16), one finds that

$$M_{AB}^{-1}(\lambda) = U_A^{-1} - \lambda U_A^{-1} b_{AB} \otimes U_A^{-1} n_{AB}.$$

Combining the last two equations and after a short calculation, we deduce that

$$\begin{aligned} M^{-T}(\lambda,\Lambda) \;=\; & U_A^{-1} - \lambda U_A^{-1} n_{AB} \otimes U_A^{-1} b_{AB} - \Lambda U_A^{-1} n_{AA'} \otimes U_A^{-1} b_{AA'} \\ & + \Lambda\lambda U_A^{-1} n_{AA'} \otimes U_A^{-1} b_{AB} (U_A^{-1} n_{AB} \cdot b_{AA'} + \eta). \end{aligned} \tag{3.3.25}$$

Above we have used the fact that

$$U_A^{-1} n_{AA'} \cdot b_{AB} = 0; \tag{3.3.26}$$

this is trivial since $n_{AA'} = e_2$, $b_{AB} = \rho U_A e_1$ and in (3.3.11) we established that $e_1 \cdot e_2 = 0$. Using the expressions for M and M^{-T} we infer that

$$g(\lambda, \Lambda) = \det(A_0 + \lambda A_1 + \Lambda A_2 + \lambda\Lambda A_3), \tag{3.3.27}$$

where

$$\begin{aligned} A_0 &= U_A^2 - 1 \\ A_1 &= U_A b_{AB} \otimes n_{AB} + n_{AB} \otimes U_A^{-1} b_{AB} \\ A_2 &= U_A b_{AA'} \otimes n_{AA'} + n_{AA'} \otimes U_A^{-1} b_{AA'} \\ A_3 &= -(U_A^{-1} n_{AB} \cdot b_{AA'} + \eta) n_{AA'} \otimes U_A^{-1} b_{AB} \\ &\quad -\eta U_A b_{AB} \otimes n_{AA'}. \end{aligned} \tag{3.3.28}$$

Note that for fixed λ, the expression multiplying Λ is of rank two and similarly, for fixed Λ, the expression multiplying λ is of the same rank. Hence, g only contains terms with λ and Λ of powers no greater than two. Then,

$$\begin{aligned} g(\lambda, \Lambda) &= \alpha + \beta\lambda + \gamma\Lambda + a\lambda^2 + b\Lambda^2 + c\lambda\Lambda + d\lambda\Lambda^2 \\ &\quad + e\lambda^2\Lambda + f\lambda^2\Lambda^2. \end{aligned} \tag{3.3.29}$$

The above expression simplifies further by noting that for all $\Lambda \in (0, 1)$,

$$g(0, \Lambda) = g(1, \Lambda) \tag{3.3.30}$$

and, respectively, for all $\lambda \in (0, 1)$,

$$g(\lambda, 0) = g(\lambda, 1). \tag{3.3.31}$$

These are not trivial to obtain; however, using Corollary 2.2.7, it becomes simple. As far as (3.3.30) is concerned, Corollary 2.2.7 says that $U_B + \Lambda b_{BB'} \otimes n_{BB'} = QU_AQ + \Lambda Q b_{AA'} \otimes Q n_{AA'}$ where $Q = Q[\pi, e_1]$ is such that $QU_BQ = U_A$ and $QU_{B'}Q = U_{A'}$. Then, by (3.3.6) and (3.3.14)

$$\begin{aligned} M^T(1, \Lambda) M(1, \Lambda) &= (U_B + \Lambda n_{BB'} \otimes b_{BB'})(U_B + \Lambda b_{BB'} \otimes n_{BB'}) \\ &= Q(U_A + \Lambda n_{AA'} \otimes b_{AA'})(U_A + \Lambda n_{AA'} \otimes b_{AA'}) Q \\ &= QM^T(0, \Lambda) M(0, \Lambda) Q. \end{aligned}$$

In turn, (3.3.30) is trivially implied. Similarly, (3.3.31), is obtained by considering the unique rotation $R = R[\pi, e_2]$ such that $RU_AR = U_{A'}$ and $RU_BR = U_{B'}$.

Corollary 2.2.7 now says that $U_{A'} + \lambda b_{A'B'} \otimes n_{A'B'} = RU_AR + \lambda R b_{AB} \otimes Rn_{AB}$, i.e.

$$\begin{aligned} M^T(\lambda,1)\,M(\lambda,1) &= (U_{A'} + \lambda n_{A'B'} \otimes b_{A'B'})\,(U_{A'} + \lambda b_{A'B'} \otimes n_{A'B'}) \\ &= R\,(U_A + \lambda n_{AB} \otimes b_{AB})\,(U_A + \lambda n_{AB} \otimes b_{AB})\,R \\ &= RM^T(\lambda,0)\,M(\lambda,0)\,R, \end{aligned}$$

proving (3.3.31). Next, from equations (3.3.29)-(3.3.31) we may write g as

$$g(\lambda,\Lambda) = a_0 + a_1(\lambda^2 - \lambda) + a_2(\Lambda^2 - \Lambda) + a_3(\lambda^2 - \lambda)(\Lambda^2 - \Lambda). \tag{3.3.32}$$

for some constants a_i, $i = 0, \ldots, 3$ and the lemma is proved. □

Making use of equations (3.3.27) and (3.3.32) we may specify the coefficients a_0, a_1, a_2, a_3 in the expression for $g(\lambda,\Lambda)$. Firstly,

$$a_0 = g(0,0) = \det(U_A^2 - 1). \tag{3.3.33}$$

Also $a_1 = -\frac{\partial g}{\partial \lambda}(0,0)$, $a_2 = -\frac{\partial g}{\partial \Lambda}(0,0)$ and, after a simple calculation, we deduce that

$$a_1 = -2b_{AB} \cdot U_A \mathrm{cof}(U_A^2 - 1)n_{AB} \quad \text{and} \tag{3.3.34}$$

$$a_2 = -2b_{AA'} \cdot U_A \mathrm{cof}(U_A^2 - 1)n_{AA'}. \tag{3.3.35}$$

As for the last coefficient, we note that $a_3 = \frac{\partial^2 g}{\partial\lambda\partial\Lambda}(0,0) = \nabla_{A_2}\mathrm{cof}\,A_0 \cdot A_1 + \mathrm{cof}\,A_0 \cdot A_3$ where, for a matrix A, ∇_A denotes the derivative in the direction of A. This expression becomes too involved when expanded and, alternatively, we write this as

$$a_3 = 4\left(\frac{\partial g}{\partial \lambda}(0,1/2) + a_1\right) = 4\mathrm{cof}(A_0 + \frac{1}{2}A_2) \cdot (A_1 + \frac{1}{2}A_3) + 4a_1 \tag{3.3.36}$$

which is an easier expression for computations.

Remark. We note that for $\Lambda = 0$, only the Type-II structure is present in the martensitic configuration. The Type-II system can form a compatible interface with the identity and, in this case, one obtains

$$g(\lambda,0) = a_0 + a_1(\lambda^2 - \lambda).$$

Trivially this becomes zero for $\lambda^2 - \lambda = -\frac{a_0}{a_1}$; we denote this solution $\lambda = k^* \in (0, 1/2]$ and we note that it agrees with the value of the classical volume fraction obtained in Theorem 2.2.12.

Finding solutions to the equation $g(\lambda,\Lambda)=0$ provides us with the pairs (λ,Λ) that make an eigenvalue of $M^T(\lambda,\Lambda)M(\lambda,\Lambda)$ equal to one. Nevertheless, to apply Theorem 2.2.3 we need to make sure that this is the middle eigenvalue.

Lemma 3.3.3. *Suppose that for some* $(\lambda^*,\Lambda^*)\in[0,1]\times[0,1]$, $M^T(\lambda^*,\Lambda^*)M(\lambda^*,\Lambda^*)$ *has the unordered triple of eigenvalues* 1, λ_1, λ_3. *Then,* λ_1 *and* λ_3 *bound* 1 *from above and below if and only if,*

$$\begin{aligned}\operatorname{tr}U_A^2-\det U_A^2 \quad -2 \quad &+(\lambda^{*\,2}-\lambda^*)\left|b_{AB}\right|^2+(\Lambda^{*\,2}-\Lambda^*)\left|b_{AA'}\right|^2\\ &+\quad (\lambda^{*\,2}-\lambda^*)(\Lambda^{*\,2}-\Lambda^*)\eta^2\left|b_{AB}\right|^2\geq 0.\end{aligned}\tag{3.3.37}$$

Proof. It is the middle eigenvalue of $M^T(\lambda^*,\Lambda^*)M(\lambda^*,\Lambda^*)$ which is equal to 1 if and only if $(1-\lambda_1)(\lambda_3-1)\geq 0$, i.e. if and only if

$$\operatorname{tr}M^T(\lambda^*,\Lambda^*)M(\lambda^*,\Lambda^*)-\det M^T(\lambda^*,\Lambda^*)M(\lambda^*,\Lambda^*)-2\geq 0.$$

We have already seen that $\det M^TM=\det U_A^2$ and it remains to calculate the expression for the trace. Note that, using the compatibility equations,

$$U_B^2=(U_A+n_{AB}\otimes b_{AB})(U_A+b_{AB}\otimes n_{AB}).$$

Taking traces and noting that, since U_A and U_B are symmetry related, $\operatorname{tr}U_B^2=\operatorname{tr}U_A^2$,

$$0=2U_Ab_{AB}\cdot n_{AB}+|b_{AB}|^2\tag{3.3.38}$$

and, by (3.3.38), it becomes straightforward to see that

$$\operatorname{tr}M_{AB}^T(\lambda)M_{AB}(\lambda)=\operatorname{tr}U_A^2+\left(\lambda^2-\lambda\right)|b_{AB}|^2.\tag{3.3.39}$$

However, we know that $M_{A'B'}(\lambda)=M_{AB}(\lambda)+b_*(\lambda)\otimes n_{AA'}$ and that for $R=R[\pi,e_2]$, $RM_{A'B'}(\lambda)R=M_{AB}(\lambda)$; in particular, they are symmetry related. Then, in a fashion almost identical to the case of the twinning system (U_B,U_A) above, we deduce that

$$0=2M_{AB}^T(\lambda)b_*(\lambda)\cdot n_{AA'}+|b_*(\lambda)|^2.\tag{3.3.40}$$

As $M(\lambda,\Lambda)=M_{AB}(\lambda)+\Lambda b_*(\lambda)\otimes n_{AA'}$, we find that

$$\begin{aligned}\operatorname{tr}M^TM &= \operatorname{tr}M_{AB}^T(\lambda)M_{AB}(\lambda)+2\Lambda M_{AB}(\lambda)b_*(\lambda)\cdot n_{AA'}+\Lambda^2|b_*(\lambda)|^2\\ &= \operatorname{tr}U_A^2+\left(\lambda^2-\lambda\right)|b_{AB}|^2+\left(\Lambda^2-\Lambda\right)|b_*(\lambda)|^2.\end{aligned}$$

Finally, $b_*(\lambda) = b_{AA'} - \lambda\eta b_{AB}$ where $\eta = \frac{2}{|b_{AB}|^2} b_{AA'} \cdot b_{AB}$ and therefore,

$$|b_*(\lambda)|^2 = |b_{AA'}|^2 + \left(\lambda^2 - \lambda\right)\eta^2 |b_{AB}|^2.$$

Substituting into the expression for $\operatorname{tr} M^T M$ we infer the result. □

We may now state and prove the theorem regarding the existence of rank-one connections between the parallelogram microstructure and $SO(3)$ for a cubic-to-orthorhombic transition; that is, the existence of a map $R(\lambda, \Lambda) \in SO(3)$ and non-zero vector-valued $c(\lambda, \Lambda)$, $p(\lambda, \Lambda)$ with $|p(\lambda, \Lambda)| = 1$ that solve the habit plane equation:

$$M(\lambda, \Lambda) = R(\lambda, \Lambda)(1 + c(\lambda, \Lambda) \otimes p(\lambda, \Lambda)) \quad \forall \lambda \in [0, 1]. \tag{3.3.41}$$

For the purposes of the following theorem we wish to exclude solutions of (3.3.41) with $\lambda = 0$ or $\lambda = 1$. Such solutions correspond to interfaces between a compound twinning system and austenite which, in accordance with Seiner's specimen, we assume are not possible. On the contrary, we assume that the Type-II systems can indeed form compatible interfaces with austenite.

Theorem 3.3.4. *Let $M(\lambda, \Lambda)$ be as in (3.3.14). Suppose that the compatibility equations (3.3.2)-(3.3.5) as well as (3.3.6) hold with $n_{AA'} = n_{BB'}$ and that the lattice parameters are such that $2\beta^2 + \alpha^2 + \gamma^2 \neq 4$. Further assume that the Type-II twins (U_B, U_A), $(U_{B'}, U_{A'})$ can form compatible interfaces with austenite, i.e. the conditions of Theorem 2.2.12 are satisfied with $U_A = U$, $U_B = V$ and with $U_{A'} = U$, $U_{B'} = V$ and that*

$$\frac{a_1}{a_3} \notin [0, 1/4]. \tag{3.3.42}$$

If $a_0 a_3 \neq a_1 a_2$, necessary and sufficient conditions for equation (3.3.41) to admit solutions satisfying $\lambda^* \in (0, 1)$ for all $\Lambda^* \in [0, 1]$ are

$$0 < \frac{4a_0 - a_2}{4a_1 - a_3} \leq \frac{1}{4} \tag{3.3.43}$$

and

$$\begin{aligned} \operatorname{tr} U_A^2 - \det U_A^2 \quad -2 \quad & +(\lambda^{*\,2} - \lambda^*)\,|b_{AB}|^2 + (\Lambda^{*\,2} - \Lambda^*)\,|b_{AA'}|^2 \\ + \quad & (\lambda^{*\,2} - \lambda^*)(\Lambda^{*\,2} - \Lambda^*)\eta^2\,|b_{AB}|^2 \geq 0 \end{aligned} \tag{3.3.44}$$

for all (λ^*, Λ^*) such that

$$\lambda^{*2} - \lambda^* = -\frac{a_0 + a_2(\Lambda^{*2} - \Lambda^*)}{a_1 + a_3(\Lambda^{*2} - \Lambda^*)}. \tag{3.3.45}$$

For each $\Lambda^* \in (0,1/2)\cup(1/2,1)$, there are four distinct solutions to (3.3.41) provided that strict inequality holds in (3.3.44). These are given by

$$\begin{aligned}
&\left(R_1, \lambda^*, \Lambda^*, c_1^+ \otimes p_1^+\right), \\
&\left(R_2, \lambda^*, \Lambda^*, c_1^- \otimes p_1^-\right), \\
&\left(R_3, 1-\lambda^*, \Lambda^*, c_2^+ \otimes p_2^+\right), \\
&\left(R_4, 1-\lambda^*, \Lambda^*, c_2^- \otimes p_2^-\right),
\end{aligned} \tag{3.3.46}$$

where the superscripts $\pm$ correspond to solutions of the twinning equation given by Theorem 2.2.3 with $\kappa = \pm 1$ and

$$\lambda^* = \frac{1-\sqrt{1-4\frac{a_0+a_2(\Lambda^{*2}-\Lambda^*)}{a_1+a_3(\Lambda^{*2}-\Lambda^*)}}}{2} \in (0,1/2]\,. \tag{3.3.47}$$

If for some $\Lambda^* \in (0,1/2)\cup(1/2,1)$ equality holds in (3.3.44) then there are precisely two solutions, one with Type-II volume fraction λ^* and one with $1-\lambda^*$. If in addition strict inequality holds in (3.3.43), there are four distinct solutions with $\Lambda^* = 1/2$ provided that strict inequality holds in (3.3.44) and two otherwise; if equality holds in (3.3.43), there are two solutions with $\Lambda^* = 1/2$ when strict inequality holds in (3.3.44) and one otherwise. At $\Lambda = 0$ or $\Lambda = 1$, Theorem 2.2.12 applies.

On the other hand, if $a_0 a_3 = a_1 a_2$, necessary and sufficient conditions for equation (3.3.41) to admit solutions satisfying $\lambda^* \in (0,1)$ for all $\Lambda^* \in [0,1]$ are

$$0 < \frac{a_0}{a_1} \leq \frac{1}{4} \tag{3.3.48}$$

and (3.3.44) with $\Lambda^* \in [0,1]$ and

$$\lambda^{*2} - \lambda^* = -\frac{a_0}{a_1}.$$

Then, for each $\Lambda^* \in [0,1]$ there are four distinct solutions to the habit plane equation (3.3.41) satisfying $\lambda^* = k^*$, with k^* the classical volume fraction, provided that strict inequality holds in (3.3.44) and $a_0/a_1 \neq 1/4$. If equality holds either in (3.3.44) or (3.3.48) there are two solutions and one if equality holds in both.

Proof. For notational convenience let $C(\lambda^*,\Lambda^*) = M^T(\lambda^*,\Lambda^*)(\lambda^*,\Lambda^*)$; we follow a proof on the lines of Theorem 2.2.12. By Theorem 2.2.3 and the polar decomposition theorem, necessary and sufficient conditions that equation (3.3.41) has a solution with $(\lambda,\Lambda) = (\lambda^*,\Lambda^*)$ are that the eigenvalues $\lambda_1 \leq \lambda_2 \leq \lambda_3$ of $C(\lambda^*,\Lambda^*)$ satisfy $\lambda_2 = 1$, $\lambda_1 > 0$ and $(\lambda_1-1)^2 + (\lambda_3-1)^2 \neq 0$. Since $\det M(\lambda^*,\Lambda^*) = \det U_A > 0$, the

condition $\lambda_1 > 0$ is immediately satisfied and, if $\lambda_2 = 1$, the condition $2\beta^2+\alpha^2+\gamma^2 \neq 4$ on the lattice parameters guarantees that λ_1 and λ_3 cannot both be 1.

To see this, suppose that $C(\lambda^*, \Lambda^*) = \mathbf{1}$ and consider the vector e_1 appearing in the defining formula for b_{AB} and n_{AB} in (3.3.8). Then, e_1 is a unit vector parallel to $U_A^{-1} b_{AB}$ for which (3.3.16) and (3.3.26) say that $U_A^{-1} b_{AB} \cdot n_{AB} = U_A^{-1} b_{AB} \cdot n_{AA'} = 0$. Then, it is easy to check that

$$\begin{aligned} e_1 &= C(\lambda^*, \Lambda^*)\, e_1 \\ &= U_A^2 e_1 + \lambda (U_A b_{AB} \cdot e_1)\, n_{AB} + \Lambda (U_A b_{AA'} \cdot e_1)\, n_{AA'} - \Lambda\lambda\eta (U_A b_{AB} \cdot e_1)\, n_{AA'} \end{aligned}$$

and taking the inner product with e_1, we deduce that

$$1 = U_A^2 e_1 \cdot e_1.$$

The vector e_1 is unique once the variants are fixed and, by a close investigation of the relevant rotations in Appendix A, we deduce that this amounts to $2\beta^2 + \alpha^2 + \gamma^2 = 4$, a contradiction[4].

Hence, we need only show that (3.3.43) and (3.3.44) are equivalent to $\lambda_2 = 1$; note that, once an eigenvalue of $C(\lambda^*, \Lambda^*)$ is 1, Lemma 3.3.3 establishes (3.3.44) as both necessary and sufficient for that eigenvalue to be the middle one. We now claim that, under our assumptions, (3.3.43) is equivalent to $C(\lambda, \Lambda)$ having an eigenvalue equal to 1 for each $\Lambda^* \in [0, 1]$ and λ^* satisfying (3.3.45) or equivalently, that $g(\lambda^*, \Lambda^*) = 0$ where by Lemma 3.3.2, $g(\lambda, \Lambda) = \det(C(\lambda, \Lambda) - 1)$ can be written as

$$g(\lambda, \Lambda) = a_0 + a_1\left(\lambda^2 - \lambda\right) + a_2\left(\Lambda^2 - \Lambda\right) + a_3\left(\lambda^2 - \lambda\right)\left(\Lambda^2 - \Lambda\right).$$

Suppose that $a_0 a_3 \neq a_1 a_2$; by (3.3.42) and the fact that $\Lambda^2 - \Lambda \in [-1/4, 0]$ whenever $\Lambda \in [0, 1]$, the expression $a_1 + a_3(\Lambda^2 - \Lambda)$ is non-zero. Then, letting

$$f(\Lambda) = \frac{a_0 + a_2(\Lambda^2 - \Lambda)}{a_1 + a_3(\Lambda^2 - \Lambda)},$$

we deduce that

$$g(\lambda^*, \Lambda^*) = 0 \Leftrightarrow \lambda^{*2} - \lambda^* + f(\Lambda^*) = 0.$$

But $\lambda^2 - \lambda + f(\Lambda) = 0$ admits solutions in $(0, 1)$ for all $\Lambda \in [0, 1]$ if and only if

$$0 < f(\Lambda) \leq \frac{1}{4} \quad \text{for all } \Lambda \in [0, 1], \tag{3.3.49}$$

[4]For example, suppose that $A = 1$ or $A = 2$; depending on the choice of B, the vector e_1 is given by $(i_1 \pm i_2)/\sqrt{2}$ or $(i_1 \pm i_3)/\sqrt{2}$. A quick calculation shows that, in all cases, $U_A^2 e_1 \cdot e_1 = (2\beta^2+\alpha^2+\gamma^2)/4$. The symmetry of the martensitic variants might convince the reader that this remains true for all other choice of A.

since the case $f(\Lambda^*) = 0$ amounts to $\lambda^* = 1$ or $\lambda^* = 0$ and it is thus excluded.

The necessity of (3.3.43) is now trivial as it corresponds to $0 < f(1/2) \leq 1/4$; as for the sufficiency, note that the conditions on the compatibility of the Type-II structures with the austenite (see Theorem 2.2.12) require that $\delta \leq -2$; but this is equivalent to

$$0 < \frac{a_0}{a_1} = f(0) = f(1) \leq \frac{1}{4},$$

where we exclude the case $f(0) = f(1) = 0$ as it amounts to $a_0 = \det(U_A^2 - \mathbf{1}) = 0$ and hence to the variant U_A having an eigenvalue equal to 1, contradicting the assumptions of Theorem 2.2.12. However,

$$f'(\Lambda) = \frac{(2\Lambda - 1)(a_1 a_2 - a_0 a_3)}{(a_1 + a_3(\Lambda^2 - \Lambda))^2}$$

which is always well-defined by (3.3.42) and becomes zero precisely at $\Lambda = 1/2$ with a constant and opposite sign in the intervals $[0, 1/2)$ and $(1/2, 1]$. In particular, this means that for any $\Lambda \in [0, 1]$,

$$f(\Lambda) \in \left[\frac{a_0}{a_1}, \frac{4a_0 - a_2}{4a_1 - a_3}\right] \quad \text{or} \quad f(\Lambda) \in \left[\frac{4a_0 - a_2}{4a_1 - a_3}, \frac{a_0}{a_1}\right], \tag{3.3.50}$$

depending on which one is greater. In either case, (3.3.49) follows.

Hence, (3.3.43) is sufficient for $g(\lambda, \Lambda) = 0$ to admit solutions λ^*, $1 - \lambda^* \in (0, 1)$ for all $\Lambda^* \in [0, 1]$, these being given by

$$\lambda^* = \frac{1 - \sqrt{1 - 4f(\Lambda^*)}}{2}.$$

Note that the solutions λ^* and $1 - \lambda^*$ are distinct for any $\Lambda^* \in (0, 1)$ except possibly at $\Lambda^* = 1/2$. This is because the solutions being distinct for some Λ is equivalent to $f(\Lambda) \neq 1/4$. To reach a contradiction suppose that, without loss of generality, there exists $\Lambda_0 \in (0, 1/2)$ such that $f(\Lambda_0) = 1/4$. Then, since f is bounded between its values at 0 and $1/2$, it must be the case that $f(0) = 1/4$ or $f(1/2) = 1/4$; in either case, by an application of Rolle's theorem, we deduce that there exists some $\Lambda_1 \in (0, \Lambda_0)$ or $\Lambda_1 \in (\Lambda_0, 1/2)$ such that $f'(\Lambda_1) = 0$; but this contradicts the fact that for $a_1 a_2 \neq a_0 a_3$, the only root of f' is at $1/2$. In particular, if strict inequality holds in (3.3.43), the solutions must be distinct for $\Lambda^* = 1/2$ and thus for all $\Lambda^* \in (0, 1)$.

The solutions are then given by Theorem 2.2.3 and for all $\Lambda^* \in (0, 1)$ they have the form (3.3.46) if strict inequality holds in (3.3.43) and (3.3.44), whereas, if equality holds in (3.3.44), they reduce to two solutions - one for each Type-II volume fraction. If equality holds in (3.3.43), the only difference is at $\Lambda^* = 1/2$, where there are two

solutions if strict inequality holds in (3.3.44) and one otherwise. At the points $\Lambda^* = 0$ and $\Lambda^* = 1$, the structure of the solutions is governed by Theorem 2.2.12 as these cases correspond to classical interfaces between a Type-II structure and austenite.

Finally, we treat the non-generic case $a_0 a_3 = a_1 a_2$. Note that since U_A does not have an eigenvalue equal to 1, $a_0 \neq 0$ and writing $a_3 = a_1 a_2 / a_0$, we find that $g(\lambda, \Lambda) = 0$ if and only if

$$\left(a_0 + a_1\left(\lambda^2 - \lambda\right)\right)\left(a_0 + a_2\left(\Lambda^2 - \Lambda\right)\right) = 0. \tag{3.3.51}$$

Since $a_1/a_3 \notin [0, 1/4]$, we immediately infer that

$$\frac{a_0}{a_2} \notin [0, 1/4]$$

and $a_0 + a_2(\Lambda^2 - \Lambda) \neq 0$ for all $\Lambda \in [0, 1]$. Thus, by (3.3.51), $g(\lambda, \Lambda) = 0$ admits solutions λ^* and $1 - \lambda^* \in (0, 1)$ for all $\Lambda^* \in [0, 1]$ if and only if

$$a_0 + a_1\left(\lambda^{*2} - \lambda^*\right) = 0$$

admits solutions in $(0, 1)$. However, from the classical case, we have seen that this is possible if and only if $\delta \leq -2$ in Theorem 2.2.12 which is equivalent to (3.3.48). Then (3.3.51) admits two solutions with $\lambda^* = k^*$ and k^* as in the classical case. These solutions are distinct if and only if strict inequality holds in (3.3.48).

By Lemma 3.3.3, equation (3.3.41) admits solutions for all $\Lambda^* \in [0, 1]$ if and only if (3.3.48) holds as well as (3.3.44) with $\lambda^{*2} - \lambda^* = -a_0/a_1$. There are four solutions if strict inequality holds in (3.3.44) and (3.3.48), two if equality holds in either and one if equality holds in both. □

The algebra for the cubic-to-orthorhombic transformation gets too involved and we are unable to provide explicit formulae for the habit plane normal p and shearing vector c in (3.3.41). For this reason, we proceed numerically.

Numerical Simulation

For the remainder of this section we present a numerical calculation where, in accordance with [120], the lattice parameters for CuAlNi are chosen to be $\alpha = 1.06372$, $\beta = 0.91542$ and $\gamma = 1.02368$. The martensitic variants used are the ones obtained from the experimental observations; that is, $A = 3$, $B = 6$ with $A' = 4$, $B' = 5$ their compound counterparts. Following the above analysis, we calculated the zeros of g,

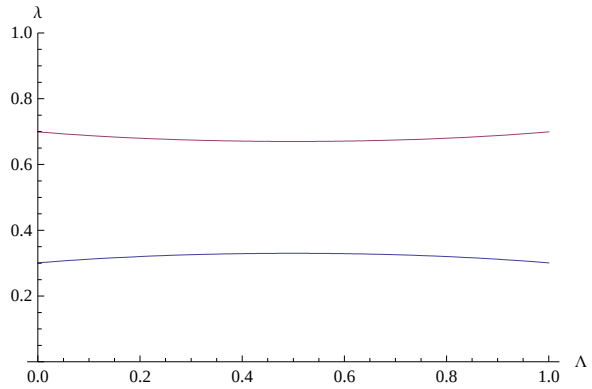

Figure 3.8: Values of λ that make the interface possible for $0 \leq \Lambda \leq 1$.

i.e. the values of (λ, Λ) that allow the interface to occur. Relations (3.3.42)-(3.3.44) were satisfied and we plotted λ against Λ as shown in Fig. 3.8.

It is easily seen that the value of λ does not change significantly from k^*, corresponding to the classical interface between the Type-II twinning system and the austenite, i.e. $\Lambda = 0$. This is rather promising as in the experimental observations it seems that the only significant variation is found in the compound volume fraction.

Moreover, using the algebraic procedure of Theorem 2.2.3, we calculated the different normals $m(\lambda, \Lambda)$ for (λ, Λ) on the curves of Fig. 3.8 and a plot of these is given in Fig. 3.9, where the normals are depicted as points on the unit sphere. These normals lie on four curves on the unit sphere whose endpoints correspond to the eight possible normals of classical interfaces between the Type-II twinning structures and the austenite, i.e. four normals for the interface between M_{AB} and the austenite (corresponding to $\Lambda = 0$) and another four normals for the interface between $M_{A'B'}$ and the austenite (corresponding to $\Lambda = 1$). We note that, unlike the admissible normals to non-classical interfaces in the two-well problem investigated by Ball and James [13], these curves do not form arcs of circles but rather, they form normals to a developable surface.

Concluding remarks

To the best of the author's knowledge, such non-classical interfaces have never been observed or analyzed before[5]. By discarding the inhomogeneity of the microstructure, in this section, we have shown that these are consistent with the commonly accepted nonlinear elasticity model for an arbitrary volume fraction of the compound laminate.

[5]We note that Q.P. Sun [131, 130] has observed different austenite-martensite interfaces in CuAlNi which are strongly deformed and non-planar.

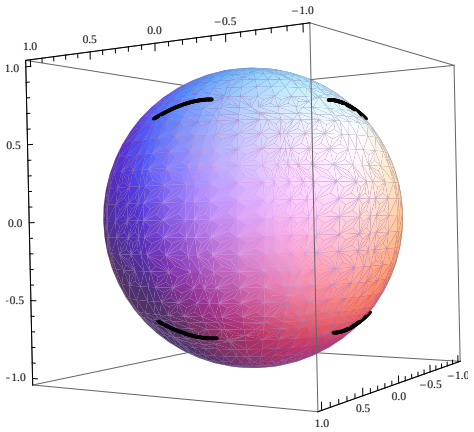

Figure 3.9: Plot of the unit normals $p(\lambda, \Lambda)$ in the compatibility equation (3.3.41) for (λ, Λ) as in Fig. 3.8.

Since the relation (3.3.45) between the compound volume fraction Λ and the volume fraction λ of the Type-II laminates, compatibly intersecting the compound twins, was derived analytically for a general cubic-to-orthorhombic transition, the analysis can be easily applied to predict the existence of similar non-classical interfaces in any other shape-memory alloy with the same class of transition (e.g. CuAlMn) as well as for materials undergoing cubic-to-tetragonal transitions (since the tetragonal symmetry is a member of the orthorhombic symmetry class.)

Moreover, the numerical simulations carried out reveal that the habit plane orientation depends on the compound volume fraction for the CuAlNi alloy. This finding is consistent with the optical observations of slightly curved non-classical interfaces between austenite and the twin-crossing microstructure with heterogeneous compound volume fraction (Fig. 3.6). In the following section we investigate the possibility of the occurrence of a curved interface.

3.4 Theoretical Construction of a Curved Interface

The curved interfaces observed by Seiner result from the fact that the pattern of compound twins is never exactly homogeneous, i.e. the compound volume fraction varies as a function of the position vector. The analysis provided in Section 3.3 admits an exact relation between the Type-II and the compound volume fractions

which allows for the habit plane interface. In order to predict the curved interface as a stress-free microstructure there are two obvious approaches.

Firstly, one might be tempted to simply let the compound volume fraction Λ vary in a suitable way as a function of the position, i.e. $\Lambda = \Lambda(x)$. Then all other quantities which depend on the compound volume fraction will also become functions of x. One difficulty with this approach is that we do not yet know of an appropriate version of the Hadamard jump condition between the inhomogeneous martensite and the austenite which ensures that the overall deformation remains continuous across a non-planar interface. Such a condition will be proved shortly and leads to a relation between the two gradients at either side of the interface given by $\mathbf{1}$ and $R(x)M(x)$, respectively, where $R : \Omega \to SO(3)$ is such that, at each x_0 on the interface, $R(x_0)$ solves the habit plane equation

$$R(x_0)M(x_0) = 1 + c(x_0) \otimes p(x_0) \quad \text{for some } c,\, p \in C^0(\mathbb{R}^3, \mathbb{R}^3).$$

However, the cubic-to-orthorhombic transition of CuAlNi, results in such complicated algebra that even the task of determining whether $R(x)M(x)$ is a gradient, and consequently the entire approach, becomes intractable.

The second possibility is an argument that would compatibly 'patch' together homogeneous regions of parallelogram microstructures with different volume fractions and, by applying the analysis of the homogeneous case in each 'patch', one would hope that this will result in a piecewise planar interface, separating the austenite and a piecewise constant gradient. Then, in some appropriate limit, one would expect to have constructed a curved interface. Even in its simplest form of only two regions (see Fig. 3.10), this construction requires the simultaneous compatibility of two parallelogram regions, each being compatible with the identity and with very special mutual rotations so that these add up to the identity. In this simple case, an analysis similar to that of Section 3.3 is still possible and formulae are simplified considerably; however, not enough to allow us to check for solutions analytically. Instead, numerical simulations indicate that for a wide range of realistic lattice parameters this interface cannot be constructed stress-free. In fact, the construction of the interface fails quickly as even the non-trivial compatibility of two parallelogram microstructures seems to be impossible. The analysis, apart from being inconclusive, contains tedious calculations and we shall not elaborate any further.

As explicit attempts to construct the curved interface of Seiner's experiment in a compatible way seem to be either intractable or impossible, in this section, we shall

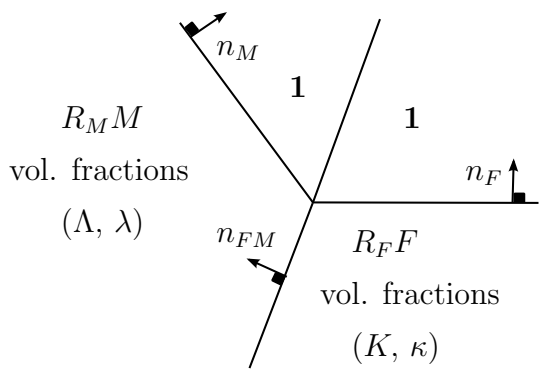

(a) $R_M M - \mathbf{1} = b_M \otimes n_M$

(b) $R_F F - \mathbf{1} = b_F \otimes n_F$

(c) $R_{FM} M - F = b_{FM} \otimes n_{FM}$

(d) $R_F^T R_M = R_{FM}$

Figure 3.10: Schematic depiction of a possible piecewise planar interface between two parallelogram microstructures of martensite M and F and austenite. For non-zero vectors b_M, b_F, b_{FM} and rotations R_M, R_F, R_{FM}, relations (a), (b), (c) and (d) are necessary for the kinematic compatibility of this construction.

employ a theoretical approach to prove the existence of a stress-free curved austenite-martensite interface in a rather more general fashion and for some appropriate set K of martensitic wells - to the best of the author's knowledge, this is the first theoretical construction of such a curved austenite-martensite interface.

As we alluded to at the beginning of this section, for the construction of a curved austenite-martensite interface, the classical Hadamard jump condition will no longer suffice. Below, we state and prove an appropriate modification that serves for the purposes of the construction that follows. However, we first clarify the notation and terminology to be used.

Notation/Terminology.

- Let $k > 0$. A domain Ω is of class C^k if for each $\xi \in \partial\Omega$ there exist $r > 0$, a Cartesian coordinate system in $B(\xi, r)$, with coordinates $(\bar{x}, x_d)$ where $\bar{x} = (x_1, \ldots, x_{d-1})$, and a C^k function $g : \mathbb{R}^{d-1} \to \mathbb{R}$ such that

$$\begin{aligned} \Omega \cap B(\xi, r) &= \{x \in B(\xi, r) \,:\, x_d > g(\bar{x})\}\,, \\ \partial\Omega \cap B(\xi, r) &= \{x \in B(\xi, r) \,:\, x_d = g(\bar{x})\}\,. \end{aligned}$$

  Interchangeably, we may refer to Ω simply as a C^k domain, locally C^k or a domain with a C^k boundary (respectively Lipschitz).

- A $(d-1)$-surface Γ is a connected, relatively compact manifold of dimension $d-1$ embedded in $\mathbb{R}^d$ such that $\Gamma = \text{int}\Gamma$, in the sense that every point of Γ has an open neighbourhood in Γ homeomorphic to a ball in $\mathbb{R}^{d-1}$. We say that

a $(d-1)$-surface Γ is of class C^k if for each $\xi \in \Gamma$ there exist $r > 0$, a Cartesian coordinate system in $B(\xi, r)$, with coordinates $(\bar{x}, x_d)$, and a C^k function $g : \mathbb{R}^{d-1} \to \mathbb{R}$ such that

$$\Gamma \cap B(\xi, r) = \{x \in B(\xi, r) \,:\, x_d = g(\bar{x})\}.$$

We note that the reference to the dimension may be dropped when this is obvious and, similarly to the definition of a C^k domain, we may refer to Γ as a locally C^k or simply C^k surface.

- We say that a function $y : \Omega \to \mathbb{R}$ belongs to the space $C^1\left(\overline{\Omega}\right)$, if $y \in C^1(\Omega)$ and y can be extended to a continuously differentiable function in an open set containing $\overline{\Omega}$. A map $y = (y_1, \ldots, y_d) : \Omega \to \mathbb{R}^d$ is in the space $C^1\left(\overline{\Omega}, \mathbb{R}^d\right)$ if $y_i \in C^1\left(\overline{\Omega}\right)$ for all $i = 1, \ldots, d$.

- Lastly, we remind the reader that throughout this thesis the term *domain* is reserved for an open and connected set.

Theorem 3.4.1. *(Modified jump condition) Let $d \geq 2$. Let $\Omega \subset \mathbb{R}^d$ be a bounded C^1 domain and suppose that Ω can be written in the form $\Omega = \Omega^+ \cup \Omega^- \cup \Gamma$ where Ω^+, Ω^- are disjoint open sets and $\Gamma = \Omega \cap \partial\Omega^+ = \Omega \cap \partial\Omega^-$ is a $(d-1)$-surface which is locally C^1. Further, assume that $y^{\pm} \in C^1\left(\overline{\Omega^{\pm}}, \mathbb{R}^d\right)$ and let $n \in C\left(\Gamma, \mathbb{R}^d\right)$ be the outward unit normal to Γ with respect to Ω^+. There exists a map $z \in W^{1,\infty}\left(\Omega, \mathbb{R}^d\right)$ such that*

$$Dz(x) = \begin{cases} Dy^+(x), & x \in \Omega^+ \\ \\ Dy^-(x), & x \in \Omega^-, \end{cases}$$

if and only if,

$$Dy^+(x) = Dy^-(x) + a(x) \otimes n(x) \tag{3.4.1}$$

for all $x \in \Gamma$ and some $a \in C\left(\Gamma, \mathbb{R}^d\right)$.

Remark. Under the hypotheses of Theorem 3.4.1, Ω^+ and Ω^- locally lie on either side of the surface Γ.

For the construction of the curved austenite-martensite interface we will be interested in the special case where, say, $Dy^- = \mathbf{1}$ represents the pure phase of austenite, whereas Dy^+ represents a microstructure of martensite, i.e. $Dy^+(x)$ is almost everywhere equal to the centre of mass of a gradient Young measure supported on an appropriate set K of martensitic wells; see Figure 3.11.

Before proving Theorem 3.4.1, we present a lemma which is used in the proof.

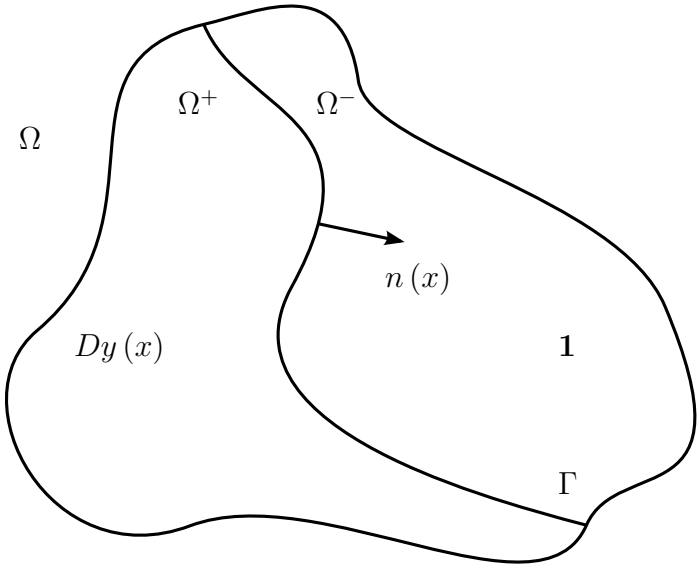

Figure 3.11: Schematic depiction of a deformation gradient Dz taking the values Dy and $\mathbf{1}$ on either side of a curved interface Γ; for an austenite-martensite interface $Dy \in K^{qc}$ a.e. for some appropriate set K of martensitic wells. The deformation z remains continuous across Γ provided that $Dy\,(x) = \mathbf{1} + a\,(x) \otimes n\,(x)$ for all $x \in \Gamma$.

Lemma 3.4.2. *Suppose that $\Gamma \subset \mathbb{R}^d$ is a $(d-1)$-surface which is of class C^1 and let $x^0 \in \Gamma$. Then, for all $x \in \Gamma$ there exists a continuous, piecewise continuously differentiable path $\gamma : [0,1] \to \Gamma$ such that $\gamma\,(0) = x^0$ and $\gamma\,(1) = x$.*

Proof. Let x^0, $x \in \Gamma$; since Γ is a connected manifold, it is also path-connected (see e.g. [95]) and there exists a continuous path connecting x^0 and x. Note that the set of points on the path is compact since it is closed and contained in a relatively compact set. Also, Γ being C^1, we can cover the path with balls $B(x, r_x)$ centred at x of radius r_x such that $\Gamma \cap B(x, r_x)$ is the graph of a C^1 function $g_x : \mathbb{R}^{d-1} \to \mathbb{R}$.

Extracting a finite subcover, we may assume that there are points $x^0, \ldots, x^N = x \in \Gamma$ such that the balls $B(x^j, r_j)$, $j = 0, 1, \ldots, N$, cover the path and that there exist local coordinate systems, say $(\bar{x}^{c_j}, x_d^{c_j})$ with $\bar{x}^{c_j} = (x_1^{c_j}, \ldots, x_{d-1}^{c_j})$, and C^1 functions $g_j : \mathbb{R}^{d-1} \to \mathbb{R}$ such that

$$\Gamma \cap B(x^j, r_j) = \left\{ x \in B(x^j, r_j) \,:\, x_d^{c_j} = g_j(\bar{x}^{c_j}) \right\}.$$

Above, the superscript c_j denotes the coordinate system in the ball $B(x^j, r_j)$. Trivially, we may also assume that for $j = 0, 1, \ldots, N-1$, there exists some $y^{j+1} \in B(x^j, r_j) \cap B(x^{j+1}, r_{j+1})$.

For $j = 0, \ldots, N$, we may define N continuously differentiable paths γ_j in each $B(x^j, r_j)$ such that $\gamma_j(0) = y^j$ and $\gamma_j(1) = y^{j+1}$, where we make the identification

$x^0 = y^0$ and $x^N = y^{N+1}$, by

$$\gamma_j(t) = \left(\bar{y}^{j,c_j} + t\left(\bar{y}^{j+1,c_j} - \bar{y}^{j,c_j}\right), g\left(\bar{y}^{j,c_j} + t\left(\bar{y}^{j+1,c_j} - \bar{y}^{j,c_j}\right)\right)\right),$$

where the superscript j, c_j denotes the point y^j expressed in the coordinate system c_j in $B(x^j, r_j)$. Then, the composition of $\gamma_0, \ldots, \gamma_N$ gives a continuous, piecewise continuously differentiable path $\gamma : [0,1] \to \Gamma$ such that $\gamma(0) = x^0$ and $\gamma(1) = x$. $\square$

Proof of modified jump condition. To prove necessity of the compatibility condition (3.4.1) suppose that there exists a map $z \in W^{1,\infty}\left(\Omega, \mathbb{R}^d\right)$ such that

$$Dz\left(x\right) = \begin{cases} Dy^+\left(x\right), & x \in \Omega^+ \\ \\ Dy^-\left(x\right), & x \in \Omega^-. \end{cases}$$

We use a blow-up argument to reduce the problem to the classical Hadamard condition of Lemma 2.1.8 (see also Hadamard [71].). Let $x_0 \in \Gamma$. Consider a positive and decreasing sequence of blow-up radii $\{r_j\}$ such that $r_j \to 0$ as $j \to \infty$ and r_1 - the first term in the sequence - is so small that $x_0 + r_1 B \subset \Omega$ and the C^1 surface Γ can be represented as the graph of a continuously differentiable function $g : \mathbb{R}^{d-1} \to \mathbb{R}$ in $B(x_0, r_1)$; above, $B = B\left(0,1\right)$ denotes the until ball in $\mathbb{R}^d$. In particular, there exists a continuously differentiable map f defined by $f(x) = x_d - g(\bar{x})$, where $(\bar{x}, x_d)$ refers to the coordinate system in the definition of the C^1 surface, such that

$$\Gamma \cap B(x_0, r_1) = \left\{x \in B(x_0, r_1) \,:\, f(x) = 0\right\}.$$

We note that the unit normal to a point $x \in B(x_0, r_1)$ is given by $n(x) = \nabla f(x)/|\nabla f(x)|$ and, in addition,

$$\Omega^{\pm} \cap B(x_0, r_1) = \left\{x \in B(x_0, r_1) \,:\, \pm f(x) > 0\right\}.$$

Next, define a sequence of functions $z_j : B \to \mathbb{R}^d$ by

$$z_j\left(x\right) = \frac{1}{r_j}\left[z\left(x_0 + r_j x\right) - z\left(x_0\right)\right].$$

Since $z \in W^{1,\infty}\left(\Omega, \mathbb{R}^d\right)$, $z_j(0) = 0$ and $Dz_j(x) = Dz(x_0 + r_j x)$, the maps z_j are uniformly bounded in $W^{1,\infty}\left(B, \mathbb{R}^d\right)$ and, up to a subsequence, converge weak$*$ to some map, say $\tilde{z} \in W^{1,\infty}\left(B, \mathbb{R}^d\right)$. We claim that

$$D\tilde{z}\left(x\right) = \begin{cases} Dy^+\left(x_0\right) & , \quad x \in B^+_{n(x_0)} \\ \\ Dy^-\left(x_0\right) & , \quad x \in B^-_{n(x_0)} \end{cases} \tag{3.4.2}$$

where for a unit vector $n \in S^{d-1}$, $B_n^{\pm} = \{x \in B : \pm x \cdot n > 0\}$.

Let $x \in B^+_{n(x_0)}$ and note that, up to a subsequence (not relabelled), $f(x_0+r_jx) > 0$. To see this, suppose otherwise; then $f(x_0 + r_jx) \leq 0$ for all j. However, since f is continuously differentiable, by Taylor's theorem,

$$\frac{1}{r_j} f(x_0 + r_j x) = \nabla f(x_0) \cdot x + \frac{o(|r_j x|)}{r_j}$$

since $x_0 \in \Gamma \cap B(x_0, r_1)$ implies $f(x_0) = 0$. Note that the left hand side of the above equation is always non-positive and letting $j \to \infty$, we obtain

$$\nabla f(x_0) \cdot x = |\nabla f(x)| n(x_0) \cdot x \leq 0$$

which is a contradiction. But then, for $x \in B^+_{n(x_0)}$, the continuity of Dy^+ implies that

$$Dz_j(x) = Dz(x_0 + r_j x) = Dy^+(x_0 + r_j x) \to Dy^+(x_0) \text{ as } j \to \infty.$$

Similarly, $Dz_j(x) \to Dy^-(x_0)$ as $j \to \infty$ whenever $x \in B^-_{n(x_0)}$. Hence, Dz_j converges (uniformly) to $D\tilde{z}$. As $\tilde{z} \in W^{1,\infty}\left(B, \mathbb{R}^d\right)$, the tangential derivatives on the hyper-plane $x \cdot n\left(x_0\right) = 0$ are equal, i.e. assuming that $|n(x_0)| = 1$,

$$\begin{aligned}
& Dy^+\left(x_0\right) n^{\perp} = Dy^-\left(x_0\right) n^{\perp}, \quad \text{for any } n^{\perp} \in \mathbb{R}^d \text{ such that } n^{\perp} \cdot n\left(x_0\right) = 0 \\
\Leftrightarrow \quad & \left[Dy^+\left(x_0\right) - Dy^-\left(x_0\right)\right]\left(x - \left(x \cdot n\left(x_0\right)\right) n\left(x_0\right)\right) = 0, \quad \text{for all } x \in \mathbb{R}^d \\
\Leftrightarrow \quad & \left[Dy^+\left(x_0\right) - Dy^-\left(x_0\right)\right] x = \left[\left(Dy^+\left(x_0\right) - Dy^-\left(x_0\right)\right) n\left(x_0\right) \otimes n\left(x_0\right)\right] x \\
\Leftrightarrow \quad & Dy^+\left(x_0\right) - Dy^-\left(x_0\right) = a\left(x_0\right) \otimes n\left(x_0\right).
\end{aligned}$$

The above is in fact a proof of Lemma 2.1.8. To conclude the proof of necessity, we are left to show that the map a, defined by the blow-up argument at each $x \in \Gamma$ is indeed continuous. But this follows easily as, for each $x \in \Gamma$,

$$a\left(x\right) = \left[Dy^+\left(x\right) - Dy^-\left(x\right)\right] n\left(x\right),$$

and all other maps involved are continuous.

To prove sufficiency, let $x_0 \in \Gamma$ be fixed and, by adding an appropriate constant, also assume that $y^+\left(x_0\right) = y^-\left(x_0\right) = 0$. Then, it is enough to deduce that for all $x \in \Gamma$, $y^+\left(x\right) = y^-\left(x\right)$ as the map defined by

$$z\left(x\right) = \begin{cases} y^+\left(x\right), & x \in \Omega^+ \\ \\ y^-\left(x\right), & x \in \Omega^- \end{cases}$$

will be continuous across Γ and its gradient will have the required form.

Let $x \in \Gamma$; since Γ is of class C^1, by Lemma 3.4.2, we can define a piecewise continuously differentiable path $\gamma : [0,1] \to \Gamma$ such that $\gamma(0) = x_0$ and $\gamma(1) = x$. Then,

$$y^+(x) - y^-(x) = \int_0^1 \left[Dy^+(\gamma(t)) - Dy^-(\gamma(t))\right] \dot{\gamma}(t)\, dt.$$

Note that for a.e. $t \in [0,1]$, $\dot{\gamma}(t)$ is tangential to the path and, in particular, perpendicular to the normal at the point $\gamma(t) \in \Gamma$, i.e. $\dot{\gamma}(t) \cdot n(\gamma(t)) = 0$. On the other hand, we know that for all $x \in \Gamma$, $Dy^+(x) - Dy^-(x) = a(x) \otimes n(x)$ and therefore,

$$y^+(x) - y^-(x) = \int_0^1 \left[n(\gamma(t)) \cdot \dot{\gamma}(t)\right] a(\gamma(t))\, dt = 0. \qquad \square$$

Remark. If one assumes that Ω is a simply connected subset of $\mathbb{R}^d$, condition (3.4.1) ensures that the map $F : \Omega \to M^{d\times d}$ defined by

$$F(x) = \begin{cases} Dy^+(x), & x \in \Omega^+ \\ \\ Dy^-(x), & x \in \Omega^- \end{cases}$$

is curl-free (in the distributional sense) and Theorem 1 in [4] shows that this is equivalent to the existence of a distribution with a distributional derivative given by F. Then, Maz'ya in Section 1.1.11 of [101] shows that a distribution whose derivatives of order k belong to an L^p space must itself be a function and an element of the Sobolev space $W^{k,p}$; sufficiency then follows. In this case, one need not assume that Γ is connected.

Also note that if Γ is disconnected (and Ω is not simply connected) the result is in general false. As an example, consider $\Omega = A \times (0,1)$ where A is the annulus

$$\{(x_1, x_2) : 1 < x_1^2 + x_2^2 < 4\}.$$

Let $\Omega^\pm = \{(x_1, x_2, x_3) : \pm x_1 < 0,\ x_3 \in (0,1)\}$ and $\Gamma = \Gamma_1 \cup \Gamma_2$ where

$$\Gamma_1 = \{(x_1, x_2, x_3) : x_1 = 0, x_2 > 1, x_3 \in (0,1)\}$$
$$\Gamma_2 = \{(x_1, x_2, x_3) : x_1 = 0, x_2 < -1, x_3 \in (0,1)\}.$$

A planar section perpendicular to the x_3 axis is depicted in Fig. 3.12 below. Let $y^+(x) = 0$ in Ω^+, $y^-(x) = 0$ for $x \in \Omega^- \cap \{x_2 > 1\}$, $y^-(x) = ax_1 + e_2$ for $x \in \Omega^- \cap \{x_2 < -1\}$ and interpolate smoothly for $x_2 \in [-1,1]$, where a is a non-zero vector and $x_1 = x \cdot e_1$, e_i being the standard basis of $\mathbb{R}^3$; trivially, the compatibility condition

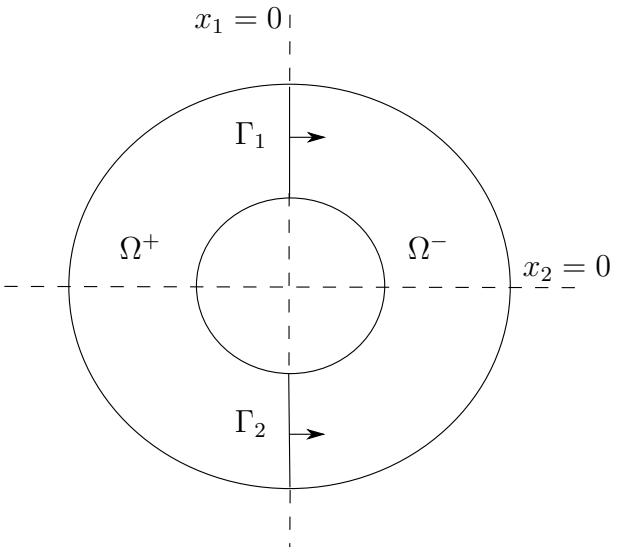

Figure 3.12: The manifold $\Gamma = \Gamma_1 \cup \Gamma_2$ is disconnected, Ω is not simply connected, and the conclusion of Theorem 3.1 no longer holds.

(3.4.1) is satisfied across Γ, with $Dy^+ - Dy^- = 0$ on Γ_1 and $Dy^+ - Dy^- = a \otimes e_1$ on Γ_2. Next suppose that there exists $z \in W^{1,\infty}(\Omega, \mathbb{R}^3)$ such that

$$Dz(x) = \begin{cases} Dy^+(x), & x \in \Omega^+ \\ Dy^-(x), & x \in \Omega^- \end{cases} = \begin{cases} 0, & x \in \Omega^+ \\ Dy^-(x), & x \in \Omega^-. \end{cases}$$

Then, since $\Omega^\pm$ are connected, $z(x) = c$ in Ω^+ for some constant c, whereas, in Ω^-, $z(x) = y^-(x) + d$ for some other constant d. But continuity across Γ_1 requires that $d = c$ and hence on Γ_2 that $c = c + e_2$ - a contradiction.

Finally, we remark that a particularly interesting problem arises when the maps $y^\pm$ are merely Lipschitz continuous. It had been thought that, in this case, the polyconvex hulls of the essential ranges of the differentials, denoted by $[Dy^\pm]^{pc}$,[6] must satisfy Hadamard's jump condition or are at least be rank-one connected. Iwaniec et al. [80] showed that this is not true as long as $d \geq 3$.

Having established an appropriate jump condition, we next present a general method for constructing a curved interface at zero stress. The method is rather general in the sense that it is applicable to any set of martensitic wells K provided that there exists a rank-one connection between $SO(3)$, the austenitic well, and the relative interior of the quasiconvex hull of K, $\operatorname{rint} K^{qc}$. Here, the interior of K^{qc} is taken relative to the set

$$\mathcal{D} := \{A \in M^{d\times d} : \det A = \det U\}$$

[6]The essential range of the differential, $[Dy^\pm]$, is defined as the smallest closed subset K of $M^{d\times d}$ such that $Dy^\pm(x) \in K$ for a.e. $x \in \Omega^\pm$.

where $\det U$ denotes the common value of the determinant of the martensitic variants.

Lemma 3.4.3. *(construction of a curved interface) Let $K \subset \mathcal{D}$ be a compact set such that $\operatorname{rint} K^{qc} \neq \emptyset$. Further, assume that there exist $F \in \operatorname{rint} K^{qc}$, $\epsilon > 0$ and non-zero vectors a, $n \in \mathbb{R}^d$ such that:*

$$\begin{aligned} B(F, \epsilon) \cap \mathcal{D} &\subset K^{qc}, \\ F &= 1 + a \otimes n. \end{aligned} \tag{3.4.3}$$

Then, for some open ball $\Omega = B(0, r) \subset \mathbb{R}^d$ and a non-planar $(d-1)$-surface Γ, as in Theorem 3.4.1, there exists a gradient Young measure $(\nu_x)_{x \in \Omega}$ satisfying $\nu_x = \delta_{\mathbf{1}}$ in Ω^- and $\operatorname{supp} \nu_x \subset K$ in Ω^+ with an underlying deformation $z \in W^{1,\infty}\left(\Omega, \mathbb{R}^d\right)$ such that

$$Dz(x) = \begin{cases} Dy^+(x), & x \in \Omega^+ \\ \mathbf{1}, & x \in \Omega^- \end{cases}$$

and $y^+ \in C^1\left(\overline{\Omega^+}, \mathbb{R}^d\right)$. That is, there exists a microstructure of martensite which borders compatibly with a pure phase of austenite along a non-planar interface Γ.

Proof. Let $f \in C^1(B(0,1))$ satisfy the following properties:

- $f(0) = 0$ and $\nabla f(0) = n$,
- $\|\nabla f - n\|_\infty < \epsilon / |a|$
- $\nabla f(x) \cdot a = n \cdot a$ for all $x \in B(0,1)$ and
- for all sufficiently small $r \in (0,1)$, $\nabla f / |\nabla f|$ is not constant on $\{x \in B(0,r) : f(x) = 0\}$.

Such a function exists and an example is given after the proof. Choose an orthonormal system of coordinates $(\bar{x}, x_d)$ with origin at 0 and $e_d = n$. Consider the map $g : B(0,1) \to \mathbb{R}^d$ defined by $g(x) = (\bar{x}, f(x))$. Since $\nabla g(0) = \mathbf{1} \neq 0$ it follows from the inverse function theorem that for $r > 0$ sufficiently small and some neighbourhood V of $0 \in \mathbb{R}^d$ the map $g : B(0,r) \to V$ is invertible with C^1 inverse g^{-1}, and that

$$\{x \in B(0,r) : f(x) = 0\} = \{x \in B(0,r) : x_d = h(\bar{x})\},$$

where $h(\bar{x}) = g^{-1}(\bar{x}, 0) \cdot n$. Let $\Omega = B(0,r)$, $\Omega^\pm = \{x \in \Omega : \pm f(x) > 0\}$ and $\Gamma = \{x \in \Omega : f(x) = 0\}$. Note that Γ is a $(d-1)$-surface of class C^1 and that the

unit normal $n(x)$ to a point $x \in \Gamma$ is given by $n(x) = \nabla f(x)/|\nabla f(x)|$. Also since on Γ, $\nabla f/|\nabla f|$ cannot be constant, Γ defines a non-planar interface.

To establish the claim, we now need to construct the appropriate Young measure. Define $y^+ : \Omega^+ \to \mathbb{R}^d$ by

$$y^+(x) = x + af(x). \tag{3.4.4}$$

As $f \in C^1(B(0,1))$ and $\Omega \subset\subset B(0,1)$, it follows that $y^+ \in C^1\left(\overline{\Omega^+}, \mathbb{R}^d\right)$ and $Dy^+(x) = \mathbf{1} + a \otimes \nabla f(x)$. Moreover, we note that at $x = 0 \in \Gamma$,

$$Dy^+(0) = \mathbf{1} + a \otimes n = F \in \operatorname{rint} K^{qc}.$$

But then there exists a homogeneous gradient Young measure μ_0 which is supported on K and satisfies $\bar{\mu}_0 = F$.

For all other $x \in \Gamma$, Dy^+ is rank-one connected to the identity and, in addition, it satisfies the determinant constraint $Dy^+(x) \in \mathcal{D}$ for all $x \in \overline{\Omega^+}$. This follows directly from our assumption that $\nabla f(x) \cdot a = n \cdot a$ for all $x \in B(0,1)$. What is more, $(3.4.3)_1$ states that $B(F,\epsilon) \cap \mathcal{D} \subset K^{qc}$ for some $\epsilon > 0$ and therefore, for all $x \in \overline{\Omega^+}$,

$$|Dy^+(x) - F| = |a||\nabla f(x) - n| < \epsilon,$$

since f satisfies $\|\nabla f - n\|_\infty < \epsilon/|a|$, i.e.

$$Dy^+(x) \in B(F,\epsilon) \cap \mathcal{D} \subset K^{qc}.$$

This implies that, for each $x \in \overline{\Omega^+}$, there exists a homogeneous gradient Young measure μ_x supported on K such that $\bar{\mu}_x = Dy^+(x)$. By Theorem 6.1 in [86], the family of measures $\mu = (\mu_x)_{x \in \Omega^+}$ satisfying $\operatorname{supp} \mu_x \subset K$ for a.e. $x \in \Omega^+$ defines a $(W^{1,\infty})$ gradient Young measure provided that the map y^+ such that $\bar{\mu}_x = Dy^+(x)$ is an element of $W^{1,\infty}(\Omega^+, \mathbb{R}^3)$; this is trivially the case since $y^+ \in C^1\left(\overline{\Omega^+}, \mathbb{R}^3\right)$.

On the other hand, for $x \in \overline{\Omega^-}$, consider the homogeneous measure $\delta_{\mathbf{1}}$. The compatibility condition along Γ between Dy^+ and the identity is satisfied and, hence, the parametrized measure $\nu = (\nu_x)_{x \in \Omega}$ defined by

$$\nu_x = \begin{cases} \mu_x, & x \in \Omega^+ \\ \delta_{\mathbf{1}}, & x \in \Omega^- \end{cases}$$

is a gradient Young measure itself since its centre of mass is given by

$$Dz(x) = \begin{cases} Dy^+(x), & x \in \Omega^+ \\ \mathbf{1}, & x \in \Omega^- \end{cases}$$

and $z \in W^{1,\infty}(\Omega, \mathbb{R}^3)$. This concludes the proof. $\square$

Depending on the choice of function f defining the implicit surface Γ, one can obtain a variety of interfaces. A rather interesting example in three dimensions is given below:

Example. Let $h \in C^1(\mathbb{R})$ be such that $\dot{h}$ is not constant, $h(0) = \dot{h}(0) = 0$ and

$$\|\dot{h}\|_\infty < \frac{\epsilon}{|a|^2}.$$

Assume $a, n \in \mathbb{R}^3$ are nonparallel and define $f \in C^1(\mathbb{R}^3)$ by

$$f(x) = x \cdot n + h(x \cdot (a \wedge n)),$$

where $a \wedge n$ denotes the vector product of a and n. If a and n are parallel, we can proceed similarly replacing $a \wedge n$ by any vector perpendicular to them. Then, $f(0) = 0$ and

$$\nabla f(x) = n + \dot{h}(x \cdot a \wedge n) a \wedge n,$$

so that $\nabla f(0) = n$. Moreover, $a \cdot \nabla f(x) = a \cdot n$. By the orthogonality of n and $a \wedge n$, $\Gamma := \{f^{-1}(0)\} = \{(-h(x_{a\wedge n}), x_{a\wedge n}, x_m) : (x_{a\wedge n}, x_m) \in \mathbb{R}^2\}$ in some appropriate coordinate system where x_n, $x_{a\wedge n}$ and x_m are coordinates in the directions n, $a \wedge n$ and some vector $m \in \mathbb{R}^3$ perpendicular to both n and $a \wedge n$, respectively. This defines a C^1 surface which extends indefinitely in the direction of $a \wedge n$ and m and $\Omega \subset \mathbb{R}^3$ can be chosen to be any domain intersecting Γ and not just the possibly small neighbourhood of Lemma 3.4.3. Also, Γ is non-planar as otherwise $\dot{h}(x_{a\wedge n}) = \dot{h}(y_{a\wedge n})$ for all x, $y \in \Gamma$ which is impossible since $\dot{h}$ is not constant.

Moreover, note that $\nabla f(x)$ only changes along the direction $a \wedge n$ and the vector m is always tangential to the surface. Then, the two-dimensional cross-sections of Γ with planes parallel to the one spanned by the vectors n and $a \wedge n$ are the same so that the cross-section with the plane $x \cdot m = k$ is parametrized by $r(t) = (-h(t), t, k)$; see Fig. 3.13 for an example.

Remark. It is worth noting that if $\det U = 1$ then, at least for martensitic transformations with cubic austenite, one can always find a sequence y^k, uniformly bounded in $W^{1,\infty}(\Omega, \mathbb{R}^3)$, such that each y^k agrees with the identity map on the boundary $\partial\Omega$ and generates a Young measure with support in K, the set of martensitic energy wells - see Bhattacharya [26]. Then, by averaging the associated Young measure, we find a homogeneous ($W^{1,\infty}$) gradient Young measure with centre of mass equal to

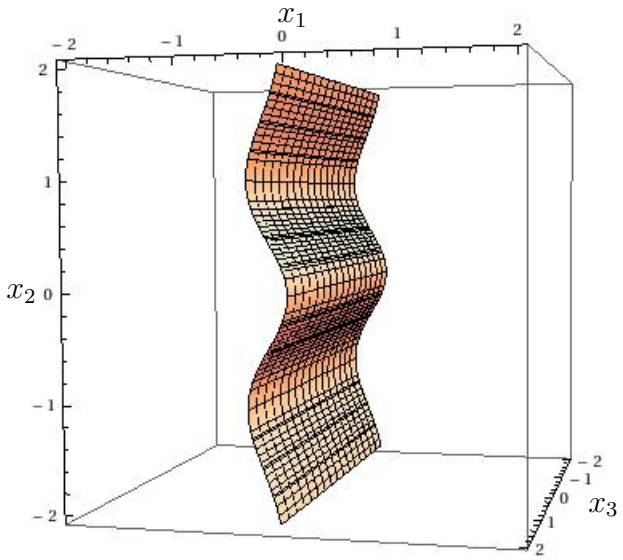

Figure 3.13: Example of a surface produced with $h(t) = t^2 e^{-t^2}$; x_1, x_2, x_3 denote the coordinates in the direction of n, $a \wedge n$ and the vector perpendicular to both n and $a \wedge n$ respectively. The vectors $n = (1, 0, 0)^T$ and $a = (0, 0, 1)^T$ have been chosen arbitrarily for simplicity and there is no smallness assumption imposed on $\|\dot{h}\|_\infty$ so that the curvature of the surface is clearly seen.

the identity matrix (see [86]), i.e. the identity matrix is an element of K^{qc} and the underlying martensitic microstructure can form any curved interface with the identity as compatibility is trivial.

In proving Lemma 3.4.3, we assumed that there exists a relatively interior point of K^{qc} which is rank-one connected to $SO(d)$. This is by no means a trivial assumption and, next, we wish to address this point.

In the context of martensitic transformations, one is interested in compact subsets of $M^{d\times d}$ of the form

$$K = \bigcup_{i=1}^{N} SO(d)\, U_i$$

where, for all i, U_i is positive definite, symmetric with $\det U_i = \det U$. For $d = 2$, there is a characterization of K^{qc} (Theorem 2.2.3, in [52]) which we present next:

Theorem 3.4.4. *Let $K = \bigcup_{i=1}^{N} SO(2)\, U_i \subset M^{2\times 2}$ be as above. Then,*

$$K^{qc} = K^{rc} = K^{pc} = K^{(2)}.$$

Further, define the set of corners $\mathcal{C}$ *by*

$$\mathcal{C} = \left\{ U_i : \exists\, v \in S^1 \ s.t\ |U_i v|^2 > \max_{j \neq i} |U_j v|^2 \right\}.$$

Then there exists a set $\mathcal{E} = \{e_1, \ldots, e_l\} \subset S^1$ $(l \leq N)$ *such that*

$$K^{(2)} = \{F : \det F = \det U \text{ and } |Fe_i|^2 \leq \max_{U \in \mathcal{C}} |Ue_i|^2,\ i = 1, \ldots, l\}.$$

Using this characterization one can show the following:

Lemma 3.4.5. *Let* $K \subset M^{2\times 2}$ *be as above. Then*

$$F \in K^{(2)} \setminus K^{(1)} \Rightarrow F \in \operatorname{rint} K^{qc},$$

i.e. all double laminates are relative interior points of K^{qc}*.*

Proof. The only non-trivial part is showing that the set of constrained points lies in $K^{(1)}$, i.e.

$$\{F : \det F = \det U \text{ and } \exists\, i \in \{1, \ldots, l\} \text{ s.t. } |Fe_i|^2 = \max_{U \in \mathcal{C}} |Ue_i|^2\} \subset K^{(1)}.$$

A proof of this can be found as Step 6 of the proof of Theorem 2.2.3 in [52]. Next, let F be an unconstrained point in K^{qc}, i.e.

$$|Fe_i| < \max_{U \in \mathcal{C}} |Ue_i| \quad \text{for all } i = 1, \ldots, l.$$

For any such F, let $\epsilon > 0$ and consider a point $G \in B_\epsilon(F) \cap \mathcal{D}$, where as before $\mathcal{D} = \{A \in M^{2\times 2} : \det A = \det U\}$. Then, $\forall\, i = 1, \ldots, l$

$$\begin{aligned} |Ge_i| &\leq |(G - F)\, e_i| + |Fe_i| \\ &\leq C|G - F||e_i| + M_i \text{ for some } C,\ M_i > 0 \text{ such that } |Fe_i| = M_i < \max_{U \in \mathcal{C}} |Ue_i| \\ &\leq \max_{U \in \mathcal{C}} |Ue_i|, \end{aligned}$$

for small enough $\epsilon > 0$, i.e. the unconstrained points of K^{qc} lie in the relative interior. Clearly, the set of unconstrained points contains $K^{qc} \setminus K^{(1)} = K^{(2)} \setminus K^{(1)}$, implying that all double laminates are relative interior points of K^{qc}. □

In two dimensions, it is indeed possible to find rank-one connections between double laminates and $SO(2)$. For example, Ball and Carstensen [13], give explicit conditions for finding rank-one connections from $K^{(2)} \subset M^{3\times 3}$ to $SO(3)$ in the case of two wells and

$$U_1 = \operatorname{diag}(\eta_2, \eta_1, \eta_1), \quad U_2 = \operatorname{diag}(\eta_1, \eta_2, \eta_1).$$

The fact that U_1 and U_2 have a common eigenvalue for the eigenvector $(0,0,1)^T$ allows one to reduce this to a two dimensional problem and we can find the appropriate rank-one connections; hence, for $d=2$ non-planar austenite-martensite interfaces can be constructed. As we are mostly interested in the case $d=3$, we do not extend further on the two dimensional case.

Similarly, finding the quasiconvex hull of $K = SO(3)U_1 \cup SO(3)U_2$ can be reduced to two dimensions (see e.g. [52]) and Theorem 3.4.4 gives $K^{qc} = K^{(2)}$. Also, Ball and James [19] directly and explicitly calculated the above quasiconvex hull. As mentioned in the beginning of the chapter, they showed that $K^{qc} = SO(3)\mathcal{F}$ where $\mathcal{F}$ consists of all matrices F such that

$$F^T F = \begin{pmatrix} a & c & 0 \\ c & b & 0 \\ 0 & 0 & \eta_1^2 \end{pmatrix}$$

where $ab - c^2 = \eta_1^2\eta_2^2$ and $a+b+2|c| \leq \eta_1^2+\eta_2^2$. Due to the determinant constraint, this is trivially a two-dimensional set which implies that K^{qc} is of dimension 5 (since $SO(3)$ has dimension 3). On the other hand, were the relative interior of K^{qc} non-empty, it would have dimension 8, i.e. of full dimension minus the determinant constraint. Therefore, $\mathrm{rint} K^{qc} = \emptyset$ and we cannot construct curved interfaces.

Hence, for $K \subset M^{3\times 3}$ we shall follow a different approach to prove the existence of a relative interior point, rank-one connected to $SO(3)$; this originated in an idea of Bernd Kirchheim.

Lemma 3.4.6. *(Dolzmann and Kirchheim [53]) Let $\kappa > 0$, $\kappa \neq 1$ and assume that $\tilde{K} \subset \{A \in M^{3\times 3} : \det A = 1\}$ is compact and that $\tilde{K}^{qc}$ contains a three-well configuration $\tilde{K}_{ct}$ given by*

$$\begin{aligned} \tilde{K}_{ct} &= \bigcup_{i=1}^{3} SO(3)\tilde{U}_i \quad \textit{where} \\ \tilde{U}_1 &= \mathrm{diag}\left(\kappa^2, \frac{1}{\kappa}, \frac{1}{\kappa}\right),\ \tilde{U}_2 = \mathrm{diag}\left(\frac{1}{\kappa}, \kappa^2, \frac{1}{\kappa}\right),\ \tilde{U}_3 = \mathrm{diag}\left(\frac{1}{\kappa}, \frac{1}{\kappa}, \kappa^2\right). \end{aligned}$$

Then there exists $\epsilon > 0$ such that

$$B(\mathbf{1}, \epsilon) \cap \left\{A \in M^{3\times 3} : \det A = 1\right\} \subset \tilde{K}^{qc}.$$

In particular, $\mathbf{1} \in \mathrm{rint}\tilde{K}^{qc}$.

Remark. The three well configuration $\tilde{K}_{ct}$ corresponds to a cubic-to-tetragonal transformation for which $\eta_1^2 = 1/\eta_2$. Also, in [53], Dolzmann and Kirchheim provide a specific bound for this neighbourhood of the identity; in particular, if $\kappa < 3/2$,

$$B\left(\mathbf{1}, \frac{(\kappa-1)^2}{62}\right) \cap \left\{A \in M^{3\times 3} \,:\, \det A = 1\right\} \subset \tilde{K}^{qc}.$$

The assumption that $\kappa < 3/2$ is realistic as for shape-memory alloys the lattice parameters are typically close to 1. Henceforth, without loss of generality, we assume that $\epsilon < 1$.

By Lemma 3.4.6 we deduce the following:

Theorem 3.4.7. *(Existence of a relative interior point, rank-one connected to the identity) Let $\kappa > 0$, $\kappa \neq 1$ and $\Delta > 0$ such that*

$$\frac{|\Delta - 1|}{\Delta}\sqrt{\Delta^4 + 2\Delta^3 + \Delta^2 + 2} < \epsilon \tag{3.4.5}$$

where, by Lemma 3.4.6, $0 < \epsilon < 1$ is such that $B(\mathbf{1}, \epsilon) \cap \{A \in M^{3\times 3} : \det A = 1\} \subset \tilde{K}^{qc}$. Further, let $\eta_1 = \frac{\Delta}{\kappa}$, $\eta_2 = \Delta\kappa^2$ and assume that $K \subset \{A \in M^{3\times 3} \,:\, \det A = \Delta^3\}$ is compact and that K^{qc} contains a three-well configuration K_{ct} given by

$$\begin{aligned} K_{ct} &= \bigcup_{i=1}^{3} SO(3)\, U_i \quad \textit{where} \\ U_1 &= \operatorname{diag}(\eta_2, \eta_1, \eta_1),\ U_2 = \operatorname{diag}(\eta_1, \eta_2, \eta_1),\ U_3 = \operatorname{diag}(\eta_1, \eta_1, \eta_2). \end{aligned} \tag{3.4.6}$$

Then there exist a, $n \in \mathbb{R}^3$ and $F \in \operatorname{rint} K^{qc}$ such that $F = \mathbf{1} + a \otimes n$.

In proving the above Theorem, we shall use two very simple observations which we now prove in the form of a lemma.

Lemma 3.4.8. *Under the notation of Lemma 3.4.6 and Theorem 3.4.7 the following hold:*

(i) $K_{ct}^{qc} = \Delta \tilde{K}_{ct}^{qc}$ *and*

(ii) $\operatorname{rint} K_{ct}^{qc} = \Delta \operatorname{rint} \tilde{K}_{ct}^{qc}$. *In particular,*

$$\begin{aligned} &B(\tilde{F}, \epsilon) \cap \left\{A \in M^{3\times 3} : \det A = 1\right\} \subset \tilde{K}_{ct}^{qc} \Leftrightarrow \\ &B(F, \Delta\epsilon) \cap \left\{A \in M^{3\times 3} : \det A = \Delta^3\right\} \subset K^{qc}. \end{aligned}$$

where $F = \Delta\tilde{F}$.

Proof. (i) For notational convenience let $K = K_{ct} = \bigcup_{i=1}^{3} SO(3)\, U_i$ and similarly, $\tilde{K} = \tilde{K}_{ct} = \bigcup_{i=1}^{3} SO(3)\, \tilde{U}_i$. We note that

$$\Delta \tilde{U}_i = U_i \quad \text{and thus,} \quad \Delta \tilde{K} = K.$$

To show that $\Delta \tilde{K}^{qc} \subset K^{qc}$, let $\tilde{F} \in \tilde{K}^{qc}$. By the characterization of the elements of $\tilde{K}^{qc}$ as weak$*$ limits (see Section 2.1), there exists a sequence $\tilde{y}^k$ uniformly bounded in $W^{1,\infty}(\Omega, \mathbb{R}^3)$, for some bounded domain $\Omega \subset \mathbb{R}^3$, such that

$$\operatorname{dist}(D\tilde{y}^k, \tilde{K}) \to 0 \ \text{ in measure,}$$

$$D\tilde{y}^k \overset{*}{\rightharpoonup} \tilde{F} \ \text{ in } L^\infty(\Omega, M^{3\times 3}).$$

Define $y^k(x) = \tilde{y}^k(\Delta x)$; by our assumptions on $\tilde{y}^k$, y^k is uniformly bounded in $W^{1,\infty}((1/\Delta)\Omega, \mathbb{R}^3)$ and the gradients $Dy^k(x) = \Delta D\tilde{y}^k(\Delta x)$ satisfy

$$\operatorname{dist}(Dy^k, \Delta \tilde{K}) \to 0 \ \text{ in measure,}$$

$$Dy^k \overset{*}{\rightharpoonup} \Delta \tilde{F} \ \text{ in } L^\infty((1/\Delta)\Omega, M^{3\times 3}).$$

But $\Delta \tilde{K} = K$ implying that $\Delta \tilde{F} \in K^{qc}$.

For the converse inclusion we need to show that whenever $F \in K^{qc}$, $F/\Delta \in \tilde{K}^{qc}$. This is almost identical to the above and the proof is omitted.

(ii) Using the same notation as for part (i), let $\tilde{F} \in \operatorname{rint} \tilde{K}^{qc}$; then there exists $\epsilon > 0$ such that

$$B(\tilde{F}, \epsilon) \cap \{ A \in M^{3\times 3} : \det A = 1\} \subset \tilde{K}^{qc}.$$

Let $F = \Delta \tilde{F}$; then $F \in K^{qc}$ by part (i). We wish to conclude that $F \in \operatorname{rint} K^{qc}$ and, in particular, that $B(F, \Delta\epsilon) \cap \{ A : \det A = \Delta^3\} \subset K^{qc}$. It is easy to see that for any $G \in B(F, \Delta\epsilon) \cap \{ A : \det A = \Delta^3\}$,

$$|G - F| < \Delta\epsilon \Rightarrow |\Delta^{-1}(G - F)| < \epsilon \Rightarrow |\Delta^{-1}G - \tilde{F}| < \epsilon$$

and

$$\det \Delta^{-1} G = \Delta^{-3}\Delta^3 = 1.$$

Therefore,

$$\Delta^{-1}G \in B(\tilde{F}, \epsilon) \cap \{ A \in M^{3\times 3} : \det A = 1\} \subset \tilde{K}^{qc}$$

so that $\Delta^{-1}G \in \tilde{K}^{qc} = \Delta^{-1}K^{qc}$ from part (i) and $G \in K^{qc}$.

Conversely, let $F \in \operatorname{rint} K^{qc}$ and $\tilde{F} = \Delta^{-1}F \in \tilde{K}^{qc}$ by part (i); Then there exists $\epsilon > 0$ such that

$$B(F, \Delta\epsilon) \cap \{ A \in M^{3\times 3} : \det A = \Delta^3\} \subset K^{qc}.$$

Let $\tilde{G} \in M^{3\times 3}$ such that $|\tilde{G} - \tilde{F}| < \epsilon$ and $\det \tilde{G} = 1$; we wish to conclude that $\tilde{G} \in \tilde{K}^{qc}$. But, like before,

$$|\tilde{G} - \tilde{F}| < \epsilon \Rightarrow |\tilde{G} - \Delta^{-1}F| < \epsilon \Rightarrow |\Delta\tilde{G} - F| < \Delta\epsilon$$

and

$$\det \Delta\tilde{G} = \Delta^3$$

so that $\Delta\tilde{G} \in B(F, \Delta\epsilon) \cap \{ A \in M^{3\times 3} : \det A = \Delta^3\} \subset K^{qc}$. Then,

$$\tilde{G} \in \Delta^{-1}K^{qc} = \tilde{K}^{qc}$$

completing the proof. □

Proof of Theorem 3.4.7. We shall prove the result for the case $K = K_{ct}$ and the general statement then follows. From Lemma 3.4.6 and Lemma 3.4.8, we know that the relative interior of K^{qc} is non-empty and, in particular, $\Delta\mathbf{1} \in \operatorname{rint} K^{qc}$. The idea behind the proof is then rather natural: if we choose $\Delta > 0$ close enough to 1, we can surely find a rank-one direction, say $a \otimes n$, such that the 'line'

$$\mathbf{1} + ta \otimes n,\ t \in \mathbb{R}$$

intersects the relative neighbourhood of $\Delta\mathbf{1}$, $B(\Delta\mathbf{1}, \Delta\epsilon) \cap \{A \in M^{3\times 3} : \det A = \Delta^3\}$. Then, the point of intersection, say F, will itself be in K^{qc} and there will exist some $\bar{\epsilon} > 0$ such that

$$B(F, \bar{\epsilon}) \cap \left\{A \in M^{3\times 3} : \det A = \Delta^3\right\} \subset K^{qc}.$$

Choose any vector $n \in \mathbb{R}^3$, $|n| = 1$ and let $a = (\Delta^3 - 1)n$. We claim that $F = \mathbf{1} + a \otimes n$ is the desired point. Trivially, $\det F = 1 + a \cdot n = \Delta^3$ and it remains to show that

$$|F - \Delta\mathbf{1}| < \Delta\epsilon.$$

But, with $a = (\Delta^3 - 1)n$, we obtain that

$$\begin{aligned} |F - \Delta\mathbf{1}|^2 &= |(1 - \Delta)\mathbf{1} + a \otimes n|^2 \\ &= 3(1 - \Delta)^2 + 2(1 - \Delta)a \cdot n + |a|^2 \\ &= (1 - \Delta)^2(\Delta^4 + 2\Delta^3 + \Delta^2 + 2) < \Delta^2\epsilon^2, \end{aligned}$$

where the last inequality follows from (3.4.5). This completes the proof. □

Combining the above result with our construction of the curved interface in Lemma 3.4.3 we deduce that under the hypotheses of Theorem 3.4.7, we can construct a stress-free curved austenite-martensite interface for a set of martensitic wells containing the three well configuration K_{ct}. As remarked already, the configuration K_{ct} in (3.4.7) is indeed a realistic one in the context of martensitic transformations as it corresponds to a cubic-to-tetragonal transition; nevertheless, such interfaces have never been observed in materials with such high symmetry in the martensitic phase. Thus, proving the existence of this relative interior point for transformations with lower martensitic symmetry is desirable. Indeed, through Theorem 3.4.7, we can prove the existence of a relative interior point, rank-one connected to the identity for a cubic-to-orthorhombic transformation (with special lattice parameters) which is the transition undergone by Seiner's specimen. Since the lattice parameters of Seiner's CuAlNi specimen are known, this also allows us to directly check the possibility of such an interface occurring in the specific crystal; however, as we shall see, the determinant of the martensitic variants of the CuAlNi specimen is too far from 1. To be more specific:

Lemma 3.4.9. *Let $K = \bigcup_{i=1}^{6} SO(3)U_i$ denote the union of the martensitic variants for a cubic-to-orthorhombic transition where the matrices U_i, $i = 1, \dots, 6$ are as in (3.3.1). Then, the set K^{qc} contains the three-well configuration K_{ct} given by*

$$\begin{aligned} K_{ct} &= \bigcup_{i=1}^{3} SO(3)\, V_i \quad \textit{where} \\ V_1 &= \operatorname{diag}(\beta, \sqrt{\alpha\gamma}, \sqrt{\alpha\gamma}),\ V_2 = \operatorname{diag}(\sqrt{\alpha\gamma}, \beta, \sqrt{\alpha\gamma}),\ V_3 = \operatorname{diag}(\sqrt{\alpha\gamma}, \sqrt{\alpha\gamma}, \beta) \end{aligned} \tag{3.4.7}$$

and α, β and γ are the lattice parameters and eigenvalues of the matrices U_i.

Proof. Under the notation of (3.3.1) let us restrict attention to the pairs of variants (U_1, U_2), (U_3, U_4) and (U_5, U_6); these are precisely the pairs that form compound twinning systems. For example, the matrices U_1, U_2 are given by

$$U_1 = \begin{pmatrix} \beta & 0 & 0 \\ 0 & \frac{\alpha+\gamma}{2} & \frac{\alpha-\gamma}{2} \\ 0 & \frac{\alpha-\gamma}{2} & \frac{\alpha+\gamma}{2} \end{pmatrix} \qquad U_2 = \begin{pmatrix} \beta & 0 & 0 \\ 0 & \frac{\alpha+\gamma}{2} & \frac{\gamma-\alpha}{2} \\ 0 & \frac{\gamma-\alpha}{2} & \frac{\alpha+\gamma}{2} \end{pmatrix}$$

and they have a common basis of eigenvectors consisting of the unit vectors

$$(1,0,0)^T,\ \frac{1}{\sqrt{2}}(0,1,1)^T,\ \frac{1}{\sqrt{2}}(0,-1,1)^T$$

with corresponding eigenvalues β, α, γ for U_1 and β, γ, α for U_2 respectively. Letting

$$Q = \begin{pmatrix} 1 & 0 & 0 \\ 0 & \frac{1}{\sqrt{2}} & -\frac{1}{\sqrt{2}} \\ 0 & \frac{1}{\sqrt{2}} & \frac{1}{\sqrt{2}} \end{pmatrix} \in SO(3)$$

be the rotation with these eigenvectors as columns and defining $D_i := Q^T U_i Q$ for $i = 1, 2$, we infer that

$$D_1 = \operatorname{diag}(\beta, \alpha, \gamma) \quad \text{and} \quad D_2 = \operatorname{diag}(\beta, \gamma, \alpha).$$

By the characterization of the quasiconvex hull of two wells with equal determinant (see Section 3.1 or part prior to Lemma 3.4.6), we trivially deduce that

$$V_1 = \operatorname{diag}(\beta, \sqrt{\alpha\gamma}, \sqrt{\alpha\gamma}) \in (SO(3)D_1 \cup SO(3)D_2)^{qc}.$$

We claim that $QV_1Q^T \in (SO(3)U_1 \cup SO(3)U_2)^{qc} \subset K^{qc}$; then, we also deduce that $V_1 = QV_1Q^T \subset K^{qc}$. As in Lemma 3.4.8, since $V_1 \in (SO(3)D_1 \cup SO(3)D_2)^{qc}$, there exists a sequence z^k uniformly bounded in $W^{1,\infty}(\Omega, \mathbb{R}^3)$, for some bounded $\Omega \subset \mathbb{R}^3$, such that

$$\operatorname{dist}(Dz^k, SO(3)D_1 \cup SO(3)D_2) \to 0 \ \text{ in measure},$$

$$Dz^k \overset{*}{\rightharpoonup} V_1 \ \text{ in } L^\infty(\Omega, M^{3\times 3}).$$

Define $y^k(x) = Qz^k(Q^Tx)$; the sequence y^k is uniformly bounded in $W^{1,\infty}(Q\Omega, \mathbb{R}^3)$ and the gradients $Dy^k(x) = QDz^k(Q^Tx)Q^T$ satisfy

$$\operatorname{dist}(Dy^k, Q(SO(3)D_1 \cup SO(3)D_2)Q^T) \to 0 \ \text{ in measure},$$

$$Dy^k \overset{*}{\rightharpoonup} QV_1Q^T \ \text{ in } L^\infty(Q\Omega, M^{3\times 3}).$$

But $Q(SO(3)D_1 \cup SO(3)D_2)Q^T = SO(3)U_1 \cup SO(3)U_2$ and hence

$$QV_1Q^T = V_1 \in (SO(3)U_1 \cup SO(3)U_2)^{qc} \subset K^{qc}.$$

By considering the pairs (U_3, U_4) and (U_5, U_6) and repeating the above argument, we find that

$$\begin{aligned} V_2 &= \operatorname{diag}(\sqrt{\alpha\gamma}, \beta, \sqrt{\alpha\gamma}) \in (SO(3)U_3 \cup SO(3)U_4)^{qc} \subset K^{qc} \quad \text{and} \\ V_3 &= \operatorname{diag}(\sqrt{\alpha\gamma}, \sqrt{\alpha\gamma}, \beta) \in (SO(3)U_5 \cup SO(3)U_6)^{qc} \subset K^{qc}. \end{aligned}$$

Then, K^{qc} being invariant under the action of $SO(3)$, $K_{ct} \subset K^{qc}$ and the proof is complete. □

Theorem 3.4.7 now allows us to deduce the existence of a relative interior point, rank-one connected to the identity for a cubic-to-orthorhombic transition:

Corollary 3.4.10. *Let $\kappa > 0$, $\kappa \neq 1$ and $\Delta > 0$ such that*

$$\frac{|\Delta - 1|}{\Delta}\sqrt{\Delta^4 + 2\Delta^3 + \Delta^2 + 2} < \epsilon$$

where $0 < \epsilon < 1$ is as in Lemma 3.4.6. Further, let K denote the union of the martensitic wells in a cubic-to-orthorhombic transition and assume that the lattice parameters α, β, γ satisfy

$$\sqrt{\alpha\gamma} = \frac{\Delta}{\kappa}, \;\; \beta = \Delta\kappa^2.$$

Then there exist a, $n \in \mathbb{R}^3$ and $F \in \operatorname{rint} K^{qc}$ such that $F = \mathbf{1} + a \otimes n$.

Proof. Follows immediately from Theorem 3.4.7 and Lemma 3.4.9. □

Given the above result, an interesting question to ask is whether we can indeed predict a curved austenite-martensite interface in the CuAlNi specimen of Seiner. This is entirely dependent on the lattice parameters of the specimen and whether they are such that the determinant of the martensitic variants is close enough to 1, as required by Theorem 3.4.7. In accordance with [120], let $\alpha = 1.06372$, $\beta = 0.91542$ and $\gamma = 1.02368$; then $\Delta = (\alpha\beta\gamma)^{1/3} = 0.998935$ and $\kappa = \beta^{1/3}(\alpha\gamma)^{-1/6} = 0.957286$. In particular, $\kappa < 3/2$ and we may take $\epsilon = (\kappa - 1)^2/62 = 2.94277 \times 10^{-5}$. This means that we can apply the above result as long as

$$2.60824 \times 10^{-3} = \frac{|\Delta - 1|}{\Delta}\sqrt{\Delta^4 + 2\Delta^3 + \Delta^2 + 2} > \epsilon = 2.94277 \times 10^{-5},$$

which is impossible. Nevertheless, it should be noted that the failure mechanism lies within the value of the determinant of the martensitic variants and not the lattice parameters themselves. Perhaps, for other materials undergoing the cubic-to-orthorhombic transition the determinant may indeed be sufficiently close to 1 so that our result on the existence of a curved interface applies.

Concluding Remarks. Our method of constructing a curved interface for a set of martensitic wells K is entirely dependent on the existence of a relative interior point of K^{qc} which can be rank-one connected to the identity. As we saw, this poses a difficult problem for which little is known in the existing literature.

Moreover, the analysis does not reveal much about the structure of the relative interior point. Based on the analysis in [53], this point must lie in the lamination convex hull of K, K^{lc}, but we cannot be more explicit.

For transformations with lower martensitic symmetry, e.g. cubic-to-orthorhombic, one might expect that the structure of the relative interior of the respective quasiconvex hulls is much richer and this is a direction worth investigating. Above, we provided the existence of the desired point for a cubic-to-orthorhombic transition but the method of doing so remains the same and we do not exploit this potentially rich structure. In this case, we saw the restriction on the determinant seems much too strong for typical values of the lattice parameters. Possibly, via enlarging the neighbourhood of $\mathbf{1} \in M^{3\times 3}$ from Lemma 3.4.6, we might indeed be able to predict non-planar interfaces for existing alloys or even Seiner's CuAlNi specimen. Of course, there could also be entirely new ways of constructing curved interfaces at a stress-free state and these might come with less stringent assumptions on the lattice parameters. This is ultimately a problem on quasiconvex hulls and appropriate jump conditions, both of which pose deep and interesting questions.

Lastly, we have mentioned already that R. D. James and others [44, 83] have extensively investigated the case when the middle eigenvalue $\lambda_2(U_i)$ of the martensitic variants equals 1 and the so-called *cofactors condition* (see e.g. [83]) holds, both theoretically, and experimentally by appropriately 'tuning' the lattice parameters of alloys. This work has established a strong connection between these conditions and low thermal hysteresis. Under the cofactor condition, one is able to theoretically construct non-planar interfaces with a pure phase of austenite, without the need for a boundary layer; however, this is restricted to this special case and the fact that martensitic twins are directly compatible with the austenite [82].

Chapter 4

Quasiconvexity at faces and edges and the nucleation of austenite in martensite by localized heating

4.1 Introduction

Consider a general variational problem of the form

$$I(y) = \int_{\Omega} W(x, y(x), Dy(x))\, dx$$

over the class of admissible deformations

$$\mathcal{A} = \left\{ y : \Omega \to \mathbb{R}^N : \, y \in X \text{ and } y_{|\partial\Omega_1} = \bar{y} \right\}$$

where $\Omega \subset \mathbb{R}^d$ is a bounded C^1 domain, $W : \overline{\Omega} \times \mathbb{R}^N \times M^{N\times d} \to \mathbb{R}$ satisfies certain conditions, X is an appropriate function space and $\bar{y} \in X$ is a specified function.

Definition 4.1.1. *We say that $y_0 \in \mathcal{A}$ is a strong local minimizer of I if there exists an $\epsilon > 0$ such that $I(y_0) \leq I(y)$ for all $y \in \mathcal{A}$ with $\|y_0 - y\|_\infty < \epsilon$.*
Similarly, $y_0 \in \mathcal{A}$ is a weak local minimizer of I if there exists an $\epsilon > 0$ such that $I(y_0) \leq I(y)$ for all $y \in \mathcal{A}$ with $\|y_0 - y\|_{1,\infty} < \epsilon$.

The Weierstrass problem consists of finding necessary and sufficient conditions for a deformation $y_0 \in \mathcal{A}$ to be a strong local minimizer of I. Of course, the function space X and the conditions on the stored energy function W are themselves part of the problem. This is an old and long-standing problem in the calculus of variations which is fairly well understood in the so-called scalar cases of $d = 1$ (Weierstrass) or $N = 1$ (Hestenes [78]). However, in the vectorial case of d, $N \geq 2$, which is of interest to us, the problem remained largely open.

Let $X = C^1\left(\overline{\Omega}, \mathbb{R}^N\right)$ and define the set $\mathcal{R} = \left\{(y_0(x), Dy_0(x)) : x \in \overline{\Omega}\right\}$ where y_0 is a strong local minimizer of I. Assume that $W(x, y, F)$ is continuous and that its partial derivatives of first and second order in (y, F) exist and are continuous on $\overline{\Omega} \times \mathcal{O}$ where $\mathcal{O}$ is a bounded and open neighbourhood of $\mathcal{R}$ in $\mathbb{R}^N \times M^{N\times d}$. Letting

$$Var\left(\mathcal{A}\right) = \left\{\varphi \in C^1\left(\overline{\Omega}, \mathbb{R}^N\right) : \varphi_{|\partial\Omega_1} = 0\right\},$$

known necessary conditions for the map y_0 to be a strong local minimizer of I are the following:

(i) Satisfaction of the weak form of the Euler-Lagrange equations, i.e.

$$\int_\Omega \left[W_y\left(x, y_0\left(x\right), Dy_0\left(x\right)\right) \cdot \varphi\left(x\right) + W_F\left(x, y_0\left(x\right), Dy_0\left(x\right)\right) \cdot D\varphi\left(x\right)\right] dx = 0$$

for all $\varphi \in Var\left(\mathcal{A}\right)$, where W_y and W_F denote the derivatives of W with respect to y and $F = Dy$ respectively.

(ii) Positivity of the second variation, i.e.

$$\delta^2 I\left(y_0\right) = \frac{d^2}{d\epsilon^2} I\left(y_0 + \epsilon\varphi\right)|_{\epsilon=0} \geq 0$$

for all $\varphi \in Var\left(\mathcal{A}\right)$.

(iii) Quasiconvexity in the interior, i.e. for all $x_0 \in \Omega$

$$\int_B W\left(x_0, y\left(x_0\right), Dy\left(x_0\right) + D\varphi\left(x\right)\right) dx \geq \int_B W\left(x_0, y\left(x_0\right), Dy\left(x_0\right)\right) dx$$

for all $\varphi \in C_0^\infty\left(B, \mathbb{R}^N\right)$ where $B = B\left(0, 1\right)$ denotes the unit ball in $\mathbb{R}^d$.

(iv) Quasiconvexity at the boundary, i.e. for all $x_0 \in \partial\Omega \setminus \overline{\partial\Omega_1}$ - the free boundary -

$$\int_{B^-_{n(x_0)}} W\left(x_0, y\left(x_0\right), Dy\left(x_0\right) + D\varphi\left(x\right)\right) dx \geq \int_{B^-_{n(x_0)}} W\left(x_0, y\left(x_0\right), Dy\left(x_0\right)\right) dx$$

for all $\varphi \in V_{n(x_0)}$ where $n\left(x_0\right)$ is the outward unit normal to Ω at x_0 and

$$V_{n(x_0)} = \left\{\varphi \in C^\infty\left(\overline{B^-_{n(x_0)}}, \mathbb{R}^N\right) : \varphi \equiv 0 \text{ on } \partial B \cap \overline{B^-_{n(x_0)}}\right\}.$$

Here, $B^-_{n(x_0)} = \{x \in B : x \cdot n\left(x_0\right) < 0\}$.

Conditions (i) and (ii) are classical conditions in the sense that these hold true in the scalar cases. The necessity of condition (iii) was shown by Ball in [7] - although this can also be deduced from the arguments of Meyers [102] - and can be thought of as a multi-dimensional version of the Weierstrass positivity condition; in fact, it reduces to it when $d = 1$. Condition (iv) was introduced by Ball and Marsden [22] and is a genuinely new condition valid for the vectorial case.

For such C^1 functions, Grabovsky and Mengesha published a seminal paper in 2009 which showed that a slightly strengthened version of the above necessary conditions is in fact sufficient for a map y_0 to be a strong local minimizer of I. This is a deep result which can be found in [70] and settled a conjecture of Ball in [12] calling for quasiconvexity-based sufficient conditions; see also Grabovsky and Mengesha [69] and Grabovsky [68] for investigations on the problems of sufficient conditions for $W^{1,\infty}$ weak$*$ local minimizers and necessary conditions for $W^{1,\infty}$ strong local minimizers, respectively.

In this section, we examine a problem which has been motivated by an experimental observation of Seiner. This concerns the nucleation of austenite in mechanically stabilized martensite, induced by localized heating in a rectangular specimen of CuAlNi (see Section 4.2 below) and, in a simplified setting, has much in common with the Weierstrass problem. The work in [70], though maybe extendable to domains with edges and corners, works for C^1 domains and is not directly applicable to our case; nevertheless, there are similarities and concluding remarks on the connection with the work of Grabovsky and Mengesha are drawn at the end of this chapter.

4.2 Experimental observations

The shape-recovery process, i.e. the thermally driven transition from the low temperature phase (martensite) into the high-temperature phase (austenite), is a fundamental part of the shape-memory effect. For many shape-memory alloys, the critical temperature for initiation of the shape-recovery process is strongly dependent on the microstructure of martensite entering the transition. When heating is applied to a thermally induced martensitic microstructure obtained by the stress-free cooling of the austenitic phase, the transition starts at a certain temperature which we denote as A_S (austenite start). However, if the material in the martensitic phase is, prior to the heating, deformed (i.e. if the microstructure is reoriented by application of external mechanical loads), this critical temperature can be shifted significantly upwards. This effect is called the mechanical stabilization of martensite and has been

documented for both single crystals and polycrystalline shape-memory alloys (SMAs) [97, 113].

The difference between the shape-recovery process from the mechanically stabilized martensite and from the thermally induced martensitic microstructure was clearly illustrated by acoustic emission (AE) measurements by Landa et al. [94]. The AE method is based on detecting and counting the number of acoustic signals emitted by the material during the course of the transition (see [93, 141] for an example of the use of AE for characterization of the martensitic transitions in SMAs). Fig. 4.1 gives an illustrative example of the comparison of AE records obtained for the same single crystal of the CuAlNi alloy undergoing the transition in these two different regimes. For the thermally induced microstructure, more than 90% of AE events occur in a temperature range between the austenite start temperature A_S and the austenite finish temperature A_F, which is in agreement with DSC measurements for the same material[1]. The transition in this temperature interval is preceded by a small number of events (less than 10%) appearing below A_S. These events can be ascribed to the formation of nuclei of austenite in the thermally induced martensitic microstructure. Above A_S, these nuclei grow successively through the material and provide the transition. For the stabilized martensite, more than 90% of the events are recorded within a very narrow temperature interval. As observed by Seiner et al. [124], the transition from the mechanically stabilized martensite is provided by the formation and propagation of special interfacial microstructures, which interpolate between austenite and mechanically stabilized martensite ensuring the kinematically compatible connection between them. These microstructures are able to exist and propagate in a wide range of temperatures and thermal gradients [122]. Thus, the AE record for the stabilized martensite can be interpreted as follows: the small number of AE events detected below the narrow interval corresponds to the nucleation of austenite. As soon as the nucleation barrier is overcome, the interfacial microstructure propagates abruptly through the specimen and no further increase of the temperature is necessary. This shows how essential the nucleation process is for the effect of mechanical stabilization and the shape-recovery process in general.

The observations that follow were made on a single crystal of CuAlNi, prepared by the Bridgeman method at the Institute of Physics, ASCR. The specimen was a prismatic bar of dimensions $12\times3\times3\text{mm}^3$ in the austenite with edges approximately

[1]These temperatures, however, differ from the transition temperatures of the material used for the experimental observations that follow, since the heat treatment of the material used by Landa et al. [94] was slightly different.

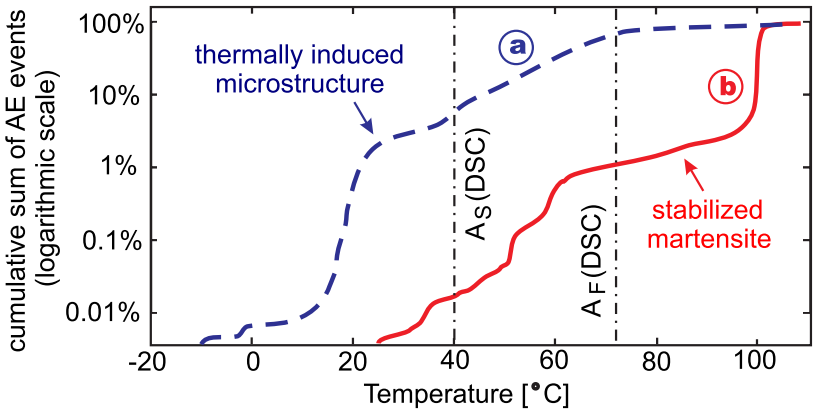

Figure 4.1: Illustrative comparison of AE records for the transitions of CuAlNi single crystal from the thermally induced and mechanically stabilized states. (a) gradual increase of the number of events between A_S and A_F for the thermally induced microstructure; (b) abrupt transition of the stabilized martensite within a narrow temperature interval. The 100% corresponds to $\sim 10^7$ events. Taken from [94] with courtesy of M. Landa.

along the principal directions of the austenitic phase (see [124] for a detailed description), i.e. along the standard basis vectors i_1, i_2, i_3. The martensite-to-austenite transition temperatures determined by DSC were $A_S = -6°\mathrm{C}$ and $A_F = 22°\mathrm{C}$. The critical temperature T_C for the transition from the stabilized martensite induced by homogeneous heating for this specimen was $\sim 60°\mathrm{C}$. This was estimated from optical observations of the transition in this specimen with one of its faces laid on and thermally contacted with a gradually heated Peltier cell, using a heat conducting gel.

The specimen was subjected to the following experimental procedure:

a) by unidirectional compression along its longest edge, the specimen was transformed into a single variant of mechanically stabilized 2H martensite. Due to the mechanical stabilization effect the reverse transition did not occur during unloading.

b) the specimen was then freely laid on a slightly pre-stressed, free-standing polyethylene (PE) foil (thickness 10μm, temperature resistance up to 140°C). This ensured that there were minimal mechanical constraints to the specimen during the observations.

c) the specimen was locally heated by touching its surface with an ohmically heated tip of the Solomon SL-30 (Digital) soldering iron with temperature electronically controlled to be 200°C (control accuracy $\sim \pm 5°\mathrm{C}$), i.e. significantly above the A_S and T_C temperatures. The nucleation of austenite was optically observed and

recorded by a conventional CCD camera (7× optical zoom, 25 frames/second, PAL resolution with `mpeg` compression).

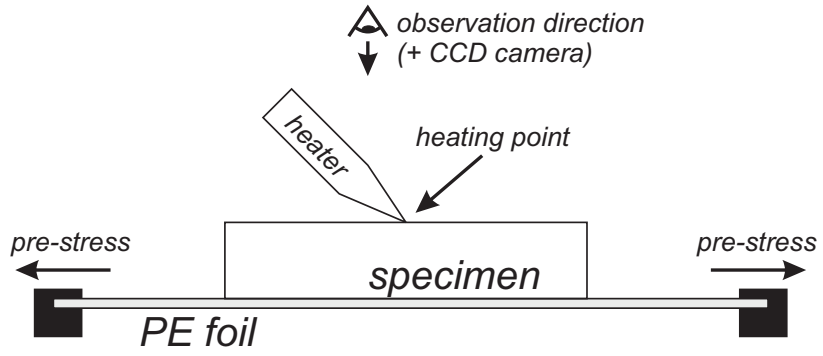

Figure 4.2: Schematic outline of the experimental procedure.

The localized heating was applied in three different ways: (i) with the tip touching one of the corners surrounding the upper face; (ii) with the tip touching one of the edges, approximately in the middle between two corners; (iii) with the tip touching approximately at the centre of the upper face. These experiments were repeated for various orientations of the specimen, i.e. with various faces chosen to be the upper (observed) ones.

When heating was applied at a corner, the nucleation was always induced exactly at that corner and occurred nearly immediately after touching the specimen with the tip. When heating either an edge or the centre of the upper face, the nucleation occurred at one of the corners as well, i.e. the localized heating did not result in formation of the nucleus under the tip. Moreover, the nucleus was only observable after 30-60s, which was enough time for the corner to reach the T_C temperature. In different tests the nuclei were observed at different corners (including those lying on the PE foil) and the exact choice was probably governed by imperfections of the stabilized martensite. After the nucleation, the transition front formed and propagated through the specimen. The velocity of the transition front probably depended on the actual overheating of the specimen. For some runs of the experiment, it propagated at a few millimetres per second (comparable to the transition front propagating in a thermal gradient citePrEASc); for other runs, the whole specimen transformed fully within less than one second. This also supports the conjecture that the nucleation is affected by the local microstructure in the corners: if the nucleation barrier in one of the corners is lowered e.g. by imperfections in the stabilized martensite, the nucleation occurs earlier (i.e. at a lower temperature) and the transition front, which lowers the temperature of the material by the latent heat [122], propagates more slowly.

In Fig. 4.3, snapshots from the observations are seen[2]. The transition fronts have morphologies of the interfacial microstructures described in [124] ($X-$ and $\lambda-$interfaces), in which the mechanically stabilized martensite is separated from austenite by a twinned region ensuring kinematical compatibility.

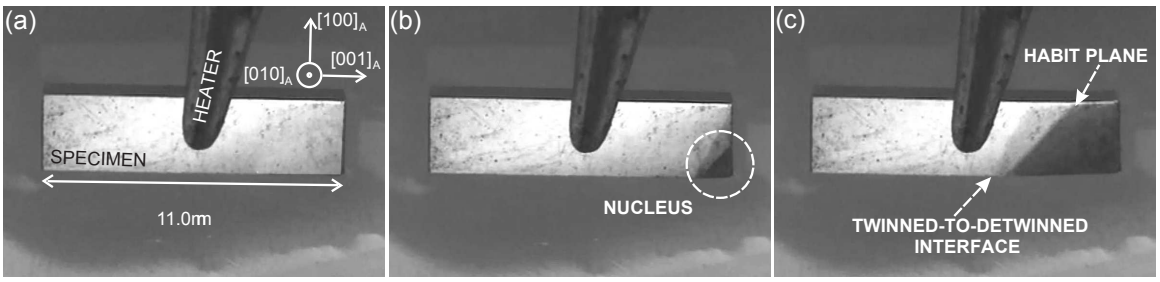

Figure 4.3: Snapshots of the recorded video taken during the optical observations of the nucleation process. (a) the initial state with the length and crystallographic orientation of the specimen given in the coordinate system of the austenitic lattice (indicated by the subscript A); (b) formation of the nucleus at a corner (the first frame of the recorded video in which the nucleus was clearly visible); (c) the fully formed transition front propagating through the specimen. The morphology of the interfacial microstructure is outlined by the arrows indicating the austenite-to-twinned martensite interface (the habit plane) and the twinned-to-detwinned interface between the laminate and the stabilized martensite.

It is only natural to treat this problem as one concerning local minimizers and using a simplified nonlinear elasticity model we propose here an explanation for the location of the nucleation points based on ideas of the modern calculus of variations. It is shown that the stabilized martensite is a local minimizer of the energy with respect to localized variations in the interior, on faces, and at edges of the sample, but not at all corners, where a localized microstructure can lower the energy.

4.3 The Ciarlet-Nečas constraint

At this point, we introduce an additional ingredient which will enter into our model in the form of the constraint set by Ciarlet & Nečas in [39]. In particular, for $\Omega \subset \mathbb{R}^3$ Lipschitz, consider the minimization problem

$$\mathcal{E}(y) = \int_\Omega f(Dy(x))\,dx$$

over the set $\mathcal{A} = \left\{ y \in W^{1,p}(\Omega, \mathbb{R}^3) : y_{|\partial\Omega_1} = y_0, \det Dy > 0 \text{ a.e.} \right\}$ of admissible deformations, for some $p > 3$; this is typical for elasticity. Ciarlet and Nečas proposed to

[2]The recorded video can be seen in the electronic version of [21]

set an additional constraint on the admissible deformations that

$$\int_\Omega \det Dy(x)\, dx \leq \mathcal{L}^3(y(\Omega)). \tag{C-N}$$

In [39], they showed that by imposing condition (C-N) the associated minimization problem results in a mathematical model for matter to come into frictionless contact with, but not interpenetrate, itself. In particular, they showed that under this constraint any admissible deformation, say y, is injective a.e. in $\overline{\Omega}$ in the sense that

$$\operatorname{card} y^{-1}(x') = 1 \quad \text{for almost all } x' \in y(\overline{\Omega}).$$

They also showed that condition (C-N) is closed under weak convergence in $W^{1,p}(\Omega, \mathbb{R}^3)$ for $p > 3$ (weak$*$ if $p = \infty$) so that minimizers of the associated problem remain a.e. injective. To retain completeness we show precisely how condition (C-N) results in almost everywhere injective maps and, as such, we do not elaborate further on the work of Ciarlet and Nečas.

Remark. The interpenetration of matter and the invertibility of Sobolev mappings is a problem that many authors have contributed to, particularly in the case of pure displacement problems; e.g. Ball [8] establishes global invertibility for orientation preserving maps in $W^{1,p}(\Omega, \mathbb{R}^3)$, $p > 3$, under an integrability condition and the assumption that these agree with an injective map on the boundary mapping Ω to a sufficiently regular set; Šverák [132] extends Ball's work proving various continuity properties as well as the invertibility of a class of functions relevant to nonlinear elasticity. Moreover, Ciarlet and Destuynder [38] and Valent [140] establish global injectivity in nonlinear elasticity under the assumption that the applied body force density is small in the space L^p, $p > 3$, within the existence theory based on the implicit function theorem. The book of Fonseca and Gangbo [61] is a very good reference as it contains insightful results regarding general invertibility problems for Sobolev mappings within the context of degree theory. The reader is also referred to Csörnyei, Hencl and Malý [43], Hencl et al. [75, 76, 77] as well as Henao and Mora-Corral [73, 74] for other works on the invertibility of Sobolev (and BV) mappings.

In our context, the (C-N) constraint results in deformations which are homeomorphic in Ω rather than simply a.e. injective. This is because our admissible deformations also satisfy an additional property, namely that of having bounded distortion, a class of functions which we define next. We note that our admissible deformations being homeomorphic is a powerful result and allows us to extend our methods and

main result to a set of domains which is much larger than the one obtained without (C-N).

Definition 4.3.1. *Let $\Omega \subset \mathbb{R}^d$ be open. A continuous map $y : \Omega \to \mathbb{R}^d$ is called a mapping of bounded distortion if:*

- $y \in W^{1,d}_{\mathrm{loc}}(\Omega; \mathbb{R}^d)$,
- $\det Dy(x)$ *does not change sign in* Ω *and*
- *there exists a number* $M \geq 1$ *such that*

$$\|Dy(x)\|^d \leq M |\det Dy(x)|$$

for almost all $x \in \Omega$.

Here, $\|Dy(x)\| = \sup_{|z|\leq 1} |Dy(x)z| = \sigma_{\max}(Dy(x))$ *- the maximum singular value of* $Dy(x)$.

Mappings of bounded distortion share remarkable properties and below we present one of them which is crucial for our purposes; the proof of the following lemma can be found in Reshetnyak [116].

Lemma 4.3.1. *Every mapping y of bounded distortion from an open domain Ω to the space $\mathbb{R}^d$ which is not identically constant is an open mapping.*

We end this section by proving an auxilliary result which will be used to establish the regularity of our deformations under the (C-N) constraint and that of being mappings of bounded distortion.

Lemma 4.3.2. *Let $\Omega \subset \mathbb{R}^3$ be a bounded Lipschitz domain. Suppose that $y \in W^{1,\infty}(\Omega, \mathbb{R}^3)$ is a mapping of bounded distortion, satisfying (C-N) and $\det Dy(x) \geq r > 0$ a.e. in Ω. Then, y is a homeomorphism between Ω and $y(\Omega)$, its inverse y^{-1} belongs to $W^{1,\infty}(y(\Omega), \mathbb{R}^3)$ and*

$$Dy^{-1}(x') = \left[Dy(y^{-1}(x'))\right]^{-1}$$

for a.e. $x' \in y(\Omega)$.

Proof. We first show how the (C-N) constraint results in y being a.e. injective. For Ω a bounded and open subset of $\mathbb{R}^3$ and $y \in W^{1,p}(\Omega, \mathbb{R}^3)$, $p > 3$, a theorem of Marcus and Mizel [99] shows that

$$\int_\Omega |\det\, Dy(x)|\, dx = \int_{y(\Omega)} \operatorname{card} y^{-1}(x')\, dx' \tag{4.3.1}$$

whenever one of the two integrals is meaningful. In our case, $y \in W^{1,\infty}(\Omega, \mathbb{R}^3)$ and the integral on the left side of (4.3.1) is bounded. Then, using (4.3.1) and the (C-N) constraint we infer that

$$\mathcal{L}^3(y(\Omega)) = \int_{y(\Omega)} dx' \leq \int_{y(\Omega)} \operatorname{card} y^{-1}(x')\, dx' = \int_\Omega \det\, Dy(x)\, dx \leq \mathcal{L}^3(y(\Omega))$$

from which we obtain the required a.e. injectivity, i.e.

$$\operatorname{card} y^{-1}(x') = 1 \quad \text{for a.e. } x' \in y(\Omega).$$

Injectivity everywhere in Ω now follows due to the fact that y has bounded distortion. In particular, if the mapping y is identically equal to a constant, it cannot be a.e. injective and Lemma 4.3.1 implies that y is an open mapping. To reach a contradiction, suppose that there exist $x_1, x_2 \in \Omega$ such that $y(x_1) = y(x_2) = y_0 \in \mathbb{R}^3$, so that y fails to be injective. Note that $y_0 \in y(\Omega)$ which is open since Ω is open and y maps open sets to open sets; hence, there exists $\epsilon > 0$ such that $B(y_0, \epsilon) \subset y(\Omega)$.

By the continuity of y the inverse image of $B(y_0, \epsilon)$, $y^{-1}(B(y_0, \epsilon))$, is an open set. However, x_1, $x_2 \in y^{-1}(B(y_0, \epsilon))$ and we can thus find open neighbourhoods U, V of x_1, x_2 respectively such that

$$U, V \subset y^{-1}(B(y_0, \epsilon)),\ x_1 \in U,\ x_2 \in V \ \text{ and } \ U \cap V = \emptyset.$$

As y is an open mapping, $y(U)$ and $y(V)$ are open sets. Furthermore, $y(U) \cap y(V)$ is open and non-empty, since $y_0 \in y(U) \cap y(V)$. Thus, $\mathcal{L}^3(y(U) \cap y(V)) > 0$ and it must be the case that

$$\operatorname{card}\, y^{-1}(x') \geq 2 \ \text{ for all } \ x' \in y(U) \cap y(V),$$

contradicting a.e. injectivity. Then, y being injective and open, it is a homeomorphism from Ω to $y(\Omega)$.

As for the regularity of y^{-1}, $\det Dy(x) \geq r > 0$ for a.e. $x \in \Omega$, i.e. $[Dy]^{-1} \in L^\infty(y(\Omega), \mathbb{R}^{3\times 3})$. To conclude the proof, we deduce that $Dy^{-1}(x') = [Dy(y^{-1}(x'))]^{-1}$ in the sense of distributions; then y^{-1} being itself bounded in $y(\Omega)$, it is an element of $W^{1,\infty}(y(\Omega), \mathbb{R}^3)$. Let $w \equiv y^{-1}$ and $\psi : \Omega \to \mathbb{R}$ a smooth, compactly supported function; letting $x' = y(x)$

$$\begin{aligned} \int_{y(\Omega)} w_i(x') \frac{\partial \psi}{\partial x'_j}(x') dx' &= \int_\Omega x_i \frac{\partial \psi}{\partial x'_j}(y(x)) \det Dy(x)\, dx \\ &= \int_\Omega x_i \frac{\partial \psi}{\partial x_k}(y(x)) [Dy(x)]^{-1}_{kj} \det Dy(x)\, dx \end{aligned}$$

by the chain rule, the fact that $y \in W^{1,\infty}$ is differentiable a.e. and $[Dy]^{-1} \in L^{\infty}(\Omega, \mathbb{R}^{3\times 3})$. Using Piola's identity and integrating by parts,

$$\begin{aligned}\int_{y(\Omega)} w_i(x')\frac{\partial \psi}{\partial x'_j}(x')dx' &= -\int_{\Omega} \delta_{ik}\psi(y(x))(\operatorname{cof} Dy(x))_{jk}\,dx \\ &= -\int_{\Omega} \frac{(\operatorname{cof} Dy(x))_{ji}}{\det Dy(x)}\psi(y(x))\det Dy(x)\,dx \\ &= -\int_{y(\Omega)} \frac{(\operatorname{cof} Dy(w(x')))_{ji}}{\det Dy(w(x'))}\psi(x')\,dx',\end{aligned}$$

completing the proof. □

Remark. We note that y^{-1} becomes itself a map of bounded distortion which also implies that y^{-1} is differentiable a.e. (see [116]).

We also remark that since $y \in W^{1,\infty}(\Omega, \mathbb{R}^3)$ is a homeomorphism with bounded distortion, a theorem from [43][3] asserts that its inverse already lies in the space $W^{1,1}_{\mathrm{loc}}(y(\Omega), \mathbb{R}^3)$. In particular, y^{-1} is absolutely continuous on almost all lines parallel to the axes, i.e. y^{-1} admits classical first partial derivatives a.e. and these coincide with the generalized derivatives (see e.g. [3, 101, 104, 117]).

Moreover, note that y being a $W^{1,\infty}$ homeomorphism, one cannot expect that $y^{-1} \in W^{1,1}_{\mathrm{loc}}(y(\Omega), \mathbb{R}^3)$. As an example, consider the map $f(x) = x + u(x)$, $x \in \mathbb{R}$, where u is the usual Cantor ternary function and let $g \equiv f^{-1}$. Then g^{-1} fails to be absolutely continuous. By setting $h(x) = (g(x_1), x_2, x_3)$, one obtains a Lipschitz homeomorphism whose inverse is not in $W^{1,1}_{\mathrm{loc}}(y(\Omega), \mathbb{R}^3)$.

In [43], the additional condition set on y is that it has finite distortion - a notion satisfied for our admissible functions - and provides an inverse map which is of finite distortion as well. Without this assumption, y^{-1} can only be expected to be in $BV_{loc}(y(\Omega), \mathbb{R}^3)$, the space of functions with locally bounded variation. The theory of mappings of finite distortion and quasi-conformal maps has played an important role in the regularity of inverses of Sobolev (and BV) maps and the reader is referred to [75, 76, 77, 110, 151] and references therein for similar results.

4.4 A simplified model

For the purposes of this exposition we derive an appropriate variational model which is based on the Young measure approach. The main reason for this is that Young

[3] In fact, in dimension 3, it only requires that $y \in W^{1,2}_{\mathrm{loc}}(\Omega, \mathbb{R}^3)$ and is a homeomorphism of finite distortion; a notion weaker than that of bounded distortion.

measures are conceptually simpler and arise more naturally in the context of microstructure. In terms of Young measures, the problem becomes that of minimizing

$$I_\theta(\nu) = \int_\Omega \langle \nu_x, \varphi \rangle \, dx \tag{4.4.1}$$

over some set of admissible gradient Young measures. We recall that, for the minimization problem (4.4.1), the underlying deformation gradient of a Young measure minimizer ν, given by $\bar{\nu}_x$, corresponds to the macroscopic deformation gradient.

We note that in our approach we do not assume any coercivity or growth for our energy density φ and, therefore, the minimization problem in terms of Young measures does not necessarily serve as a relaxation method for the gradient problem.

To set up our model, let $\Omega \subset \mathbb{R}^3$ - a bounded domain - describe the rectangular specimen in austenite at the critical temperature θ_c and let

$$K := SO(3) \cup \bigcup_{i=1}^{6} SO(3) U_i$$

denote the union of the energy wells of the austenite and the martensite; for the cubic-to-orthorhombic transition of CuAlNi the martensitic variants U_i, $i = 1, \ldots, 6$ being given in (3.3.1).

Henceforth, we make the assumption on the lattice parameters that $\det U_s \leq 1$ and $\lambda_{\max}(\operatorname{cof} U_s) \geq 1$, where $\lambda_{\max}(A)$ denotes the largest eigenvalue of the matrix A; in particular, the same holds for all martensitic variants as they are symmetry related. This is a technical assumption and it should be noted that it is consistent with the lattice parameters of the CuAlNi specimen used in the experiment.

For our energy density $\varphi : M^{3\times 3} \to \overline{\mathbb{R}} = \mathbb{R} \cup \{+\infty\}$ we only assume lower semicontinuity. Moreover, as described in the experimental observations, the temperature of the iron tip exceeded the critical temperature significantly and it was only after the lapse of sufficient time for the corner to reach the critical temperature that the transformation initiated; thus, we make the assumption that $\theta > \theta_c$, i.e. the austenite is energetically preferable to the martensitic variants. Specifically, on the energy wells K, we assume that

$$\varphi(F) = \begin{cases} -\delta, & F \in SO(3) \\ \\ 0, & F \in \bigcup_{i=1}^{6} SO(3) U_i \end{cases} \tag{4.4.2}$$

where $\delta > 0$ is such that $\min_{M^{3\times 3}} \varphi = -\delta$ (the austenite minimizes φ); in particular, φ is bounded below.

The above form for φ is natural and as for the lower semicontinuity, this is the least we can assume to make the minimization problem meaningful. As noted above, we do not impose any coercivity or growth conditions for our minimization problem. However, the question of local minimizers is dependent on the growth of φ off the energy wells and in order to make the problem more tractable, we wish to work with an energy functional which captures the essential behaviour of φ but becomes infinite off the set K. This allows one to disregard the growth of φ and instead concentrate only on microstructures supported on the wells; moreover, any configuration that lowers the energy will necessarily be partly supported on the austenitic well, $SO(3)$, so that austenite has nucleated. To derive this functional rigorously we invoke Γ-convergence, the definition of which we now recall in some generality:

Definition 4.4.1. *Let (X, d) be a metric space. We say that a sequence $I^k : X \to \mathbb{R} \cup \{\pm\infty\}$ $\Gamma(d)$-converges to $I : X \to \mathbb{R} \cup \{\pm\infty\}$ if for all $x \in X$ we have:*

(i) (liminf inequality) for every sequence x^k converging to x

$$I(x) \leq \liminf_k I^k\left(x^k\right); \tag{4.4.3}$$

(ii) (existence of a recovery sequence) there exists a sequence x^k converging to x such that

$$I(x) \geq \limsup_k I^k\left(x^k\right), \tag{4.4.4}$$

or, equivalently by 4.4.3,

$$I(x) = \lim_k I^k\left(x^k\right). \tag{4.4.5}$$

The function I is called the $\Gamma(d)$-limit of I^k and we write $I = \Gamma(d)\text{-}\lim_k I^k$.

The notion of Γ-convergence was first introduced by De Giorgi [50, 51] and has been a very powerful technique, particularly in homogenization problems and the passage from atomistic to continuum models. Γ-convergence defines a topology on the space of lower semicontinuous functions on X and the idea behind it is to precisely introduce a suitable notion of 'variational convergence' which is captured by the following classical theorem, see e.g. [36].

Theorem 4.4.1. *Let (X, d) be a metric space and suppose that the sequence of functions $I^k : X \to \mathbb{R} \cup \{\pm\infty\}$ is equi-mildly coercive, i.e. there exists a compact set $L \subset X$ such that $\inf_X I^k = \inf_L I^k$ for all $k \in \mathbb{N}$. Suppose that the $\Gamma(d)$-limit of I^k exists and $I = \Gamma(d)\text{-}\lim_k I^k$; then $\min_X I$ exists and*

$$\min_X I = \lim_{k\to\infty} \inf_X I^k.$$

Moreover, if x^k is a converging sequence such that $\lim_k I^k\left(x^k\right) = \lim_k \inf_X I^k$ then its limit is a minimum point for I.

This type of convergence is only used to deduce our model rigorously and we do not make use of any relevant deep results. As such we do not further review Γ-convergence here and we refer the reader to the books of Braides and Defranceschi [36] as well as that of Dal Maso [49] for an extensive account.

Returning to our model, it is only natural to restrict attention to $W^{1,\infty}$ gradient Young measures since, once we consider the blown up version of our functional, any gradient Young measure with finite energy will be supported entirely within the compact set K. For notational convenience, let us denote the closed unit ball of $L^\infty_{w^*}\left(\Omega, \mathcal{M}\left(M^{3\times 3}\right)\right)$ by $\mathcal{B}$, i.e.

$$\mathcal{B} = \left\{\nu \in L^\infty_{w^*}\left(\Omega, \mathcal{M}\left(M^{3\times 3}\right)\right) : \nu_x \geq 0,\ \|\nu_x\|_{\mathcal{M}(M^{3\times 3})} \leq 1 \text{ a.e.}\right\}.$$

Any Young measure $\nu = (\nu_x)_{x\in\Omega}$ is a probability measure for a.e. x and hence belongs to $\mathcal{B}$. In our minimization problem we will be interested in a class of admissible measures which belong to the subset of $\mathcal{B}$

$$\mathcal{M}^\infty := \{\nu = (\nu_x)_{x\in\Omega} \in \mathcal{B} : \nu \text{ a } W^{1,\infty} \text{ gradient Young measure}\}$$

under certain constraints and the (C-N) constraint introduced in Section 4.3 is one of them. Of course, our model is expressed in terms of gradient Young measures and we employ condition (C-N) in the obvious way, i.e. we require that the underlying deformation of any admissible gradient Young measure satisfies this constraint. Here, for the purposes of deriving our energy via Γ-convergence, we define our functionals on the class of measures

$$\mathcal{A} := \{\nu \in \mathcal{M}^\infty : \bar{\nu}_x = Dy(x) \text{ a.e., } \det Dy(x) > 0 \text{ a.e., } y \text{ satisfies (C-N)}\}. \quad (4.4.6)$$

Note also that we will be interested in the Γ-limit with respect to the weak$*$ convergence in the space $L^\infty_{w^*}\left(\Omega, \mathcal{M}\left(M^{3\times 3}\right)\right)$. In principle, Γ-convergence can be defined for a general topological space (X, τ) where the convergence is naturally induced by the topology τ; nevertheless, one needs to be careful as some general results may not be valid.

However, the space $L^\infty_{w^*}\left(\Omega, \mathcal{M}\left(M^{3\times 3}\right)\right)$ is the dual of $L^1\left(\Omega, C_0\left(M^{3\times 3}\right)\right)$ - a separable normed vector space - and the Banach Alaoglu theorem states that $\mathcal{B}$ is weak$*$

compact. Then $\mathcal{B}$ equipped with the topology induced by the weak$*$ convergence is a metrizable space (see e.g. [62])[4] with metric given by

$$\mathrm{d}(\nu,\,\mu)=\sum_{i,j=1}^{\infty}2^{-i-j}|(\nu-\mu,h_j\otimes f_i)|=\sum_{i,j=1}^{\infty}2^{-i-j}\left|\int_{\Omega}h_j(x)\,\langle\nu_x-\mu_x,f_j\rangle\,dx\right| \quad (4.4.7)$$

where $\{f_i\}$ and $\{h_j\}$ are countable dense subsets in the unit balls of $C_0(M^{3\times3})$ and $L^1(\Omega)$ respectively. Henceforth, we will freely use the term Γ-convergence with respect to the weak$*$ topology in $\mathcal{B}$ without referring to the above argument about its metrization.

Let us consider a function $\psi:M^{3\times3}\to\mathbb{R}$ and assume that

$$\psi(F)\geq0,\ \psi(F)=0\Leftrightarrow F\in K\ \text{ and }\ -d+c|F|^p\leq\psi(F), \quad (4.4.8)$$

for some $d,\ c>0$ and $p>3$. Let $\varphi^k:=k\psi+\varphi$ and for each $k\in\mathbb{N}$ define the functional $I^k:\mathcal{A}\to\overline{\mathbb{R}}$ by

$$I^k(\nu):=\int_{\Omega}\langle\nu_x,\varphi^k\rangle\,dx. \quad (4.4.9)$$

The function ψ vanishes on the energy wells K, whereas, away from them it is strictly positive and increasing. In the limit $k\to\infty$, one expects that the increasing term $k\psi$ will force the limiting functional to blow up whenever a measure is supported anywhere off the set K, while, for measures with support contained in K the functional should capture the behaviour of φ.

Lemma 4.4.2. *Let $\varphi,\ \psi:M^{3\times3}\to\overline{\mathbb{R}}$ be lower semicontinuous functions satisfying (4.4.2) and (4.4.8) respectively and for $k\in\mathbb{N}$ write $\varphi^k=k\psi+\varphi$. Let $I^k:\mathcal{A}\to\mathbb{R}$ be as in (4.4.9). Then, $I=\Gamma\text{-}\lim_{k\to\infty}I^k$ with respect to the weak$*$ convergence of Young measures, where*

$$I(\nu)=\begin{cases}-\delta\int_{\Omega}\nu_x(SO(3))\,dx, & \operatorname{supp}\nu\subset K\\ +\infty, & \text{otherwise}\end{cases} \quad (4.4.10)$$

and $\nu_x(SO(3))=\int_{SO(3)}d\nu_x(A)$.

Remark. In terms of microstructures, the expression $\nu_x(SO(3))$ represents the volume fraction of $SO(3)$ in the microstructure corresponding to ν_x at $x\in\Omega$.

[4]In general, suppose that X is a separable normed space and let $L\subset X^*$ be compact in the weak$*$ topology. Then L equipped with the weak$*$ topology is a metrizable space.

Proof. Note that since $\psi \geq 0$, the sequence φ^k is increasing and therefore so is I^k, i.e. the Γ-limit exists and is given by the supremum of the lower semicontinuous envelopes of the functionals I^k, see e.g. [49]. To establish the lim inf-inequality, let $\nu^k \in \mathcal{A}$ such that

$$\nu^k \overset{*}{\rightharpoonup} \nu \quad \text{in} \quad L^\infty_{w^*}\left(\Omega,\, \mathcal{M}\left(\mathbb{R}^{3\times 3}\right)\right).$$

Let us show that $\nu \in \mathcal{A}$. Clearly, we may assume that $\liminf_k I^k\left(\nu^k\right) < \infty$. In particular, this implies that $\operatorname{supp}\nu_x \subset K$ a.e. in Ω; otherwise, ν has part of its support outside K. Then, letting $f \in C_0(\mathbb{R}^{3\times 3})$ such that $0 \leq f \leq \psi$ and $f(A) = 0$ if and only if $A \in K$, we deduce by the weak$*$ convergence of ν^k that

$$\int_\Omega \langle \nu^k_x, f\rangle\, dx \to \int_\Omega \langle \nu_x, f\rangle\, dx = C > 0$$

since $f > 0$ outside K and ν has at least part of its support outside K. Hence, for k large enough,

$$\begin{aligned} I^k(\nu^k) &= k\int_\Omega \langle \nu^k_x, \psi\rangle\, dx + \int_\Omega \langle \nu^k_x, \varphi\rangle\, dx \\ &\geq k\int_\Omega \langle \nu^k_x, f\rangle\, dx - \delta|\Omega| \\ &\geq k\frac{C}{2} - \delta|\Omega|. \end{aligned}$$

But $\liminf_k I^k\left(\nu^k\right) < \infty$, leading to a contradiction.

Also, since $\liminf_k I^k\left(\nu^k\right) < \infty$, up to a subsequence, we may also assume that $\sup_k I^k(\nu^k) < \infty$ and, by (4.4.8), we deduce that, for some constant C,

$$\sup_k \int_\Omega \int_{\mathbb{R}^{3\times 3}} |A|^p\, d\nu^k_x(A)dx \leq C. \tag{4.4.11}$$

In particular, this implies that ν_x is a probability measure a.e. (e.g. Theorem 3.6, [137]) and that (e.g. Theorem 3.7, [137])

$$\bar{\nu}^k \rightharpoonup \bar{\nu} \ \text{ in } L^p(\Omega, \mathbb{R}^{3\times 3}). \tag{4.4.12}$$

In particular, we may assume that the functions y^k underlying the measures ν^k are uniformly bounded in $W^{1,p}(\Omega, \mathbb{R}^3)$ and in view of (4.4.12), $y^k \rightharpoonup y$ in $W^{1,p}(\Omega, \mathbb{R}^3)$ where $Dy(x) = \bar{\nu}_x$ a.e. in Ω; note, that a priori $y^k \in W^{1,\infty}(\Omega, \mathbb{R}^3)$ for each k but the bound is not uniform.

By Proposition 4.6 in [137], we infer that ν is a $W^{1,p}$ gradient Young measure and, since $\operatorname{supp}\nu_x \subset K$ a.e., Zhang's lemma says that $\nu \in \mathcal{M}^\infty$. The remaining conditions

now follow: the determinant constraint follows from the minors relations (2.1.12) and the fact that $\operatorname{supp}\nu_x \subset K$ a.e. in Ω since then

$$\begin{aligned} 0 < \min(\det U_s, 1) &= \min_{F\in K} \det F \leq \langle \nu_x, \det\rangle = \det \bar{\nu}_x \\ &= \det Dy(x) \leq \max_{F\in K} \det F = \max(\det U_s, 1) \end{aligned} \tag{4.4.13}$$

and (C-N) follows by the fact that each y^k satisfies (C-N) and $y^k \rightharpoonup y$ in $W^{1,p}(\Omega, \mathbb{R}^3)$, $p > 3$ (see [39]).

Having established that $\nu \in \mathcal{A}$, let us prove the lim inf-inequality. Note that any non-negative lower semicontinuous function f on $\mathbb{R}^{3\times 3}$ (generally, on a metric space) is the pointwise supremum of a non-decreasing sequence of functions in $C_0(\mathbb{R}^{3\times 3})$, e.g. given f, its Lipschitz regularizations

$$f_n(F) := \inf_{A\in\mathbb{R}^{3\times 3}} (f(A) + n|F - A|)$$

satisfy $f_1 \leq f_2 \leq \ldots \leq f$ and $f_n(F) \to f(F)$ for all $F \in \mathbb{R}^{3\times 3}$. Multiplying each f_n by a suitable decaying and continuous function, we obtain the required sequence in $C_0(\mathbb{R}^{3\times 3})$. Next, consider the map $\varphi + \delta$; this is non-negative, lower semicontinuous and, hence, there exists a non-decreasing sequence of functions, say $\varphi_n \in C_0(M^{3\times 3})$ with $0 \leq \varphi_n \leq \varphi + \delta$ converging pointwise to $\varphi + \delta$. Then, by weak$*$ convergence and the fact that $\varphi_n \leq \varphi + \delta$, for $n \in \mathbb{N}$

$$\begin{aligned} \int_\Omega \langle \nu_x, \varphi_n\rangle \, dx &= \liminf_{k\to\infty} \int_\Omega \langle \nu_x^k, \varphi_n\rangle \, dx \\ &\leq \liminf_{k\to\infty} \int_\Omega \langle \nu_x^k, \varphi + \delta\rangle \, dx \\ &\leq \liminf_{k\to\infty} \int_\Omega \langle \nu_x^k, k\psi + \varphi + \delta\rangle \, dx = \liminf_{k\to\infty} I^k(\nu^k) + \delta|\Omega| \end{aligned}$$

since $\psi \geq 0$ and ν_x^k is a probability measure for a.e. x. But, $0 \leq \varphi_n$ for all n and letting $n \to \infty$, we obtain the lim inf inequality by monotone convergence and the fact that ν_x is a probability measure a.e. in Ω.

For the recovery sequence, let $\nu \in \mathcal{A}$ and assume that $I(\nu) < \infty$ as otherwise the result follows; in particular, $\operatorname{supp}\nu_x \subset K$ a.e. in Ω. The recovery sequence is simply given by the constant sequence $\nu^k = \nu$, as trivially $\nu^k \in \mathcal{A}$, $\nu^k \overset{*}{\rightharpoonup} \nu$ and

$$I^k(\nu^k) = I^k(\nu) = k\int_\Omega \langle \nu_x, \psi\rangle \, dx + \int_\Omega \langle \nu_x, \varphi\rangle \, dx = \int_\Omega \langle \nu_x, \varphi\rangle \, dx.$$

since $\operatorname{supp}\nu_x \subset K$ a.e and $\psi = 0$ on K. $\square$

Remark. Alternatively, we write our energy functional $I(\nu)$ as

$$I(\nu) = \int_\Omega \langle \nu_x, W \rangle \, dx$$

where the energy density $W : M^{3\times 3} \to \overline{\mathbb{R}}$ is given by

$$W(F) = \begin{cases} -\delta, & F \in \mathrm{SO}(3) \\ 0, & F \in \bigcup_{i=1}^{6} \mathrm{SO}(3)\, U_i \\ +\infty, & \text{otherwise.} \end{cases} \tag{4.4.14}$$

Admissible measures

Having established the form of our energy we next define the set of admissible measures, i.e. the set of $W^{1,\infty}$ gradient Young measures competing in the minimization. Throughout the rest of this thesis, we denote the mechanically stabilized variant of martensite by U_s. Then, the homogeneous gradient Young measure δ_{U_s} corresponds to a pure phase of the martensitic variant U_s.

In our minimization problem, we only consider variations of δ_{U_s} which are localized in the interior, on faces, edges and at corners. In particular, let S_i, S_f, S_e, $S_c \subset \Omega$ be as in Fig. 4.4.

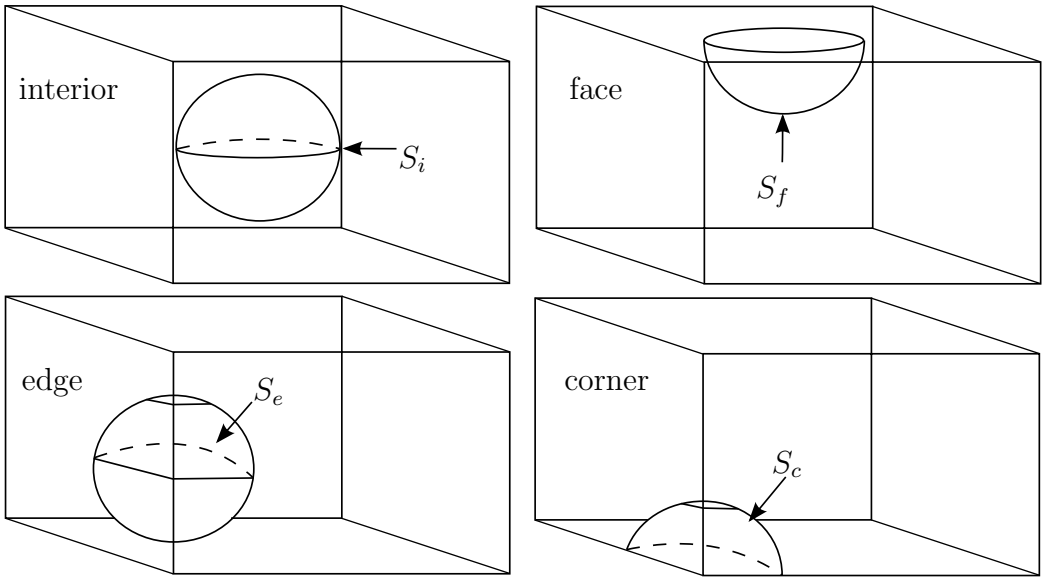

Figure 4.4: Subsets of Ω used for testing whether nucleation of austenite can occur in the interior, on a face, an edge and at a corner; these are given respectively by the intersection of Ω with a small ball centred at a point in the interior, on a face, an edge or a corner.

More precisely, let $B(x_0, r)$ be the ball of radius $r > 0$ centered at x_0.

- (interior) Let $x_0 \in \Omega$; $S_i = B(x_0, r)$ for some $r > 0$ such that $\overline{S_i} \subset \Omega$.
- (face) Suppose that a face F is contained in the plane $\{x \cdot n = k\}$ where $n \in S^2$ is outward pointing and $k \in \mathbb{R}$. Let $x_0 \in F$; then $S_f = \{x \in B(x_0, r) : x \cdot n < k\}$ for some $r > 0$ such that $\overline{S_f} \setminus \{x \cdot n = k\} \subset \Omega$.
- (edge) Suppose that an edge E is the intersection of two faces contained in the planes $\{x \cdot n_1 = k_1\}$ and $\{x \cdot n_2 = k_2\}$ where $n_i \in S^2$ are outward pointing and $k_i \in \mathbb{R}$, $i = 1, 2$. Let $x_0 \in E$; then $S_e = \{x \in B(x_0, r) : x \cdot n_i < k_i \ \forall\, i = 1, 2\}$ for some $r > 0$ such that $\overline{S_e} \setminus \bigcup_{i=1}^{2} \{x \cdot n_i = k_i\} \subset \Omega$.
- (corner) Suppose that a corner C is the intersection of three faces contained in the planes $\{x \cdot n_i = k_i\}$ where $n_i \in S^2$ are outward pointing and $k_i \in \mathbb{R}$, $i = 1, 2, 3$. Let $x_0 \in C$; then $S_c = \{x \in B(x_0, r) : x \cdot n_i < k_i \ \forall\, i = 1, 2, 3\}$ for some $r > 0$ such that $\overline{S_c} \setminus \bigcup_{i=1}^{3} \{x \cdot n_i = k_i\} \subset \Omega$.

Definition 4.4.2. *Let $\omega \in \{i, f, e, c\}$. We say that a measure $\nu = (\nu_x)_{x \in \Omega}$ is admissible for the interior (resp. a face, an edge or a corner) if $\nu \in \mathcal{A}_i$ (resp. $\mathcal{A}_f$, $\mathcal{A}_e$ or $\mathcal{A}_c$) where*

$$\mathcal{A}_\omega = \left\{ \begin{array}{r} \nu \in \mathcal{M}^\infty : \nu_x = \delta_{U_s} \text{ a.e. outside } S_\omega \text{ and its underlying deformation } y \\ \text{satisfies (C-N), } \det Dy > 0 \text{ a.e. and } y(x) = U_s x \text{ on } \partial S_\omega \cap \Omega \end{array} \right\}.$$

Remark. Note that the sets S_i, S_f, S_e, S_c are chosen to be (parts of) balls for simplicity; clearly, no matter what the shape of a 'nucleation region' is, it can always be embedded in (part of) such a ball.

Moreover, with the above notation and for $S \in \{S_i, S_f, S_e, S_c\}$ we can write ∂S as the disjoint union of $\partial S \cap \Omega$ and $\partial S \cap \partial\Omega$, which are relatively open and closed subsets of ∂S respectively, where relative means with respect to ∂S.

For faces, edges and corners $\partial S_f \cap \partial\Omega$, $\partial S_e \cap \partial\Omega$ and $\partial S_c \cap \partial\Omega$ act as free boundaries; these are comprised of part of the given face, parts of the two faces that meet at the given edge and parts of the three faces that meet at the given corner, respectively.

Note that any deformation y underlying an admissible Young measure is required to be in $W^{1,\infty}(\Omega, \mathbb{R}^3)$ and to satisfy the linear boundary condition $y(x) = U_s x$ on $\partial S \cap \Omega$. By the Sobolev embeddings, y is continuous up to the boundary of Ω and hence, whenever $y(x) = U_s x$ on $\partial S \cap \Omega$ then also $y(x) = U_s x$ on $\overline{\partial S \cap \Omega}$.

We now end this section by showing how condition (C-N) leads to finite-energy deformations which, as claimed, are homeomorphic in Ω.

Theorem 4.4.3. *Let $\omega \in \{i, f, e, c\}$ and $\nu \in \mathcal{A}_\omega$. Suppose that* $\operatorname{supp}\nu_x \subset K$ *a.e. in* Ω *and let* $y \in W^{1,\infty}(\Omega, \mathbb{R}^3)$ *be the underlying deformation of* ν*. Then* y *is a homeomorphism between* Ω *and* $y(\Omega)$*, its inverse* y^{-1} *belongs to* $W^{1,\infty}(y(\Omega), \mathbb{R}^3)$ *and*

$$Dy^{-1}(x') = [Dy(y^{-1}(x'))]^{-1} \text{ for a.e. } x' \in y(\Omega).$$

Proof. In view of Lemma 4.3.2, we need only prove that y is a mapping of bounded distortion and that $\det Dy(x) \geq r > 0$ a.e. in Ω. The determinant constraint follows by the minors relations and the fact that $\operatorname{supp}\nu_x \subset K$ a.e. in Ω as in (4.4.13). To show that y has bounded distortion, note that Ω being Lipschitz, $y \in W^{1,\infty}(\Omega, \mathbb{R}^3)$ is continuous. Moreover, $\operatorname{supp}\nu_x \subset K$ a.e. and the norm on $\mathbb{R}^{3\times 3}$, $\|F\| = \sigma_{\max}(F)$ is quasiconvex, i.e.

$$\|\bar{\nu}_x\| = \|Dy(x)\| \leq \max_{F\in K} \|F\| \text{ for a.e. } x \in \Omega.$$

Also, by (4.4.13), $\det Dy(x)$ is bounded above and below a.e. and does not change sign in Ω. Then, for a.e. $x \in \Omega$,

$$\frac{\|Dy(x)\|^3}{|\det Dy(x)|} \leq \frac{\max_{F\in K} \|F\|^3}{\min_{F\in K} \det F} := M,$$

where $M \geq 1$ and y is a mapping of bounded distortion. □

Having established the required regularity of the finite-energy deformations in our simplified model, we proceed with the analysis of the experimental observations and state our main result.

4.5 Proposed explanation for the location of the nucleation points

Our main result implies that nucleation is only possible at a corner but this will be dependent on the directions along which the specimen is cut. We proceed with two definitions and introduce the class of 'admissible' domains, i.e. the domains for which our result will be proved to hold. We note that for any admissible measure ν with finite energy, $\operatorname{supp}\nu_x \subset K = SO(3) \cup \bigcup_{i=1}^{6} SO(3) U_i$ a.e. which implies that $\bar{\nu}_x \in K^{qc}$ a.e. in Ω. In particular, for any quasiconvex function $f : M^{3\times 3} \to \mathbb{R}$

$$f(\bar{\nu}_x) \leq \max_{F\in K} f(F) \quad \text{for a.e. } x \in \Omega.$$

This motivates the following definition.

Definition 4.5.1. *Let $K = SO(3) \cup \bigcup_{i=1}^{6} SO(3)\, U_i$ and $s \in \{1, \dots, 6\}$. We say that a vector $e \in S^2$ - the unit sphere in $\mathbb{R}^3$ - is a maximal direction for U_s if*

$$|U_s e| = \max_{F \in K} |Fe| = \max_{i \in \{1,\dots,6\}} \{|U_i e|, 1\}.$$

Similarly, we say that a vector $e \in S^2$ is a maximal direction for U_s^{-1} if

$$\begin{aligned} |\operatorname{cof} U_s e| \quad &> \quad \max_{F \in K \setminus SO(3) U_s} |\operatorname{cof} Fe| = \max_{i \in \{1,\dots,6\} \setminus \{s\}} \{|\operatorname{cof} U_i e|, 1\} \\ \textit{or} \qquad & \qquad e = e_{\max}(\operatorname{cof} U_s), \end{aligned}$$

where $e_{\max}(\operatorname{cof} U_s)$ denotes the eigenvector of $\operatorname{cof} U_s$ corresponding to its largest eigenvalue[5]*. We denote the set of maximal directions for U_s and U_s^{-1} by $\mathcal{M}_s$ and $\mathcal{M}_s^{-1}$ respectively.*

Definition 4.5.2. *Let $\Omega \subset \mathbb{R}^3$ be a parallelepiped domain. We say that an edge of Ω is admissible for U_s if it is in the direction of a vector in $\mathcal{M}_s \cup U_s^{-2}\mathcal{M}_s^{-1}$. Similarly, a face of Ω is admissible for U_s if the normal to the face is perpendicular to a vector in $\mathcal{M}_s \cup U_s^{-2}\mathcal{M}_s^{-1}$. Then, we say that the domain Ω is admissible for U_s if all of its edges are in the direction of a vector in $\mathcal{M}_s \cup U_s^{-2}\mathcal{M}_s^{-1}$.*

Remark. Due to the condition that $\lambda_{\max}(\operatorname{cof} U_s) \geq 1$, the sets $\mathcal{M}_s$ and $\mathcal{M}_s^{-1}$ are non-empty. We also remark that we view the set $U_s^{-2}\mathcal{M}_s^{-1}$ as a subset of S^2; that is $e \in U_s^{-2}\mathcal{M}_s^{-1}$ if there exists $f \in \mathcal{M}_s^{-1}$ such that $e = U_s^{-2} f / |U_s^{-2} f|$. In particular, $e_{\max}(\operatorname{cof} U_s) \in U_s^{-2}\mathcal{M}_s^{-1}$.

Moreover, note that if an edge is admissible it follows that the faces intersecting at that edge are also admissible since the normals are necessarily perpendicular to that edge. Therefore, for Ω to be admissible we need not require that its faces are admissible too.

We are now in a position to state and prove our main result:

Theorem 4.5.1. *Let $\Omega \subset \mathbb{R}^3$ be admissible for U_s and assume that $\det U_s \leq 1$ as well as $\lambda_{\max}(cofU_s) \geq 1$. Let $\nu \in \mathcal{A}_i \cup \mathcal{A}_f \cup \mathcal{A}_e \cup \mathcal{A}_c$ be such that $I(\nu) < I(\delta_{U_s})$. Then, $\nu \in \mathcal{A}_c$.*

Furthermore, for the CuAlNi specimen of the experiment described in Section 4.2, there exist four corners and, for each of these corners, an admissible measure $\nu \in \mathcal{A}_c$ such that $I(\nu) < I(\delta_{U_s})$.

[5] We note that $e_{\max}(\operatorname{cof} U_s)$ may or may not satisfy the maximality condition above.

Remark. For the simplified model constructed above, δ_{U_s} being a local minimizer with respect to variations in, e.g. $\mathcal{A}_f$, says in particular that no nucleation can occur on that face. This should be clear from the form of our energy as $I(\delta_{U_s}) = 0$ and

$$I(\nu) < 0 \Leftrightarrow \int_\Omega \nu_x(SO(3))\,dx = \int_\Omega \int_{SO(3)} d\nu_x(A) > 0.$$

On the other hand, if there exists $\nu \in \mathcal{A}_f$ such that $I(\nu) < I(\delta_{U_s})$, we infer that ν must be partly supported on $SO(3)$; in particular, austenite has nucleated.

The first part of Theorem 4.5.1 says that δ_{U_s} is a local minimizer with respect to localized variations in the interior, on faces and at edges of Ω and no nucleation can occur there. The second part says that, for Seiner's specimen, δ_{U_s} is not a local minimizer with respect to localized variations at some corner and, hence, the austenite can indeed nucleate at that corner. Therefore, Theorem 4.5.1 states that austenite must and indeed can nucleate at a corner.

We should point out that the requirement that Ω is admissible for U_s as well as the conditions on the lattice parameters and the constraint (C-N) are only relevant for faces and edges; for corners and the interior no such conditions are required.

Quasiconvexity conditions.

At this stage we introduce a set of quasiconvexity conditions in the interior, on faces, edges and at corners; we use these to prove the first part of Theorem 4.5.1.

Definition 4.5.3. *Let $W : M^{3\times 3} \to \overline{\mathbb{R}}$, $\Omega \subset \mathbb{R}^3$ a parallelepiped domain and write $B = B(0,1) = \{x \in \mathbb{R}^3 : |x| < 1\}$, the unit ball in $\mathbb{R}^3$.*

- *(interior) We say that W is quasiconvex at $F \in M^{3\times 3}$ in the interior of Ω if*

$$\langle \mu, W\rangle \geq W(F)$$

for all $\mu \in \mathcal{B}_i$ where

$$\mathcal{B}_i = \{\text{homogeneous } W^{1,\infty} \text{ gradient Young measures } \mu\text{: } \bar{\mu} = F.\}$$

- *(face) Let a face of Ω be contained in the plane $\{x \cdot n = k\}$ for some outward pointing normal $n \in S^2$ and $k \in \mathbb{R}$; let $B_f = \{x \in B : x \cdot n < 0\}$. We say that W is quasiconvex at $F \in M^{3\times 3}$ on that face if*

$$\int_{B_f} \langle \mu_x, W\rangle\,dx \geq \int_{B_f} W(F)\,dx$$

for all $\mu \in \mathcal{B}_f$ *where*

$$\mathcal{B}_f = \left\{ \begin{array}{c} W^{1,\infty} \text{ gradient Young measures } \mu = (\mu_x)_{x \in B_f} \text{: } \bar{\mu}_x = Dz(x) \\ \text{a.e. in } B_f, \ z \text{ satisfies (C-N) and } z(x) = Fx \text{ on } \operatorname{int}\left(\partial B \cap \overline{B_f}\right) \end{array} \right\},$$

the interior being relative to ∂B.

- *(edge) Let an edge of* Ω *be the intersection of two faces contained in the planes* $\{x \cdot n_1 = k_1\}$ *and* $\{x \cdot n_2 = k_2\}$ *for some outward pointing normals* $n_i \in S^2$ *and* $k_i \in \mathbb{R}$, $i = 1, 2$*; let* $B_e = \{x \in B : x \cdot n_i < 0 \ \forall\, i = 1, 2\}$. *We say that* W *is quasiconvex at* $F \in M^{3\times 3}$ *at that edge if*

$$\int_{B_e} \langle \mu_x, W \rangle \, dx \geq \int_{B_e} W(F) \, dx$$

for all $\mu \in \mathcal{B}_e$ *where*

$$\mathcal{B}_e = \left\{ \begin{array}{c} W^{1,\infty} \text{ gradient Young measures } \mu = (\mu_x)_{x \in B_e} \text{: } \bar{\mu}_x = Dz(x) \\ \text{a.e. in } B_e, \ z \text{ satisfies (C-N) and } z(x) = Fx \text{ on } \operatorname{int}\left(\partial B \cap \overline{B_e}\right) \end{array} \right\},$$

the interior being relative to ∂B.

- *(corner) Let a corner of* Ω *be the intersection of three faces contained in the planes* $\{x \cdot n_i = k_i\}$ *for some outward pointing normals* $n_i \in S^2$ *and* $k_i \in \mathbb{R}$, $i = 1, 2, 3$*; let* $B_c = \{x \in B : x \cdot n_i < 0 \ \forall\, i = 1, 2, 3\}$. *We say that* W *is quasiconvex at* $F \in M^{3\times 3}$ *at that corner if*

$$\int_{B_c} \langle \mu_x, W \rangle \, dx \geq \int_{B_c} W(F) \, dx$$

for all $\mu \in \mathcal{B}_c$ *where*

$$\mathcal{B}_c = \left\{ \begin{array}{c} W^{1,\infty} \text{ gradient Young measures } \mu = (\mu_x)_{x \in B_c} \text{: } \bar{\mu}_x = Dz(x) \\ \text{a.e. in } B_c, \ z \text{ satisfies (C-N) and } z(x) = Fx \text{ on } \operatorname{int}\left(\partial B \cap \overline{B_c}\right) \end{array} \right\},$$

the interior being relative to ∂B.

Notation. As remarked already, it is useful to view the free boundary of the nucleation region as being closed and the prescribed boundary as being open relative to the boundary of the region; as such we retain this for the sets B_ω, $\omega \in \{f, e, c\}$, in Definition 4.5.3 in contrast to the definition of quasiconvexity at the boundary given in Section 4.1. This makes no real difference since the deformations underlying our admissible measures are continuous up to the boundary. Then, for convenience and in order to not depart from the notation used so far, we shall denote the free and

prescribed parts of the boundary of B_ω by $\partial B_\omega \cap \partial\Omega$ and $\partial B_\omega \cap \Omega$ respectively rather than $\overline{\left(B \cap \overline{B_\omega}\right)}$ and $\operatorname{int}\left(\partial B \cap \overline{B_\omega}\right)$.

Remark. We note that whenever a measure $\mu \in \mathcal{B}_\omega$ satisfies $\operatorname{supp}\mu_x \subset K$, its underlying deformation z becomes a mapping of bounded distortion and it thus inherits the property of being homeomorphic with an inverse in the space $W^{1,\infty}\left(z\left(B_\omega\right), \mathbb{R}^3\right)$.

Moreover, if we suppose that the map W is finite everywhere and ignore the determinant and (C-N) constraints, the quasiconvexity conditions in the interior and on a face are essentially the standard quasiconvexity conditions in the interior and at the boundary but phrased in terms of Young measures. To see this, suppose that W is quasiconvex in the interior at F in the sense of Definition 4.5.3 and let $z \in Fx + W_0^{1,\infty}(\Omega, \mathbb{R}^3)$; consider the measure $\nu = \delta_{Dz(\cdot)}$ which is clearly a $W^{1,\infty}$ gradient Young measure and define $\mu = \operatorname{Av}\nu$, the average of ν, through its action on a continuous function f by

$$\langle \mu, f \rangle = \frac{1}{|\Omega|}\int_\Omega \langle \nu_x, f\rangle \, dx.$$

Then μ is a homogeneous gradient Young measure and satisfies $\bar{\mu} = F$ (see e.g. [112]). By the quasiconvexity of W we get that

$$\langle \mu, W\rangle \geq W(F) \Rightarrow \frac{1}{|\Omega|}\int_\Omega \langle \nu_x, W\rangle \, dx \geq W(F) \Rightarrow \frac{1}{|\Omega|}\int_\Omega W\left(Dz(x)\right) \, dx \geq W(F).$$

Conversely, suppose that W is quasiconvex in the 'gradient' sense. Let μ be a homogeneous $W^{1,\infty}$ gradient Young measure with $\bar{\mu} = F$ and consider its generating sequence z^k. We may assume that this lies in $W^{1,\infty}(\Omega, \mathbb{R}^3)$ and, by a standard modification (e.g. [1, 98]), we may also assume that $z^k \in Fx + W_0^{1,\infty}(\Omega, \mathbb{R}^3)$. Using the quasiconvexity of W (and implied continuity) and taking the limit $k \to \infty$,

$$\frac{1}{|\Omega|}\int_\Omega W\left(Dz^k\right) \, dx \geq W(F) \Rightarrow \frac{1}{|\Omega|}\int_\Omega \langle \mu, W\rangle \, dx \geq W(F) \Rightarrow \langle \mu, W\rangle \geq W(F)$$

since μ is homogeneous. The case of a face is similar but simpler since no averaging is required.

In regards to the other two conditions, these are natural extensions of the quasiconvexity conditions in the interior and at a face. To the best of the author's knowledge, quasiconvexity conditions at an edge or a corner have not been considered before.

Next we prove that the above quasiconvexity conditions in the interior, on a face, an edge or at a corner are sufficient for the measure δ_{U_s} to be a minimizer with respect to localized variations in the interior, on a face, an edge or at a corner respectively.

Lemma 4.5.2. *Let $\Omega \subset \mathbb{R}^3$ be a parallelepiped and suppose that $W : M^{3\times 3} \to \overline{\mathbb{R}}$ is quasiconvex at U_s in the interior (resp. on faces, edges or at corners) of Ω in the sense of Definition 4.5.3. Then $I(\delta_{U_s}) \leq I(\nu)$ for any $\nu \in \mathcal{A}_i$ (resp. $\mathcal{A}_f$, $\mathcal{A}_e$ or $\mathcal{A}_c$).*

Proof. The proof for faces, edges and corners is similar and we only treat the case of a face; the case of the interior differs from the rest and we treat it last.

Suppose that W is quasiconvex at U_s at a face contained in $\{x \cdot n = k\}$ where $n \in S^2$ is outward pointing and $k \in \mathbb{R}$; let $\nu = (\nu)_{x\in\Omega} \in \mathcal{A}_f$ with underlying deformation $y \in W^{1,\infty}(\Omega, \mathbb{R}^3)$ be admissible for that face. We wish to deduce that $I(\nu) \geq I(\delta_{U_s})$. Since $W = +\infty$ outside K, we may also assume that

$$\operatorname{supp} \nu_x \subset K \quad \text{a.e.}$$

as, otherwise, $I(\nu) > I(\delta_{U_s})$ and there is nothing to prove.

The set $S_f \subset \Omega$ where ν differs from δ_{U_s} is of the form $\{x \in B(x_0, r) : x \cdot n < k\}$ for some x_0 in the interior of the face and some $r > 0$; clearly $k = x_0 \cdot n$ and

$$S_f = x_0 + rB_f,$$

where $B_f = \{x \in B(0,1) : x \cdot n < 0\}$. Then also $x_0 + r(\partial B_f \cap \partial\Omega) = \partial S_f \cap \partial\Omega$ and $x_0 + r(\partial B_f \cap \Omega) = \partial S_f \cap \Omega$.

We note that, since ν is a $W^{1,\infty}$ gradient Young measure, the parametrized measure $(\nu_x)_{x\in S_f}$ is a $W^{1,\infty}$ gradient Young measure too with underlying deformation $y|_{S_f}$; this follows directly from Theorem 2.1.5. Also, $y|_{S_f}$ satisfies the (C-N) constraint since y, and thus $y|_{S_f}$, are injective.

Define $\mu = (\mu_x)_{x\in B_f}$ by

$$\mu_x = \nu_{x_0+rx}.$$

We claim that μ is a $W^{1,\infty}$ gradient Young measure. Suppose that $y^k \in W^{1,\infty}(S_f, \mathbb{R}^3)$ generates $(\nu_x)_{x\in S_f}$; in particular, we may assume that $y^k \overset{*}{\rightharpoonup} y|_{S_f}$ in $W^{1,\infty}(S_f, \mathbb{R}^3)$. For $x \in B_f$, define $z^k(x) = \frac{1}{r}[y^k(x_0 + rx) - U_s x_0]$; this is a sequence uniformly bounded in $W^{1,\infty}(B_f, \mathbb{R}^3)$ and for any $\xi \in L^1(B_f)$, $\psi \in C_0(M^{3\times 3})$,

$$\begin{aligned}
\int_{B_f} \xi(x)\psi(Dz^k(x))\,dx &= \frac{1}{r^3}\int_{S_f} \xi\Big(\frac{x'-x_0}{r}\Big)\psi(Dy^k(x'))\,dx' \quad \text{letting } x' = x_0 + rx \\
&\to \frac{1}{r^3}\int_{S_f} \xi\Big(\frac{x'-x_0}{r}\Big)\langle \nu_{x'}, \psi\rangle\,dx' \quad \text{since } y^k \text{ generates } (\nu_x)_{x\in S_f} \\
&= \int_{B_f} \xi(x)\langle \mu_x, \psi\rangle\,dx
\end{aligned}$$

by changing back to the variables $x = (x' - x_0)/r$, i.e. the sequence z^k generates the $W^{1,\infty}$ gradient Young measure μ. Note also that $z(x) = \frac{1}{r}[y(x_0 + rx) - U_s x_0]$ is the underlying deformation of μ and, for $x \in \partial B_f \cap \Omega$, $z(x) = U_s x$.

Also, z satisfies the (C-N) constraint as

$$\begin{aligned}\int_{B_f} \det Dz(x)\,dx &= \frac{1}{r^3}\int_{S_f} \det Dy(x')\,dx' \\ &\leq \frac{1}{r^3}\mathcal{L}^3(y(S_f)) \text{ since } y|_{S_f} \text{ satisfies (C-N)} \\ &= \mathcal{L}^3(z(B_f)).\end{aligned}$$

In particular, $\mu \in \mathcal{B}_f$ and by the quasiconvexity assumption,

$$\int_{B_f} \langle \mu_x, W\rangle\,dx \geq \int_{B_f} W(U_s)\,dx.$$

Noting that $\mu_x = \nu_{x_0+rx}$, changing variables to $x' = x_0 + rx$ and multiplying by r^3, we deduce that

$$\int_{S_f} \langle \nu_z, W\rangle\,dz \geq \int_{S_f} W(U_s)\,dz. \tag{4.5.1}$$

This is precisely what we need to show since then

$$\begin{aligned}I(\nu) &= \int_{S_f} \langle \nu_x, W\rangle\,dx + \int_{\Omega\setminus S_f} W(U_s)\,dx \\ &\geq \int_{S_f} W(U_s)\,dx + \int_{\Omega\setminus S_f} W(U_s)\,dx \text{ by (4.5.1)} \\ &= I(\delta_{U_s}).\end{aligned}$$

As for the case of the interior, let $\nu = (\nu_x)_{x\in\Omega} \in \mathcal{A}_i$; as before, we may assume that for a.e. $x \in \Omega$, $\operatorname{supp}\nu_x \subset K$. Define $\mu := \operatorname{Av}\nu$, i.e. for any continuous f

$$\langle \mu, f\rangle = \frac{1}{|\Omega|}\int_\Omega \langle \nu_x, f\rangle\,dx.$$

By [86], μ is a homogeneous $W^{1,\infty}$ gradient Young measure with $\operatorname{supp}\mu \subset K$ and $\bar{\mu} = U_s$. Then $\mu \in \mathcal{B}_i$ and by the quasiconvexity assumption we deduce that

$$\langle \mu, W\rangle \geq W(U_s) \quad \text{and hence} \quad I(\mu) \geq I(\delta_{U_s}).$$

To finish the proof, it suffices to show that $I(\nu) = I(\mu)$ so that $I(\nu) \geq I(\delta_{U_s})$. Since the measures μ and, for a.e. x, ν_x are supported in K, we may replace W by any continuous function agreeing with W on K (not relabelled) and then

$$\begin{aligned}I(\nu) &= \int_\Omega \langle \nu_x, W\rangle\,dx \\ &= |\Omega|\langle \mu, W\rangle \\ &= \int_\Omega \langle \mu, W\rangle\,dx = I(\mu). \quad \square\end{aligned}$$

Remark. We note that any measure in $\mathcal{B}_i$ is trivially an element of $\mathcal{A}_i$ and the quasiconvexity condition at U_s in the interior is also necessary for δ_{U_s} to be a minimizer with respect to the localized variations in $\mathcal{A}_i$. However, for faces, edges and corners, necessity does not follow due to the (C-N) constraint. For example, assume that for a face contained in $\{x \cdot n = k\}$, δ_{U_s} is a minimizer with respect to variations in $\mathcal{A}_f$ and let $\mu \in \mathcal{B}_f$. If one neglects the (C-N) constraint, let $x_0 \in \mathbb{R}^3$ be a typical point in the interior of the face, $r > 0$ such that $x_0 + rB_f$ has the form of some S_f and define $\nu = (\nu_x)_{x\in\Omega}$ by

$$\nu_x = \begin{cases} \mu_{\frac{x-x_0}{r}}, & x \in x_0 + rB_f \\ \\ \delta_{U_s}, & x \in \Omega \setminus (x_0 + rB_f). \end{cases}$$

Similarly to the proof above, we may assume that $\operatorname{supp} \nu_x \subset K$ a.e. so that ν is a $W^{1,\infty}$ gradient Young measure and its underlying deformation preserves orientation and (up to a constant) satisfies the boundary condition, i.e. by neglecting the (C-N) constraint, $\nu \in \mathcal{A}_f$. We may now use the fact that δ_{U_s} is a minimizer to get that $I(\nu) \geq I(\delta_{U_s})$. But this implies that

$$\int_{x_0+rB_f} \langle \mu_{\frac{x-x_0}{r}}, W \rangle \, dx \geq \int_{x_0+rB_f} W(U_s) \, dx.$$

Then, making the change of variables $x' = (x - x_0)/r$ and dividing by r^3,

$$\int_{B_f} \langle \mu_{x'}, W \rangle \, dx' \geq \int_{B_f} W(U_s) \, dx',$$

proving the quasiconvexity of W at U_s on that face. However, it is entirely possible that the underlying deformation z of μ satisfies (C-N) but the underlying deformation, say y, of ν is not a.e. injective in Ω and thus does not satisfy (C-N).

This can happen whenever the image of the free boundary of B_f 'goes around a corner' and comes close to, or even into contact with, the image of the prescribed part of the boundary $\partial B_f \cap \Omega$; see Fig. 4.5 for an example.

Nevertheless, we mention that by altering the definition of the measures in $\mathcal{A}_\omega$ or $\mathcal{B}_\omega$, $\omega \in \{f, e, c\}$, it is possible to retain the necessity of the quasiconvexity conditions at U_s on a face, an edge or at a corner for the measure δ_{U_s} to be a minimizer amongst the respective localized variations.

One possibility is to add a *confinement condition* on the deformations underlying measures in $\mathcal{B}_\omega$ in the spirit of the confinement condition by Ciarlet and Nečas in [39], which generalized the constraint set by the same authors in [40] (see also Noll [108]).

To motivate this in our context, let x_0 be a typical point in the interior of an edge of Ω contained in the intersection of the planes $\{x \cdot n_i = k_i\}$, S_e an appropriate set

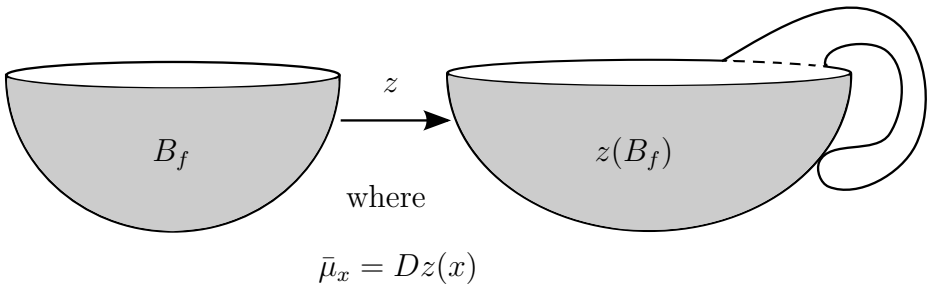

Figure 4.5: Depiction of a possible deformation z underlying a measure $\mu \in \mathcal{B}_f$ which may satisfy the (C-N) constraint but the underlying deformation of ν cannot; in particular, $\nu \notin \mathcal{A}_f$.

of the form $B(x_0, r) \cap \Omega$ and y a deformation underlying a measure in $\mathcal{A}_e$ so that $y(x) = U_s x$ outside S_e. Writing $S_e = x_0 + rB_e$ we see that the deformation z defined for $x \in B_e$ by $z(x) = \frac{1}{r}[y(x_0 + rx) - U_s x_0]$ is injective not only in B_e but also in the larger set $D_r \subset \mathbb{R}^3$ such that $\Omega = x_0 + rD_r$; then, z can be extended linearly by $U_s x$ to D_r while satisfying (C-N). By blowing up around the point x_0, i.e. by letting $r \to 0$, we see that a natural confinement condition would be to require that any deformation z underlying a measure in $\mathcal{B}_e$ can be extended linearly by $U_s x$ to the 'quadrant'

$$D := \bigcup_{i=1}^{2} \{x \cdot n_i < 0\}$$

and (C-N) is satisfied over any subset of that 'quadrant' - the quadrant being in quotation marks as Ω need not be rectangular. Similarly, for faces or corners, D would be the half-space defined by the face or the 'octant' defined by the three faces meeting at the corner respectively. This would be a rather natural condition to assume so that our localized problem respects the nature of the original one.

If we employ the (C-N) constraint in the definition of quasiconvexity as above, the quasiconvexity conditions at U_s become trivially necessary for δ_{U_s} to be a minimizer in the respective class of admissible measures, but the measures in $\mathcal{B}_\omega$ are restricted dramatically and the conditions are no longer sufficient. Restricting attention to a corner say, sufficiency is lost as it is possible for a map y, underlying a measure in $\mathcal{A}_c$, to map part of S_c into the region $U_s D$, where D is the corresponding 'octant', so that the map $z(x) = \frac{1}{r}[y(x_0 + rx) - U_s x_0]$ cannot be injective in D.

Nevertheless, since finite-energy measures are supported in K a.e., one may use the resulting uniform Lipschitz condition on the maps underlying admissible measures in

$\mathcal{A}_c$ to show that, if x_0 is the corner in question, there exists a neighbourhood $B(x_0, r)$ such that δ_{U_s} remains a minimizer amongst measures in $\mathcal{A}_c$ such that $S_c \subset B(x_0, r)$, i.e. austenite cannot nucleate in $B(x_0, r) \cap \Omega$; similarly for faces and edges. Hence, employing (C-N) in this way, weakens our main result and it is thus not preferred.

Clearly, one could also assume the same confinement condition for the maps underlying our admissible measures and get both sufficiency and necessity as well as our main result. However, this is a much too strong condition and does not seem natural.

Another way of establishing both necessity and sufficiency is to require that the (C-N) condition does not hold for the entire deformation y underlying an admissible measure in $\mathcal{A}_\omega$, $\omega \in \{f, e, c\}$, but rather that it holds for $y|_{S_\omega}$, i.e. the restriction of y to the set S_ω. Then, the quasiconvexity conditions at U_s as in Definition 4.5.3 are necessary and sufficient for δ_{U_s} to be a minimizer amongst the respective admissible measures and we can still prove our main result. However, employing (C-N) for the restriction of admissible deformations means that our deformations can only be locally injective, i.e. the non-physical interpenetration of matter is not excluded.

In particular, showing that the quasiconvexity conditions at U_s hold for the interior, faces and edges would say that

$$\nu \in \mathcal{A}_i \cup \mathcal{A}_f \cup \mathcal{A}_e \cup \mathcal{A}_c \text{ and } I(\nu) < I(\delta_{U_s}) \Longrightarrow \nu \in \mathcal{A}_c,$$

proving the first part of Theorem 4.5.1. We now proceed to the proof of our main result where we distinguish between three cases: corners, interior, and faces and edges.

Corners.

To resolve the second part of Theorem 4.5.1, we construct an explicit Young measure in $\mathcal{A}_c$ that lowers the energy. As the construction depends heavily on the orientation of Ω and the lattice parameters of the material, we only show this for Seiner's specimen.

Lemma 4.5.3. *Assume that $\Omega \subset \mathbb{R}^3$ is a parallelepiped domain with edges along the principle axes of the cubic austenite and let $s \in \{1, \dots, 6\}$. For the lattice parameters of the CuAlNi specimen of the experiment described in Section 4.2, there exist four corners of Ω and, for each of these corners, a corresponding measure $\nu \in \mathcal{A}_c$ such that*

$$I(\nu) < I(\delta_{U_s}).$$

In particular, austenite can be nucleated at a corner of Ω.

Proof. Let Ω be as in the statement and, for convenience, suppose that the coordinate system is such that the edges of Ω are parallel to the axes and each corner of Ω belongs to a different octant. Fix $s \in \{1, \dots, 6\}$ and suppose that there exists $l \in \{1, \dots, 6\}$, $l \neq s$, such that

$$QU_l - U_s = a \otimes n, \tag{4.5.2}$$

$$(1-\lambda)\, U_s + \lambda\, QU_l = U_s + \lambda a \otimes n = R + b \otimes m, \tag{4.5.3}$$

for non-zero vectors a, b, n, $m \in \mathbb{R}^3$, $|n|, |m| = 1$, $\lambda \in (0,1)$ and Q, $R \in SO(3)$.

Suppose, in addition, that the twin normal n and the habit plane normal m can be chosen in such a way that they are not perpendicular to any of the edges of Ω and that n, m belong to the same octant. Consider the corner of Ω lying in that octant, say at the point x_0, and let $S_c \subset \Omega$ be an appropriate set of the form $B(x_0, r) \cap \Omega$ in which austenite will nucleate. Define

$$\begin{aligned} S^1 &:= \{x \in S_c : x \cdot m > k_m\}, \\ S^2 &:= \{x \in S_c : x \cdot m < k_m \text{ and } x \cdot n > k_n\}, \\ S^3 &:= \{x \in S_c : x \cdot m < k_n\} \end{aligned}$$

where k_m, $k_n \in \mathbb{R}^3$ are such that

$$\{x \in S_c : x \cdot m \geq k_m\} \cap \{x \in S_c : x \cdot n \leq k_n\} = \emptyset. \tag{4.5.4}$$

We note that, if one can make the above choice of normals, it is always possible to choose k_m, k_n verifying (4.5.4).

Define a parametrized measure $\nu = (\nu_x)_{x \in \Omega}$, as in Figure 4.6, by

$$\nu_x = \begin{cases} \delta_R, & x \in S^1 \\ (1-\lambda)\, \delta_{U_s} + \lambda \delta_{QU_l}, & x \in S^2 \\ \delta_{U_s}, & x \in S^3 \cup (\Omega \setminus S_c). \end{cases} \tag{4.5.5}$$

If this measure belongs to $\mathcal{A}_c$, the proof is complete as then

$$I(\nu) = -\delta \mathcal{L}^3\left(S^1\right) < 0 = I\left(\delta_{U_s}\right).$$

Let us first verify that ν defines a $W^{1,\infty}$ gradient Young measure. Note that in each of the regions S^1, S^2 and $S_3 \cup (\Omega \setminus S_c)$, ν_x is a homogeneous $W^{1,\infty}$ gradient Young measure with underlying deformation y given by

$$Dy(x) = \begin{cases} R, & x \in S^1 \\ (1-\lambda)\, U_s + \lambda\, QU_l, & x \in S^2 \\ U_s, & x \in S_3 \cup (\Omega \setminus S_c). \end{cases} \tag{4.5.6}$$

This is trivially the case for the regions S^1 and $S_3 \cup (\Omega \setminus S_c)$; as for the simple laminate in S^2 we have seen in Chapter 2 that one can construct the above simple laminate as the weak$*$ limit of a sequence y^k uniformly bounded in $W^{1,\infty}(\Omega, \mathbb{R}^3)$ such that $\operatorname{dist}(Dy^k, \{U_s, QU_l\}) \to 0$ in measure, i.e. the associated measure is a $W^{1,\infty}$ gradient Young measure supported on these two matrices.

To verify that $\nu = (\nu_x)_{x\in\Omega}$ is itself a $W^{1\infty}$ gradient Young measure, by Theorem 6.1 in [86], we simply need to check that the above y lies in $W^{1,\infty}(\Omega, \mathbb{R}^3)$. But this reduces to verifying that y remains continuous across the planar interfaces between S^1 and S^2 as well as between S^2 and S^3, i.e. it reduces to verifying Hadamard's jump condition across the interfaces $\{x \cdot m = k_m\}$ and $\{x \cdot n = k_n\}$. The compatibility equation (4.5.3) directly implies that y remains continuous across the interface $\{x \cdot m = k_m\}$, whereas, it is trivial to see that

$$[(1-\lambda)\, U_s + \lambda\, QU_l] - U_s = \lambda\,(QU_l - U_s) = \lambda\, a \otimes n.$$

Therefore, the underlying deformation y is continuous across the interface $\{x \cdot n = k_n\}$ (twinned-to-detwinned interface) and the parametrized measure $\nu = (\nu_x)_{x\in\Omega}$ is indeed a $W^{1,\infty}$ gradient Young measure.

As ν is supported in K a.e. in Ω, $\det Dy(x) > 0$ a.e. and it remains to verify the boundary condition on $\partial S_c \cap \Omega$ and the (C-N) constraint. The underlying deformation y is given by

$$y(x) = \begin{cases} Rx + k_m b - \lambda k_n a, & x \in S^1 \\ (U_s + \lambda a \otimes n)x - \lambda k_n a, & x \in S^2 \\ U_s x, & x \in S_3 \cup (\Omega \setminus S_c), \end{cases} \tag{4.5.7}$$

where the constants are chosen so that y remains continuous across the interfaces $\{x \cdot m = k_m\}$ and $\{x \cdot n = k_n\}$. Clearly, $\partial S_c \cap \Omega \subset S_3 \cup (\Omega \setminus S_c)$ and then $y|_{\partial S_c \cap \Omega} = U_s x$. As for the (C-N) constraint, it suffices to show that y is injective. To reach a contradiction, suppose that $x_i \neq x_j$ but $y(x_i) = y(x_j)$; there are three non-trivial cases to consider:

(a) $x_1 \in S^1$ and $x_2 \in S^2$;

(b) $x_2 \in S^2$ and $x_3 \in S_3 \cup (\Omega \setminus S_c)$;

(c) $x_1 \in S^1$ and $x_3 \in S_3 \cup (\Omega \setminus S_c)$.

Let us first treat case (b); $y(x_2) = y(x_3)$ implies that

$$U_s(x_2 - x_3) = \lambda(k_n - x_2 \cdot n)a. \tag{4.5.8}$$

But $U_s + a \otimes n = QU_l$ so that, by taking determinants on both sides, we infer that $(\det U_s)(1 + U_s^{-1}a \cdot n) = \det U_l$; but $\det U_s = \det U_l \neq 0$ and hence

$$U_s^{-1}a \cdot n = 0. \tag{4.5.9}$$

The above is a relation we have seen repeatedly in Chapters 2 and 3. Now multiplying (4.5.8) to the left by U_s^{-1}, taking the dot product with n and using (4.5.9), we find that $(x_2 - x_3) \cdot n = 0$ which is absurd since $x_2 \cdot n > k_n$ and $x_3 \cdot n < k_n$.

Next we treat case (a). Now, $y(x_1) = y(x_2)$ implies that

$$R(x_1 - x_2) = (x_2 \cdot m - k_m)b, \tag{4.5.10}$$

where we have made use of (4.5.3). Also, taking determinants in (4.5.3) and using (4.5.9), we infer that $\det U_s = 1 + R^T b \cdot m$ and hence

$$-1 < R^T b \cdot m \leq 0, \tag{4.5.11}$$

since we are also assuming that $0 < \det U_s \leq 1$. Multiplying (4.5.10) to the left by R^T, taking the dot product with m and using (4.5.11), we find that

$$(x_1 - x_2) \cdot m < -(x_2 \cdot m - k_m),$$

since also $x_2 \cdot m < k_m$. But this is absurd since $x_1 \cdot m > k_m$. We simply note that if $\det U_s > 1$, then $R^T b \cdot m > 0$ and by (4.5.10) we deduce that $(x_1 - x_2) \cdot m < 0$, a contradiction.

As for case (c), we repeat a similar argument which reduces the injectivity of y to the sign of a dot product. However, we are unable to check this sign for general lattice parameters and, instead, we verify this numerically for Seiner's specimen. In particular, suppose that $y(x_1) = y(x_3)$, i.e.

$$Rx_1 + k_m b - \lambda k_n a = U_s x_3.$$

By (4.5.3), we may write $R = U_s + \lambda a \otimes n - b \otimes m$ so that $y(x_1) = y(x_3)$ becomes

$$U_s(x_1 - x_3) = \lambda(k_n - x_1 \cdot n)a + (x_1 \cdot m - k_m)b. \tag{4.5.12}$$

We may now multiply to the left by U_s^{-1} and take the dot product with n so that (4.5.12) becomes

$$(x_1 - x_3) \cdot n = (x_1 \cdot m - k_m)U_s^{-1}b \cdot n.$$

However, $x_1 \cdot n > k_n$ by (4.5.4) and hence $(x_1 - x_3) \cdot n > 0$; also, $x_1 \cdot m > k_m$ and we reach a contradiction provided that $U_s^{-1}b \cdot n < 0$.

We note that taking $\tilde{a} = -a$, $\tilde{n} = -n$, $\tilde{b} = -b$ and $\tilde{m} = -m$ in (4.5.2) and (4.5.3) does not alter anything in the above argument. Then, if the construction is possible for a corner in the quadrant $\{x_1 > 0, x_2 > 0, x_3 > 0\}$ say, it is also possible for the corner in the quadrant $\{x_1 < 0, x_2 < 0, x_3 < 0\}$.

To complete the proof, we need to establish that for each $s \in \{1, \dots, 6\}$ we may indeed choose two sets of solutions to the twin and habit plane equations (4.5.2) and (4.5.3) respectively, such that the twin and habit plane normals are not perpendicular to any edge and they lie in the same quadrant as a corner - the quadrant, and hence the corner, being different for each set of solutions. Then, the construction of a microstructure lowering the energy is possible at four distinct corners provided that, for each choice of twin and habit plane solutions, $U_s^{-1} b \cdot n < 0$. This is indeed possible and we refer the reader to Appendix B for the details. There, in Tables B.7 and B.8, one may also find a summary of the results for all values of $s \in \{1, \dots, 6\}$. $\square$

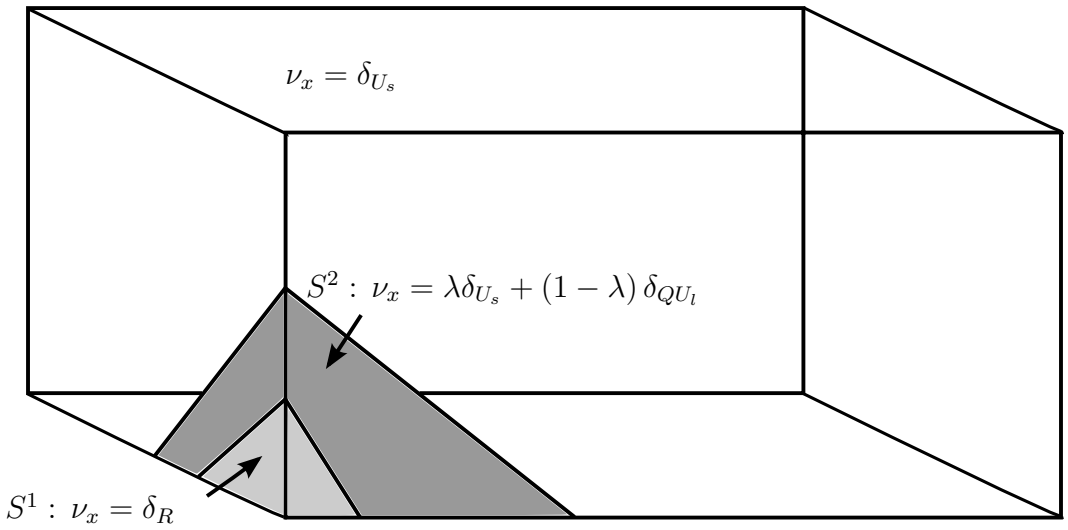

Figure 4.6: Depiction of a measure $\nu \in \mathcal{A}_c$ such that $I(\nu) < I(\delta_{U_s})$. In the region S_c^1, $\nu_x = \delta_R$ for some $R \in SO(3)$ so that austenite has nucleated at a corner; in the region S_c^2, $\nu_x = \lambda\delta_{U_s} + (1-\lambda)\,\delta_{QU_l}$ for some $Q \in SO(3)$ and $l \in \{1, \dots, 6\}$ such that the matrices R and $\lambda U_s + (1-\lambda)\,QU_l$ are rank-one connected, i.e. ν_x corresponds to a simple laminate between U_s and QU_l there, forming a compatible interface with R. Note that the normals to the interfaces between austenite and the simple laminate (habit plane) and between the simple laminate and the pure phase of U_s (twinned-to-detwinned interface) are different.

Interior

For the case of the interior we wish to deduce that the stabilized martensite δ_{U_s} is indeed a minimizer with respect to the localized variations in $\mathcal{A}_i$. In particular, we prove the following:

Lemma 4.5.4. *The map $W : M^{3\times 3} \to \overline{\mathbb{R}}$ given by (4.4.14) is quasiconvex at U_s in the interior.*

By the above lemma, along with Lemma 4.5.2, we may immediately infer the required result which we provide for completeness in the form of a corollary.

Corollary 4.5.5. *Assume that $\Omega \subset \mathbb{R}^3$ is a parallelepiped. Then,*

$$\nu \in \mathcal{A}_i \Longrightarrow I(\nu) \geq I(\delta_{U_s}).$$

In particular, nucleation cannot occur in the interior.

Proof of Lemma 4.5.4. Let μ be a homogeneous gradient Young measure satisfying $\bar{\mu} = U_s$; we may assume that $\operatorname{supp}\mu \subset K$ as otherwise, $\langle \mu, W\rangle = +\infty > 0 = W(U_s)$. Using the minors relation for the determinant, we deduce that

$$\begin{aligned}
\det U_s &= \det \bar{\mu} \\
&= \langle \mu, \det\rangle \\
&= \int_{SO(3)} \det A \, d\mu(A) + \int_{\bigcup_i SO(3)U_i} \det A \, d\mu(A) \\
&= \int_{SO(3)} 1 \, d\mu(A) + \int_{\bigcup_i SO(3)U_i} \det U_s \, d\mu(A). \qquad (4.5.13)
\end{aligned}$$

On the other hand, as μ is a probability measure,

$$\det U_s = \int_{SO(3)} \det U_s \, d\mu(A) + \int_{\bigcup_i SO(3)U_i} \det U_s \, d\mu(A). \qquad (4.5.14)$$

Subtracting equations (4.5.13) and (4.5.14), we obtain

$$\int_{SO(3)} (1 - \det U_s) \, d\mu(A) = 0.$$

Therefore,

$$\mu(SO(3)) = 0 \quad \text{or} \quad \det U_s = 1.$$

The former case is precisely what we need to prove. So, let $\det U_s = \alpha\beta\gamma = 1$ where α, β and γ are the lattice parameters and eigenvalues of U_s. By the AM-GM inequality

$$\frac{|U_s|^2}{3} = \frac{\alpha^2+\beta^2+\gamma^2}{3} \geq \left(\alpha^2\beta^2\gamma^2\right)^{1/3} = 1$$

and thus $|U_s|^2 > 3 = |\mathbf{1}|^2$. Note that the inequality is strict as otherwise $\alpha = \beta = \gamma = 1$ and $U_i = \mathbf{1}$ for all $i = 1, \ldots, 6$.

Since the map $F \mapsto |F|^2$ is convex,

$$\begin{aligned} |U_s|^2 &= |\bar{\mu}|^2 \\ &\leq \langle \mu, |\cdot|^2 \rangle \\ &= \int_{SO(3)} |A|^2 \, d\mu\,(A) + \int_{\bigcup_i SO(3)U_i} |A|^2 \, d\mu\,(A) \\ &= \int_{SO(3)} 3 \, d\mu\,(A) + \int_{\bigcup_i SO(3)U_i} |U_s|^2 \, d\mu\,(A) \end{aligned} \tag{4.5.15}$$

as the martensitic variants are symmetry related and the norm stays constant. Moreover, as μ is a probability measure,

$$|U_s|^2 = \int_{SO(3)} |U_s|^2 \, d\mu\,(A) + \int_{\bigcup_i SO(3)U_i} |U_s|^2 \, d\mu\,(A)\,. \tag{4.5.16}$$

Subtracting equations (4.5.15) and (4.5.16), we infer that

$$\int_{SO(3)} \left(3 - |U_s|^2\right) \, d\mu\,(A) \geq 0.$$

However, $|U_s|^2 > 3$ and hence, $\mu\,(SO\,(3)) = 0$ which completes the proof. □

Remark. The proof of Lemma 4.5.4 only uses the fact that $\bar{\mu} = U_s$. For an inhomogeneous measure $\mu = (\mu_x)_{x\in B}$ with $\operatorname{supp}\mu_x \subset K$ and $\bar{\mu}_x = U_s$ a.e. in B, the same argument applies to show that for a.e. $x \in B$, $\mu_x\,(SO\,(3)) = 0$. We keep this remark in mind as it will be central in proving quasiconvexity at faces and edges.

Faces and Edges

We argue about faces and edges in a similar manner and so we treat them simultaneously. Both for faces and edges, we wish to conclude that δ_{U_s} is a minimizer of I in $\mathcal{A}_f$ and $\mathcal{A}_e$, respectively, which in turn implies that nucleation cannot occur there. To prove this we establish the quasiconvexity of W at U_s on faces and edges.

Lemma 4.5.6. *Assume that $\Omega \subset \mathbb{R}^3$ is a parallelepiped domain which is admissible for U_s and let $W : M^{3\times 3} \to \overline{\mathbb{R}}$ as in (4.4.14). Then W is quasiconvex at U_s on all faces and edges of Ω.*

Then, by Lemma 4.5.2 we immediately deduce:

Corollary 4.5.7. *Assume that $\Omega \subset \mathbb{R}^3$ as above is admissible for U_s. Then,*

$$\begin{aligned} \nu \in \mathcal{A}_f \implies I(\nu) \geq I(\delta_{U_s}) \quad &\text{for a face and} \\ \nu \in \mathcal{A}_e \implies I(\nu) \geq I(\delta_{U_s}) \quad &\text{for an edge.} \end{aligned}$$

In particular, nucleation cannot occur at any face or edge.

Remark. Note that the statement of Lemma 4.5.6 requires that Ω be admissible for U_s and it is here that we use this condition for the first time. The (C-N) constraint as well as the conditions $\det U_s \leq 1$, $\lambda_{\max}(\operatorname{cof} U_s)$ enter here too. This will become apparent in the proofs that follow.

Firstly, we prove a claim (Lemma 4.5.8) to which the proof of Lemma 4.5.6 will eventually be reduced; note that Ω being admissible for U_s, condition (C-N) and the assumption on the lattice parameters are not required.

Notation. As the cases of a face and an edge are treated simultaneously, for convenience, we shall use the subscript f, e in e.g. $\mathcal{A}_{f,e}$ or $B_{f,e}$ to mean 'either $\mathcal{A}_f$ or $\mathcal{A}_e$' and 'either B_f or B_e', respectively.

Lemma 4.5.8. *Assume that for a face or an edge $\mu \in \mathcal{B}_{f,e}$ satisfies $\bar{\mu}_x = U_s$ for a.e. $x \in B_{f,e}$. Then,*

$$\int_{B_{f,e}} \langle \mu_x, W \rangle \, dx \geq \int_{B_{f,e}} W(U_s) \, dx,$$

i.e. W is quasiconvex at U_s on that face or edge. In particular, if $\operatorname{supp} \mu_x \subset K$ a.e. then $\mu_x(SO(3)) = 0$ for a.e. $x \in B_{f,e}$.

Proof. See Remark after Lemma 4.5.4. □

Thus, to prove Lemma 4.5.6, it suffices to show that all measures in $\mathcal{B}_f$ and $\mathcal{B}_e$ satisfy $\bar{\mu}_x = U_s$. In the case of the interior we reduced the problem to (homogeneous) measures μ such that $\bar{\mu} = U_s$ due to the fact that the boundary condition on deformations underlying measures in $\mathcal{A}_i$ was set throughout the boundary of S_i

and, crucially, that the averaged measure did not change the energy. However, on a face or at an edge, averaging the measures does not work as part of the boundary is free. Therefore, we follow a different approach in order to establish that $\bar{\mu}_x = U_s$ which is dependent on the orientation of Ω or, equivalently, the directions in which the specimen is cut.

At this stage we invoke the notions of maximal directions for U_s and U_s^{-1} from Definition 4.5.1. For the convenience of the reader, we recall that a vector $e \in S^2$ belongs to $\mathcal{M}_s$, the set of maximal directions for U_s, if

$$|U_s e| = \max_{i\in\{1,\dots,6\}} \{|U_i e|, 1\}.$$

and to $\mathcal{M}_s^{-1}$, the set of maximal directions for U_s^{-1}, if

$$|\operatorname{cof} U_s e| > \max_{i\in\{1,\dots,6\}\setminus\{s\}} \{|\operatorname{cof} U_i e|, 1\} \text{ or } e = e_{\max}(\operatorname{cof} U_s)$$

The maximal directions allow us to use a rigidity argument to deduce that $\bar{\mu}_x = U_s$ a.e. in $B_{f,e}$ for all measures in $\mathcal{B}_{f,e}$, provided that Ω is admissible itself. This argument is the basis of our method; it is presented in Lemma 4.5.9 and applied in Lemma 4.5.10 and Lemma 4.5.12.

Lemma 4.5.9. *Let t^-, $t^+ \in \mathbb{R}$ with $t^- < t^+$ and suppose that $\sigma : [t^-, t^+] \to \mathbb{R}^d$, $d \geq 1$, is differentiable almost everywhere. Then*

$$\forall\, t \quad |\frac{d}{dt}\sigma(t)| \leq \frac{|\sigma(t^+) - \sigma(t^-)|}{|t^+ - t^-|} \Rightarrow \forall\, t \quad \frac{d}{dt}\sigma(t) = \frac{\sigma(t^+) - \sigma(t^-)}{t^+ - t^-}.$$

In particular, $\sigma(t) = \sigma(t^-) + (t - t^-)(\sigma(t^+) - \sigma(t^-))/(t^+ - t^-)$.

Proof. By the Fundamental Theorem of Calculus and the uniform bound on the derivative of σ,

$$\begin{aligned} 0 &\leq \int_{t^-}^{t^+} |\frac{d}{dt}\sigma(t) - \frac{\sigma(t^+) - \sigma(t^-)}{t^+ - t^-}|^2\, dt \\ &= \int_{t^-}^{t^+} |\frac{d}{dt}\sigma(t)|^2 + |\frac{\sigma(t^+) - \sigma(t^-)}{t^+ - t^-}|^2 - 2\frac{d}{dt}\sigma(t) \cdot \frac{\sigma(t^+) - \sigma(t^-)}{t^+ - t^-}\, dt \\ &= \int_{t^-}^{t^+} |\frac{d}{dt}\sigma(t)|^2 - |\frac{\sigma(t^+) - \sigma(t^-)}{t^+ - t^-}|^2\, dt \leq 0. \end{aligned}$$

That is $\frac{d}{dt}\sigma(t) = (\sigma(t^+) - \sigma(t^-))/(t^+ - t^-)$ and the result follows. □

We may now apply Lemma 4.5.9 to obtain the following result:

Lemma 4.5.10. *Let $\mu \in \mathcal{B}_{f,e}$ with $\operatorname{supp}\mu_x \subset K$ a.e. in $B_{f,e}$ and $z \in W^{1,\infty}(B_{f,e}, \mathbb{R}^3)$ such that $Dz(x) = \bar{\mu}_x$ a.e. in $B_{f,e}$. In addition, let $e \in \mathcal{M}_s$ and suppose that $D \subset B_{f,e}$ is an open set with the property that for each $x \in D$ the line segment parametrized by $r_x(t) = x + te$, $t \in [t_x^-, t_x^+]$, where*

$$\begin{aligned} t_x^- &= \sup\{t < 0 : x + te \notin B_{f,e}\} \\ t_x^+ &= \inf\{t > 0 : x + te \notin B_{f,e}\}, \end{aligned}$$

lies in D for all $t \in (t_x^-, t_x^+)$ and $x + t_x^{\pm} e \in \partial B_{f,e} \cap \Omega$, the prescribed part of the boundary of $B_{f,e}$. Then, for a.e. $x \in D$,

$$z(r_x(t)) = U_s r_x(t) \text{ for all } t \in [t_x^-, t_x^+].$$

Proof. For $x \in D$, let $r_x(t)$, $t \in [t_x^-, t_x^+]$, as in the statement and

$$\sigma_x(t) = z(r_x(t)).$$

Note that the map $z \in W^{1,\infty}$ is differentiable a.e. in $B_{f,e}$ and the classical and generalized derivatives coincide a.e. in $B_{f,e}$. Hence, by Fubini's theorem, z is differentiable at a.e. point of a.e. line segment parallel to a given direction and the directional and generalized derivatives coincide, i.e. for a.e. $x \in D$, $\sigma_x(t) = z(r_x(t))$ is differentiable for a.e. $t \in [t_x^-, t_x^+]$. Then, for a.e. $t \in (t_x^-, t_x^+)$,

$$\frac{d}{dt}\sigma_x(t) = \frac{d}{dt} z(r_x(t)) = Dz(r_x(t))e. \tag{4.5.17}$$

Note that for any fixed $e \in \mathbb{R}^3$ the function $F \mapsto |Fe|$ is a convex function of the matrix F. But, $\bar{\mu}_x = Dz(x) \in K^{qc}$ a.e. and, again by Fubini's theorem, a.e. point of a.e. line segment parallel to the vector e belongs to the subset of $B_{f,e}$ where $Dz(x) \in K^{qc}$. That is, for a.e. $x \in D$ and a.e. $t \in (t_x^-, t_x^+)$,

$$|Dz(r_x(t))e| \leq \max_i \{1, |U_i e|\} = |U_s e|,$$

since $e \in S^2$ is a maximal direction for U_s. Combining with (4.5.17) we deduce that for a.e. $x \in D$,

$$\left|\frac{d}{dt}\sigma_x(t)\right| = |Dz(r_x(t))e| \leq |U_s e| = \frac{|\sigma_x(t_x^+) - \sigma_x(t_x^-)|}{|t_x^+ - t_x^-|}. \tag{4.5.18}$$

Applying Lemma 4.5.9, we infer that for a.e. $x \in D$ and all $t \in (t_x^-, t_x^+)$,

$$z(r_x(t)) = z(r_x(t_x^-)) + (t - t_x^-)\frac{z(r_x(t_x^+)) - z(r_x(t_x^-))}{t_x^+ - t_x^-} = U_s r_x(t). \quad \square$$

Remark. We note that since the region $D \subset B_{f,e}$ can be covered by line segments joining points on the prescribed boundary $\partial B_{f,e} \cap \Omega$ and on a.e. such line segment, z agrees with $U_s x$, $z(x) = U_s x$ for a.e. $x \in D$; in particular, assuming z to be the continuous representative, the same is true for all $x \in D$.

The idea is now simple; let $e \in \mathcal{M}_s$ and suppose that we may take $D = B_{f,e}$, i.e. the entire set $B_{f,e}$ can be covered by line segments in the direction of e joining points on the prescribed boundary. Then, by Lemma 4.5.10, we immediately deduce that for any $\mu \in \mathcal{B}_{f,e}$ such that $\operatorname{supp} \mu_x \subset K$ a.e.,

$$\bar{\mu}_x = U_s \quad \text{for a.e. } x \in B_{f,e}$$

and using Lemma 4.5.8 we infer the quasiconvexity of W at U_s on a face or an edge. In particular, we can prove the following:

Lemma 4.5.11. *Let $\Omega \subset \mathbb{R}^3$ be a parallelepiped and suppose that $e \in \mathcal{M}_s$ is a vector parallel to an edge or perpendicular to a normal of a face of Ω. Then W is quasiconvex at U_s on that face or edge. In particular, $I(\nu) \geq I(\delta_{U_s})$ for every $\nu \in \mathcal{A}_{f,e}$.*

Proof. Let $\mu \in \mathcal{B}_{f,e}$; we may assume that $\operatorname{supp} \mu_x \subset K$ a.e. as otherwise the result follows trivially irrespective of the directions. Hence, it suffices to show that if the normal to a face is perpendicular to, or an edge is parallel to, $e \in \mathcal{M}_s$ then any respective region $B_{f,e}$ can be covered by line segments in the direction of $e \in \mathcal{M}_s$, joining points on the prescribed boundary $\partial B_{f,e} \cap \Omega$. Then, Lemma 4.5.10 says that $\bar{\mu}_x = U_s$ a.e. and Lemma 4.5.8 proves the claim.

Trivially, the set $B_{f,e}$ can be covered by lines parallel to any direction joining points on its boundary. Hence, it is a question of making sure that, if these are in the direction of e, they never intersect the free boundary $\partial B_{f,e} \cap \partial\Omega$.

Note that for the case of a face, $\partial B_f \cap \partial\Omega$ is flat and for an edge, $\partial B_e \cap \partial\Omega$ is piecewise flat, as it comprises of parts of the two faces that meet at the given edge. Recalling that e is perpendicular to the normal of the face in question or parallel to the edge, let $x \in \partial B_{f,e} \cap \partial\Omega$ - the free boundary - and define

$$\begin{aligned} t^+ &= \sup\{t > 0 : x + te \in \partial B_{f,e} \cap \partial\Omega\} \quad \text{and} \\ t^- &= \inf\{t < 0 : x + te \in \partial B_{f,e} \cap \partial\Omega\}. \end{aligned}$$

The infimum and supremum above are attained since $\partial B_{f,e} \cap \partial\Omega$ is compact. Then, the line $x + te$, $t \in \mathbb{R}$ must lie on $\partial B_{f,e} \cap \partial\Omega$ for all $t \in [t^-, t^+]$ whereas, for $t < t^-$ or $t > t^+$, $x + te \notin \overline{B_{f,e}}$.

Now, to reach a contradiction, suppose that for some $x_0 \in \partial B_{f,e} \cap \Omega$, there exists $t_0 \in \mathbb{R}$ such that $x_0 + t_0 e \in \partial B_{f,e} \cap \partial\Omega$. But then, there exists some $x \in \partial B_{f,e} \cap \partial\Omega$ such that $x_0 + t_0 e = x$, i.e. $x - t_0 e \in \partial B_{f,e} \cap \Omega$. Note that this cannot be the case since, by the above argument, either $x_0 - t_0 e \notin \overline{B_{f,e}}$ or $x_0 - t_0 e \in \partial B_{f,e} \cap \partial\Omega$ and $(\partial B_{f,e} \cap \partial\Omega) \cap (\partial B_{f,e} \cap \Omega) = \emptyset$. $\square$

Note that, so far, we have not made use of the (C-N) constraint or the assumptions on the lattice parameters. We employ these next where we follow a similar method as for the maximal directions for U_s, this time basing our argument on the inverse deformation and maximal directions for U_s^{-1}. This method allows us to add more directions along which the underlying deformations of measures in $\mathcal{B}_{f,e}$ agree with $U_s x$; indeed, for the cubic-to-orthorhombic transition of CuAlNi, we will see in the following section that all added directions are in fact new.

In Theorem 4.4.3 we established that measures in $\mathcal{A}_{f,e}$ whose support is contained in K have underlying deformations that are homeomorphic and remarked that this property is naturally inherited by measures in $\mathcal{B}_{f,e}$. We now restrict attention to the deformed configuration $z(B_{f,e})$ and the maps $z^{-1} : z(B_{f,e}) \to B_{f,e}$. The underlying idea of our arguments is essentially the same as in Lemma 4.5.10 but we consider an open set in the deformed configuration, covered by line segments along directions in $U_s^{-2}\mathcal{M}_s^{-1}$ joining points on $z(\partial B_{f,e} \cap \Omega)$. We claim that almost all of these lines necessarily deform linearly under the inverse map z^{-1} and according to U_s^{-1}; then, returning to the forward deformation, we can establish that the pre-image of these segments deforms under z as $U_s x$.

Nevertheless, as Fig. 4.7 below suggests for the case of a face (similarly for an edge), we need to make sure that such an open set can actually 'fit' in the deformed region $z(B_{f,e})$; this will become possible due to the (C-N) constraint.

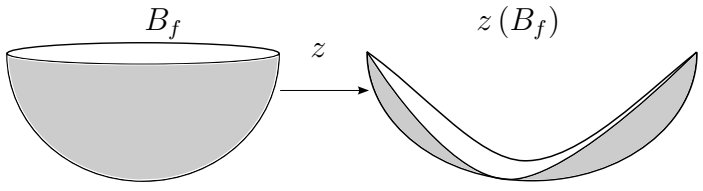

Figure 4.7: Depiction of a deformation at a face; in this case, the method of maximal directions for U_s^{-1} is not applicable.

For now we assume that this is indeed the case and we return to it after proving the result analogous to Lemma 4.5.10 concerning the maximal directions for U_s^{-1}.

Lemma 4.5.12. *Let $\mu \in \mathcal{B}_{f,e}$ with $\operatorname{supp}\mu_x \subset K$ a.e. in $B_{f,e}$ and $z \in W^{1,\infty}(B_{f,e},\mathbb{R}^3)$ such that $Dz(x) = \bar{\mu}_x$ a.e. in $B_{f,e}$. In addition, let $e \in U_s^{-2}\mathcal{M}_s^{-1}$ and suppose that $D \subset B_{f,e}$ is an open set with the property that for each $x \in D$ the line segment parametrized by $r_x(t) = x + te$, $t \in [t_x^-, t_x^+]$, where*

$$\begin{aligned} t_x^- &= \sup\{t < 0 : x + te \notin B_{f,e}\} \\ t_x^+ &= \inf\{t > 0 : x + te \notin B_{f,e}\}, \end{aligned}$$

lies in D for all $t \in (t_x^-, t_x^+)$ and $x + t_x^{\pm}e \in \partial B_{f,e} \cap \Omega$, the prescribed part of the boundary of $B_{f,e}$. Then, for a.e. $x \in D$,

$$z(r_x(t)) = U_s r_x(t) \ \text{ for all } t \in [t_x^-, t_x^+],$$

provided that $U_s D \subset z(B_{f,e})$.

Proof. For $x \in D$, let $r_x(t)$, $t \in [t_x^-, t_x^+]$, as in the statement and write $\rho_x(t) = U_s r_x(t) = U_s x + tU_s e$. Let $w : z(B_{f,e}) \to B_{f,e}$ be the inverse of z. We have remarked that maps underlying measures in $\mathcal{B}_{f,e}$ inherit the properties of maps underlying measures in $\mathcal{A}_{f,e}$ so that, by Theorem 4.4.3, $w \in W^{1,\infty}(z(B_{f,e}),\mathbb{R}^3)$ is differentiable a.e. in $z(B_{f,e})$ and

$$Dw(v) = [Dz(w(v))]^{-1}$$

for a.e. $v \in z(B_{f,e})$.

Also, for every $x \in D$, $r_x(t) \in D$ for all $t \in (t_x^-, t_x^+)$ and therefore, for $t \in (t_x^-, t_x^+)$, $\rho_x(t) \in U_s D \subset z(B_{f,e})$ by assumption; also, for each $x \in D$, the line segments parametrized by ρ_x are all in the direction of the vector $U_s e$. Hence, as in Lemma 4.5.10, for a.e. $x \in D$, $w(\rho_x(t))$ is differentiable for a.e. $t \in (t_x^-, t_x^+)$ and the classical and generalized derivatives coincide.

Lastly, we note that $\bar{\mu}_x = Dz(x) \in K^{qc}$ a.e. and hence, for a.e. $x \in D$ and a.e. $t \in (t_x^-, t_x^+)$,

$$Dz(w(\rho_x(t))) \in K^{qc}.$$

To see this, note that the set $N \subset D$ such that $Dz(x) \notin K^{qc}$ satisfies $\mathcal{L}^3(N) = 0$; since $z \in W^{1,\infty}(B_{f,e},\mathbb{R}^3)$ and $B_{f,e} \subset \mathbb{R}^3$ is open and bounded, z maps sets of measure zero to sets of measure zero (see [99]), i.e. $\mathcal{L}^3(z(N)) = 0$. Then, a.e. point of a.e. line in the direction of $U_s e$ in the deformed configuration does not belong to the set $z(N)$ and their pre-image does not belong to N.

Now assume that $e = e_{\max}(\operatorname{cof} U_s)$ and let

$$\sigma_x(t) = w(\rho_x(t)).$$

The function $F \mapsto |\mathrm{cof}\, F^T e| = |\mathrm{adj}\, Fe|$ is polyconvex. Since all the U_i's are symmetric, $U_s e \parallel e$ and, for a.e. $x \in D$ and a.e. $t \in (t_x^-, t_x^+)$, $Dz(w(\rho_x(t))) \in K^{qc}$, we infer that

$$\begin{aligned}
|\frac{d}{dt}\sigma_x(t)| &= |Dw(\rho_x(t))U_s e| \\
&= \frac{1}{\det Dz(w(\rho_x(t))}|(\mathrm{adj}\ Dz(w(\rho_x(t)))U_s e| \\
&\leq \frac{1}{\det U_s} \max_{i,R\in SO(3)} \{|\mathrm{cof}\ U_i R U_s e|, |U_s e|\} \\
&= \frac{1}{\det U_s}\lambda_{\max}(\mathrm{cof}\, U_s)|U_s e| \\
&= \frac{1}{\det U_s}|(\mathrm{cof}\, U_s)U_s e| = 1 = \frac{|\sigma_x(t_x^+) - \sigma_x(t_x^-)|}{|t_x^+ - t_x^-|}. \qquad (4.5.19)
\end{aligned}$$

Above we have used the fact that the map $F \mapsto \det F$ is quasiaffine and, since $\det U_s \leq 1$, $\det U_s \leq \det Dz(w(\rho_x(t))) \leq 1$. Now Lemma 4.5.9 applies to give that

$$w(\rho_x(t)) = w(\rho_x(t_x^-)) + (t - t_x^-)\frac{w(\rho_x(t_x^+)) - w(\rho_x(t_x^-))}{t_x^+ - t_x^-} = r_x(t),$$

i.e. $z(r_x(t)) = U_s r_x(t)$ for a.e. $x \in D$ and $t \in [t_x^-, t_x^+]$.

Next, assume that $e \in U_s^{-2}\mathcal{M}_s^{-1}$, $e \neq e_{\max}(\mathrm{cof}\, U_s)$, and let

$$\sigma_x(t) = U_s^2 e \cdot w(\rho_x(t)).$$

Then, for a.e. $x \in D$ and a.e. $t \in (t_x^-, t_x^+)$,

$$\frac{d}{dt}\sigma_x(t) = \frac{d}{dt}U_s^2 e \cdot w(\rho_x(t)) = U_s^2 e \cdot [Dz(w(\rho_x(t)))]^{-1}U_s e. \qquad (4.5.20)$$

However, the function $F \mapsto |(\mathrm{cof}\, F)U_s^2 e \cdot U_s e|$ is polyconvex and since, for a.e. $x \in D$ and a.e. $t \in (t_x^-, t_x^+)$, $Dz(w(\rho_x(t))) \in K^{qc}$, we infer that

$$\begin{aligned}
|(\mathrm{cof}\, Dz(w(\rho_x(t))))U_s^2 e \cdot U_s e| &\leq \max_{i,R\in SO(3)} \left\{R(\mathrm{cof}\, U_i)U_s^2 e \cdot U_s e, RU_s^2 e \cdot U_s e\right\} \\
&\leq \max_i \left\{|(\mathrm{cof}\, U_i)U_s^2 e||U_s e|, |U_s^2 e||U_s e|\right\} \\
&= |(\mathrm{cof}\, U_s)U_s^2 e||U_s e| = \det\, U_s|U_s e|^2 \qquad (4.5.21)
\end{aligned}$$

since $e \in U_s^{-2}\mathcal{M}_s^{-1}$ and U_s is symmetric. As before, $F \mapsto \det F$ is quasiaffine and $\det U_s \leq 1$, hence

$$|U_s^2 e \cdot [Dz(w(\rho_x(t)))]^{-1}U_s e| \leq |U_s e|^2.$$

Combining with (4.5.20) we deduce that for a.e. $x \in D$ and a.e. $t \in (t_x^-, t_x^+)$

$$|\frac{d}{dt}\sigma_x(t)| \leq |U_s e|^2 = |U_s^2 e \cdot e| = \frac{|\sigma_x(t_x^+) - \sigma_x(t_x^-)|}{|t_x^+ - t_x^-|} \qquad (4.5.22)$$

and applying the rigidity argument of Lemma 4.5.9, we infer that for a.e. $x \in D$ and all $t \in (t_x^-, t_x^+)$,

$$U_s^2 e \cdot Dw(\rho_x(t)) U_s e = \frac{U_s^2 e \cdot w(\rho_x(t_x^+)) - U_s^2 e \cdot w(\rho_x(t_x^-))}{t_x^+ - t_x^-} = |U_s e|^2. \tag{4.5.23}$$

To finish the proof, note that by (4.5.21)

$$|\operatorname{cof} Dz(w(\rho_x(t))) U_s^2 e \cdot U_s e| \leq \det U_s |U_s e|^2.$$

However, (4.5.23) says that

$$|\operatorname{cof} Dz(w(\rho_x(t))) U_s^2 e \cdot U_s e| = \det Dz(w(\rho_x(t))) |U_s e|^2 \geq \det U_s |U_s e|^2$$

by our assumption that $\det U_s \leq 1$. But then $\det Dz(w(\rho_x(t))) = \det U_s$ and

$$|(\operatorname{cof} Dz(w(\rho_x(t)))) U_s^2 e \cdot U_s e| = \det U_s |U_s e|^2 = |(\operatorname{cof} U_s) U_s^2 e \cdot U_s e|.$$

Letting $\psi : \mathbb{R}^{3\times 3} \to \mathbb{R}$ be the polyconvex function $\psi(F) = |(\operatorname{cof} F) U_s^2 e \cdot U_s e|$ and using the fact that the measure $\mu = (\mu_x)_{x \in B_{f,e}}$ underlying the deformation z is a $W^{1,\infty}$ gradient Young measure, we deduce that for a.e. $x \in D$ and $t \in (t_x^-, t_x^+)$,

$$\begin{aligned}
|(\operatorname{cof} U_s) U_s^2 e \cdot U_s e| &= \psi(Dz(w(\rho_x(t)))) \\
&\leq \langle \mu_{w(\rho_x(t))}, \psi \rangle \\
&= \int_{SO(3)} |A U_s^2 e \cdot U_s e| \, d\mu_{w(\rho_x(t))}(A) \\
&\quad + \sum_i \int_{SO(3)U_i} |(\operatorname{cof} A) U_s^2 e \cdot U_s e| \, d\mu_{w(\rho_x(t))}(A) \\
&\leq \mu_{w(\rho_x(t))}(SO(3)) |U_s^2 e| |U_s e| + \\
&\quad \sum_i \mu_{w(\rho_x(t))}(SO(3)U_i) |(\operatorname{cof} U_i) U_s^2 e| |U_s e|.
\end{aligned} \tag{4.5.24}$$

On the other hand, since $(\operatorname{cof} U_s) U_s^2 e$ is parallel to $U_s e$, we also deduce that

$$\begin{aligned}
|(\operatorname{cof} U_s) U_s^2 e \cdot U_s e| &= |(\operatorname{cof} U_s) U_s^2 e| |U_s e| \\
&= \mu_{w(\rho_x(t))}(SO(3)) |(\operatorname{cof} U_s) U_s^2 e| |U_s e| + \\
&\quad \sum_i \mu_{w(\rho_x(t))}(SO(3)U_i) |(\operatorname{cof} U_s) U_s^2 e| |U_s e|.
\end{aligned} \tag{4.5.25}$$

Subtracting equation (4.5.25) from (4.5.24), we obtain

$$\begin{aligned}
0 \leq\ & \mu_{w(\rho_x(t))}(SO(3)) \left[|U_s^2 e| |U_s e| - |(\operatorname{cof} U_s) U_s^2 e| |U_s e| \right] + \\
& \sum_{i \neq s} \mu_{w(\rho_x(t))}(SO(3)U_i) \left[|(\operatorname{cof} U_i) U_s^2 e| |U_s e| - |(\operatorname{cof} U_s) U_s^2 e| |U_s e| \right].
\end{aligned}$$

However, since $e \in U_s^{-2}\mathcal{M}_s^{-1}$, all terms in the brackets are strictly negative and hence, for a.e. $x \in D$ and $t \in (t_x^-, t_x^+)$,

$$\mu_{w(\rho_x(t))}(SO(3)) = \mu_{w(\rho_x(t))}(SO(3)U_i) = 0 \text{ for all } i \neq s,$$

implying that $\operatorname{supp} \mu_{w(\rho_x(t))} \subset SO(3)U_s$ for a.e. $x \in D$ and $t \in (t_x^-, t_x^+)$. By standard results (see e.g. [10]), the quasiconvex hull of one well is trivial and any Young measure supported on one well must be homogeneous; in particular, since the endpoints of the curves parametrized by $w(\rho_x(t))$ deform linearly by U_s,

$$\mu_{w(\rho_x(t))} = \delta_{U_s},$$

for a.e. $x \in D$ and $t \in (t_x^-, t_x^+)$. Trivially one now obtains that $Dw(\rho_x(t)) = [Dz(w(\rho_x(t)))]^{-1} = U_s^{-1}$ and

$$w(\rho_x(t)) = \int_{t_x^-}^{t} Dw(\rho_x(s))U_s e \, ds + w(\rho_x(t_x^-)) = x + te = r_x(t),$$

i.e. $z(r_x(t)) = U_s r(t)$ for a.e. $x \in D$ and $t \in (t_x^-, t_x^+)$. $\square$

The idea is now almost identical to that of maximal directions for U_s; if we are able to take $D = B_{f,e}$, i.e. if we can cover $B_{f,e}$ by segments in the direction of $e \in U_s^{-2}\mathcal{M}_s^{-1}$ joining points on the prescribed boundary $\partial B_{f,e} \cap \Omega$, we can immediately deduce that $\bar{\mu}_x = U_s$ a.e. and Lemma 4.5.8 will provide the required quasiconvexity condition. However, there is a crucial obstacle: in the statement of Lemma 4.5.12 we assumed that the image of the set D under U_s lies entirely in $z(B_{f,e})$.

In fact, proving this for $D = B_{f,e}$ would prove that $z(x) = U_s x$ throughout $B_{f,e}$ which is precisely our goal. To see this, let's restrict attention at an edge assumed parallel to $e \in U_s^{-2}\mathcal{M}_s^{-1}$. Clearly, any region B_e can be covered by lines in the direction of e, i.e. parallel to the edge, joining points on $\partial B_e \cap \Omega$. If we knew that the image of any such segment under the linear map $U_s x$ was contained in $z(B_e)$ then Lemma 4.5.12 would say that almost all of the region B_e transforms like $U_s x$ and therefore, by the continuity of z, $z(x) = U_s x$ in B_e. We proceed with two lemmata to show that this is indeed the case.

Firstly, we wish to show that points in $B_{f,e}$, sufficiently close to the prescribed boundary $\partial B_{f,e} \cap \Omega$, have the property that their image under the linear map $U_s x$ lies in $z(B_{f,e})$ for any deformation z underlying an admissible measure in $\mathcal{B}_{f,e}$ supported within K. This allow us to cover a small region in $B_{f,e}$, sufficiently close to $\partial B_{f,e} \cap \Omega$, by the appropriate line segments such that their image under $U_s x$ lies in $z(B_{f,e})$,

i.e. one appropriate set D exists. This is described in Lemma 4.5.13 below and, as its proof is applicable to both faces and edges, we treat them together. We note that Lemma 4.5.12 will then say that this (possibly small) region necessarily transforms like $U_s x$ and the idea is that this process can be continued to exhaust $B_{f,e}$.

Lemma 4.5.13. *Let z be a map underlying a measure in $\mathcal{B}_{f,e}$ with support contained in K a.e. and suppose that $C \subset \partial B_{f,e} \cap \Omega$ is closed. There exists some $\epsilon > 0$ such that whenever $x \in B_{f,e}$ satisfies* $\operatorname{dist}(x, C) < \epsilon$ *then $U_s x \in z(B_{f,e})$, where for any two sets A, $B \subset \mathbb{R}^3$, dist$(A, B) = \inf\{|a - b|,\ a \in A,\ b \in B\}$.*

In particular, if $r : [0, a] \to \overline{B_{f,e}}$ is the parametrization of a line segment such that $r(0), r(a) \in C$ and for all $t \in (0, a)$, $r(t) \in B_{f,e}$ then

$$\{U_s r(t) \,:\, t \in (0, a)\} \subset z(B_{f,e})$$

whenever $\operatorname{dist}(r(t), C) < \epsilon$ *for all $t \in [0, a]$.*

Proof. Since $C \subset \partial B_{f,e} \cap \Omega$ is closed and the sets $\partial B_{f,e} \cap \Omega$, $\partial B_{f,e} \cap \partial\Omega$ are disjoint, there must exist $\delta > 0$ such that $\operatorname{dist}(C, \partial B_{f,e} \cap \partial\Omega) = \delta$. Let $c_0 \in C$; then $\operatorname{dist}(c_0, \partial B_{f,e} \cap \partial\Omega) \geq \delta$. Restrict z to $B(c_0, \delta) \cap B_{f,e}$ and extend it to $\tilde{z} : B(c_0, \delta) \to \mathbb{R}^3$ by $U_s x$, i.e.

$$\tilde{z}(x) = \begin{cases} z(x), & x \in B(c_0, \delta) \cap B_{f,e} \\ \\ U_s x, & x \in B(c_0, \delta) \setminus B_{f,e}. \end{cases}$$

Note that $\tilde{z}$ is continuous, an element of $W^{1,\infty}(B(c_0, \delta), \mathbb{R}^3)$ and has bounded distortion. Thus, since $\tilde{z}$ is not identically equal to a constant, Lemma 4.3.1 says that $\tilde{z}$ is an open mapping.

Then, $\tilde{z}(B(c_0, \delta))$ is an open set and there exists ϵ_0 such that $B(\tilde{z}(c_0), \epsilon_0) \subset \tilde{z}(B(c_0, \delta))$, i.e.

$$B(z(c_0), \epsilon_0) = B(U_s c_0, \epsilon_0) \subset \tilde{z}(B(c_0, \delta)).$$

We now claim that $U_s[B(c_0, \epsilon_0/\|U_s\|) \cap B_{f,e}] \subset z(B_{f,e})$ where $\|U_s\| = \sigma_{max}(U_s)$; trivially, $U_s B(c_0, \epsilon_0/\|U_s\|) \subset B(U_s c_0, \epsilon_0)$ and hence

$$U_s[B(c_0, \epsilon_0/\|U_s\|) \cap B_{f,e}] \subset \tilde{z}(B(c_0, \delta)) = z(B(c_0, \delta) \cap B_{f,e}) \cup U_s(B(c_0, \delta) \setminus B_{f,e}).$$

But $B(c_0, \epsilon_0/\|U_s\|) \cap B_{f,e}$ and $B(c_0, \delta) \setminus B_{f,e}$ are disjoint and, since U_s is invertible (even positive definite), the linear map $U_s x$ is injective, i.e.

$$U_s[B(c_0, \epsilon_0/\|U_s\|) \cap B_{f,e}] \subset z(B(c_0, \delta) \cap B_{f,e}) \subset z(B_{f,e}).$$

To conclude the proof, it suffices to find an ϵ such that $U_s\left[B(c,\epsilon)\cap B_{f,e}\right]\subset z(B_{f,e})$ for all $c\in C$; by the above argument, for any $c\in C$ there exists $\epsilon_c>0$ such that

$$U_s\left[B(c,\epsilon_c)\cap B_{f,e}\right]\subset z(B_{f,e})$$

and the family of sets $\{B(c,\epsilon_c)\}_{c\in C}$ is an open cover of C. Since C is closed, it is also compact and there exist $c_i\in C$, $i=1,\dots,N$ such that the sets $\{B(c_i,\epsilon_{c_i})\}_{i=1,\dots,N}$ cover C; let

$$\epsilon=\operatorname{dist}([\bigcup_{i=1}^{N}B(c_i,\epsilon_{c_i})]^c,C),$$

where for a set $A\subset\mathbb{R}^3$, A^c denotes its complement in $\mathbb{R}^3$. Note that $\epsilon>0$ since otherwise, both sets being closed, there would exist $x\in[\bigcup_{i=1}^{N}B(c_i,\epsilon_{c_i})]^c$ and $c\in C$ such that $x=c$. But this is absurd as the point $c\in C$ would not belong to the cover of C. Also, for any $\tilde{x}\in[\bigcup_{i=1}^{N}B(c_i,\epsilon_{c_i})]^c$ and $c\in C$, $|\tilde{x}-c|\geq\epsilon$ and hence, whenever $x\in B_{f,e}$ satisfies $\operatorname{dist}(x,C)<\epsilon$, $x\in(\bigcup_{i=1}^{N}B(c_i,\epsilon_{c_i}))\cap B_{f,e}$ and $U_sx\in z(B_{f,e})$. □

Remark. We note that the above result excludes a certain kind of 'one-sided' contact between $\partial B_{f,e}\cap\Omega$ and $\partial B_{f,e}\cap\partial\Omega$, the prescribed and free parts of the boundary of $B_{f,e}$ respectively. In particular, it says that for any $x_0\in\partial B_{f,e}\cap\Omega$ there exists an $\epsilon_0>0$ such that the set $U_s\left[B(x_0,\epsilon_0)\cap B_{f,e}\right]$, lies in $z(B_{f,e})$ and hence does not intersect the image of the free boundary $z(\partial B_{f,e}\cap\partial\Omega)$. By abusing terminology, $U_s\left[B(x_0,\epsilon_0)\cap B_{f,e}\right]$ can be thought of as a 'neighbourhood' of $z(x_0)$ lying entirely within $z(B_{f,e})$.

Moreover, let $r(t)$, $t\in[0,a]$ be the parametrization of a line segment with endpoints on $\partial B_{f,e}\cap\Omega$ such that $r(t)\in B_{f,e}$ for any $t\in(0,a)$ and suppose that

$$\{U_sr(t):t\in(0,a)\}\subset z(B_{f,e}).$$

For any $t_0\in(0,a)$, $U_sr(t_0)\in z(B_{f,e})$ which is open, i.e. there exists $\epsilon_0>0$ such that $B(U_sr(t_0),\epsilon_0)\subset z(B_{f.e})$ and hence

$$U_s[B(r(t_0),\frac{\epsilon_0}{\|U_s\|})]\subset z(B_{f,e}).$$

Treating endpoints, or generally boundary points, as in the proof of Lemma 4.5.13 and repeating the argument, one can find $\epsilon>0$ such that whenever $x\in B_{f,e}$ and $\operatorname{dist}(x,\{r(t):t\in[0,a]\})<\epsilon$, then $U_sx\in z(B_{f,e})$. In particular, whenever $\rho(t)$, $t\in[0,b]$ is another line segment in the direction of e with endpoints on $\partial B_{f,e}\cap\Omega$ with the property that

$$\operatorname{dist}(\rho(t),\{r(t):t\in[0,a]\})<\epsilon\quad\forall\,t\in[0,b],$$

then the set $\{U_s\rho(t) : t \in (0,b)\}$ lies in $z(B_{f,e})$; we note this as it will be used shortly in the proof of Lemma 4.5.14.

To see how one can use Lemma 4.5.13, let $e \in U_s^{-2}\mathcal{M}_s^{-1}$ be a vector parallel to the edge or perpendicular to the normal of the face in question and consider some closed set $C \subset \partial B_{f,e} \cap \Omega$ such that the region (partly) enclosed by C can be covered by line segments in the direction of e contained in $B_{f,e}$ with endpoints on C. Lemma 4.5.13 says that for any such line segment sufficiently close to C, its image under the linear map $U_s x$ lies within the image of $B_{f,e}$ under any map z underlying an admissible Young measure with support contained in K.

In particular, this means that we can cover an open region D contained in $B_{f,e}$ by such lines. Since each of these is in the direction of e and $e \in U_s^{-2}\mathcal{M}_s^{-1}$, Lemma 4.5.12 says that for a.e. $x \in D$ the line segment through x, in the direction of e, joining points on the prescribed boundary $\partial B_{f,e} \cap \Omega$, parametrized by $r_x(t)$, $t \in [t_x^-, t_x^+]$ satisfies

$$z(r(t)) = U_s r(t) \quad \text{for all } t \in [0,a],$$

i.e. almost all the region D transforms linearly and according to $U_s x$.

By the continuity of z, z must agree with the linear map $U_s x$ on the closure of D and we may as well assume that $B_{f,e}$ is reduced; in particular, part of the prescribed boundary of the reduced region $B_{f,e}$ is now flat and covered by the appropriate line segments - see Figure 4.8 for an example in the case of a face.

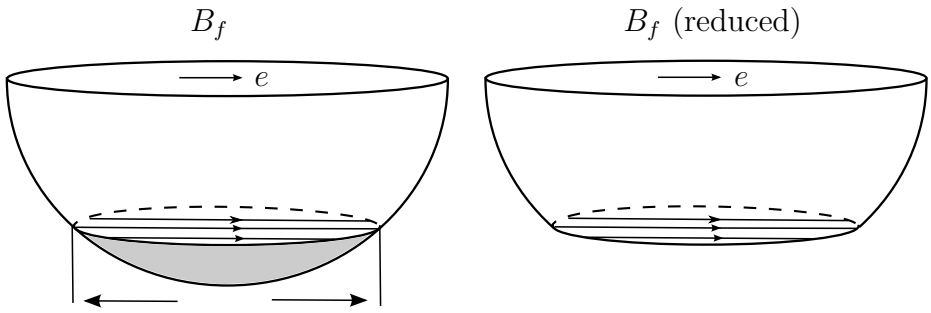

Figure 4.8: The shaded region - covered by the appropriate line segments - necessarily deforms like $U_s x$ and can be removed, thus reducing the set B_f.

Let $r_x(t)$, $t \in [t_x^-, t_x^+]$ be the parametrization of such a line segment now lying on the prescribed part of the boundary of $B_{f,e}$. As before, using Lemma 4.5.13 with $\{r_x(t) : t \in [t_x^-, t_x^+]\} \subset C$, we can repeat the process and cover a greater part of $B_{f,e}$

with the appropriate line segments, this time close to the flat boundary of the reduced set $B_{f,e}$, each having the property that its image under $U_s x$ lies within $z(B_{f,e})$, i.e. the map z agrees with $U_s x$ in the closure of this larger region and the process can be repeated. Then one may naturally expect that the entire region $B_{f,e}$ must transform under the linear map $U_s x$.

The following lemma shows that this is indeed true and resolves the case of a face and an edge. As before we treat both simultaneously.

Lemma 4.5.14. *Let $\Omega \subset \mathbb{R}^3$ be a parallelepiped domain and suppose that the vector $e \in U_s^{-2}\mathcal{M}_s^{-1}$ is parallel to an edge or perpendicular to the normal of a face of Ω. Let $z \in W^{1,\infty}(B_{f,e}, \mathbb{R}^3)$ be a map underlying a Young measure in $\mathcal{B}_{f,e}$ with support contained in K a.e. in $B_{f,e}$. Then*

$$z(x) = U_s x \quad \text{for all } x \in B_{f,e}.$$

Proof. Let $\mu \in \mathcal{B}_{f,e}$ with support a.e. in K and suppose that $z \in W^{1,\infty}(B_{f,e}, \mathbb{R}^3)$ is its underlying deformation. As in Lemma 4.5.11, we may cover $B_{f,e}$ with line segments in the direction of $e \in U_s^{-2}\mathcal{M}_s^{-1}$ whose endpoints lie on $\partial B_{f,e} \cap \Omega$. In particular, for any $x \in B_{f,e}$ let

$$\begin{aligned} t_x^- &= \sup\{t < 0 : x + te \notin B_{f,e}\} \text{ and} \\ t_x^+ &= \inf\{t > 0 : x + te \notin B_{f,e}\}, \end{aligned}$$

where both the supremum and infimum above are attained as $B_{f,e}$ is open. Then, $r_x(t) = x + te$, $t \in [t_x^-, t_x^+]$ is a parametrization of the unique line segment through x, in the direction of e, with endpoints on $\partial B_{f,e} \cap \Omega$.

Let E be the maximal subset of $B_{f,e}$ with the property that for every $x \in E$, $r_x(t) \in E$ for all $t \in (t_x^-, t_x^+)$ and $\{U_s r_x(t) : t \in (t_x^-, t_x^+)\} \subset z(B_{f,e})$, i.e. E is the maximal subset of $B_{f,e}$ that can be covered by line segments in the direction of e, joining points on $\partial B_{f,e} \cap \Omega$ such that their image under the linear map $x \mapsto U_s x$ lies in $z(B_{f,e})$. Such a maximal set clearly exists.

We aim to show that E is a non-empty, open and closed subset of $B_{f,e}$ where open and closed is meant in terms of the induced topology on $B_{f,e}$ as a subset of $\mathbb{R}^3$. Then, $B_{f,e}$ being connected, $E = B_{f,e}$; by Lemma 4.5.12 and the continuity of z we then deduce that $z(x) = U_s x$ for all $x \in B_{f,e}$.

Firstly, by choosing an appropriate closed set $C \subset \partial B_{f,e} \cap \Omega$, Lemma 4.5.13 says that there exists $\epsilon > 0$ such that any line segment in the direction of e with endpoints

on C - say parametrized by $r(t)$, $t \in [0,a]$ - with $\operatorname{dist}(r(t), C) < \epsilon$ for all $t \in [0,a]$ satisfies

$$\{U_s r(t) \,:\, t \in (0,a)\} \subset z(B_{f,e}).$$

In particular, $\{r(t) : t \in (0,a)\} \subset E$ and E is non-empty.

Let $x_0 \in E$ and $r_{x_0}(t)$, $t \in [t_{x_0}^-, t_{x_0}^+]$, be the parametrization of the corresponding line segment. By the remark following Lemma 4.5.13, there exists yet another $\epsilon > 0$ such that whenever $\rho(t)$, $t \in [0,b]$, is a line segment in the direction of e with endpoints on $\partial B_{f,e} \cap \Omega$ with the property that

$$\operatorname{dist}(\rho(t), \{r_{x_0}(t) : t \in [t_{x_0}^-, t_{x_0}^+]\}) < \epsilon \quad \forall\, t \in [0,b],$$

then $\{U_s\rho(t) : t \in (0,b)\} \subset z(B_{f,e})$. In particular, this defines a neighbourhood of $\{r_{x_0}(t) : t \in (t_{x_0}^-, t_{x_0}^+)\}$, say D, which is open in $B_{f,e}$ such that for any point $\tilde{x} \in D$, the image under $U_s x$ of the corresponding line segment parametrized by $r_{\tilde{x}}(t)$, $t \in [t_{\tilde{x}}^-, t_{\tilde{x}}^+]$ lies in $z(B_{f,e})$ - except for the endpoints. But E is the maximal subset of $B_{f,e}$ with this property and hence $D \subset E$. Trivially,

$$x_0 = r_{x_0}(0) \in D \subset E$$

and E is indeed open.

We note an important fact: since E is open and can be covered by line segments in the direction of e with endpoints on $\partial B_{f,e} \cap \Omega$ whose image under $U_s x$ lies in $z(B_{f,e})$, by Lemma 4.5.12 and the continuity of z, $z(x) = U_s x$ for all $x \in \overline{E}$. Note that, since z is continuous up to the boundary of $B_{f,e}$, this is also true if $\overline{E}$ is viewed as the closure of E in $\mathbb{R}^3$.

It is now easy to infer that E is also closed: let $x_k \in E$ be a sequence of points such that $x_k \to x \in B_{f,e}$[6]. Let $r_x(t)$, $t \in [t_x^-, t_x^+]$ be the parametrization of the line segment through x and similarly $r_{x_k}(t)$ for the points x_k. The idea is to show that $z(r_x(t)) = U_s r_x(t)$ for all $t \in (t_x^-, t_x^+)$; then surely $U_s r_x(t) \in z(B_{f,e})$ for all $t \in (t_x^-, t_x^+)$ and, by the maximality of E, $x \in E$.

We saw above that $z(x) = U_s x$ for all $x \in E$; thus $z(x_k) = U_s x_k$ and $z(x) = U_s x$ by the convergence of x_k to x. Let $t_0 \in (t_x^-, t_x^+)$ and consider the point $r_x(t_0) = x + t_0 e$; trivially,

$$r_{x_k}(t_0) = x_k + t_0 e \to x + t_0 e = r_x(t_0) \tag{4.5.26}$$

[6]Since we have restricted attention to $B_{f,e}$ with the induced topology, a sequence $\{x_k\}_k \subset B_{f,e}$ such that $x_k \to x \in \overline{B_{f,e}}$ is convergent in $\mathbb{R}^3$ but not in $B_{f,e}$; in $B_{f,e}$ it is only Cauchy.

and since $r_x(t_0) \in B_{f,e}$, for k large enough, $r_{x_k}(t_0)$ must belong to $B_{f,e}$, i.e. $r_{x_k}(t_0) \in E$ for k large and therefore $z(r_{x_k}(t_0)) = U_s r_{x_k}(t_0)$. But then $z(r_x(t_0)) = U_s r_x(t_0)$ by (4.5.26) and, hence, E is also closed. □

We can now easily deduce Lemma 4.5.6 regarding the quasiconvexity of W at U_s at any face or edge of a domain admissible for U_s as well as establish our main result, Theorem 4.5.1. These are presented next:

Proof of Lemma 4.5.6. Suppose that $\mu \in \mathcal{B}_{f,e}$ is such that $\operatorname{supp} \mu_x \subset K$; otherwise the quasiconvexity follows trivially. Combining Lemma 4.5.11 and Lemma 4.5.14, we deduce that whenever Ω is admissible for U_s, then $\bar{\mu}_x = U_s$ a.e. in $B_{f,e}$ and the quasiconvexity of W at U_s on a face or edge follows by Lemma 4.5.8. □

Proof of Theorem 4.5.1. The second part of the Theorem was established in Lemma 4.5.3. As for the first part, it suffices to show that W is quasiconvex at U_s in the interior, on faces and edges; but this is immediate by Lemma 4.5.5 for the interior and Lemma 4.5.6 for faces and edges. □

In particular, we have shown that if the specimen has been cut in such a way that its edges are parallel to vectors in $\mathcal{M}_s \cup U_s^{-2}\mathcal{M}_s^{-1}$, the austenite cannot nucleate anywhere in the interior, on faces or edges and we have shown how nucleation can occur at a corner for Seiner's specimen. We now turn our attention to the cubic-to-orthorhombic transition of CuAlNi, calculate the sets of maximal directions for each $s = 1, \dots, 6$ and infer whether our simplified model and main result can indeed provide an explanation for the location of the nucleation points in Seiner's experiment.

4.6 Admissible domains: cubic-to-orthorhombic

In this section we identify the maximal directions for U_s and U_s^{-1}, $s = 1, \dots, 6$ for the cubic-to-orthorhombic variants given in (3.3.1). These directions are of course dependent on the lattice parameters and, as a very simple example, consider the unit vector $e = (1, 0, 0)^T$ and the matrices U_1 and U_3, where

$$U_1 = \begin{pmatrix} \beta & 0 & 0 \\ 0 & \frac{\alpha+\gamma}{2} & \frac{\alpha-\gamma}{2} \\ 0 & \frac{\alpha-\gamma}{2} & \frac{\alpha+\gamma}{2} \end{pmatrix} \qquad U_3 = \begin{pmatrix} \frac{\alpha+\gamma}{2} & 0 & \frac{\alpha-\gamma}{2} \\ 0 & \beta & 0 \\ \frac{\alpha-\gamma}{2} & 0 & \frac{\alpha+\gamma}{2} \end{pmatrix}.$$

We see immediately that $|U_1 e|^2 = \beta^2$ while $|U_3 e|^2 = (\alpha^2 + \gamma^2)/2$ and there is no general relation between these quantities for arbitrary α, β, γ and, therefore, further assumptions on the lattice parameters must be made.

Assumptions on lattice parameters. We make the following assumptions on the lattice parameters α, β, γ of the cubic-to-orthorhombic transformation:

(A1) $\beta \leq 1 \leq \gamma < \alpha$;

(A2) $2\alpha^2 + \beta^2 \geq 3$; equivalently $|U_s|^2 \geq 3 + \gamma^2 - \alpha^2$;

(A3) $\alpha^2\gamma^2 + \alpha^2\beta^2 + \beta^2\gamma^2 \geq 3$; equivalently $|\mathrm{cof}\, U_s|^2 \geq 3$;

(A4) $A - B > 0$ where $A = \alpha^2\gamma^2 - \beta^2(\alpha^2 + \gamma^2)/2 > 0$ and $B = \beta^2(\alpha^2 - \gamma^2) > 0$.

We note that these assumptions are in accordance with the CuAlNi specimen used in the experiment of Seiner where $\alpha = 1.06372$, $\beta = 0.91542$ and $\gamma = 1.02368$. Then, $|U_s|^2 - \gamma^2 + \alpha^2 = 3.10099$, $|\mathrm{cof}\, U_s|^2 = 3.01206$ and $A - B = 0.202513$.

For the remainder of this section we prove a series of results concerning the maximal directions for U_s and U_s^{-1}; we warn the reader that the proofs of these rely on simple, but often long, calculations.

Lemma 4.6.1. *Assume that the lattice parameters α, β, γ satisfy (A1) and (A2) and for a vector $e \in S^2$ write $e = (e_1, e_2, e_3)^T$. Then, for each $s = 1, \ldots, 6$,*

$$\mathcal{M}_s = \left\{ e \in S^2 : (-1)^{s-1} e_2 e_3 \geq 0,\ \ |e_1| \leq \min\left\{|e_2|, |e_3|\right\} \right\}, \quad \textit{for } s = 1, 2$$

$$\mathcal{M}_s = \left\{ e \in S^2 : (-1)^{s-1} e_1 e_3 \geq 0,\ \ |e_2| \leq \min\left\{|e_1|, |e_3|\right\} \right\}, \quad \textit{for } s = 3, 4$$

$$\mathcal{M}_s = \left\{ e \in S^2 : (-1)^{s-1} e_1 e_2 \geq 0,\ \ |e_3| \leq \min\left\{|e_1|, |e_2|\right\} \right\}, \quad \textit{for } s = 5, 6.$$

Proof. We first prove this for $s = 1$. Writing out the expressions for $|U_i e|^2$ we get

$$\begin{aligned}
|U_s e|^2 &= \beta^2 e_1^2 + \frac{\alpha^2 + \gamma^2}{2}\left(e_2^2 + e_3^2\right) + (-1)^{s-1}\left(\alpha^2 - \gamma^2\right) e_2 e_3 \quad \text{for } s = 1, 2, \\
|U_s e|^2 &= \beta^2 e_2^2 + \frac{\alpha^2 + \gamma^2}{2}\left(e_1^2 + e_3^2\right) + (-1)^{s-1}\left(\alpha^2 - \gamma^2\right) e_1 e_3 \quad \text{for } s = 3, 4, \\
|U_s e|^2 &= \beta^2 e_3^2 + \frac{\alpha^2 + \gamma^2}{2}\left(e_1^2 + e_2^2\right) + (-1)^{s-1}\left(\alpha^2 - \gamma^2\right) e_1 e_2 \quad \text{for } s = 5, 6.
\end{aligned}$$

We show that $e \in \mathcal{M}_1$ with the above representation is necessary and sufficient for $|U_1 e| = \max_i |U_i e|$. The condition on the norm of U_s is related to $|U_1 e| \geq 1$ and we treat this last. Writing $N = \left(\frac{\alpha^2+\gamma^2}{2} - \beta^2\right) > 0$ and $P = (\alpha^2 - \gamma^2) > 0$,

$$\begin{aligned}
|U_1 e|^2 - |U_2 e|^2 &= 2Pe_2e_3, && (4.6.1)\\
|U_1 e|^2 - |U_3 e|^2 &= -N(e_1^2 - e_2^2) + Pe_3(e_2 - e_1), && (4.6.2)\\
|U_1 e|^2 - |U_4 e|^2 &= -N(e_1^2 - e_2^2) + Pe_3(e_2 + e_1), && (4.6.3)\\
|U_1 e|^2 - |U_5 e|^2 &= -N(e_1^2 - e_3^2) + Pe_2(e_3 - e_1), && (4.6.4)\\
|U_1 e|^2 - |U_6 e|^2 &= -N(e_1^2 - e_3^2) + Pe_2(e_3 + e_1). && (4.6.5)
\end{aligned}$$

Trivially, (4.6.1) is non-negative if and only if $e_2e_3 \geq 0$, i.e. $|e_2e_3| = e_2e_3$. Then

$$\begin{aligned}
|U_1 e|^2 - |U_3 e|^2 &= -N(|e_1|^2 - |e_2|^2) + P|e_3e_2| - Pe_3e_1,\\
|U_1 e|^2 - |U_4 e|^2 &= -N(|e_1|^2 - |e_2|^2) + P|e_3e_2| + Pe_3e_1
\end{aligned}$$

and the minimum between (4.6.2) and (4.6.3) is given by

$$-N(|e_1|^2 - |e_2|^2) + P|e_3e_2| - P|e_3e_1| = (|e_1| - |e_2|)\left[-N|e_1| - N|e_2| - P|e_3|\right]. \quad (4.6.6)$$

Simply by interchanging the roles of e_2 and e_3, the minimum between (4.6.4) and (4.6.5) is given by

$$-N(|e_1|^2 - |e_3|^2) + P|e_2e_3| - P|e_2e_1| = (|e_1| - |e_3|)\left[-N|e_1| - N|e_3| - P|e_2|\right]. \quad (4.6.7)$$

Then, (4.6.1)-(4.6.5) are all non-negative if and only if $e_2e_3 \geq 0$ and both (4.6.6) and (4.6.7) are non-negative, i.e. $e_2e_3 \geq 0$ and $|e_1| \leq \min\{|e_2|, |e_3|\}$.

It now suffices to show that any vector e as above satisfies $|U_1 e|^2 \geq 1$. This is a consequence of the constraint $|U_1|^2 \geq 3 + \gamma^2 - \alpha^2$. Since $e \in S^2$, $e_1^2 + e_2^2 + e_3^2 = 1$ and

$$\begin{aligned}
|U_1 e|^2 - 1 &= \beta^2 e_1^2 + \frac{\alpha^2+\gamma^2}{2}\left(e_2^2 + e_3^2\right) + \left(\alpha^2 - \gamma^2\right)e_2e_3 - 1\\
&= \left(\beta^2 - 1\right)e_1^2 + \left(\frac{\alpha^2+\gamma^2}{2} - 1\right)\left(e_2^2 + e_3^2\right) + \left(\alpha^2 - \gamma^2\right)e_2e_3.
\end{aligned}$$

But $|e_1| \leq \min\{|e_2|, |e_3|\}$ and $e_2e_3 \geq 0$ implies that $2e_1^2 \leq e_2^2 + e_3^2$ and $e_1^2 \leq e_2e_3$. Noting that $|U_1|^2 \geq 3 + \gamma^2 - \alpha^2$,

$$\begin{aligned}
|U_1 e|^2 - 1 &\geq \left(\beta^2 - 1\right)e_1^2 + 2\left(\frac{\alpha^2+\gamma^2}{2} - 1\right)e_1^2 + \left(\alpha^2 - \gamma^2\right)e_1^2\\
&= \left(|U_1|^2 - 3 + \alpha^2 - \gamma^2\right)e_1^2 \geq 0.
\end{aligned}$$

For the remaining variants, the proof is almost identical. Also note that the result follows easily due to the symmetry relations between the martensitic variants (see Appendix A). Suppose we wish to calculate the maximal directions for U_s. There exists a rotation $Q = Q[\pi, a]$ about an axis $a \in \mathbb{R}^3$ such that $U_s = QU_1Q$. But then,

$$\begin{aligned} e \in \mathcal{M}_s &\Leftrightarrow |U_s e| = \max_i\{|U_i e|,\ 1\} \\ &\Leftrightarrow |QU_1Qe| = \max_i\{|U_i e|,\ 1\} \\ &\Leftrightarrow |U_1(Qe)| = \max_j\{|U_j Qe|,\ 1\} \Leftrightarrow Qe \in \mathcal{M}_1 \end{aligned}$$

since for each $j = 1, \ldots, 6$ there exists a unique $i \in \{1, \ldots, 6\}$ such that $QU_jQ = U_i$ and hence $|U_jQe| = |U_ie|$. For e.g. U_2, $Q_{17}U_2Q_{17} = U_1$ where $Q_{17} = Q[\pi, i_3]$ and

$$e \in \mathcal{M}_2 \Leftrightarrow Q_{17}e \in \mathcal{M}_1 \Leftrightarrow (-e_1, -e_2, e_3) \in \mathcal{M}_1 \Leftrightarrow e_2e_3 \leq 0 \text{ and } |e_1| \leq \min\{|e_2|,\ |e_3|\}.$$

Using the appropriate rotations we can easily compute the rest. □

Remark. The assumption on the lattice parameters that $\beta \leq 1 \leq \gamma < \alpha$ can indeed be relaxed. What is needed here is that $\alpha, \gamma \geq 1$ and that $\beta \leq \min\{\alpha, \gamma\}$. In fact, if $\beta \geq 1$ the condition on the norm of U_s is immediately satisfied and if $\gamma > \alpha$ then simply $\mathcal{M}_i$ assumes the form of $\mathcal{M}_j$ where U_j is the compound counterpart of U_i and vice versa. Nevertheless, we need the assumption for the characterization of the maximal directions for U_s^{-1}.

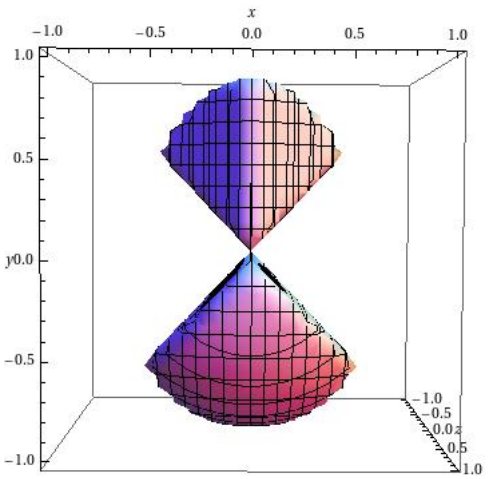

Figure 4.9: All vectors $e \in \mathcal{M}_1$ calculated using the lattice parameters of the CuAlNi specimen in Seiner's experiment.

We now turn our attention to the problem of calculating the maximal directions for U_s^{-1} and see whether they indeed add new directions along which we can deduce that the underlying deformation of an admissible measure coincides with $U_s x$.

Lemma 4.6.2. *Assume that the lattice parameters satisfy (A1),(A3) and (A4). For a vector $e \in S^2$ write $e = (e_1, e_2, e_3)^T$. Then, for each $s = 1, \ldots, 6$,*

$$\mathcal{M}_s^{-1} = \left\{ e \in S^2 : (-1)^{s-1} e_2 e_3 < 0,\ |e_1| > \max\left\{|e_2|, |e_3|\right\} \right\} \cup (1,0,0)^T,\ s = 1,2,$$

$$\mathcal{M}_s^{-1} = \left\{ e \in S^2 : (-1)^{s-1} e_1 e_3 < 0,\ |e_2| > \max\left\{|e_1|, |e_3|\right\} \right\} \cup (0,1,0)^T,\ s = 3,4,$$

$$\mathcal{M}_s^{-1} = \left\{ e \in S^2 : (-1)^{s-1} e_1 e_2 < 0,\ |e_3| > \max\left\{|e_1|, |e_2|\right\} \right\} \cup (0,0,1)^T,\ s = 5,6.$$

Proof. We only prove this for $s = 1$. The rest follows from the symmetry relations, since $|\mathrm{cof}\,(QU_1Q)e| = |\mathrm{cof}\,U_1\,(Qe)\,|$. First note that $\lambda_{\max}(\mathrm{cof}\,U_1) = \alpha\gamma$ by (A1), so that $e_{\max}(\mathrm{cof}\,U_1) = (1,0,0)^T$. As for the remaining maximal directions, the relevant expressions here are

$$\begin{aligned}
|\mathrm{cof}\,U_s e|^2 &= \alpha^2\gamma^2 e_1^2 + \beta^2 \frac{\alpha^2+\gamma^2}{2}\left(e_2^2+e_3^2\right) + (-1)^{s-1}\beta^2\left(\gamma^2-\alpha^2\right)e_2e_3,\ s=1,2,\\
|\mathrm{cof}\,U_s e|^2 &= \alpha^2\gamma^2 e_2^2 + \beta^2 \frac{\alpha^2+\gamma^2}{2}\left(e_1^2+e_3^2\right) + (-1)^{s-1}\beta^2\left(\gamma^2-\alpha^2\right)e_1e_3,\ s=3,4,\\
|\mathrm{cof}\,U_s e|^2 &= \alpha^2\gamma^2 e_3^2 + \beta^2 \frac{\alpha^2+\gamma^2}{2}\left(e_1^2+e_2^2\right) + (-1)^{s-1}\beta^2\left(\gamma^2-\alpha^2\right)e_1e_2,\ s=5,6.
\end{aligned}$$

First we show that $e \in \mathcal{M}_1^{-1}$, $e \neq e_{\max}(\mathrm{cof}\,U_s)$, with the above representation is necessary and sufficient for $|\mathrm{cof}\,U_1 e| > \max_{i\neq 1}|\mathrm{cof}\,U_i e|$. The condition on the norm of cof U_s is again related to $|\mathrm{cof}\,U_s e| > 1$ and we treat this last. With $A > 0$, $B > 0$ as in the statement,

$$\begin{aligned}
|\mathrm{cof}\,U_1 e|^2 - |\mathrm{cof}\,U_2 e|^2 &= -2Be_2e_3 && (4.6.8)\\
|\mathrm{cof}\,U_1 e|^2 - |\mathrm{cof}\,U_3 e|^2 &= A(e_1^2-e_2^2) - Be_3(e_2-e_1) && (4.6.9)\\
|\mathrm{cof}\,U_1 e|^2 - |\mathrm{cof}\,U_4 e|^2 &= A(e_1^2-e_2^2) - Be_3(e_2+e_1) && (4.6.10)\\
|\mathrm{cof}\,U_1 e|^2 - |\mathrm{cof}\,U_5 e|^2 &= A(e_1^2-e_3^2) - Be_2(e_3-e_1) && (4.6.11)\\
|\mathrm{cof}\,U_1 e|^2 - |\mathrm{cof}\,U_6 e|^2 &= A(e_1^2-e_3^2) - Be_2(e_3+e_1). && (4.6.12)
\end{aligned}$$

Trivially, (4.6.8) is positive if and only if $e_2e_3 < 0$; in particular, $|e_2e_3| = -e_2e_3$. Then,

$$\begin{aligned}
|\mathrm{cof}\,U_1 e|^2 - |\mathrm{cof}\,U_3 e|^2 &= A(|e_1|^2-|e_2|^2) + B|e_3e_2| + Be_3e_1|,\\
|\mathrm{cof}\,U_1 e|^2 - |\mathrm{cof}\,U_4 e|^2 &= A(|e_1|^2-|e_2|^2) + B|e_3e_2| - Be_3e_1|
\end{aligned}$$

and the minimum between (4.6.9) and (4.6.10) is given by

$$A(|e_1|^2 - |e_2|^2) + B|e_3e_2| + B|e_3e_1| = (|e_1| - |e_2|)\left[A|e_1| + A|e_2| - B|e_3|\right]. \quad (4.6.13)$$

Similarly, for (4.6.11) and (4.6.12), we need only interchange the roles of e_2 and e_3 and the minimum is given by

$$A(|e_1|^2 - |e_3|^2) + B|e_2e_3| + B|e_2e_1| = (|e_1| - |e_3|)\left[A|e_1| + A|e_3| - B|e_2|\right]. \quad (4.6.14)$$

Since $A > B$, if $|e_1| > \max\{|e_2|, |e_3|\}$, both (4.6.13) and (4.6.14) are positive and so are (4.6.9)-(4.6.12), establishing sufficiency.

Conversely, suppose that (4.6.9)-(4.6.12) are all positive. In particular,

$$\begin{aligned} (|e_1| - |e_2|)\left[A|e_1| + A|e_2| - B|e_3|\right] &> 0 \quad (4.6.15)\\ (|e_1| - |e_3|)\left[A|e_1| + A|e_3| - B|e_2|\right] &> 0. \quad (4.6.16)\end{aligned}$$

Note that if $|e_1| > |e_3|$,

$$A|e_1| + A|e_2| - B|e_3| > 0$$

since $A > B$ and $e \neq 0$. Then (4.6.15) says that $|e_1| > |e_2|$. Similarly, if $|e_1| > |e_2|$,

$$A|e_1| + A|e_3| - B|e_2| > 0$$

and (4.6.16) says that $|e_1| > |e_3|$, i.e.

$$|e_1| > |e_3| \Leftrightarrow |e_1| > |e_2|.$$

So, if $A|e_1| + A|e_2| - B|e_3| > 0$ or $A|e_1| + A|e_3| - B|e_2| > 0$, by the above argument, $|e_1| > |e_2|$ and $|e_1| > |e_3|$ and we need only worry about the case

$$A|e_1| + A|e_2| - B|e_3| \leq 0 \text{ and } A|e_1| + A|e_3| - B|e_2| \leq 0.$$

But this is impossible since by adding them up, $2A|e_1| + (A - B)(|e_2| + |e_3|) \leq 0$ which is a contradiction since $A > B$.

To finish the proof, we show that for all vectors $e \in \mathcal{M}_1^{-1}$, $e \neq e_{\max}(\operatorname{cof} U_s)$, $|\operatorname{cof} U_1 e|^2 - 1 > 0$. This is a consequence of the constraint $|\operatorname{cof} U_1|^2 \geq 3$. Note that, since $|e| = 1$,

$$\begin{aligned} |\operatorname{cof} U_1 e|^2 - 1 &= \alpha^2\gamma^2 e_1^2 + \beta^2 \frac{\alpha^2 + \gamma^2}{2}\left(e_2^2 + e_3^2\right) + \beta^2\left(\gamma^2 - \alpha^2\right) e_2e_3 - e_1^2 - e_2^2 - e_3^2 \\ &= \left(\alpha^2\gamma^2 - 1\right) e_1^2 + \left(\beta^2\alpha^2 + \beta^2\gamma^2 - 2\right)\frac{e_2^2 + e_3^2}{2} + \beta^2\left(\gamma^2 - \alpha^2\right) e_2e_3\end{aligned}$$

However, $|e_1| > \max\{|e_2|, |e_3|\}$, so that

$$|e_1|^2 > \frac{|e_2|^2 + |e_3|^2}{2}.$$

Then,

$$\begin{aligned} |\operatorname{cof} U_1 e|^2 - 1 &\geq \left(\alpha^2\gamma^2 + \alpha^2\beta^2 + \beta^2\gamma^2 - 3\right)\frac{e_2^2 + e_3^2}{2} + \beta^2\left(\gamma^2 - \alpha^2\right)e_2e_3 \\ &= \left(|\operatorname{cof} U_1|^2 - 3\right)\frac{e_2^2 + e_3^2}{2} + \beta^2\left(\alpha^2 - \gamma^2\right)|e_2e_3| \quad \text{since } e_2e_3 < 0 \\ &> 0 \quad \text{since } |\operatorname{cof} U_1|^2 \geq 3 \text{ and } \alpha > \gamma. \quad \square \end{aligned}$$

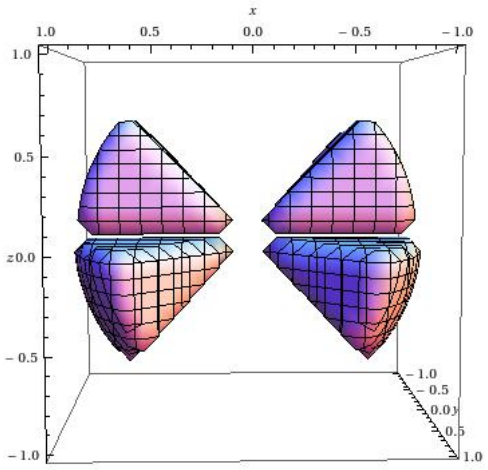

Figure 4.10: All vectors $e \in \mathcal{M}_1^{-1}$ calculated using the lattice parameters of the CuAlNi specimen in Seiner's experiment.

Naturally, one would ask whether we are actually adding any new directions compared to the ones we had already obtained from $\mathcal{M}_s$. The answer is that all the directions in $U_s^{-2}\mathcal{M}_s^{-1}$ are in fact new. To demonstrate this, consider a vector $f = (f_1, f_2, f_3) \in \mathcal{M}_1^{-1}$, say, and write $f \| U_1^2 e$ for some unit vector $e = (e_1, e_2, e_3)^T$ in $U_1^{-2}\mathcal{M}_1^{-1}$. We claim that $e \notin \mathcal{M}_1$, where

$$\mathcal{M}_1 = \left\{e \in S^2 : e_2e_3 \geq 0,\ |e_1| \leq \min\left\{|e_2|, |e_3|\right\}\right\}.$$

This is because,

$$f = U_1^2 e = \left(\beta^2 e_1, \frac{\alpha^2 + \gamma^2}{2}e_2 + \frac{\alpha^2 - \gamma^2}{2}e_3, \frac{\alpha^2 - \gamma^2}{2}e_2 + \frac{\alpha^2 + \gamma^2}{2}e_3\right)$$

must satisfy $f_2 f_3 < 0$ (being in $\mathcal{M}_1^{-1}$), i.e.

$$\frac{\alpha^4 - \gamma^4}{4}\left(e_2^2 + e_3^2\right) + \frac{\alpha^4 + \gamma^4}{2} e_2 e_3 < 0 \tag{4.6.17}$$

However, the first term in the sum is non-negative and so is $\frac{\alpha^4+\gamma^4}{2}$. So, it must be the case that $e_2 e_3 < 0$ and thus, $e \notin \mathcal{M}_1$, i.e. $\mathcal{M}_1$ and $U_1^{-1}\mathcal{M}_1^{-1}$ are disjoint, so that we are genuinely adding new directions. On the other hand, it is clear that if $f \| U_1^2 e_{\max}(\operatorname{cof} U_1)$ is a unit vector, then $f = e_{\max}(\operatorname{cof} U_1) \notin \mathcal{M}_1$.

An important issue is whether these directions can cover the unit sphere and hence exhaust all possible domains or, in terms of the experiment, whether we can deduce that for any bar-shaped specimen, the nucleation can only occur at a corner. The answer is easily seen to be negative as the union of the sets $\mathcal{M}_s$ and $U_s^{-2}\mathcal{M}_s^{-1}$ is a proper subset of the unit sphere. For example, consider $s = 1$ and the unit vector $e = \frac{1}{\sqrt{2}}(0,\ 1,\ -1)^T$. Since $e_2 e_3 = -1 < 0$, it becomes clear that $e \notin \mathcal{M}_1$ and on the other hand,

$$U_1^2 e = \gamma^2 e.$$

But then, $[U_1^2 e]_1 = 0$ and $U_1^2 e \notin \mathcal{M}_1^{-1}$ or, equivalently, $e \notin U_1^{-2}\mathcal{M}_1^{-1}$. We note that writing out an explicit expression for all vectors outside $\mathcal{M}_s \bigcup U_s^{-2}\mathcal{M}_s^{-1}$ becomes a tedious task and, instead, we see these numerically for $s = 1$ and the lattice parameters of Seiner's specimen in Fig. 4.11 below.

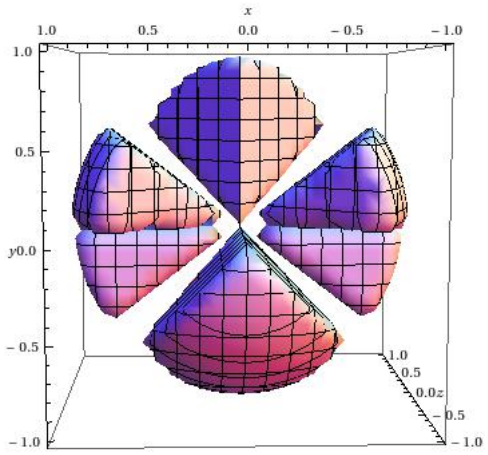

Figure 4.11: All vectors $e \in \mathcal{M}_1 \cup U_1^{-2}\mathcal{M}_1$ calculated using the lattice parameters of the CuAlNi specimen in Seiner's experiment.

However, in the case of a face, this does not reveal much. The fact that the above directions do not cover the unit sphere, does not necessarily imply that the normal

vectors to these directions do not cover the sphere as well. Moreover, it would be more convenient to know all the possible normals to the faces that the method can decide on rather than the possible vectors lying on the face. The rest of this section aims to do precisely that. Let

$$\begin{aligned} \mathcal{N}_s &= \{n \in S^2 : \exists e \in \mathcal{M}_s \text{ with } e \cdot n = 0\} \quad \text{and} \\ \mathcal{N}_s^{-1} &= \{n \in S^2 : \exists e \in \mathcal{M}_s^{-1} \text{ with } e \cdot n = 0\}. \end{aligned}$$

The set we are then interested in is $\mathcal{N}_s \cup U_s^2 \mathcal{N}_s^{-1}$. To see this, let $n \in \mathcal{N}_s \cup U_s^2 \mathcal{N}_s^{-1}$.

- If $n \in \mathcal{N}_s$ there exists $e \in \mathcal{M}_s$ such that $e \cdot n = 0$ and we can apply the method to any face with normal n as there will exist a maximal direction e which lies on the face.
- On the other hand, if $n \in U_s^2 \mathcal{N}_s^{-1}$ then there exists $m \in \mathcal{N}_s^{-1}$ such that $n = U_s^2 m$. Since $m \in \mathcal{N}_s^{-1}$ there exists $e \in \mathcal{M}_s^{-1}$ such that $e \cdot m = 0$. Once again, we can then apply the method to any face with normal n as

  $$U_s^{-2} e \cdot n = U_s^{-2} e \cdot U_s^2 m = e \cdot m = 0,$$

  i.e. $U_s^{-2} e$ lies on the face with normal n and e is a maximal direction for U_s^{-1}.

Let us characterize these sets and see whether these can exhaust the unit sphere, i.e. whether our methods can be applied to all possible faces.

Lemma 4.6.3. *Under the assumptions (A1) and (A2) on the lattice parameters and for each* $s = 1, \ldots, 6$

$$\mathcal{N}_s = \left\{ n \in S^2 : (-1)^{s-1} n_2 n_3 \leq 0 \text{ or } |n_1| \geq |n_2| + |n_3| \right\}, \quad s = 1, 2$$

$$\mathcal{N}_s = \left\{ n \in S^2 : (-1)^{s-1} n_1 n_3 \leq 0 \text{ or } |n_2| \geq |n_1| + |n_3| \right\}, \quad s = 3, 4$$

$$\mathcal{N}_s = \left\{ n \in S^2 : (-1)^{s-1} n_1 n_2 \leq 0 \text{ or } |n_3| \geq |n_1| + |n_2| \right\}, \quad s = 5, 6.$$

Proof. We only prove this for $s = 1$. The rest follow easily due to symmetry.
Sufficiency. We show that if a vector $n \in S^2$ has the above representation then there exists $e \in \mathcal{M}_1$ such that $e \cdot n = 0$.

Suppose that n satisfies $n_2 n_3 \leq 0$. If $n_2 = n_3 = 0$ then $n = \pm (1, 0, 0)^T$ and $e = (0, 1, 0)^T \in \mathcal{M}_1$ satisfies $e \cdot n = 0$. So, assume that $|n_2| + |n_3| \neq 0$ and let $e \in \mathcal{M}_1$ be the vector $\frac{1}{\rho}(0, |n_3|, |n_2|)$ where $\rho > 0$ is a constant making e of unit length. Then,

$$\rho e \cdot n = n_2 |n_3| + n_3 |n_2| = 0$$

as either one of n_2, n_3 is zero or they have opposite sign. On the other hand, suppose that $|n_1| \geq |n_2|+|n_3|$. Clearly, we may additionally assume that $n_2 n_3 > 0$ as otherwise it reduces to the previous case. Note that if $e = (e_1, e_2, e_3)^T$ satisfies $e \cdot n = 0$ then

$$f \cdot (n_1, -n_2, -n_3)^T = 0$$

for $f = (e_1, -e_2, -e_3)^T$ and if $e \in \mathcal{M}_1$ so is f. Hence, without loss of generality, we may assume that $n_2 > 0$ and $n_3 > 0$. Then,

$$|n_2| + |n_3| = n_2 + n_3 \quad \text{and} \quad \frac{|n_2 + n_3|}{|n_1|} \leq 1$$

by assumption. So, let $e \in \mathcal{M}_1$ be the vector $\frac{1}{\rho}\left(-\left(n_2 + n_3\right)/n_1, 1, 1\right)^T$, where $\rho > 0$ forces $|e| = 1$, to get

$$\rho e \cdot n = -\left(n_2 + n_3\right) + n_2 + n_3 = 0$$

and sufficiency is established.
Necessity. To reach a contradiction, suppose that $n \cdot e = 0$ for some $e \in \mathcal{M}_1$ but

$$n_2 n_3 > 0 \quad \text{and} \quad |n_1| < |n_2| + |n_3|.$$

Since $n_2 n_3 > 0$ and $e_2 e_3 \geq 0$, it must be the case that $\left(n_2 e_2\right)\left(n_3 e_3\right) \geq 0$ and hence

$$|n_2 e_2 + n_3 e_3| = |n_2 e_2| + |n_3 e_3|. \tag{4.6.18}$$

If $n_1 e_1 + n_2 e_2 + n_3 e_3 = 0$,

$$\begin{aligned} |n_1 e_1| &= |n_2 e_2| + |n_3 e_3| \ \text{ by (4.6.18)} \\ &\geq \min\{|e_2|, |e_3|\}\left(|n_2| + |n_3|\right) \\ &\geq |e_1|\left(|n_2| + |n_3|\right), \end{aligned}$$

so that $|n_1| \geq |n_2|+|n_3|$, a contradiction proving necessity. Note that for the remaining variants

$$\begin{aligned} n \in \mathcal{N}_s &\Leftrightarrow \exists e \in \mathcal{M}_s \text{ such that } \quad e \cdot n = 0 \\ &\Leftrightarrow \exists f \in \mathcal{M}_1 \text{ such that } \quad Qf \cdot n = 0 \text{ where } QU_1Q = U_s \\ &\Leftrightarrow Qn \in \mathcal{N}_1 \end{aligned}$$

and the result follows easily. □

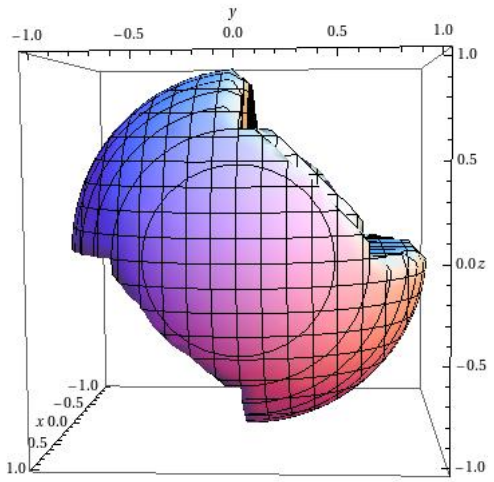

Figure 4.12: All vectors $n \in \mathcal{N}_1$ calculated using the lattice parameters of the CuAlNi specimen in Seiner's experiment.

Lemma 4.6.4. *Under the assumptions (A1), (A3) and (A4) on the lattice parameters*

$$\begin{aligned}
\mathcal{N}_s^{-1} = \; & \left\{n \in S^2 : (-1)^{s-1} n_2 n_3 \leq 0 \text{ and } |n_1| < |n_2| + |n_3|\right\} \\
& \bigcup \left\{n \in S^2 : (-1)^{s-1} n_2 n_3 \geq 0 \text{ and } |n_1| < \max\{|n_2|,\ |n_3|\}\right\} \\
& \bigcup \{n \in S^2 : n \cdot (1,0,0)^T = 0\}, \qquad s = 1, 2, \\
\mathcal{N}_s^{-1} = \; & \left\{n \in S^2 : (-1)^{s-1} n_1 n_3 \leq 0 \text{ and } |n_2| < |n_1| + |n_3|\right\} \\
& \bigcup \left\{n \in S^2 : (-1)^{s-1} n_1 n_3 \geq 0 \text{ and } |n_2| < \max\{|n_1|,\ |n_3|\}\right\} \\
& \bigcup \{n \in S^2 : n \cdot (0,1,0)^T = 0\}, \qquad s = 3, 4, \\
\mathcal{N}_s^{-1} = \; & \left\{n \in S^2 : (-1)^{s-1} n_1 n_2 \leq 0 \text{ and } |n_3| < |n_1| + |n_2|\right\} \\
& \bigcup \left\{n \in S^2 : (-1)^{s-1} n_1 n_2 \geq 0 \text{ and } |n_3| < \max\{|n_1|, |n_2|\}\right\}, \\
& \bigcup \{n \in S^2 : n \cdot (0,0,1)^T = 0\}, \qquad s = 5, 6.
\end{aligned}$$

Proof. We only show this for $s = 1$ and the rest follows easily due to symmetry. Note that the plane $\{n \in S^2 : n \cdot (1,0,0)^T = 0\}$ corresponds precisely to the set of vectors perpendicular to $e_{\max}(\operatorname{cof} U_1)$ and, in the proof below, we only deal with the remaining maximal directions.

Sufficiency. Assume that $n \in S^2$ has the representation above; we wish to conclude

that $e \cdot n = 0$ for some $e \in \mathcal{M}_1^{-1}$. Firstly, note that n_2 and n_3 cannot both be zero and we may also assume that $n_1 \neq 0$ as otherwise

$$n \cdot (1, 0, 0)^T = 0.$$

Next, suppose that either $n_2 = 0$ or $n_3 = 0$; without loss of generality assume that $n_3 = 0$. Then, from the above representations, it must be the case that $|n_1| < |n_2|$ so that the vector $e = \frac{1}{\rho}(n_2, -n_1, n_1)$ is an element of $\mathcal{M}_1^{-1}$ ($\rho > 0$ forces $|e| = 1$) and satisfies

$$\rho e \cdot n = n_2 n_1 - n_1 n_2 = 0.$$

Hence, we may assume that $n_1 n_2 n_3 \neq 0$. Let us consider the case $n_2 n_3 < 0$ and $|n_1| < |n_2| + |n_3|$. Since $n_2 n_3 < 0$ we infer that

$$|n_2 - n_3| = |n_2| + |n_3|,$$

i.e. $|n_2 - n_3| > |n_1|$ and the normalized vector $\frac{1}{\rho}(n_2 - n_3, -n_1, n_1)^T$ is an element of $\mathcal{M}_1^{-1}$ satisfying

$$\frac{1}{\rho}(n_2 - n_3, -n_1, n_1)^T \cdot n = 0.$$

Next let $n_2 n_3 > 0$ and $|n_1| < \max\{|n_2|, |n_3|\}$ - this case is seemingly more elaborate. Without loss of generality, suppose that $|n_3| \geq |n_2|$ and let $\alpha \geq 1$ be any number such that

$$\alpha \frac{|n_3|}{|n_1|} - \frac{|n_2|}{|n_1|} > \alpha.$$

The existence of α is trivial since $|n_3| > |n_1|$. With $\rho > 0$ a normalizing factor, define the vector

$$e = \frac{1}{\rho}(\alpha n_3 - n_2, n_1, -\alpha n_1)^T.$$

Clealry, $e \cdot n = 0$ and we are left to show that $e \in \mathcal{M}_1^{-1}$. But $e_2 e_3 = -\alpha n_1^2 < 0$ since we are assuming that $n_1 \neq 0$ and

$$\begin{aligned} |e_1| &= |\alpha n_3 - n_2| \\ &= \alpha |n_3| - |n_2|, \quad \text{since } n_2 n_3 > 0 \\ &> \alpha |n_1|, \quad \text{by assumption} \\ &= \max\{|e_2|, |e_3|\} \quad \text{since } \alpha \geq 1. \end{aligned}$$

This completes the proof of sufficiency.

Necessity. Assume that $n \in S^2$ and that there exists $e \in \mathcal{M}_1^{-1}$ such that $e \cdot n = 0$. Then,

$$|n_1 e_1| = |n_2 e_2 + n_3 e_3| \tag{4.6.19}$$

and we distinguish between two cases depending on the sign of n_2n_3. Note that since $e \in \mathcal{M}_1^{-1}$, it must be the case that $e_2e_3 < 0$.

If $n_2n_3 \leq 0$, $(n_2e_2)\,(n_3e_3) \geq 0$ and $|n_2e_2 + n_3e_3| = |n_2e_2| + |n_3e_3|$, i.e. by (4.6.19),

$$\begin{aligned} |n_1e_1| &= |n_2e_2| + |n_3e_3| \\ &\leq \max\{|e_2|, |e_3|\}\,(|n_2| + |n_3|) \\ &< |e_1|\,(|n_2| + |n_3|) \end{aligned}$$

since $e \in \mathcal{M}_1^{-1}$. Now $e_1 \neq 0$ as otherwise, e belonging to $\mathcal{M}_1^{-1}$, forces $e_2 = e_3 = 0$. Therefore, $|n_1| < |n_2| + |n_3|$ and this case is finished.

On the other hand, if $n_2n_3 \geq 0$ we get that $(n_2e_2)\,(n_3e_3) \leq 0$ and consequently, $|n_1e_1| = ||n_2e_2| - |n_3e_3||$. Then, by (4.6.19),

$$\begin{aligned} |n_1e_1| &= ||n_2e_2| - |n_3e_3|| \\ &\leq \max\{|n_2e_2|, |n_3e_3|\} \\ &< |e_1| \max\{|n_2|, |n_3|\} \end{aligned}$$

since $e \in \mathcal{M}_1^{-1}$. But $e_1 \neq 0$ now says that $|n_1| < \max\{|n_2|, |n_3|\}$ and the proof is complete. □

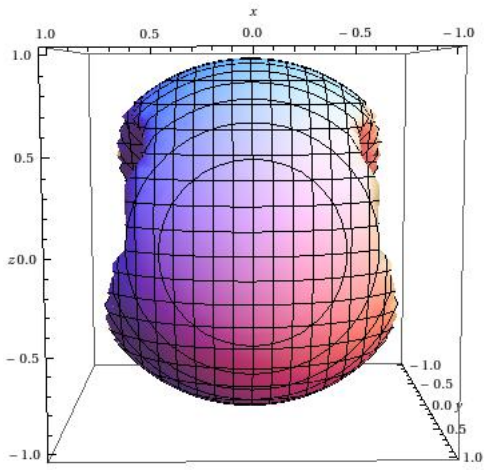

Figure 4.13: All vectors $n \in \mathcal{N}_1^{-1}$ calculated using the lattice parameters of the CuAlNi specimen in Seiner's experiment.

As described already, we are interested in the set $\mathcal{N}_s \cup U_s^2\mathcal{N}_s^{-1}$ and, in particular, we are interested in whether it can cover the entire unit sphere. If so, then our result regarding faces will not depend on the orientation of the domain; however, the answer is negative.

Lemma 4.6.5. *Suppose that a unit vector n satisfies $n \notin \mathcal{N}_s \cup \mathcal{N}_s^{-1}$. Then,*

$$U_s^2 n \notin \mathcal{N}_s \cup U_s^2 \mathcal{N}_s^{-1}.$$

In particular, there exists $m \in S^2$ such that $m \notin \mathcal{N}_s \cup U_s^2 \mathcal{N}_s^{-1}$.

Proof. We only prove this for $s = 1$ and the rest are identical. Let us first show that

$$n \notin \mathcal{N}_1 \Rightarrow U_1^2 n \notin \mathcal{N}_1. \tag{4.6.20}$$

Let $n \notin \mathcal{N}_1$ so that $n_2 n_3 > 0$ and $|n_1| < |n_2| + |n_3|$. Then,

$$U_1^2 n = \left(\beta^2 n_1,\ \frac{\alpha^2 + \gamma^2}{2} n_2 + \frac{\alpha^2 - \gamma^2}{2} n_3,\ \frac{\alpha^2 - \gamma^2}{2} n_2 + \frac{\alpha^2 + \gamma^2}{2} n_3 \right)$$

and

$$\left[U_1^2 n\right]_2 \left[U_1^2 n\right]_3 = \frac{\alpha^4 - \gamma^4}{4} \left(n_2^2 + n_3^2\right) + \frac{\alpha^4 + \gamma^4}{2} n_2 n_3 > 0$$

since $n_2 n_3 > 0$ and $\alpha > \gamma > 0$. Moreover,

$$\begin{aligned}
|\left[U_1^2 n\right]_1| &= \beta^2 |n_1| \\
&< \alpha^2 \left(|n_2| + |n_3|\right) \quad \text{as } n \notin \mathcal{N}_1 \text{ and } \beta \leq \alpha \\
&= \alpha^2 |n_2 + n_3| \quad \text{since } n_2 n_3 > 0 \\
&= \left| \left(\frac{\alpha^2 + \gamma^2}{2} n_2 + \frac{\alpha^2 - \gamma^2}{2} n_3 \right) + \left(\frac{\alpha^2 - \gamma^2}{2} n_2 + \frac{\alpha^2 + \gamma^2}{2} n_3 \right) \right| \\
&= |\left[U_1^2 n\right]_2 + \left[U_1^2 n\right]_3| = |\left[U_1^2 n\right]_2| + |\left[U_1^2 n\right]_3|
\end{aligned}$$

as $[U_1^2 n]_2 [U_1^2 n]_3 > 0$ and (4.6.20) is established. Then,

$$n \notin \mathcal{N}_1 \cup \mathcal{N}_1^{-1} \Rightarrow U_1^2 n \notin \mathcal{N}_1 \cup U_1^2 \mathcal{N}_1^{-1}.$$

Finally, it is easy to check that whenever $n = (n_1, n_2, n_3)^T$ satisfies

$$n_2 n_3 > 0 \text{ and } \max\{|n_2|, |n_3|\} \leq |n_1| < |n_2| + |n_3|,$$

then $n \notin \mathcal{N}_1 \cup \mathcal{N}_1^{-1}$, i.e. $m = U_1^2 n \notin \mathcal{N}_1 \cup U_1^2 \mathcal{N}_1^{-1}$. □

The edges of the CuAlNi specimen in Seiner's experiment were oriented very nearly along the principal directions of the cubic austenite, i.e. along $(1,0,0)^T$, $(0,1,0)^T$ and $(0,0,1)^T$ and our result becomes applicable for any $s = 1, \ldots, 6$. In particular, suppose that the mechanically stabilized variant of martensite is U_1.

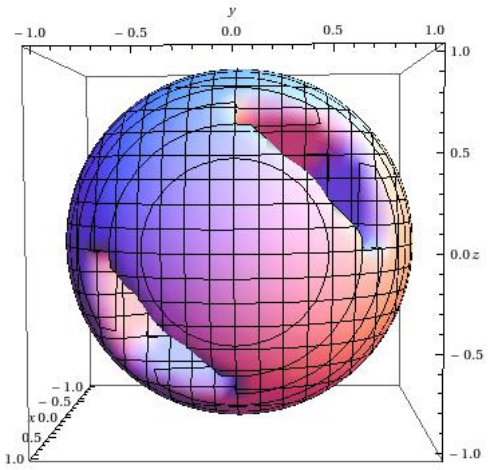

Figure 4.14: All vectors $n \in \mathcal{N}_1 \cup U_1^2 \mathcal{N}_1^{-1}$ calculated using the lattice parameters of the CuAlNi specimen in Seiner's experiment.

As remarked already, the lattice parameters of Seiner's specimen satisfy assumptions (A1)-(A4) and the representations of $\mathcal{M}_1$ and $\mathcal{M}_1^{-1}$ given in Lemma 4.6.1 and Lemma 4.6.2 hold. In particular, the maximal directions for U_1 and U_1^{-1} are

$$\begin{aligned} \mathcal{M}_1 &= \left\{ e \in S^2 : e_2 e_3 \geq 0, \ \ |e_1| \leq \min\left\{|e_2|, |e_3|\right\} \right\}, \\ \mathcal{M}_1^{-1} &= \left\{ e \in S^2 : e_2 e_3 < 0, \ \ |e_1| > \max\left\{|e_2|, |e_3|\right\} \right\} \cup (1,0,0)^T. \end{aligned}$$

But the vectors $(0,1,0)^T$, $(0,0,1)^T$ belong to $\mathcal{M}_1$ and the vector $(1,0,0)^T$ is an element of $\mathcal{M}_1^{-1}$ and, being an eigenvector of U_1, it is also an element of $U_1^{-2}\mathcal{M}_1^{-1}$. Therefore, one can cover any nucleation region B_f on a face or B_e at an edge and our main result applies, i.e. for Seiner's CuAlNi specimen, nucleation can only occur at a corner.

Concluding remarks. It is worth mentioning that the set of maximal directions - as calculated in Lemma 4.6.2, say for $s = 1$, (similarly for the rest) - is the interior of the set

$$\left\{ e \in S^2 : e_2 e_3 \leq 0, \ |e_1| \geq \max\left\{|e_2|, |e_3|\right\} \right\},$$

where strict inequalities have been replaced with inequalities. In particular, we note that the above set contains the vector $e_{\max}(\operatorname{cof} U_1)$. Then, defining the set

$$\bar{\mathcal{M}}_s^{-1} := \left\{ e \in S^2 : |\operatorname{cof} U_s e| = \max_i \left\{|\operatorname{cof} U_i e|, 1\right\} \right\}$$

it is possible to use a continuity argument and deduce the quasiconvexity conditions at any face with normal perpendicular to, or any edge in the direction of, a vector in

$U_s^{-2}\bar{\mathcal{M}}_s^{-1}$. For example, suppose that a face has normal perpendicular to a vector in $U_s^{-2}\bar{\mathcal{M}}_s^{-1}$ and let $x_0 \in B_f$. Consider a plane through the point x_0, whose boundary is contained in the prescribed boundary of B_f, $\partial B_f \cap \Omega$, and whose normal, n' say, is perpendicular to a vector in $U_s^{-2}\mathcal{M}_s^{-1}$. Such a plane always exists as the vectors in $\mathcal{M}_s^{-1}$ are dense in $\bar{\mathcal{M}}_s^{-1}$. Then, we may restrict attention to the half-ball

$$B_f^{'} := \{x \in B(0,1) : x \cdot n' < 0\}$$

and view the plane $\{x \in B(0,1) : x \cdot n' = 0\}$ as part of a face with normal perpendicular to a vector in $U_s^{-2}\mathcal{M}_s^{-1}$. We may then repeat our arguments for the new set $B_f^{'}$ to deduce that $z(x) = U_s x$ for all $x \in \overline{B_f^{'}}$ and, in particular, $z(x_0) = U_s x_0$. But $x_0 \in B_f$ is arbitrary so that the same holds for all $x \in B_f$. The case of an edge is similar. However, it has not been possible to show that the set $\mathcal{M}_s^{-1}$ is the interior of $\bar{\mathcal{M}}_s^{-1}$ simply by exlpoiting the general structure of the martensitic and austenitic energy wells, i.e. prior to computing the sets $\mathcal{M}_s^{-1}$, $\bar{\mathcal{M}}_s^{-1}$ explicitly for specific transformations.

Also, we note that for any $s = 1, \ldots, 6$ and appropriate lattice parameters, the set $\mathcal{M}_s \cup U_s^{-2}\mathcal{M}_s^{-1}$ contains several sets of three linearly independent directions and our methods apply to a variety of parallelepipeds with edges along these directions. In fact, the method can also be extended to any convex polyhedron with edges along directions in $\mathcal{M}_s \cup U_s^{-2}\mathcal{M}_s^{-1}$. However, $\mathcal{M}_s \cup U_s^{-2}\mathcal{M}_s^{-1}$ does not exhaust the unit sphere. Hence our result leaves open the possibility that for differently cut specimens nucleation could occur at a face or an edge.

It should also be mentioned that our analysis would carry forward even if we departed from the exact form of the energy wells of the cubic-to-orthorhombic transition. This exact form of the set K is only relevant for the calculation of the maximal directions and our analysis remains applicable for any number of martensitic variants and any other transformation. In fact, for our analysis to apply we need only require that

$$K = SO(3) \cup \bigcup_{i=1}^{N} SO(3)\, U_i$$

is such that the variants U_i are symmetry related and satisfy the constraint on the determinant and the largest eigenvalue of the cofactor matrix. Of course, this is not necessarily the case for the construction at a corner.

We note that the argument of maximal directions reduces to measuring the length of lines; having fixed the endpoints of the deformed segments, the definition of a maximal direction ensures that its length cannot be greater than the length of the straight line joining the endpoints and, thus, it must precisely be that straight line. It is

worth remarking here that similar ideas are also used in Sivaloganathan and Spector [129] to show that for an incompressible cylinder under uniaxial extension, the unique minimizer is a homogeneous, isoaxial deformation (under additional constitutive hypotheses on the stored-energy function). Similarly, the cofactor matrix relates areas and one might think of an argument in which, having fixed the boundary values of a deformed planar section, we can use the quasiconvexity of the cofactors to compare areas and show that the plane must have deformed linearly. We mention, however, that such a method allows one to deduce the quasiconvexity condition on faces with normals in $\mathcal{M}_s^{-1}$ and does not seem applicable to edges. In particular, since $\mathcal{M}_s^{-1} \subset \mathcal{N}_s$, we would add no new faces and one would not be able cover Seiner's specimen. Nevertheless, other methods based on the cofactor matrix may be possible and it is worth investigating.

Also, as we alluded to in the introduction to this chapter, there are connections between our work and that of Grabovsky and Mengesha [70]. In particular, Grabovsky and Mengesha base their sufficiency proof on a decomposition lemma (see also [63, 92]) which splits arbitrary variations of the dependent variable into a strong and a weak part. The core of their proof lies in showing that these two parts act on the functional independently. In particular, they show that the action of the weak part can be described in terms of the second variation, whereas, the action of the strong part is 'localized', in the sense that it can be described as a superposition of 'Weierstrass needles'. Then, it is the (uniform) positivity of the second variation and the (uniform) quasiconvexity conditions, respectively, that prevent the weak and the strong part from decreasing the functional.

In our analysis, we have restricted attention to localized variations corresponding to the localized nucleation of austenite. Nevertheless, if we depart from our simplified setting of the singular energy, one expects to be able to prove something stronger using the machinery of Grabovsky and Mengesha; in particular, one might be able to show that whenever ν is a $W^{1,\infty}$ gradient Young measure such that $\mathrm{d}\left(\delta_{U_s}, \nu\right)$ is sufficiently small and $I\left(\nu\right) < I\left(\delta_{U_s}\right)$, then ν must necessarily involve nucleation at a corner. Here, the distance $\mathrm{d}\left(\cdot, \cdot\right)$, given by (4.4.7), comes from the metrization of the weak$*$ topology in $L^{\infty}_{w^*}\left(\Omega, \mathcal{M}\left(M^{3\times 3}\right)\right)$. This is another direction worth investigating further.

Concluding our final remarks, we mention that the same nucleation mechanism was also observed by Seiner for a CuAlNi specimen which was mechanically stabilized as a compound twin. We recall that, for typical lattice parameters, compound twins are also unable to form directly compatible interfaces with austenite so that the

mechanical stabilization effect comes into play. We note that our methods, presented in this chapter, may be applicable to this case as well.

Lastly, similar situations in which the incompatibility of gradients results in hysteresis have been documented before in other contexts, e.g. Ball, Chu and James [15]. There, though in a different way, the mathematical analysis argues that despite the existence of a state with lower energy than a certain martensitic variant, it is necessarily geometrically incompatible with it, giving rise to an energy barrier which keeps the specific martensitic variant stable. In general, in the context of microstructure formation, the incompatibility of gradients gives rise to very rich and interesting phenomena and the observations in Chapter 3 provide such an example.

Appendix A

Symmetry relations between the cubic-to-orthorhombic variants

The following relations between the cubic-to-orthorhombic variants can be found in Hane [72].

	1	Q_1	Q_2	Q_3	Q_4	Q_5	Q_6	Q_7	Q_8	Q_9	Q_{10}	Q_{11}
U_1	1	3	5	6	4	5	4	6	3	4	3	6
U_2	2	4	6	5	3	6	3	5	4	3	4	5
U_3	3	5	1	2	5	2	6	1	6	2	1	3
U_4	4	6	2	1	6	1	5	2	5	1	2	4
U_5	5	1	3	3	2	4	1	4	2	5	5	2
U_6	6	2	4	4	1	3	2	3	1	6	6	1
	Q_{12}	Q_{13}	Q_{14}	Q_{15}	Q_{16}	Q_{17}	Q_{18}	Q_{19}	Q_{20}	Q_{21}	Q_{22}	Q_{23}
U_1	5	1	1	1	2	2	2	2	5	6	4	3
U_2	6	2	2	2	1	1	1	1	6	5	3	4
U_3	3	6	5	4	3	4	6	5	4	4	1	2
U_4	4	5	6	3	4	3	5	6	3	3	2	1
U_5	1	4	3	6	6	5	3	4	2	1	6	6
U_6	2	3	4	5	5	6	4	3	1	2	5	5

Table A.1: Symmetry relations amongst the variants of a cubic-to-orthorhombic transformation, where the rotations of the cubic Laue group are given below.

As an example of how Table A.1 is meant to be understood, consider the variant U_3 and the rotation Q_{14}; the number corresponding to these is 5. Then, the table says that $Q_{14}U_3Q_{14}^T = U_5$.

Cubic Laue group

Below the orthonormal vectors $\{i_1, i_2, i_3\}$ correspond to the cubic basis and $Q = Q[\phi, e]$ denotes a rotation by angle ϕ about the axis e.

$$
\begin{aligned}
\mathbf{1} &= i_1 \otimes i_1 + i_2 \otimes i_2 + i_3 \otimes i_3 \\
Q_1 &= Q[2\pi/3, i_1 + i_2 + i_3] = i_1 \otimes i_3 + i_2 \otimes i_1 + i_3 \otimes i_2 \\
Q_2 &= Q[-2\pi/3, i_1 + i_2 + i_3] = i_1 \otimes i_2 + i_2 \otimes i_3 + i_3 \otimes i_1 \\
Q_3 &= Q[2\pi/3, -i_1 + i_2 + i_3] = -i_1 \otimes i_2 + i_2 \otimes i_3 - i_3 \otimes i_1 \\
Q_4 &= Q[-2\pi/3, -i_1 + i_2 + i_3] = -i_1 \otimes i_3 - i_2 \otimes i_1 + i_3 \otimes i_2 \\
Q_5 &= Q[2\pi/3, i_1 - i_2 + i_3] = -i_1 \otimes i_2 - i_2 \otimes i_3 + i_3 \otimes i_1 \\
Q_6 &= Q[-2\pi/3, i_1 - i_2 + i_3] = i_1 \otimes i_3 - i_2 \otimes i_1 - i_3 \otimes i_2 \\
Q_7 &= Q[2\pi/3, i_1 + i_2 - i_3] = i_1 \otimes i_2 - i_2 \otimes i_3 - i_3 \otimes i_1 \\
Q_8 &= Q[-2\pi/3, i_1 + i_2 - i_3] = -i_1 \otimes i_3 + i_2 \otimes i_1 - i_3 \otimes i_2 \\
Q_9 &= Q[\pi, i_1 + i_2] = i_1 \otimes i_2 + i_2 \otimes i_1 - i_3 \otimes i_3 \\
Q_{10} &= Q[\pi, i_1 - i_2] = -i_1 \otimes i_2 - i_2 \otimes i_1 - i_3 \otimes i_3 \\
Q_{11} &= Q[\pi, i_1 + i_3] = i_1 \otimes i_3 - i_2 \otimes i_2 + i_3 \otimes i_1 \\
Q_{12} &= Q[\pi, i_1 - i_3] = -i_1 \otimes i_3 - i_2 \otimes i_2 - i_3 \otimes i_1 \\
Q_{13} &= Q[\pi, i_2 + i_3] = -i_1 \otimes i_1 + i_2 \otimes i_3 + i_3 \otimes i_2 \\
Q_{14} &= Q[\pi, i_2 - i_3] = -i_1 \otimes i_1 - i_2 \otimes i_3 - i_3 \otimes i_2 \\
Q_{15} &= Q[\pi, i_1] = i_1 \otimes i_1 - i_2 \otimes i_2 - i_3 \otimes i_3 \\
Q_{16} &= Q[\pi, i_2] = -i_1 \otimes i_1 + i_2 \otimes i_2 - i_3 \otimes i_3 \\
Q_{17} &= Q[\pi, i_3] = -i_1 \otimes i_1 - i_2 \otimes i_2 + i_3 \otimes i_3 \\
Q_{18} &= Q[\pi/2, i_1] = i_1 \otimes i_1 - i_2 \otimes i_3 + i_3 \otimes i_2 \\
Q_{19} &= Q[-\pi/2, i_1] = i_1 \otimes i_1 + i_2 \otimes i_3 - i_3 \otimes i_2 \\
Q_{20} &= Q[\pi/2, i_2] = i_1 \otimes i_3 + i_2 \otimes i_2 - i_3 \otimes i_1 \\
Q_{21} &= Q[-\pi/2, i_2] = -i_1 \otimes i_3 + i_2 \otimes i_2 + i_3 \otimes i_1 \\
Q_{22} &= Q[\pi/2, i_3] = -i_1 \otimes i_2 + i_2 \otimes i_1 + i_3 \otimes i_3 \\
Q_{23} &= Q[-\pi/2, i_3] = i_1 \otimes i_2 - i_2 \otimes i_1 + i_3 \otimes i_3
\end{aligned}
$$

Appendix B

Twin and habit plane elements for CuAlNi

In this Appendix we give the details of the proof of Lemma 4.5.3. In order to do so, we need to summarize the results concerning the twin and habit plane shears and normals for all variant pairs (l, s) in the cubic-to-orthorhombic transition of CuAlNi, i.e. the vectors a, n (twin plane) and the vectors b, m (habit plane) such that

$$QU_l - U_s = a \otimes n, \tag{B.0.1}$$

$$U_s + \lambda a \otimes n = R\left(\mathbf{1} + b \otimes m\right). \tag{B.0.2}$$

We use the following notation:

a^I, n^I : Type-I twin plane shear and normal respectively;

a^{II}, n^{II} : Type-II twin plane shear and normal respectively;

b_1^+, m_1^+ : habit plane shear and normal respectively, using the Type-II twinning elements a^{II}, n^{II}, $\kappa = +1$ in the solutions given by Theorem 2.2.3 and volume fraction $\lambda \in (0, 1/2)$;

b_1^-, m_1^- : habit plane shear and normal respectively, using the Type-II twinning elements a^{II}, n^{II}, $\kappa = -1$ in the solutions given by Theorem 2.2.3 and volume fraction $\lambda \in (0, 1/2)$;

b_2^+, m_2^+ : habit plane shear and normal respectively, using the Type-II twinning elements a^{II}, n^{II}, $\kappa = +1$ in the solutions given by Theorem 2.2.3 and volume fraction $\lambda \in (1/2, 1)$;

b_2^-, m_2^- : habit plane shear and normal respectively, using the Type-II twinning elements a^{II}, n^{II}, $\kappa = -1$ in the solutions given by Theorem 2.2.3 and volume fraction $\lambda \in (1/2, 1)$.

The Type-I and Type-II twinning elements can also be found in Hane [72]. The algebra for the habit plane elements of the austenite - Type-II twinned martensite interfaces becomes too involved and we calculate the components numerically using *Mathematica*. The procedure involved in the numerical calculation simply verifies the hypotheses of Theorem 2.2.12 and calculates the solutions directly by Theorem 2.2.3. We note that the lattice parameters of Seiner's specimen are given by $\alpha = 1.06372$, $\beta = 0.91542$ and $\gamma = 1.02368$. For these parameters and the Type-II twinning elements of any variant pair, $\lambda^* = 0.300782 \in (0, 1/2)$ and

$$\delta = -2.37742 < -2, \;\; \eta = 0.0091991 > 0,$$

where λ^*, δ, η are as in Theorem 2.2.12, i.e. for each variant pair there are four distinct solutions to the habit plane equation using the Type-II twinning elements as above.

In this Appendix, we do not present the twin plane elements for compound twins as, for our lattice parameters, these cannot form compatible interfaces with austenite (see Bhattacharya [29] for the appropriate conditions on the lattice parameters allowing for austenite - compound twinned martensite interfaces) and hence cannot be used for the construction in Lemma 4.5.3 of the microstructure reducing the energy at a corner. Also, we do not give the habit plane elements for austenite - Type-I twinned martensite interfaces as the Type-I twin planes belong to the family of crystallographically equivalent planes $\{110\}$ and the corresponding twin plane normals are perpendicular to the edges of Seiner's specimen (see Table B.1), i.e. these cannot be used for our construction in Lemma 4.5.3 either.

Table B.1 gives the Type-I twin plane normal n^I and twin plane shear a^I for the variant pair (l, s). The components u_1, u_2, u_3 of the shears a^I are given by

$$\begin{pmatrix} u_1 \\ u_2 \\ u_3 \end{pmatrix} = \frac{\sqrt{2}}{2\alpha^2\gamma^2 + \beta^2(\alpha^2+\gamma^2)} \begin{pmatrix} \frac{\alpha+\gamma}{2}\left(4\alpha\gamma\beta^2 - 2\alpha^2\gamma^2 - \beta^2(\alpha^2+\gamma^2)\right) \\ \beta\left(\beta^2(\alpha^2+\gamma^2) - 2\alpha^2\gamma^2\right) \\ \frac{\gamma-\alpha}{2}\left(4\alpha\gamma\beta^2 + 2\alpha^2\gamma^2 + \beta^2(\alpha^2+\gamma^2)\right) \end{pmatrix}.$$

Table B.2 gives the Type-II twin plane normal n^{II} and twin plane shear a^{II} for the variant pair (l, s). The components t_1, t_2 of the normals n^{II} and v_1, v_2, v_3 of the shears a^{II} are given by

$$\begin{aligned} \begin{pmatrix} t_1 \\ t_2 \end{pmatrix} &= \frac{1}{\sqrt{8\beta^2(\beta^2-\alpha^2-\gamma^2) + 6\alpha^4 - 4\alpha^2\gamma^2 + 6\gamma^2}} \begin{pmatrix} 2\beta^2 - \alpha^2 - \gamma^2 \\ 2(\gamma^2 - \alpha^2) \end{pmatrix}, \\ \begin{pmatrix} v_1 \\ v_2 \\ v_3 \end{pmatrix} &= \frac{\sqrt{8\beta^2(\beta^2-\alpha^2-\gamma^2) + 6\alpha^4 - 4\alpha^2\gamma^2 + 6\gamma^2}}{\alpha^2+\gamma^2+2\beta^2} \begin{pmatrix} \frac{\alpha+\gamma}{2} \\ -\beta \\ \frac{\alpha-\gamma}{2} \end{pmatrix}. \end{aligned}$$

pair	$\sqrt{2}n^I$	a^I	pair	$\sqrt{2}n^I$	a^I
$(1,3)$	$(1,-1,0)$	(u_1,u_2,u_3)	$(3,1)$	$(1,-1,0)$	$(-u_2,-u_1,-u_3)$
$(1,4)$	$(1,1,0)$	$(u_1,-u_2,-u_3)$	$(4,1)$	$(1,1,0)$	$(-u_2,u_1,u_3)$
$(1,5)$	$(1,0,-1)$	(u_1,u_3,u_2)	$(5,1)$	$(1,0,-1)$	$(-u_2,-u_3,-u_1)$
$(1,6)$	$(1,0,1)$	$(u_1,-u_3,-u_2)$	$(6,1)$	$(1,0,1)$	$(-u_2,u_3,u_1)$
$(2,3)$	$(1,1,0)$	$(u_1,-u_2,u_3)$	$(3,2)$	$(1,1,0)$	$(-u_2,u_1,-u_3)$
$(2,4)$	$(1,-1,0)$	$(u_1,u_2,-u_3)$	$(4,2)$	$(1,-1,0)$	$(-u_2,-u_1,u_3)$
$(2,5)$	$(1,0,1)$	$(u_1,u_3,-u_2)$	$(5,2)$	$(1,0,1)$	$(-u_2,-u_3,u_1)$
$(2,6)$	$(1,0,-1)$	$(u_1,-u_3,u_2)$	$(6,2)$	$(1,0,-1)$	$(-u_2,u_3,-u_1)$
$(3,5)$	$(0,1,-1)$	(u_3,u_1,u_2)	$(5,3)$	$(0,1,-1)$	$(-u_3,-u_2,-u_1)$
$(3,6)$	$(0,1,1)$	$(-u_3,u_1,-u_2)$	$(6,3)$	$(0,1,1)$	$(u_3,-u_2,u_1)$
$(4,5)$	$(0,1,1)$	$(u_3,u_1,-u_2)$	$(5,4)$	$(0,1,1)$	$(-u_3,-u_2,u_1)$
$(4,6)$	$(0,1,-1)$	$(-u_3,-u_1,u_2)$	$(6,4)$	$(0,1,-1)$	$(u_3,-u_2,-u_1)$

Table B.1: Components of the Type-I twin plane normal and shear for the different variant pairs in a cubic-to-orthorhombic transition [72].

pair	n^{II}	a^{II}	pair	n^{II}	a^{II}
$(1,3)$	(t_1,t_1,t_2)	(v_1,v_2,v_3)	$(3,1)$	(t_1,t_1,t_2)	(v_2,v_1,v_3)
$(1,4)$	$(-t_1,t_1,t_2)$	$(-v_1,v_2,v_3)$	$(4,1)$	$(-t_1,t_1,t_2)$	$(-v_2,v_1,v_3)$
$(1,5)$	(t_1,t_2,t_1)	(v_1,v_3,v_2)	$(5,1)$	(t_1,t_2,t_1)	(v_2,v_3,v_1)
$(1,6)$	$(-t_1,t_2,t_1)$	$(-v_1,v_3,v_2)$	$(6,1)$	$(-t_1,t_2,t_1)$	$(-v_2,v_3,v_1)$
$(2,3)$	$(t_1,-t_1,t_2)$	$(v_1,-v_2,v_3)$	$(3,2)$	$(t_1,-t_1,t_2)$	$(v_2,-v_1,v_3)$
$(2,4)$	$(t_1,t_1,-t_2)$	$(v_1,v_2,-v_3)$	$(4,2)$	$(t_1,t_1,-t_2)$	$(v_2,v_1,-v_3)$
$(2,5)$	$(t_1,t_2,-t_1)$	$(v_1,v_3,-v_2)$	$(5,2)$	$(t_1,t_2,-t_1)$	$(v_2,v_3,-v_1)$
$(2,6)$	$(t_1,-t_2,t_1)$	$(v_1,-v_3,v_2)$	$(6,2)$	$(t_1,-t_2,t_1)$	$(v_2,-v_3,v_1)$
$(3,5)$	(t_2,t_1,t_1)	(v_3,v_1,v_2)	$(5,3)$	(t_2,t_1,t_1)	(v_3,v_2,v_1)
$(3,6)$	$(t_2,-t_1,t_1)$	$(v_3,-v_1,v_2)$	$(6,3)$	$(t_2,-t_1,t_1)$	$(v_3,-v_2,v_1)$
$(4,5)$	$(t_2,t_1,-t_1)$	$(v_3,v_1,-v_2)$	$(5,4)$	$(t_2,t_1,-t_1)$	$(v_3,v_2,-v_1)$
$(4,6)$	$(-t_2,t_1,t_1)$	$(-v_3,v_1,v_2)$	$(6,4)$	$(-t_2,t_1,t_1)$	$(-v_3,v_2,v_1)$

Table B.2: Components of the Type-II twin plane normal and shear for the different variant pairs in a cubic-to-orthorhombic transition [72].

We note that for Seiner's CuAlNi specimen the components of the twinning elements become:

$$\begin{pmatrix} u_1 \\ u_2 \\ u_3 \end{pmatrix} = \begin{pmatrix} 0.197977 \\ -0.173644 \\ 0.00379754 \end{pmatrix},$$

$$\begin{pmatrix} t_1 \\ t_2 \end{pmatrix} = \begin{pmatrix} -0.688388 \\ -0.228571 \end{pmatrix}, \quad \begin{pmatrix} v_1 \\ v_2 \\ v_3 \end{pmatrix} = \begin{pmatrix} 0.197977 \\ -0.173644 \\ 0.00379754 \end{pmatrix}.$$

For the habit plane elements, the calculations are purely numerical. In order to shorten the otherwise long tables that follow, let us write

$$\begin{array}{lll} s_1 = 0.141221, & s_2 = 0.668151, & s_3 = 0.730501, \\ s_4 = 0.261549, & s_5 = 0.727152, & s_6 = 0.634699, \\ z_1 = 0.0244382, & z_2 = 0.0728267, & z_3 = 0.0575181, \\ z_4 = 0.0123419, & z_5 = 0.0674388, & z_6 = 0.0671488. \end{array}$$

pair	m_1^+	b_1^+	pair	m_1^+	b_1^+
$(1,3)$	$(-s_1, s_2, -s_3)$	$(-z_1, -z_2, -z_3)$	$(3,1)$	$(-s_2, s_1, s_3)$	(z_2, z_1, z_3)
$(1,4)$	$(s_4, -s_5, -s_6)$	$(z_4, z_5, -z_6)$	$(4,1)$	$(-s_5, s_4, s_6)$	(z_5, z_4, z_6)
$(1,5)$	$(s_1, s_3, -s_2)$	(z_1, z_3, z_2)	$(5,1)$	$(-s_5, -s_6, -s_4)$	$(z_5, -z_6, -z_4)$
$(1,6)$	$(s_4, -s_6, -s_5)$	$(z_4, -z_6, z_5)$	$(6,1)$	$(-s_2, -s_3, -s_1)$	$(z_2, -z_3, -z_1)$
$(2,3)$	$(s_4, -s_5, s_6)$	(z_4, z_5, z_6)	$(3,2)$	$(-s_2, -s_1, s_3)$	$(z_2, -z_1, z_3)$
$(2,4)$	$(-s_1, s_2, s_3)$	$(-z_1, -z_2, z_3)$	$(4,2)$	$(-s_5, -s_4, s_6)$	$(z_5, -z_4, z_6)$
$(2,5)$	$(s_4, s_6, -s_5)$	(z_4, z_6, z_5)	$(5,2)$	$(-s_5, -s_6, s_4)$	$(z_5, -z_6, z_4)$
$(2,6)$	$(s_1, -s_3, -s_2)$	$(z_1, -z_3, z_2)$	$(6,2)$	$(-s_2, -s_3, s_1)$	$(z_2, -z_3, z_1)$
$(3,5)$	$(s_3, s_1, -s_2)$	(z_3, z_1, z_2)	$(5,3)$	$(s_3, -s_2, s_1)$	(z_3, z_2, z_1)
$(3,6)$	$(s_3, -s_1, -s_2)$	$(z_3, -z_1, z_2)$	$(6,3)$	$(-s_6, s_5, -s_4)$	$(-z_6, -z_5, -z_4)$
$(4,5)$	$(s_6, s_4, -s_5)$	(z_6, z_4, z_5)	$(5,4)$	$(s_3, -s_2, -s_1)$	$(z_3, z_2, -z_1)$
$(4,6)$	$(s_6, -s_4, -s_5)$	$(z_6, -z_4, z_5)$	$(6,4)$	$(-s_6, s_5, s_4)$	$(-z_6, -z_5, z_4)$

Table B.3: Components of the habit plane normal m_1^+ and shear b_1^+ for the different variant pairs in the cubic-to-orthorhombic transition of Seiner's CuAlNi specimen.

pair	m_1^-	b_1^-	pair	m_1^-	b_1^-
$(1,3)$	(s_4, s_5, s_6)	$(z_4, -z_5, z_6)$	$(3,1)$	$(-s_5, -s_4, -s_6)$	$(z_5, -z_4, -z_6)$
$(1,4)$	$(-s_1, -s_2, s_3)$	$(-z_1, z_2, z_3)$	$(4,1)$	$(-s_2, -s_1, -s_3)$	$(z_2, -z_1, -z_3)$
$(1,5)$	$(-s_4, -s_6, -s_5)$	$(-z_4, -z_6, z_5)$	$(5,1)$	$(-s_2, s_3, s_1)$	(z_2, z_3, z_1)
$(1,6)$	$(-s_1, s_3, -s_2)$	$(-z_1, z_3, z_2)$	$(6,1)$	$(-s_5, s_6, s_4)$	(z_5, z_6, z_4)
$(2,3)$	$(-s_1, -s_2, -s_3)$	$(-z_1, z_2, -z_3)$	$(3,2)$	$(-s_5, s_4, -s_6)$	$(z_5, z_4, -z_6)$
$(2,4)$	$(s_4, s_5, -s_6)$	$(z_4, -z_5, -z_6)$	$(4,2)$	$(-s_2, s_1, -s_3)$	$(z_2, z_1, -z_3)$
$(2,5)$	$(-s_1, -s_3, -s_2)$	$(-z_1, -z_3, z_2)$	$(5,2)$	$(-s_2, s_3, -s_1)$	$(z_2, z_3, -z_1)$
$(2,6)$	$(-s_4, s_6, -s_5)$	$(-z_4, z_6, z_5)$	$(6,2)$	$(-s_5, s_6, -s_4)$	$(z_5, z_6, -z_4)$
$(3,5)$	$(-s_6, -s_4, -s_5)$	$(-z_6, -z_4, z_5)$	$(5,3)$	$(-s_6, -s_5, -s_4)$	$(-z_6, z_5, -z_4)$
$(3,6)$	$(-s_6, s_4, -s_5)$	$(-z_6, z_4, z_5)$	$(6,3)$	(s_3, s_2, s_1)	$(z_3, -z_2, z_1)$
$(4,5)$	$(-s_3, -s_1, -s_2)$	$(-z_3, -z_1, z_2)$	$(5,4)$	$(-s_6, -s_5, s_4)$	$(-z_6, z_5, z_4)$
$(4,6)$	$(-s_3, s_1, -s_2)$	$(-z_3, z_1, z_2)$	$(6,4)$	$(s_3, s_2, -s_1)$	$(z_3, -z_2, -z_1)$

Table B.4: Components of the habit plane normal m_1^- and shear b_1^- for the different variant pairs in the cubic-to-orthorhombic transition of Seiner's CuAlNi specimen.

pair	m_2^+	b_2^+	pair	m_2^+	b_2^+
$(1,3)$	$(-s_2, s_1, s_3)$	(z_2, z_1, z_3)	$(3,1)$	(s_4, s_5, s_6)	$(z_4, -z_5, z_6)$
$(1,4)$	$(-s_5, s_4, s_6)$	(z_5, z_4, z_6)	$(4,1)$	$(-s_1, -s_2, s_3)$	$(-z_1, z_2, z_3)$
$(1,5)$	$(-s_5, -s_6, -s_4)$	$(z_5, -z_6, -z_4)$	$(5,1)$	$(s_1, s_3, -s_2)$	(z_1, z_3, z_2)
$(1,6)$	$(-s_2, -s_3, -s_1)$	$(z_2, -z_3, -z_1)$	$(6,1)$	$(s_4, -s_6, -s_5)$	$(z_4, -z_6, z_5)$
$(2,3)$	$(-s_2, -s_1, s_3)$	$(z_2, -z_1, z_3)$	$(3,2)$	$(s_4, -s_5, s_6)$	(z_4, z_5, z_6)
$(2,4)$	$(-s_5, -s_4, s_6)$	$(z_5, -z_4, z_6)$	$(4,2)$	$(-s_1, s_2, s_3)$	$(-z_1, -z_2, z_3)$
$(2,5)$	$(-s_5, -s_6, s_4)$	$(z_5, -z_6, z_4)$	$(5,2)$	(s_1, s_3, s_2)	$(z_1, z_3, -z_2)$
$(2,6)$	$(-s_2, -s_3, s_1)$	$(z_2, -z_3, z_1)$	$(6,2)$	$(s_4, -s_6, s_5)$	$(z_4, -z_6, -z_5)$
$(3,5)$	$(s_3, -s_2, s_1)$	(z_3, z_2, z_1)	$(5,3)$	$(s_3, s_1, -s_2)$	(z_3, z_1, z_2)
$(3,6)$	$(-s_6, s_5, -s_4)$	$(-z_6, -z_5, -z_4)$	$(6,3)$	$(s_3, -s_1, -s_2)$	$(z_3, -z_1, z_2)$
$(4,5)$	$(s_3, -s_2, -s_1)$	$(z_3, z_2, -z_1)$	$(5,4)$	$(s_6, s_4, -s_5)$	(z_6, z_4, z_5)
$(4,6)$	$(-s_6, s_5, s_4)$	$(-z_6, -z_5, z_4)$	$(6,4)$	$(s_6, -s_4, -s_5)$	$(z_6, -z_4, z_5)$

Table B.5: Components of the habit plane normal m_2^+ and shear b_2^+ for the different variant pairs in the cubic-to-orthorhombic transition of Seiner's CuAlNi specimen.

pair	m_2^-	b_2^-	pair	m_2^-	b_2^-
$(1,3)$	$(-s_5, -s_4, -s_6)$	$(z_5, -z_4, -z_6)$	$(3,1)$	$(-s_1, s_2, -s_3)$	$(-z_1, -z_2, -z_3)$
$(1,4)$	$(-s_2, -s_1, -s_3)$	$(z_2, -z_1, -z_3)$	$(4,1)$	$(s_4, -s_5, -s_6)$	$(z_4, z_5, -z_6)$
$(1,5)$	$(-s_2, s_3, s_1)$	(z_2, z_3, z_1)	$(5,1)$	$(-s_4, -s_6, -s_5)$	$(-z_4, -z_6, z_5)$
$(1,6)$	$(-s_5, s_6, s_4)$	(z_5, z_6, z_4)	$(6,1)$	$(-s_1, s_3, -s_2)$	$(-z_1, z_3, z_2)$
$(2,3)$	$(-s_5, s_4, -s_6)$	$(z_5, z_4, -z_6)$	$(3,2)$	$(-s_1, -s_2, -s_3)$	$(-z_1, z_2, -z_3)$
$(2,4)$	$(-s_2, s_1, -s_3)$	$(z_2, z_1, -z_3)$	$(4,2)$	$(s_4, s_5, -s_6)$	$(z_4, -z_5, -z_6)$
$(2,5)$	$(-s_2, s_3, -s_1)$	$(z_2, z_3, -z_1)$	$(5,2)$	$(-s_4, -s_6, s_5)$	$(-z_4, -z_6, -z_5)$
$(2,6)$	$(-s_5, s_6, -s_4)$	$(z_5, z_6, -z_4)$	$(6,2)$	$(-s_1, s_3, s_2)$	$(-z_1, z_3, -z_2)$
$(3,5)$	$(-s_6, -s_5, -s_4)$	$(-z_6, z_5, -z_4)$	$(5,3)$	$(-s_6, -s_4, -s_5)$	$(-z_6, -z_4, z_5)$
$(3,6)$	(s_3, s_2, s_1)	$(z_3, -z_2, z_1)$	$(6,3)$	$(-s_6, s_4, -s_5)$	$(-z_6, z_4, z_5)$
$(4,5)$	$(-s_6, -s_5, s_4)$	$(-z_6, z_5, z_4)$	$(5,4)$	$(-s_3, -s_1, -s_2)$	$(-z_3, -z_1, z_2)$
$(4,6)$	$(s_3, s_2, -s_1)$	$(z_3, -z_2, -z_1)$	$(6,4)$	$(-s_3, s_1, -s_2)$	$(-z_3, z_1, z_2)$

Table B.6: Components of the habit plane normal m_2^- and shear b_2^- for the different variant pairs in the cubic-to-orthorhombic transition of Seiner's CuAlNi specimen.

We note that the above components of the habit plane elements are only approximate. These are of course easily subject to verification since

$$(U_s + \lambda n \otimes a)(U_s + \lambda a \otimes n) = (\mathbf{1} + m \otimes b)(\mathbf{1} + b \otimes m).$$

We can now verify that it is indeed possible to construct the microstructure at the corner that reduces the energy as in Lemma 4.5.3. To see this we need to consider each possible value of $s \in \{1, \dots, 6\}$ and check the corners at which the required microstructure can be constructed.

As in the proof of Lemma 4.5.3, suppose that the coordinate system has been chosen in such a way that the edges of Ω are parallel to the axes and each corner of Ω lies in a different octant. Let us write $x = (x_1, x_2, x_3)^T$ for the coordinates of the point $x \in \mathbb{R}^3$ in the standard basis of $\mathbb{R}^3$ and denote the octants as follows:

$$\begin{aligned}
O_1 &:= \left\{x \in \mathbb{R}^3 : x_1 > 0,\, x_2 > 0,\, x_3 > 0\right\},\ O_5 = -O_1\\
O_2 &:= \left\{x \in \mathbb{R}^3 : x_1 < 0,\, x_2 > 0,\, x_3 > 0\right\},\ O_6 = -O_2\\
O_3 &:= \left\{x \in \mathbb{R}^3 : x_1 > 0,\, x_2 < 0,\, x_3 > 0\right\},\ O_7 = -O_3\\
O_4 &:= \left\{x \in \mathbb{R}^3 : x_1 > 0,\, x_2 > 0,\, x_3 < 0\right\},\ O_8 = -O_4.
\end{aligned}$$

The results are summarized in Tables B.7 and B.8 for the habit plane solutions using $\lambda = \lambda^* \in (0, 1/2)$ and $\lambda = 1 - \lambda^* \in (1/2, 1)$ respectively and are explained below:

s/l	1	2	3	4	5	6	O
1	-	-	m_1^-	$-m_1^+$	m_1^+	$-m_1^-$	$1,2,5,6$
2	-	-	m_1^-	m_1^+	m_1^+	m_1^-	$3,4,7,8$
3	$-m_1^-$	$-m_1^+$	-	-	m_1^-	m_1^+	$1,3,5,7$
4	m_1^+	$-m_1^-$	-	-	m_1^-	$-m_1^+$	$2,4,6,8$
5	m_1^-	$-m_1^+$	m_1^-	$-m_1^+$	-	-	$1,4,5,8$
6	m_1^+	m_1^-	m_1^-	m_1^+	-	-	$2,3,6,7$

Table B.7: For each $s \in \{1, \ldots, 6\}$, the table gives all the habit plane normals with $\lambda \in (0, 1/2)$ that lie in the same octant as the Type-II twin normal for the possible values of l. The final column gives the octants in which the construction at the corner is possible.

s/l	1	2	3	4	5	6	O
1	-	-	$-m_2^+$	m_2^-	m_2^-	m_2^+	$1,2,5,6$
2	-	-	$-m_2^+$	$-m_2^-$	m_2^-	$-m_2^+$	$3,4,7,8$
3	m_2^-	m_2^-	-	-	m_2^-	m_2^-	$1,3,5,7$
4	$-m_2^+$	m_2^+	-	-	$-m_2^+$	m_2^+	$2,4,6,8$
5	m_2^+	m_2^+	m_2^-	m_2^-	-	-	$1,4,5,8$
6	$-m_2^-$	m_2^-	m_2^+	$-m_2^+$	-	-	$2,3,6,7$

Table B.8: For each $s \in \{1, \ldots, 6\}$, the table gives all the habit plane normals with $\lambda \in (1/2, 1)$ that lie in the same octant as the Type-II twin normal for the possible values of l. The final column gives the octants in which the construction at the corner is possible.

For example, let $s = 1$. From Table B.2 and the lattice parameters of Seiner's

specimen, the Type-II twin normal is given by

$$n = n^{II} = \begin{cases} (-0.688388, -0.688388, -0.228571)^T, & l = 3 \\ (0.688388, -0.688388, -0.228571)^T, & l = 4 \\ (-0.688388, -0.228571, -0.688388)^T, & l = 5 \\ (0.688388, -0.228571, -0.688388)^T, & l = 6. \end{cases}$$

For each $l \in \{3, \dots, 6\}$ and $\lambda \in (0, 1/2)$, we see from Tables B.3 and B.4 that we may choose habit plane normal m in the same octant as n^{II} as follows:

$$m = \begin{cases} m_1^-, & l = 3 \\ -m_1^+, & l = 4 \\ m_1^+, & l = 5 \\ -m_1^-, & l = 6 \end{cases}$$

and similarly, for $\lambda \in (1/2, 1)$ and Tables B.5, B.6,

$$m = \begin{cases} -m_2^+, & l = 3 \\ m_2^-, & l = 4 \\ m_2^-, & l = 5 \\ m_2^+, & l = 6. \end{cases}$$

Note that we have multiplied some of the above habit plane normals by -1 implying that we also need to multiply the corresponding shears by -1 so that the tensor product $m \otimes b$ remains unaltered. Then, for $l = 3, 5$ the Type-II twin normal lies in O_5 and we may choose a habit plane normal m in the same octant such that neither m nor n^{II} are perpendicular to any of the edges of Ω (recall that the edges are along the principal cubic axes). Also, for $l = 4, 6$ the Type-II twin normal lies in O_6 and we may again choose an appropriate habit plane normal.

Clearly, by considering $-a^{II}$, $-n^{II}$ and respectively $-m$, $-b$, we may also choose twin and habit plane normals lying in the octants $O_1 = -O_5$ and $O_2 = -O_6$. The construction is now possible provided that the underlying deformation remains injective, i.e. provided that

$$U_1^{-1}\tilde{b} \cdot n < 0,$$

where $\tilde{b} = Rb$, $R \in SO(3)$ as in (B.0.2). Note that multiplying all the elements of the twin and habit planes by -1 leaves the above dot product unchanged. The rotation R can be easily computed in each case by calculating

$$R = (U_1 + \lambda a \otimes n)(\mathbf{1} + b \otimes m)^{-1}.$$

Then one finds that $U_1^{-1}\tilde{b} \cdot n = -0.0226521$ for any $l \in \{3, \dots, 6\}$ and any choice of the above habit plane elements.

The case $s = 2, \ldots, 6$ is identical to the above. The only non-trivial part is verifying the inequality

$$U_s^{-1}\tilde{b} \cdot n < 0,$$

for the appropriate choice of habit plane normals. In fact, the value of the above dot product remains -0.0226521 for any s and l, as long as we have chosen a habit plane normal that lies in the same quadrant as the Type-II twin normal. This is surprising and leads one to conjecture that there must be some underlying structure for this to be true; nevertheless, algebraic complexity prevents us from unravelling this structure.

Bibliography

[1] E. Acerbi and N. Fusco. Semicontinuity problems in the calculus of variations. *Arch. Rational Mech. Anal.*, 86(2):125–145, 1984.

[2] R. A. Adams. *Sobolev spaces*. Academic Press [A subsidiary of Harcourt Brace Jovanovich, Publishers], New York-London, 1975. Pure and Applied Mathematics, Vol. 65.

[3] L. V. Ahlfors. *Lectures on quasiconformal mappings*, volume 38 of *University Lecture Series*. American Mathematical Society, Providence, RI, second edition, 2006. With supplemental chapters by C. J. Earle, I. Kra, M. Shishikura and J. H. Hubbard.

[4] C. Amrouche, P. G. Ciarlet, and P. Ciarlet, Jr. Vector and scalar potentials, Poincaré's theorem and Korn's inequality. *C. R. Math. Acad. Sci. Paris*, 345(11):603–608, 2007.

[5] G. Andrews and J. M. Ball. Asymptotic behaviour and changes of phase in one-dimensional non-linear viscoelasticity. *J. Diff. Eqns.*, 44:306–341, 1982.

[6] N. W. Ashcroft and N. D. Mermin. *Solid State Physics*. Thomson Learning, U. K., 1976.

[7] J. M. Ball. Convexity conditions and existence theorems in nonlinear elasticity. *Arch. Rational Mech. Anal.*, 63(4):337–403, 1976/77.

[8] J. M. Ball. Global invertibility of Sobolev functions and the interpenetration of matter. *Proc. Roy. Soc. Edinburgh Sect. A*, 88(3-4):315–328, 1981.

[9] J. M. Ball. A version of the fundamental theorem for Young measures. In *PDEs and continuum models of phase transitions (Nice, 1988)*, volume 344 of *Lecture Notes in Phys.*, pages 207–215. Springer, Berlin, 1989.

[10] J. M. Ball. Sets of gradients with no rank-one connections. *J. Math. Pures Appl. (9)*, 69(3):241–259, 1990.

[11] J. M. Ball. Dynamic energy minimization and phase transformations in solids. In *ICIAM 91 (Washington, DC, 1991)*, pages 3–14. SIAM, Philadelphia, PA, 1992.

[12] J. M. Ball. The calculus of variations and materials science. *Quart. Appl. Math.*, 56(4):719–740, 1998. Current and future challenges in the applications of mathematics (Providence, RI, 1997).

[13] J. M. Ball and C. Carstensen. Non-classical austenite-martensite interfaces. *J. Phys. IV France*, 7:35–40, 1997.

[14] J. M. Ball and C. Carstensen. Compatibility conditions for microstructures and the austenite martensite transition. *Materials Science and Engineering A*, 273-275:231–236, 1999.

[15] J. M. Ball, C. Chu, and R. D. James. Hysteresis during stress-induced variant rearrangement. *Journal de Physique IV C8*, 5 (1):245–251, 1995.

[16] J. M. Ball and E. C. M. Crooks. Local minimizers and planar interfaces in a phase-transition model with interfacial energy. *Calc. Var. Partial Differential Equations*, 40(3-4):501–538, 2011.

[17] J. M. Ball, P. J. Holmes, R. D. James, R. L. Pego, and P. J. Swart. On the dynamics of fine structure. *J. Nonlinear Sci.*, 1(1):17–70, 1991.

[18] J. M. Ball and R. D. James. Fine phase mixtures as minimizers of energy. *Arch. Rational Mech. Anal.*, 100(1):13–52, 1987.

[19] J. M. Ball and R. D. James. Proposed experimental tests of a theory of fine microstructure and the two-well problem. *Philosophical Transactions: Physical Sciences and Engineering*, pages 389–450, 1992.

[20] J. M. Ball, K. Koumatos, and H. Seiner. An analysis of non-classical austenite-martensite interfaces in CuAiNi. In *Proceedings ICOMAT08*, pages 383–390 (also at arXiv:1108.6220v1). TMS, 2010.

[21] J. M. Ball, K. Koumatos, and H. Seiner. Nucleation of austenite in mechanically stabilized martensite by localized heating. *Journal of Alloys and Compounds, Proceedings ICOMAT11*, 2011. in press, DOI:10.1016/j.jallcom.2011.11.070.

[22] J. M. Ball and J. E. Marsden. Quasiconvexity at the boundary, positivity of the second variation and elastic stability. *Arch. Rational Mech. Anal.*, 86(3):251–277, 1984.

[23] J.M. Ball and F. Murat. $W^{1,p}$-quasiconvexity and variational problems for multiple integrals. *Journal of functional analysis*, 58(3):225–253, 1984.

[24] Z. S. Basinski and J. W. Christian. Crystallography of deformation by twin boundary movements in Indium-Thallium alloys. *Acta Metallurgica*, 2(1):101–116, 1954.

[25] K. Bhattacharya. Wedge-like microstructure in martensites. *Acta metallurgica et materialia*, 39(10):2431–2444, 1991.

[26] K. Bhattacharya. Self-accommodation in martensite. *Archive for rational mechanics and analysis*, 120(3):201–244, 1992.

[27] K. Bhattacharya. Comparison of the geometrically nonlinear and linear theories of martensitic transformation. *Contin. Mech. Thermodyn.*, 5(3):205–242, 1993.

[28] K. Bhattacharya. The kinematics of crossing twins. In *Contemporary Research in the Mechanics and Mathematics of Materials*, pages 251–261. CIMNE, 1996.

[29] K. Bhattacharya. *Microstructure of martensite: Why it forms and how it gives rise to the shape-memory effect*. Oxford Series on Materials Modelling. Oxford University Press, Oxford, 2003.

[30] K. Bhattacharya and G. Dolzmann. Relaxation of some multi-well problems. *Proc. Roy. Soc. Edinburgh Sect. A*, 131(2):279–320, 2001.

[31] K. Bhattacharya, N. B. Firoozye, R. D. James, and R. V. Kohn. Restrictions on microstructure. *Proc. Roy. Soc. Edinburgh Sect. A*, 124(5):843–878, 1994.

[32] K. Bhattacharya, R. D. James, and P. J. Swart. Relaxation in shape-memory alloys–part i. mechanical model. part ii. thermo-mechanical model and proposed experiments. *Acta materialia*, 45(11):4547–4568, 1997.

[33] K. Bhattacharya and R. V. Kohn. Symmetry, texture and the recoverable strain of shape-memory polycrystals. *Acta Mater.*, 44:529–542, 1996.

[34] K. Bhattacharya and R. V. Kohn. Energy minimization and the recoverable strains of polycrystalline shape-memory alloys. *Arch. Rat. Mech. Anal.*, 139:99–180, 1997.

[35] J. S. Bowles and J. K. MacKenzie. The crystallography of martensitic transformations I and II. *Acta Metall.*, 2(129–137):138–147, 1954.

[36] A. Braides and A. Defranceschi. *Homogenization of multiple integrals*, volume 12 of *Oxford Lecture Series in Mathematics and its Applications*. The Clarendon Press Oxford University Press, New York, 1998.

[37] A. Cellina and S. Perrotta. On a problem of potential wells. *J. Convex Anal.*, 2(1-2):103–115, 1995.

[38] P. G. Ciarlet and P. Destuynder. A justification of the two-dimensional linear plate model. *J. Mécanique*, 18(2):315–344, 1979.

[39] P. G. Ciarlet and J. Nečas. Injectivity and self-contact in nonlinear elasticity. *Arch. Rational Mech. Anal.*, 97(3):171–188, 1987.

[40] P.G. Ciarlet and J. Nečas. Unilateral problems in nonlinear, three-dimensional elasticity. *Archive for rational mechanics and analysis*, 87(4):319–338, 1985.

[41] S. Conti, G. Dolzmann, and B. Kirchheim. Existence of Lipschitz minimizers for the three-well problem in solid-solid phase transitions. *Ann. Inst. H. Poincaré Anal. Non Linéaire*, 24(6):953–962, 2007.

[42] S. Conti and B. Schweizer. Rigidity and gamma convergence for solid-solid phase transitions with SO(2) invariance. *Comm. Pure Appl. Math.*, 59(6):830–868, 2006.

[43] M. Csörnyei, S. Hencl, and J. Malý. Homeomorphisms in the Sobolev space $W^{1,n-1}$. *J. Reine Angew. Math.*, 644:221–235, 2010.

[44] J. Cui, Y. S. Chu, O. Famodu, Y. Furuya, J. Hattrick-Simpers, R. D. James, A. Ludwig, S. Thienhaus, M. Wuttig, Z. Zhang, and I. Takeuchi. Combinatorial search of thermoelastic shape-memory alloys with extremely small hysteresis width. *Nature materials*, 5(4):286–290, 2006.

[45] B. Dacorogna. Quasiconvexity and relaxation of nonconvex problems in the calculus of variations. *J. Funct. Anal.*, 46(1):102–118, 1982.

[46] B. Dacorogna. *Direct methods in the calculus of variations*, volume 78 of *Applied Mathematical Sciences*. Springer, New York, second edition, 2008.

[47] B. Dacorogna and N. Fusco. Semi-continuité des fonctionnelles avec contraintes du type $\det f > 0$. *Boll. Un. Mat. Ital*, pages 4–8, 1985.

[48] B. Dacorogna and P. Marcellini. *Implicit partial differential equations*. Progress in Nonlinear Differential Equations and their Applications, 37. Birkhäuser Boston Inc., Boston, MA, 1999.

[49] G. Dal Maso. *An introduction to* Γ*-convergence*. Progress in Nonlinear Differential Equations and their Applications, 8. Birkhäuser Boston Inc., Boston, MA, 1993.

[50] E. De Giorgi. Sulla convergenza di alcune successioni d'integrali del tipo dell'area. *Rend. Mat. (6)*, 8:277–294, 1975. Collection of articles dedicated to Mauro Picone on the occasion of his ninetieth birthday.

[51] E. De Giorgi and T. Franzoni. Su un tipo di convergenza variazionale. *Atti Accad. Naz. Lincei Rend. Cl. Sci. Fis. Mat. Natur. (8)*, 58(6):842–850, 1975.

[52] G. Dolzmann. *Variational methods for crystalline microstructure—analysis and computation*, volume 1803 of *Lecture Notes in Mathematics*. Springer-Verlag, Berlin, 2003.

[53] G. Dolzmann and B. Kirchheim. Liquid-like behavior of shape memory alloys. *C. R. Math. Acad. Sci. Paris*, 336(5):441–446, 2003.

[54] G. Dolzmann, B. Kirchheim, and J Kristensen. Conditions for the equality of hulls in the calculus of variations. *Arch. Ration. Mech. Anal.*, 154:93–100, 2000.

[55] G. Dolzmann, B. Kirchheim, S. Müller, and V. Šverák. The two-well problem in three dimensions. *Calc. Var. Partial Differential Equations*, 10(1):21–40, 2000.

[56] J. L. Ericksen. Special topics in elastostatics. In *Advances in Applied Mechanics, ed. C.S. Yih*, volume 17, pages 189–243. Academic Press, New York, 1977.

[57] J. L. Ericksen. Some phase transitions in crystals. *Arch. Rational Mech. Anal.*, 73(2):99–124, 1980.

[58] J. L. Ericksen. The Cauchy and Born hypotheses for crystals. In *Phase transformations and material instabilities in solids (Madison, Wis., 1983)*, volume 52 of *Publ. Math. Res. Center Univ. Wisconsin*, pages 61–77. Academic Press, Orlando, FL, 1984.

[59] J. L. Ericksen. Weak Martensitic transformations in Bravais lattices. *Arch. Rational Mech. Anal.*, 107(1):23–36, 1989.

[60] I. Fonseca. The lower quasiconvex envelope of the stored energy function for an elastic crystal. *J. Math. Pures Appl. (9)*, 67(2):175–195, 1988.

[61] I. Fonseca and W. Gangbo. *Degree theory in analysis and applications*, volume 2 of *Oxford Lecture Series in Mathematics and its Applications*. The Clarendon Press Oxford University Press, New York, 1995. Oxford Science Publications.

[62] I. Fonseca and G. Leoni. *Modern methods in the calculus of variations: L^p spaces*. Springer Monographs in Mathematics. Springer, New York, 2007.

[63] I. Fonseca, S. Müller, and P. Pedregal. Analysis of concentration and oscillation effects generated by gradients. *SIAM journal on mathematical analysis*, 29(3):736–756, 1998.

[64] A. Forclaz. *Variational methods in material science*. Ph.D. thesis, University of Oxford, 2002.

[65] R. L. Fosdick and B. Hertog. Material symmetry and crystals. *Arch. Rational Mech. Anal.*, 110(1):43–72, 1990.

[66] G. Friesecke. Quasiconvex hulls and recoverable strains in shape-memory alloys. In *TMR Meeting 'Phase Transitions in Crystalline Solids'*, Max Planck Institute for Mathematics in the Sciences, Leipzig, 2000.

[67] G. Friesecke and J. B. McLeod. Dynamics as a mechanism preventing the formation of finer and finer microstructure. *Arch. Rational Mech. Anal.*, 133(3):199–247, 1996.

[68] Y. Grabovsky. New necessary conditions for Lipschitz strong local minimizers, 2008.

[69] Y. Grabovsky and T. Mengesha. Direct approach to the problem of strong local minima in calculus of variations. *Calc. Var. Partial Differential Equations*, 29(1):59–83, 2007.

[70] Y. Grabovsky and T. Mengesha. Sufficient conditions for strong local minimal: the case of C^1 extremals. *Trans. Amer. Math. Soc.*, 361(3):1495–1541, 2009.

[71] J. Hadamard. *Lecons sur la Propogation des Ondes*. Hermann, Paris, 1903.

[72] K. Hane. *Microstructures in Thermoelastic Martensites*. Ph.D. thesis, University of Minnesota, 1998.

[73] D. Henao and C. Mora-Corral. Lusins condition and the distributional determinant for deformations with finite energy. *Adv. Calc. Var*, 2009.

[74] D. Henao and C. Mora-Corral. Fracture surfaces and the regularity of inverses for BV deformations. *Archive for rational mechanics and analysis*, 201(2):575–629, 2011.

[75] S. Hencl and P. Koskela. Regularity of the inverse of a planar Sobolev homeomorphism. *Arch. Ration. Mech. Anal.*, 180(1):75–95, 2006.

[76] S. Hencl, P. Koskela, and J. Malý. Regularity of the inverse of a Sobolev homeomorphism in space. *Proc. Roy. Soc. Edinburgh Sect. A*, 136(6):1267–1285, 2006.

[77] S. Hencl, P. Koskela, and J. Onninen. Homeomorphisms of bounded variation. *Arch. Ration. Mech. Anal.*, 186(3):351–360, 2007.

[78] M. R. Hestenes. Sufficient conditions for multiple integral problems in the calculus of variations. *Amer. J. Math.*, 70:239–276, 1948.

[79] Y. Huo and I. Müller. Nonequilibrium thermodynamics of pseudoelasticity. *Contin. Mech. Thermodyn.*, 5(3):163–204, 1993.

[80] T. Iwaniec, G. C. Verchota, and A. L. Vogel. The failure of rank-one connections. *Archive for Rational Mechanics and Analysis*, 163(2):125–169, 2002.

[81] R. D. James. The stability and metastability of quartz. *Institute for Mathematics and Its Applications*, 3:147, 1987.

[82] R. D. James. *Compatibility, hysteresis and the direct conversion of heat to electricity*, 2011. Talk at the PIRE and OxMOS Workshop on Pattern Formation and Multiscale Phenomena, Oxford (UK), 26-28 September.

[83] R. D. James and Z. Zhang. A way to search for multiferroic materials with unlikely combinations of physical properties. *Magnetism and structure in functional materials*, pages 159–175, 2005.

[84] A. G. Khachaturyan. *Theory of Structural Transformations in Solids.* John Wiley, New York, 1983.

[85] D. Kinderlehrer. Remarks about equilibrium configurations of crystals. In *Material instabilities in continuum mechanics (Edinburgh, 1985–1986)*, Oxford Sci. Publ., pages 217–241. Oxford Univ. Press, New York, 1988.

[86] D. Kinderlehrer and P. Pedregal. Characterizations of Young measures generated by gradients. *Arch. Rational Mech. Anal.*, 115(4):329–365, 1991.

[87] D. Kinderlehrer and P. Pedregal. Gradient Young measures generated by sequences in Sobolev spaces. *J. Geom. Anal.*, 4(1):59–90, 1994.

[88] P. Klouček and M. Luskin. The computation of the dynamics of the martensitic transformation. *Contin. Mech. Thermodyn.*, 6(3):209–240, 1994.

[89] R. V. Kohn. The relaxation of a double-well energy. *Contin. Mech. Thermodyn.*, 3(3):193–236, 1991.

[90] R. V. Kohn and S. Müller. Surface energy and microstructure in coherent phase transitions. *Comm. Pure Appl. Math.*, 47(4):405–435, 1994.

[91] J. Kristensen. On the non-locality of quasiconvexity. *Ann. Inst. H. Poincaré Anal. Non Linéaire*, 16(1):1–13, 1999.

[92] J. Kristensen, Technical University of Denmark. Mathematical Institute, and DTU. *Finite functionals and Young measures generated by gradients of Sobolev functions.* 1994.

[93] M. Landa, V. Novák, M. Blaháček, and P. Šittner. Transformation processes in shape memory alloys based on monitoring acoustic emission activity. *Journal of Acoustic Emission*, 20:163–171, 2002.

[94] M. Landa, P. Šittner, V. Novák, P. Sedlák, and H. Seiner. *Temperature dependence of elastic properties of cubic and orthorhombic phases in CuAlNi shape memory alloy near their stability limits*, 2005. Unpublished lecture, 10^{th} International Symposium on Physics of Materials, ISPMA-10, Prague (Czech Republic), August 30 - September 2.

[95] J. M. Lee. *Introduction to smooth manifolds*, volume 218. Springer, 2012.

[96] D. S. Lieberman, M. A. Schmerling, and R. S. Karz. *Ferroelastic 'memory' and mechanical properties in gold-cadmium.* Plenum Press New York, 1975.

[97] Y. Liu and D. Favier. Stabilisation of martensite due to shear deformation via variant reorientation in polycrystalline NiTi. *Acta materialia*, 48(13):3489–3499, 2000.

[98] P. Marcellini. Approximation of quasiconvex functions and lower semicontinuity of multiple integrals. *Manuscripta Math.*, 51(1-3):1–28, 1985.

[99] M. Marcus and V. J. Mizel. Transformations by functions in Sobolev spaces and lower semicontinuity for parametric variational problems. *Bull. Amer. Math. Soc.*, 79:790–795, 1973.

[100] J. P. Matos. Young measures and the absence of fine microstructures in a class of phase transitions. *European J. Appl. Math.*, 3(1):31–54, 1992.

[101] V. G. Maz'ya. *Sobolev spaces.* Springer Series in Soviet Mathematics. Springer-Verlag, Berlin, 1985. Translated from the Russian by T. O. Shaposhnikova.

[102] N. G. Meyers. Quasi-convexity and lower semi-continuity of multiple variational integrals of any order. *Trans. Amer. Math. Soc.*, 119:125–149, 1965.

[103] C. B. Morrey. Quasiconvexity and the semicontinuity of multiple integrals. *Pacific J. Math.*, 2:25–53, 1952.

[104] C. B. Morrey. *Multiple Integrals in the Calculus of Variations.* Classics in Mathematics. Springer-Verlag, 1966.

[105] S. Müller. Variational models for microstructure and phase transitions. In *Calculus of variations and geometric evolution problems (Cetraro, 1996)*, volume 1713 of *Lecture Notes in Math.*, pages 85–210. Springer, Berlin, 1999.

[106] M. Nishida, H. Ohgi, I. Itai, A. Chiba, and K. Yamauchi. Electron microscopy studies of twin morphologies in B19' martensite in the Ti-Ni shape memory alloy. *Acta metallurgica et materialia*, 43(3):1219–1227, 1995.

[107] M. Nishida, K. Yamauchi, I. Itai, H. Ohgi, and A. Chiba. High resolution electron microscopy studies of twin boundary structures in B19' martensite in the Ti-Ni shape memory alloy. *Acta metallurgica et materialia*, 43(3):1229–1234, 1995.

[108] W. Noll. A general framework for problems in the statics of finite elasticity. In *Contemporary Developments in Continuum Mechanics and Partial Differential Equations*, pages 363–387. North-Holland, 1978.

[109] V. Novák, P. Šittner, S. Ignacová, and T. Černoch. Transformation behavior of prism shaped shape memory alloy single crystals. *Materials Science and Engineering: A*, 438:755–762, 2006.

[110] J. Onninen. Regularity of the inverse of spatial mappings with finite distortion. *Calc. Var. Partial Differential Equations*, 26(3):331–341, 2006.

[111] G. P. Parry. Elasticity of monotomic crystals. *Math. Proc. Cambridge Phil. Soc.*, 80:189–211, 1976.

[112] P. Pedregal. *Parametrized measures and variational principles*. Progress in Nonlinear Differential Equations and their Applications, 30. Birkhäuser Verlag, Basel, 1997.

[113] C. Picornell, VA. Lvov, J. Pons, and E. Cesari. Experimental and theoretical study of mechanical stabilization of martensite in Cu-Al-Ni single crystals. *Materials Science and Engineering: A*, 438:730–733, 2006.

[114] M. Pitteri. Reconciliation of local and global symmetries in crystals. *J. Elasticity*, 14:175–190, 1984.

[115] M. Pitteri and G. Zanzotto. *Continuum models for phase transitions and twinning in crystals*, volume 19 of *Applied Mathematics (Boca Raton)*. Chapman & Hall/CRC, Boca Raton, FL, 2003.

[116] Yu. G. Reshetnyak. *Space mappings with bounded distortion*, volume 73 of *Translations of Mathematical Monographs*. American Mathematical Society, Providence, RI, 1989. Translated from the Russian by H. H. McFaden.

[117] S. Rickman. *Quasiregular mappings*, volume 26 of *Ergebnisse der Mathematik und ihrer Grenzgebiete (3) [Results in Mathematics and Related Areas (3)]*. Springer-Verlag, Berlin, 1993.

[118] R. T. Rockafellar. *Convex analysis*. Princeton Mathematical Series, No. 28. Princeton University Press, Princeton, N.J., 1970.

[119] G. Ruddock. A microstructure of martensite which is not a minimiser of energy: the X-interface. *Arch. Rational Mech. Anal.*, 127:1–39, 1994.

[120] P. Sedlák, H. Seiner, M. Landa, V. Novák, P. P. Šittner, and Ll. Mañosa. Elastic constants of bcc austenite and 2h orthorhombic martensite in cualni shape memory alloy. *Acta Materialia*, 53:3643–3661, 2005.

[121] H. Seiner and M. Landa. Non-classical austenite-martensite interfaces observed in single crystals of Cu-Al-Ni. *Phase Transitions*, 82(11):793–807, 2009.

[122] H. Seiner, M. Landa, and P. Sedlák. Propagation of an austenite-martensite interface in a thermal gradient. In *Proceedings Estonian Academy of Sciences*, volume 56, 2007.

[123] H. Seiner, P. Sedlák, and M. Landa. Shape recovery mechanism observed in single crystals of cu-al-ni shape memory alloy. *Phase Transitions*, 81(6):537–551, 2008.

[124] H. Seiner, P. Sedlák, and M. Landa. Shape recovery mechanism observed in single crystals of Cu-Al-Ni shape memory alloy. *Phase Transitions*, 81(6):537–551, 2008.

[125] J. A. Shaw and S. Kyriakides. Thermomechanical aspects of niti. *J. Mech. Phys. Solids*, 43:1243–1281, 1995.

[126] Y. C. Shu and K. Bhattacharya. The influence of texture on the shape-memory effect in polycrystals. *Acta Materialia*, 46:5457–5473, 1998.

[127] P. Šittner, P. Lucas, D. Neov, M. R. Daymond, V. Novak, and G.M. Swallowe. Stress-induced martensitic transformation in cu-al-zn-mn polycrystal investigated by two *in situ* neutron diffraction techniques. *Mat. Sci. Eng. A*, 324:225–234, 2002.

[128] P. Sittner, V. Noval, P. Lucas, D. Lugovsky, D. Neov, and M. Tovar. Load partiton in niti shape memory alloy polycrystals investigated by in-situ neutron diffraction and micromechanics modelling. *Mat. Sci. Forum*, 404:829–834, 2002.

[129] J. Sivaloganathan and S. J. Spector. On the stability of incompressible elastic cylinders in uniaxial tension. *Journal of Elasticity*, 105:313–330, 2011.

[130] Q. P. Sun, T. T. Xu, and X. Zhang. On deformation of am interface in single crystal shape memory alloys and some related issues. *Journal of engineering materials and technology*, 121:38, 1999.

[131] Q. P. Sun, X. Zhang, and X. Terry. Some recent advances in experimental study of shape memory alloys. In *IUTAM Symposium on Micro-and Macrostructural Aspects of Thermoplasticity*, pages 407–416. Springer, 2002.

[132] V. Šverák. Regularity properties of deformations with finite energy. *Archive for Rational Mechanics and Analysis*, 100(2):105–127, 1988.

[133] V. Šverák. Quasiconvex functions with subquadratic growth. *Proc. Roy. Soc. London Ser. A*, 433(1889):723–725, 1991.

[134] V. Šverák. Rank-one convexity does not imply quasiconvexity. *Proc. Roy. Soc. Ed.*, 120:185–189, 1992.

[135] V. Šverák. On Tartar's conjecture. *Ann. Inst. H. Poincaré Anal. Non Linéaire*, 10(4):405–412, 1993.

[136] V. Šverák. On the problem of two wells. In *Microstructure and phase transition, ed. D. Kinderlehrer, R.D. James, M. Luskin and J.L. Ericksen*, volume 54 of *IMA Vol. Math. Appl.*, pages 183–189. Springer, New York, 1993.

[137] M. A. Sychev. A new approach to Young measure theory, relaxation and convergence in energy. In *Annales de l'Institut Henri Poincare (C) Non Linear Analysis*, volume 16, pages 773–812, 1999.

[138] L. Tartar. Compensated compactness and applications to partial differential equations. In *Nonlinear analysis and mechanics: Heriot-Watt Symposium, Vol. IV*, volume 39 of *Res. Notes in Math.*, pages 136–212. Pitman, Boston, Mass., 1979.

[139] R. N. Thurston. Waves in solids. In *In: Mechanics of solids IV (Festkoerpermechanik IV). Berlin, Springer-Verlag (Handbuch der Physik. Volume VIa/4), 1974, p. 109-308.*, volume 4, pages 109–308, 1974.

[140] T. Valent. Local theorems of existence and uniqueness in finite elastostatics. In *Proceedings of the IUTAM Symposium on Finite Elasticity (Bethlehem, Pa., 1980)*, pages 401–421, The Hague, 1982. Nijhoff.

[141] T. Černoch, M. Landa, V. Novák, P. Sedlák, and P. Šittner. Acoustic characterization of the elastic properties of austenite phase and martensitic transformations in CuAlNi shape memory alloy. *Journal of alloys and compounds*, 378(1-2):140–144, 2004.

[142] Y. Wang and A. G. Khachaturyan. Three-dimenional field model and computer modeling of martensitic transformations. *Acta Materialia*, 45:759–773, 1997.

[143] M. S. Wechsler, D. S. Lieberman, and T. A. Read. On the theory of the formation of martensite. *Trans. AIME J. Metals*, 197:1503–1515, 1953.

[144] L. C. Young. *Lectures on the calculus of variations and optimal control theory.* Foreword by Wendell H. Fleming. W. B. Saunders Co., Philadelphia, 1969.

[145] G. Zanzotto. On the material symmetry group of elastic crystals and the born rule. *Archive for rational mechanics and analysis*, 121(1):1–36, 1992.

[146] K. Zhang. A construction of quasiconvex functions with linear growth at infinity. *Ann. Scuola Norm. Sup. Pisa Cl. Sci. (4)*, 19(3):313–326, 1992.

[147] K. Zhang. On the structure of quasiconvex hulls. *Ann. Inst. H. Poincaré Anal. Non Linéaire*, 15(6):663–686, 1998.

[148] K. Zhang. On various semiconvex hulls in the calculus of variations. *Calc. Var. Partial Differential Equations*, 6(2):143–160, 1998.

[149] K. Zhang. On the quasiconvex exposed points. *ESAIM Control Optim. Calc. Var.*, 6:1–19 (electronic), 2001.

[150] K. Zhang. On the equal hull problem for nontrivial semiconvex hulls. *J. Convex Anal.*, 10(2):409–417, 2003.

[151] W. P. Ziemer. Change of variables for absolutely continuous functions. *Duke Math. J.*, 36:171–178, 1969.